Experimental Evaluation of the Dynamic Performance Benefits of Roll Stability Control Systems on A-train Doubles

Andrew E. Kim

Thesis submitted to the Faculty of Virginia Polytechnic Institute
and State University in partial fulfillment for the degree of

Master of Science

in

Mechanical Engineering

Mehdi Ahmadian, Chair

Douglas J Nelson

Steve C Southward

December 11, 2017

Blacksburg, Virginia

Keywords: rollover, ride stability, roll stability, combination vehicle, A-train, doubles, outriggers, RSC, vehicle dynamics, controlled braking, track testing

Experimental Evaluation of the Dynamic Performance Benefits of Roll Stability Control Systems on A-train Doubles

Andrew E. Kim

Abstract

The ride stability of an A-train 28-foot double tractor trailer when outfitted with different Roll Stability Control (RSC) systems with the same payload and suspension configurations is studied experimentally for various dynamic maneuvers. The primary goal of the study is to determine the effect of different commercially-available RSC systems on the extent of improvements they offer for increasing roll stability of commercial vehicles with double trailers, when subjected to limit-steering maneuvers that can rise during highway driving. A semitruck and two 28-foot trailers are modified for enduring the forces and moments that can result during testing. A load structure is used for placing the ballast loads within the trailers at a suitable height for duplicating the CG height of the trailers during their commercial use. Outriggers and jackknifing arresting mechanisms are used to prevent vehicle damage and ensure safety during the tests. The test vehicle is equipped with multiple sensors and cameras for the necessary measurements and observations. The analog and video data are time-synced for correlating the measurements with visual observation of the test vehicle dynamics in post-processing.

An extensive number of tests are conducted at the Michelin Laurens Proving Grounds (MLPG) in Laurens, SC. The tests include evaluating each RSC system with different maneuvers and speeds until a rollover occurs or the vehicle is deemed to be unstable. The maneuvers that are used for the tests include: double lane change, sine-with-dwell, J-turn, and ramp steer maneuver. Both a steering robot and subjective driver are used for the tests. The test data are analyzed and the results are used to compare the three RSC systems with each other, and with trailers without RSC. The test results indicate that all three RSC systems are able to improve the speed at which rollover occurs, with a varying degree. For two of the systems, the rollover speed gained, when compared with trailers without RSC, is marginal. For one of the systems, there are more significant speed gains. Since most RSC systems are tuned for a conventional tractor-trailer, additional testing with some of the systems would be necessary to enable the manufacturers to better fine-tune the RSC control scheme to the dynamics of double trailers.

Experimental Evaluation of the Dynamic Performance Benefits of Roll Stability Control Systems on A-train Doubles

Andrew E. Kim

General Audience Abstract

The safety of driven semi-trailer trucks towing two trailers is analyzed in a study created to examine the behavior of the vehicle and its units during high speed, high maneuvering circumstances. The rolling over of a specific test truck is studied to study the ability of a common large vehicle to succeed in evasive or emergency maneuvers. Focus on the rolling over of a truck is placed in this project, as large freight vehicle rollovers are among the most popular and most dangerous type of accidents on highways today. A semi-trailer truck with two trailers, or double trailer vehicle, is instrumented with sensors and cameras to study several different characteristics associated with vehicle operation and conditions that incite rollover. The behavior of a double trailer vehicle is complicated due to the additional rotation joint between the adjacent trailers, where typical semi-trailer trucks (18-wheelers) only incorporate one: between the towing tractor and the towed trailer.

Commercially available electronic appliances called Roll Stability Control (RSC) systems were designed to automatically control and apply the vehicle brakes under rollover conditions, and are installed and used individually to evaluate any improvements on the test vehicle's ability to stay upright. Information regarding RSC system operation can be found.

All vehicle testing is completed at a professional vehicle testing location in Laurens, SC and the same four test maneuvers are used to determine the effectiveness of each of the five RSC systems tested using data collected with the instrumented sensors. Different types of RSC systems exist due to different manners of operation, and are discussed in this document and analyzed. This project develops the conclusion that the five systems used during testing all improve vehicle stability, but provide differing results in doing so, largely due to their different operations. Therefore, commercially available RSC systems are proven to work differently and provide different results. Recommendations for further testing of RSC systems is provided.

Although no recommendations are made regarding the tested RSC systems, the collected data show large, double trailer freight vehicles are more stable when using any of the tested commercially available RSC systems, especially during evasive maneuvering or emergency situations. These findings can bring immediate improvements to large freight vehicle operation and safety.

Acknowledgements

I would like to thank my family, friends, and my coworkers at the Center for Vehicle Systems and Safety at Virginia Tech. Without you, this would have been an impossible task. Specific recognition goes towards my project team: Dr. Andrew Peterson, Dr. Masood Taheri, Dr. Yang Chen, and Dr. Yunbo Hou, who served as team leaders and personal mentors throughout my time here, and were all responsible for large portions of the test vehicle preparation and testing. I would additionally like to thank Dr. Steve Southward and Dr. Doug Nelson for serving on my committee.

I would lastly like to thank Dr. Mehdi Ahmadian for giving me the opportunity to be in this position. Without your constant belief and support, I simply would not be where I am today. Words cannot explain how grateful I am.

Notation

2S1M	Two-Sensor-One-Modulator
2S2M	Two-Sensor-Two-Modulator
ABS	Anti-lock Brake System
AD	A-Double
CVeSS	Center for Vehicle Systems and Safety
DAQ	Data Acquisition System
DLC	Double Lane Change
ESC	Electronic Stability Control
GVWR	Gross Vehicle Weight Rating
LCV	Long Combination Vehicle
MLPG	Michelin Laurens Proving Ground
OE	Original Equipment (Baseline)
OERS	Original Equipment Rollover Speed/Steering
OERS+	One testing configuration past the OERS
RA	Rearward Amplification
RSC/TBRSC	Roll Stability Control (Trailer-Based Roll Stability Control)
RSM	Ramp Steer Maneuver
SRT	Static Rollover Threshold
ST	Tractor Semi-Trailer
SWD	Sine-with-Dwell
System A	2S1M System from Manufacturer A
System A-D	2S1M System from Manufacturer A with automated dolly braking included in RSC system
System B	2S1M System from Manufacturer B
System C	2S1M System from Manufacturer C
System C-2	2S2M System from Manufacturer C

Contents

List of Figures

List of Tables

Chapter 1 Introduction

With the recent surge in production and usage of multi-trailer combination vehicles within the trucking industry for increased logistical efficiency, the large number of accidents involving long combination vehicle rollover has increasingly raised concerns. These large vehicles suffer from intrinsic design faults and resultant lower directional stabilities than passenger vehicles, and A-Doubles are both the most frequently used and least stable among them. Because of the instabilities, namely in the roll direction, of these long combination vehicles, roll stability controls systems, or RSC systems, have lately been implemented across the trucking industry in efforts to aid their roll stabilities.

Roll stability control systems are commercially-available active vehicle safety systems that assist drivers in maintaining stability and control over their vehicle by monitoring rollover conditions and automatically applying brakes when deemed necessary. These control systems check several variables, most notably the lateral acceleration of the vehicle unit on which it is installed to determine impending rollover. Unfortunately, past studies, such as the National Highway Traffic Safety Administration's (NHTSA's) evaluation for their Federal Motor Vehicle Safety Standard (FMVSS) No. 136, have found both tractor- and trailer-based RSC systems to be inferior to Electronic Stability Control (ESC) systems. These evaluations are deemed unfair towards long combination vehicle usage of RSC systems not only due to the fact that these studies only use one of many commercially available RSC systems, but also because they test a tractor semi-trailer rather than a multi-trailer vehicle. This thesis does not provide a comparison of RSC systems to ESC systems on a long combination vehicle, as ESC testing is outside the scope of this project. Rather, this thesis focuses on the benefits of commercially-available RSC systems on LCVs, as well as the measurable performance differences between different RSC systems.

The Center for Vehicle Systems and Safety (CVeSS) at Virginia Tech has put effort towards studying the efficacy of different commercially-available trailer-based RSC systems on a double-trailer vehicle called an A-Double. The A-Double test vehicle, shown in Figure 1-1, is instrumented with mechanical safety structures, mechanical test structures, and a data acquisition system to safely collect vehicle data through extensive track testing, and to capture the operational performances of trailer-based RSC systems.

The RSC systems discussed in this project are all trailer-based, but operate in several different ways. Three separate comparative studies are conducted:

1. Evaluation of three double-sensor-single-modulator (2S1M) systems from different manufacturers

2. Evaluation of one of the three 2S1M systems on the dolly
3. Evaluation of one of the 2S1M systems in a slightly different configuration in which two modulators (one for each side) are used. This configuration is commonly referred to as a double-sensor-double-modulator or 2S2M system.

Figure 1-1. A-Double test vehicle.

1.1 Motivation

The primary motivation for this research is to evaluate the effectiveness and operational benefits of trailer-based RSC systems for long combination vehicles. It is intended to highlight any difference that may exist in the performance of RSC systems available from different U.S.-based manufacturers.

Past studies have extensively examined the effectiveness of Electronic Stability Control (ESC) systems for controlling oversteer and understeer conditions. Comparatively, fewer studies have been done with RSC systems for combination vehicles, in particular for double and triple configurations. This research is intended to close the gap and provide a comprehensive evaluation of RSC systems for 28-ft double trailers in A-train configuration, which is the most common form of LCVs in the U.S.

Of particular interest is the extent to which RSC systems can reduce or control rearward amplification that occurs in multiple trailer arrangements. Rearward amplification (RA) is the increased ratio of lateral accelerations between the leading unit (tractor) and the rear trailer unit, and reducing it is essential for

improving vehicle roll stability. RA is more prevalent in the rear trailer(s) of long combination vehicles (LCVs) than in tractor semi-trailers because of both increased total vehicle length and existence of an additional articulation point between adjacent trailers. The increased demands of the more complex dynamics of trucks with double trailers would perhaps make RSC systems more essential safety equipment when compared with tractor semitrailers.

1.2 Objectives

The primary objectives of this study are to:

1) Evaluate the roll stability benefits of roll stability control systems for commercial trucks with two A-train double trailers (commonly known as "A-Doubles"),
2) Determine any differences among various RSC systems marketed in the U.S.,
3) Establish any safety benefits that may be gained from equipping not only the two trailers but also the dolly with an RSC system,
4) Assess any performance differences between RSC systems with one or two modulators, and
5) Provide general recommendations for future testing of commercial trucks with RSC systems.

1.3 Approach

The above objectives are achieved through track testing an instrumented vehicle at the Michelin Laurens Proving Ground (MPLG) in Laurens, SC. The test vehicle is instrumented with various sensors and with video cameras for measuring both in analog and video forms the dynamics of the tractor and trailers during various maneuvers. A steering robot is used for conducting the selected maneuvers in a repeatable manner. The maneuvers selected for the tests are double lane change, J-hook (or J-turn), and sine-and-dwell. In addition to conducting the maneuvers with a steering robot, a subjective test driver is used to conduct some of the tests, as repeatedly as possible.

The tests are conducted at various speeds and in increasing sequence until rollover occurs. Two outriggers on each trailer are used to "catch" the trailers from rolling on their sides. The outriggers are designed such that they do not significantly alter the dynamics of the trailers. Additionally, they are equipped with load cells to measure the ground contact forces in order to assess the severity of the rollover.

Three different commercially-available systems are tested on both trailers. In one case, the dolly is also equipped with the RSC. In the case of another system, the RSC is tested in both single- and double-modulator configurations. The test results for each system are compared with each other, and with a no-RSC configuration. The comparisons are used to establish a series of recommendations, mainly on the roll

stability improvements achieved by each system. Other aspects of the systems, such as cost effectiveness, ease of installation, operational efficiency, durability, and sustainability, fall outside the scope of this study and are not considered.

1.4 Contribution

This study provides a comprehensive evaluation of RSC systems for long combination vehicles, in particular for A-Doubles. The study sheds light on how different systems perform under different dynamic conditions. The test evaluations also provide an excellent roadmap for future test studies that may involve other vehicle configurations, such as trucks with triple trailers.

1.5 Thesis Organization

This document consists of six chapters. Chapter 1 provides an introduction. Chapter 2 includes background information regarding roll stability in commercial vehicles, long combination vehicle classifications, and general RSC information, including how these systems work. Chapter 3 discusses the differences in brake characteristics of a tractor semi-trailer and A-Double that can lead to theoretical differences in RSC efficacy between the two vehicle configurations. Chapter 4 details the preparation of the A-Double test vehicle, including the installation of the outriggers and data acquisition. It also includes other aspects of the tests, such as the details on the maneuvers, test procedures, etc. Chapter 5 provides a comprehensive analysis of the data collected during track testing. Chapter 6 summarizes the findings of the study and provides recommendations for any additional future testing on other vehicle configurations.

Chapter 2 Background Information

The purpose of this chapter is to provide background information on what rollover is and what factors influence a vehicle's roll stability. It will also include a discussion on different long combination vehicles (LCVs) and how various coupling hitches influence their roll stability. The chapter ends with an overview of RSC systems, a description of general operation, and a review of some of the past studies for roll stability of articulated vehicles.

2.1 Introduction to Rollover

Heavy vehicles (defined as trucks with a gross vehicle weight rating (GVWR) greater than 10,000 pounds) continue to be the leader in freight transport methods in North America. The data shows an increasing trend to their usage, with the number of registered heavy trucks increasing steadily from 2011 to 2015 [1]. In step with this, the revenue of specialized long-distance freight trucking has increased steadily from 2008 to 2015 [2]. Naturally, with an increase in the number of heavy vehicles on the roads comes an increase in accidents involving them.

Due to their integral role in U.S. commerce, heavy vehicle accidents not only affect those directly involved, but also the businesses and companies that rely on the trucking industry for transporting commercial and consumer goods. Therefore, the safe operation of heavy vehicles is of utmost importance. Among all the dangers intrinsic to operating large mechanical vehicles, rollover incidents are of special concern and consideration due to a high center of gravity. Not only are rollover incidents one of the largest causes of severe injury and fatalities on the road (especially highways) for passenger cars, they are even more so for heavy commercial trucks. The lower directional stability exhibited by larger freight vehicles will always pose serious safety risks. This section will illustrate just how dangerous rollovers are, as well as how rollover and roll stability are defined.

2.1.1 Statistics

According to a study conducted by the Federal Motor Carrier Safety Administration (FMCSA), there were approximately 415,000 police-reported crashes involving heavy trucks in 2015. Of those, 83,000 (20%) resulted in injury and 3,598 (0.08%) resulted in death [3]. Both of these statistics saw increases from the 2014 numbers: 82,000 injuries, and 3,429 families, resulting in 12% and 5% increases, respectively. Of these 3,598 fatal crashes, 166 were caused by rollover as the first event, with countless others not necessarily directly caused by rollover, but were associated with and included large trucks overturning [3]. Only 2.1% of the 9.1 million passenger car accidents in 2010 involved rollovers, but rollovers still

accounted for almost 35% of all fatalities from passenger vehicle crashes that year [4]. Although rollover incidents and accidents are not as numerous as those caused by other reasons such as collision, they have higher injury and fatality rates than other types of crashes. In fact, it was concluded by Green in 2002 that rollover accidents are the deadliest kinds of accidents, particularly on ramps and inclines off highways [5].

There are two types of rollover: untripped and tripped. Most rollover accidents are of the latter type, in which an external object on the road serves as a tripping or collision mechanism. Up to 95% of single-vehicle rollovers are tripped [6]. However, it was found by Dilich and Goebelecker in 1997 that the great majority of rollovers were due to driver error, which includes misjudging road curves, speeding, drifting off roads, and being physically or emotionally impaired [7]. In fact, the Large Truck Crash Causation Study (LTCCS) conducted by the National Highway Traffic Safety Administration (NHTSA) and the Federal Motor Carrier Safety Administration (FMCSA) discovered that 45% of the 239 rollover crashes between 2001 and 2003 were due to speeding. These reasons correlate highly with tripped rollovers, and many can be avoided with higher-level driver responsibilities, attentiveness, and experience. On the other hand, untripped rollovers usually occur during high-speed avoidance maneuvers (and can be thought of as maneuver-induced rollovers), and are more inevitable and therefore more dangerous. Because of this, this study uses testing maneuvers to produce untripped rollovers.

2.1.2 Rollover

Most large vehicle accidents are caused by directional instability, and largely fall into three categories: (1) roll instability or rotation about the longitudinal axis, (2) yaw instability or rotation about the vertical axis, and (3) trailer yaw oscillation or rotation about the lateral axis. When the lateral forces on the vehicle surpass the stabilizing moment provided by the vehicle's wheels and track (most likely during a cornering maneuver), the vehicle will fall under the first category and roll. This lateral force causes the body's center of gravity to laterally extend past the wheels, thus causing the vehicle body to overturn.

While both light and heavy vehicles exhibit directional instability in all three rotation modes, heavy vehicles are more prone to rollover than lighter, smaller vehicles mainly due to a high center of gravity. The design of larger vehicles is why the performance limit of heavy vehicles is characterized by a loss of roll stability, instead of the typical loss of yaw stability used for lighter vehicles. Therefore, consideration of roll dynamics was chosen to be the focus of this study.

Rollover occurs when a vehicle loses directional control about its longitudinal axis, but rotation about the vertical axis, or yaw, plays a large part in the dynamics of a rollover as well. When cornering is initiated, a slip angle and thus a lateral force are generated from the steering input and the front wheels turning. A

resulting rear wheel slip angle and lateral force follows, and the vehicle starts rotating along its vertical axis. This yaw response occurs from the steady-state turning. As the trailer begins its yaw response, the attached trailers follow in similar fashion. The semi-trailer's (rear) tires develop lateral force and their own yaw response forms. When any of the lateral forces at the units' tires produced by yaw responses exceeds the respective friction limit with the ground, the tire loses control and causes the vehicle to either oversteer or understeer. In LCVs, this loss of tire-to-ground traction can also cause trailers to swing in or out of the intended path, and in worst-case scenarios, can cause jackknifing and rollover. When the generated lateral forces result in lateral accelerations that exceed the vehicle's SRT, rollover occurs. Because of the interplay of yaw and roll, both must be considered when evaluating LCV ride stability and safety. It is important to note that yaw dynamics complicate, but can also stabilize, roll behavior for articulated vehicles [8]. This is further discussed in Chapter 3.

2.1.3 Roll Stability

The roll stability, or the propensity for a vehicle to stay upright during cornering, can be quantified in a number of ways, but this paper will consistently use a maximum lateral acceleration threshold. This lateral acceleration threshold is a basic method of quantifying roll stability, and is referred to as a static rollover threshold, or an SRT. SRT values can range from a lower limit of around 0.2 g's for individual cases of heavy trucks, to an upper limit of over 1.4 g's for shorter passenger cars [8]. Roll stability limits for heavy freight vehicles are much lower than passenger vehicles because of their low track width to center of gravity (cg) height ratio [5]. For loaded heavy trucks, the rollover threshold is below 0.5 g's of lateral acceleration, compared to that of passenger cars which are always greater than 1.0 g. The lateral acceleration rollover limits for most heavy vehicles have been reported to be around 0.3 to 0.6 g's [6].

This wide range is largely due to the fact that SRTs depend on several factors, the most important of which are vehicle type, vehicle weight, weight distribution, vehicle roll stiffness and other suspension properties, cornering maneuver, and tire and road conditions. Figure 2-1 and Equation 2-1 provide a model for the relationship between several variables to a vehicle's basic roll characteristics. This steady-state roll stability has been linked to the probability of rollover in an accident by Winkler et al. [9].

Figure 2-1 shows a tractor semi-trailer from behind in the *yz*-plane in a simplified free-body diagram during cornering. This simplified model treats the vehicle, the tires, and the suspensions as a lumped-element, and tackles lateral roll only. Using Conservation of Momentum, an equation for roll moment can be derived from the forces on a vehicle during a steady-state turn:

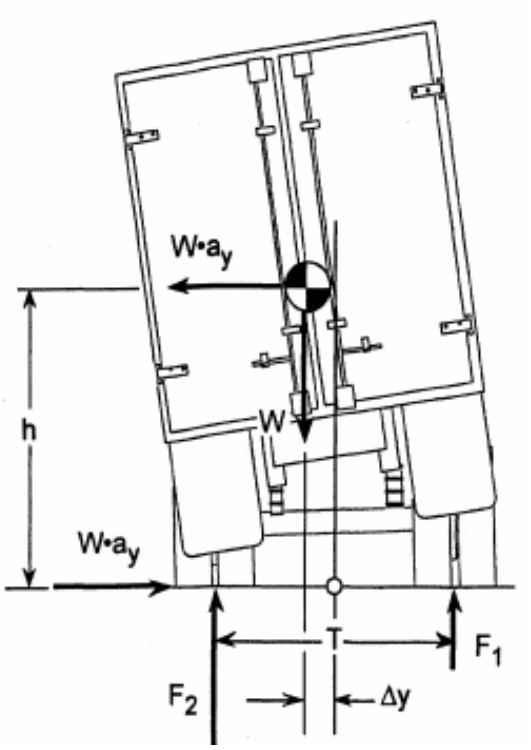

Figure 2-1. Simplified rigid roll plane model of tractor semi-trailer [8].

$$W * h * a_y = (F_2 - F_1) * \frac{T}{2} - W * \Delta y \tag{2-1}$$

where W is weight, h is the cg height, a_y is lateral acceleration, F_i is the vertical tire load, T is the track width, and Δy is the cg lateral motion due to body roll. Equation 2-1 is also known as the roll equilibrium equation for a rigid body, and lumps the vehicle into a single roll plane while assuming the vehicle will roll about its roll center indicated by a white circle on Figure 2-1. Figure 2-1 shows the major factors involved in rollover events: speed, weight, centrifugal force, track width, and center of gravity height. Speed directly affects the lateral accelerations experienced when the vehicle corners or changes direction. The ratio of cg height, h, and track width, T, is an important factor that determines at what lateral accelerations a vehicle tips over. The weight of a vehicle, W, affects rollover in multiple ways: (1) distribution can change cg locations along all axes, and (2) the heavier a vehicle is, the more prone it is to rollover [10]. Thus, rollover is more likely to occur when the vehicle has fully-loaded trailers. Tractor semi-trailers are typically loaded to its maximum GVWR of 80,000 lbs. One type of LCV called an A-Double is usually loaded to their maximum volume rather than weight rating, so is typically significantly lighter but has higher cg's than that of tractor semi-trailers. These differences are the main causes for different roll stabilities between the two vehicle types.

Figure 2-1 and Equation 2-1, however, only apply to single trailer vehicles, as roll dynamics become more complicated as additional units are incorporated. Rollovers for multi-trailer vehicles are a more significant problem than for single trailer vehicles, and the different types of these vehicles will be introduced in the following chapter.

2.2 Combination Vehicles

2.2.1 History

Commercial needs have called for a wide range of designs for both trucks and trailers. Since the two largest costs in the trucking industry are fuel and labor, the desire for larger trailers to move more payload per trip and driver grew quickly. As more emphasis was placed on cost effectiveness, trucks became bigger and longer, which was not very practical for road use. As trucks eventually started towing 53' semi-trailers to meet the demand of commercial shipping, they began reaching maneuverability limits due to a combination of their rigidity and length. By constructing vehicles that instead towed trailers with shorter wheelbases and an extra articulation point between them, very long and maneuverable vehicles that met commercial shipping needs were created. These long combination vehicles (LCVs), or multi-trailer vehicles, such as double and triple trailer trucks quickly, became popular with the help of some recent dramatic aerodynamics and tire rolling resistance improvements.

Although larger single trailer vehicles would allow the larger towing yields, dividing a truck's payload into smaller and separable units has a couple of advantages. Firstly, LCVs allow the ability to pick up and drop off entire trailers, further improving logistics for many businesses. Secondly, an extra articulation point along the vehicle body allows for better maneuverability, especially during low-speed cornering, as a normal 53' tractor semi-trailer combination tends to off-track inward of a turn, as shown in Figure 2-2.

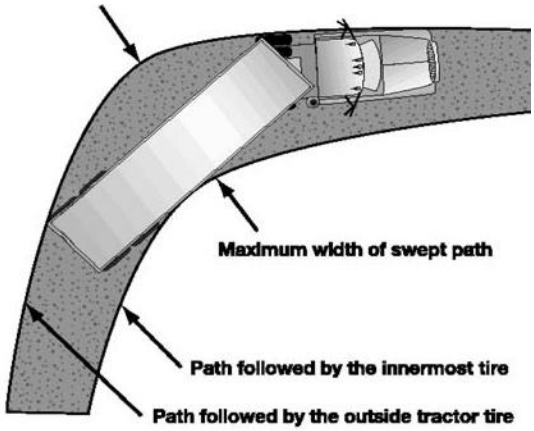

Figure 2-2. Off-tracking of a tractor semi-trailer vehicle in a 90-degree turn [11]**.**

Large vehicles can lose directional stability quite easily, and many of these incidents occur from quick maneuvers, such as avoiding obstacles around a curve or a tractor slipping through turns. When a tractor and its trailer loses directional stability or control during a curve or turn like the one shown in Figure 2-2, either understeering or oversteering events may occur. Understeering is described as a loss of directional control in a vehicle in which the front or steering wheels' traction to the road is exceeded by the lateral forces exhibited by the vehicle. This causes the front wheels to slide instead of roll, thereby not turning the vehicle enough to follow the road path. Oversteering is the same dynamic but with the rear wheels instead of the front. As a result, the rear of the vehicle will swing out of the turn or curve, and the vehicle will turn too much compared to what was intended. This can be accompanied by spinning of the vehicle.

Oversteering is considered the more dangerous of the two, because while both events result in a loss of control over the vehicle, oversteering is a yaw-unstable event compared to the yaw-stable event that is understeering. Understeering sees no increase in vehicle rotation in accordance to increased steering wheel angles, while oversteering does.

When combination vehicles oversteer, a frightening phenomenon called jackknifing can follow. If a tractor is oversteering and the semi-trailer is understeering, jackknifing occurs at a certain critical speed [12]. Due to a spin from a loss of traction at its rear, the tractor will spin towards its towed unit. The towed unit continues forward due to its mass and momentum, further worsening the tractor spinning and hitting the trailer, resulting in a combination vehicle looking like the one shown in the bottom image of Figure 2-3. Unfortunately, one of the downsides of extra articulation points in LCVs is a higher risk of jackknifing. If a truck jackknifes, there is high probability that a rollover will follow. Therefore, jackknifing is another vehicle dynamic that must be avoided in efforts to increase ride and roll stabilities.

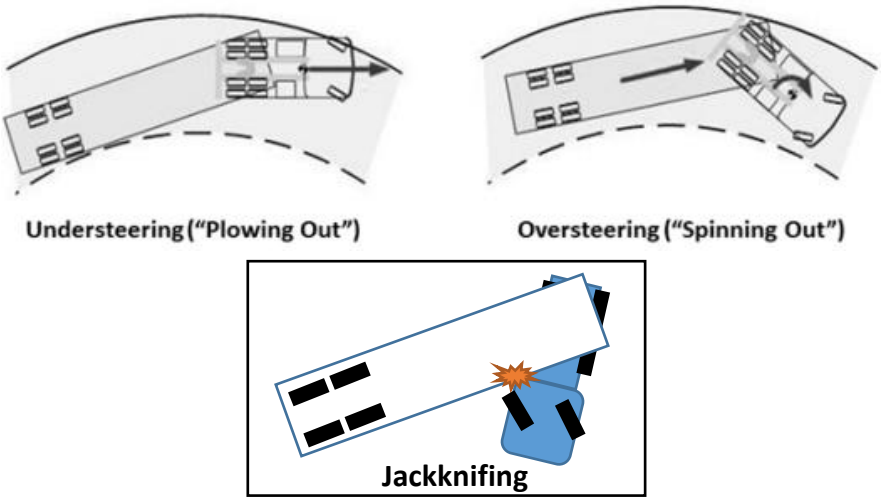

Figure 2-3. Understeer, oversteer, and jackknife [13].

2.2.2 Combination Vehicle Classifications

While there are many different types of heavy vehicles, those mentioned in this study only pertain to Classes 8, 9, 11, 12, and 13 from the Federal Highway Administration's classifications. These classes are divided by axle and towed unit type, as seen in Figure 2-4. These vehicles will be referred to as combination or articulated vehicles, as they use a towing mechanism (a tractor) and at least one towed unit (trailer). Depending on the number of towed units and the hitches used, combination vehicles can be categorized into seven generic categories that span these five classes. These categories are shown in Table 2-1, and the most common vehicle configurations, the conventional tractor and 52' semi-trailer combination (the WB64 semi-trailer) and the conventional A-Double with 28' semi-trailers (the western A-Double), are highlighted in blue. Table 2-1 also contains the features of the families, such as what the combination vehicle is comprised of and what hitches are used to attach the units.

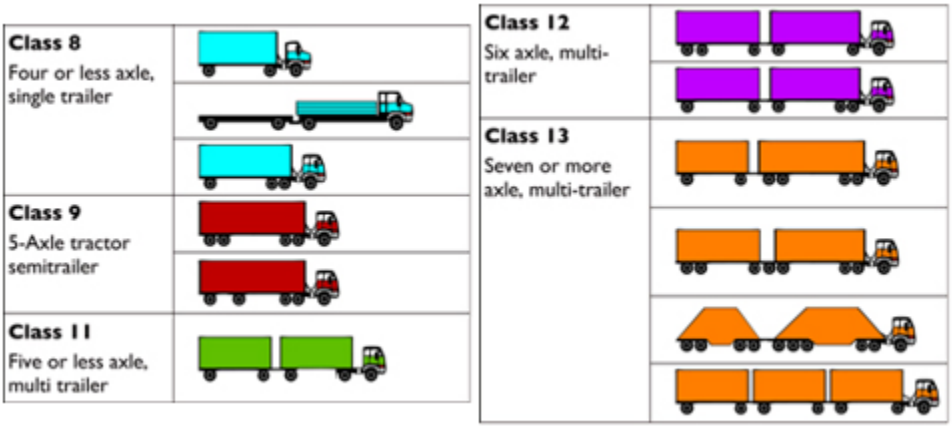

Figure 2-4. FHWA Vehicle Type Classifications [14].

Table 2-1. Combination vehicle classifications and properties.

Combination	Hitches	# of Towed Semi-trailers	Illustration
3-axle Straight Truck	N/A	N/A	
5-axle Tractor Semi-Trailers	Fifth wheel	1	
A-train Doubles	Fifth wheels, A-Dolly	2	
B-Train Doubles	Fifth wheels	2	
C-Train Doubles	Fifth wheels, B-dolly	2	
A-Train Triples	Fifth wheels, A-Dollies	3	
C-Train Triples	Fifth wheels, C-dollies	3	

The hitches listed in Table 2-1 are designed to allow rotational freedom so that connected units are not rigid. The constraints and freedoms provided by these hitches complicate the vehicle's roll dynamics, and also result in the A-train doubles being the least stable vehicle of the group. Details regarding the hitches of an A-Double are provided in the following Subsection 2.2.3. The combination of the A-Double being both the most common and least stable LCV in the U.S. is the motivation behind this project's testing of RSC efficacy with an A-Double.

2.2.3 Combination Vehicle Hitches

The most common of all commercial heavy vehicles is the widely used 53' tractor semi-trailer, or the WD-64 conventional tractor semi-trailer. This vehicle is a simple combination of a tractor and semi-trailer, as shown in Table 2-1. This unit uses a single semi-trailer connected to a tractor via fifth wheel, which permits relative yaw and pitch motions between the two units, but not roll. This is due to the design of the fifth wheel hitch and semi-trailer kingpin, shown in Figure 2-5. Fancher's yaw-roll simulation study in 1987 concluded that fifth wheel hitches couple the roll dynamics of the two connected units very strongly [15].

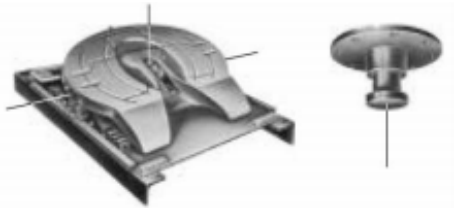

Figure 2-5. Fifth wheel hitch (left) and kingpin (right) [16].

There are several types of LCVs differentiated by the number of towed trailers and the type of coupling used between the trailers. A converter dolly is an inter-trailer coupling unit that "converts" a semi-trailer to a full trailer, and is usually used between adjacent trailers in LCVs. By connecting subsequent trailers with converter dollies, long combination vehicles can be built up. Dollies hold both a coupling point to the back of a vehicle, as well as a fifth wheel hitch to mount semitrailers. As will be discussed in this section, due to the use of converter dollies in filling the greater number of articulation points in LCVs, the stability of long combination vehicles is reduced, especially in quick steering maneuvers, such as evasive actions.

The key difference between the three dollies is how they are coupled to the back of the lead trailer. B-dollies are extensions of the rear axle of the lead trailer, while A- and C-dollies incorporate pintle hitch couplings, as shown in Figure 2-6. This design difference yields great changes in directional stabilities, as pintle hitch couplings decouple the roll motions of the connected units [15].

The two most commonly used dollies in North America are the A- and C- dollies. A-Dollies are most frequently used by common freight carriers due to logistical efficiency: A-Dollies are easier and quicker to connect and disconnect then are C-dollies, and cost less to maintain mostly due to larger tire wear from the latter [17]. The ease of use found in A-Dollies is due to the implementation of a single drawbar, or a single coupling, to connect or disconnect a towing vehicle to a towed unit. C-dollies, on the other hand, use a double coupling system. This is illustrated in Figure 2-6. Double and triple trailer configurations that integrate A-Dollies are called A-Doubles and A-triples, and the same naming convention applies for those that use C-dollies.

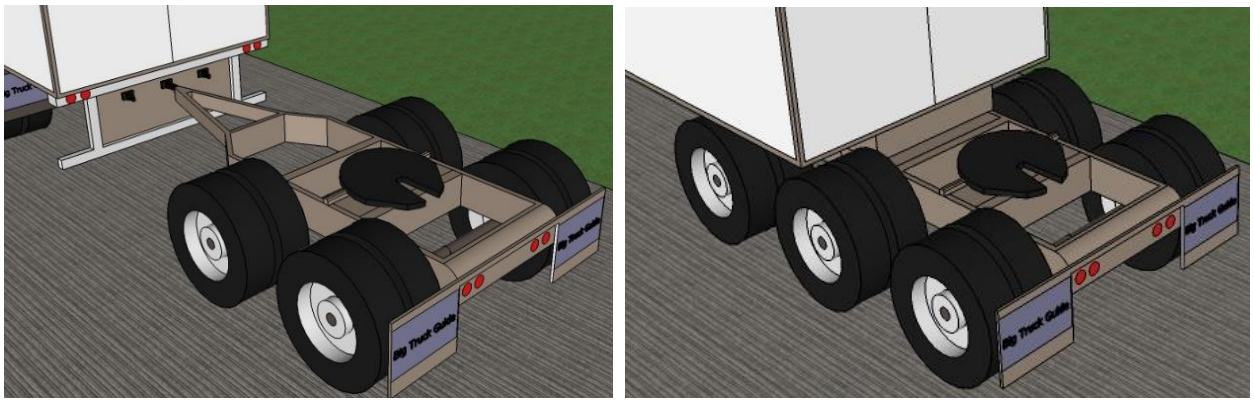

Figure 2-6. A-Train (left) and B-Train (right) secondary trailer mount comparison [18].

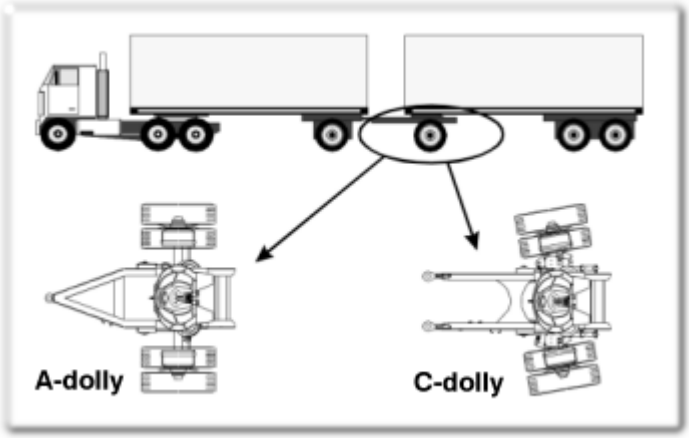

Figure 2-7. The two most commonly used dollies [17].

A-Dollies suffer tremendously from the use of pintle hitches, as problems mainly arise from its implementation of a single drawbar, shown in both Figures 2-6 and 2-7. A single pintle connection allows rotation about all directions with respect to the towing unit, and is why many consider A-Dollies to be weak roll-coupling mechanisms [19]. C-dollies, however, incorporate a second pintle hitch to eliminate yaw between the dolly and the preceding semi-trailer. A phenomenon called rearward amplification (RA) occurs most severely in A-trains due to the failure of A-Dollies to do the same, and worsens the roll stability of A-trains since yaw and roll dynamics are coupled.

2.2.4 Rearward Amplification

A main contribution to rollover events for large combination vehicles such as doubles and triples is the previously introduced phenomenon of “rearward amplification.” Rearward amplification, or RA, refers to the increase of ratio of the lateral accelerations of the towed trailers to that of the tractor. Figure 2-8 shows the results of a study of a double tanker following a simple lane change maneuver. The last trailer of the double exhibited the most rearward amplification, and trailers closer to the tractor exhibited less.

This principle of rearward amplification holds true for triples as well. This phenomenon is the biggest reason for the significantly different dynamics between LCVs and other heavy vehicles, such as tractor semi-trailer vehicles.

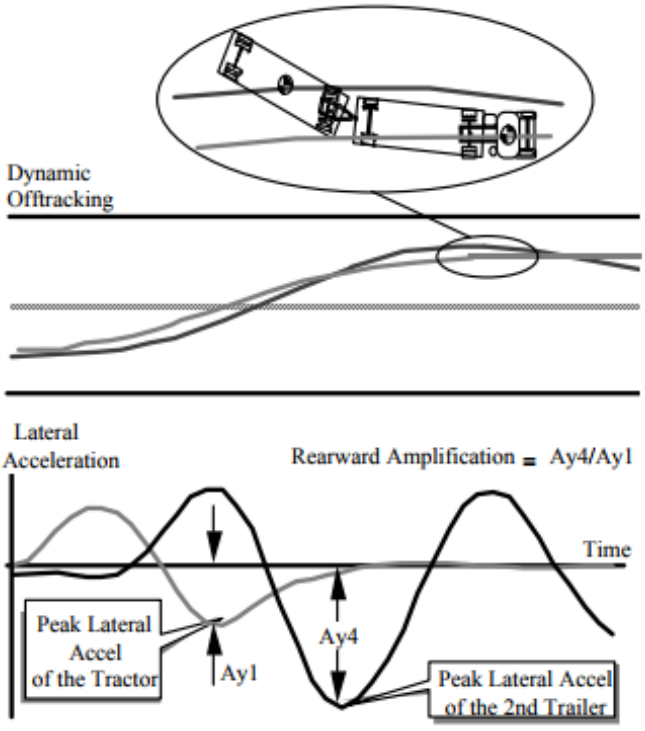

Figure 2-8. Rearward amplification in an A-Double [20].

Another crucial aspect of rearward amplification is the lag that following trailers experience during dynamic movements. A driver and tractor can be fully completed with a turn or lane change by the time the rest of the vehicle completes the maneuver. Figure 2-9 displays the rearward amplification in a two-second lane change maneuver by a double. As shown in the plot, both lateral acceleration and the roll angle of the trailers increase from and lag behind those of the tractor [8]. At around 3 *s*, the tractor recovers from its maneuver while the second trailer is experiencing its maximum lateral acceleration. This lag becomes even more dangerous when the driver is inexperienced, as the tractor has a tendency to isolate the driver from the rest of the vehicle. Without understanding rearward amplification and its lag, a driver may continue in high frequency steering without knowing that the rear trailer is experiencing dangerous levels of lateral acceleration. In addition, the lag is also applied when the vehicle is braked, so preventive action must be taken very quickly to stop potential rollover.

Rearward amplification is highly undesired because of its effects on even the simplest and slowest of LCV maneuvers, as amplified low-level lateral accelerations can cause units to roll over. The combination of

trailer lag, the increase of lateral acceleration due to rearward amplification, and cab isolation from rear trailer behavior, helps to explain why heavy combination vehicle rollover can happen quite easily. Rearward amplification also increases the probability of vehicle off-tracking and jackknifing, both of which are highly undesired outcomes during vehicle operation, but are outside of this study's scope.

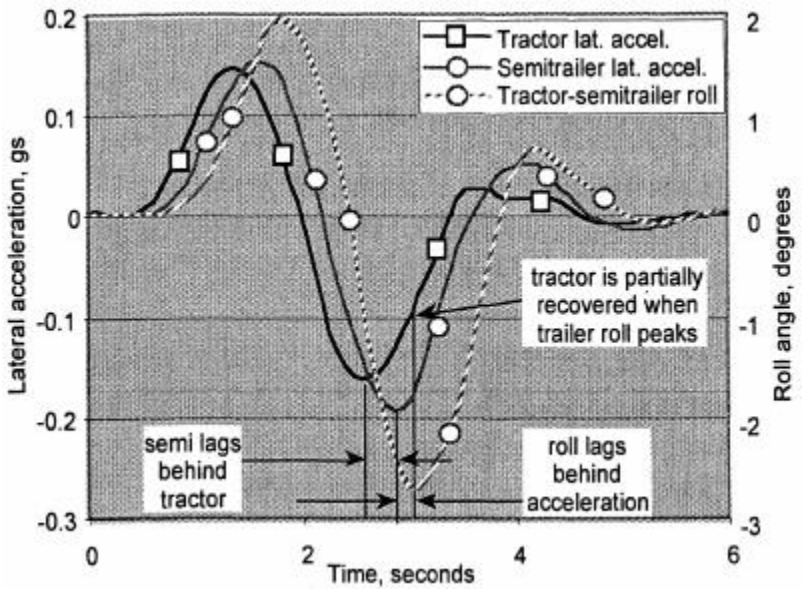

Figure 2-9. Trailer lag in an A-Double indicated by lateral accelerations over time [8].

Figure 2-9 displays this phenomenon for a doubles configuration vehicle, but the lateral acceleration results for both a tractor semi-trailer and double during an obstacle-avoidance maneuver can be interpreted. Many have compared articulated vehicles to a whip, where the longer the vehicle and whip are, the faster the end moves. The rearward amplification of a 5-axle tractor semi-trailer of a 27' semi-trailer is about 1, while that of a conventional 27' double is around 2.0 [21]. The natural increase in lateral acceleration found in "cracking the whip" has caused doubles to be considered quite discernably the less stable of the two vehicle types.

Among the doubles, ADs are notoriously known for their roll instabilities as they exhibit worse (higher) rearward amplifications than B-dollies and C-dollies [20, 21]. Many studies have proven C-dollies to be more effective and safer for high-speed heavy vehicle usage. A widely-cited study by Winkler and the University of Michigan Transportation Research Institute displayed this best by their testing of light commercial vehicles (LCVs). Winkler's results showed a reduction in rearward amplification in LCVs that used C-dollies, and a driver proclivity towards C-dollies as well [17]. Figure 2-10 shows the lateral acceleration plots for loaded triples using A-Dollies and C-dollies, which indicate that C-dollies tend to

reduce the increase of lateral accelerations for towed units due to rearward amplification [17]. A-Dollies, however, show the opposite trend. Figure 2-10 further illustrates that A-trains are significantly less stable than other types of LCVs, even though they are the most commonly used, and thus have the largest room and need for improvement.

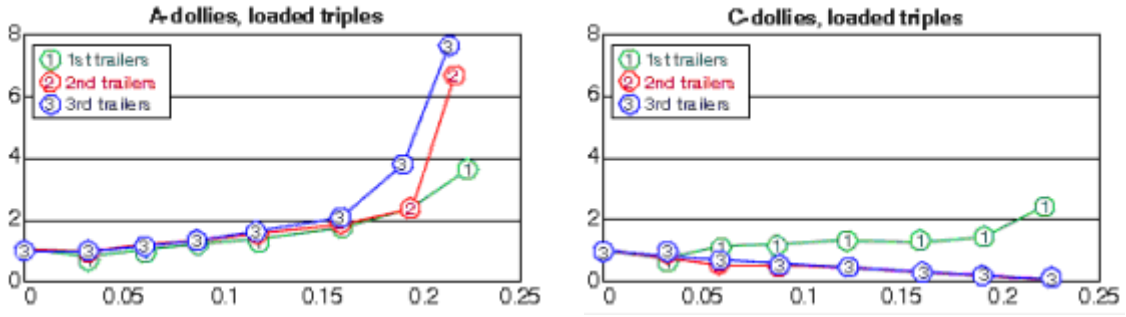

Figure 2-10. Rearward amplification on A-Dollies (left) and C-dollies (right) [17].

Vehicles that use A-Dollies exhibit the worst rearward amplification trailer lag mentioned before as well. Many have found that pitch arrangements that provide roll coupling allow lateral accelerations of following units that are actually combatted by the out-of-phase roll of the preceding units [22, 23], and stabilized. A-Dollies fail to take advantage of this stabilizing opportunity. Because this lag and rearward amplification are highly related to the maneuver and its steering frequency, several testing maneuvers must be used to fully analyze their effects on A-Doubles. The reasoning behind selected maneuvers will be discussed in Chapter 4.

As usage of combination vehicles (mainly A-Doubles) increases throughout the US, the emergence of trailer-based RSC systems as a primary system used for inhibiting vehicle roll during cornering has become more prominent. The focus of most of these RSC systems is to reduce RA, and as will be discussed in Section 2.3, RSC systems largely operate through the monitoring of lateral accelerations.

2.3 Roll Stability Control (RSC) Systems

This section will cover a brief history and general description of RSC systems. A complete RSC system includes many algorithm modules, state estimation calculations, and vehicle dynamics analyses [24]. This information is highly proprietary to RSC system manufacturers and trailer manufacturers, so this section will only detail very basic information regarding RSC systems and their operation.

2.3.1 Introduction to RSC

There are two active stability control systems for heavy vehicles available in the market today: (1) electronic stability control (ESC) systems, and (2) roll stability control (RSC) systems. While both ESC and

RSC systems were developed to assist roll instability in primarily untripped rollover events, ESC systems also additionally tackle yaw instabilities. Another key difference between the two is the area of application for the two systems, as ESC systems are only for tractors and buses, while RSC systems can be installed on tractors, buses, and semi-trailers. Therefore, hereafter, the term RSC will mean the tractor-based RSC systems, while the trailer-based RSC systems will be referred to as just that.

Active roll control for road vehicles itself is quite new, as the earliest documented case was MIT's motorcycle-based machine in 1968 [25]. This prototype used a feedback system of measured body roll angle and applied realignment moment between the body and the rear axle. With the improvement of sensor capabilities and latency, more sophisticated roll control methods came about. The idea of modern roll stability control systems has been documented by several companies and authors, with one of the more popular designs belonging to Ford Motor Company via US Patent 6,263,261 [26]. Extensive research has already been completed on the benefit of ESC on the ride stability of tractor semi-trailers, and in 2012, NHTSA established Federal Motor Vehicle Safety Standard (FMVSS) No. 136 that required ESC (which included RSC system features) on truck tractors with a gross vehicle weight rating (GVWR) greater than 26,000 pounds. ESC systems in truck tractors were designed to mitigate vehicle rollovers after NHTSA saw its FMVSS No. 126 successfully lower untripped rollover incidents for light vehicles. The implementation of ESC had significantly reduced the number of fatal crashes by 36% for passenger cars and 70% for light trucks and vans from 1997-2003 [27]. Such success led to Ford and Volvo adding RSC to their rendition of ESC (AdvanceTrac) as they looked to mitigate rollover in larger vehicles [24]. Currently, there are no government regulations regarding the use of trailer-based RSC systems.

Another large reason for RSC popularity other than their operational effectiveness is their economical utility. Diminishing the number of rollover crashes is clearly beneficial to all, but when the average cost of injury and fatal rollover accidents are $462,000 and $1,143,000, respectively, for large combination trucks [28], the biggest winner is the trucking industry. Analysis of the costs of RSC systems that have been incurred by the trucking industry by the Federal Motor Carrier Safety Administration (FMCSA) concluded that companies see positive returns on 5-year investments as company image and vehicle maintenance both benefit from less rollover incidents [28]. More specifically, costs which the use of RSC systems help avoid include:

- Labor costs (less overall training needed, less driver turnover)
- Driver injury compensation (settlements)
- Damage costs (vehicle and cargo, delivery delays, towing, company image)

- Environmental costs (clean-up)
- Legal costs (property damage, court costs, legal fees)

2.3.2 RSC and Trailer-Based RSC Operation

Like ESC systems, RSC systems rely on several sensors – most notably roll rate sensors, wheel speed sensors, and accelerometers – to identify roll instability. RSC modules communicate with these sensors with CAN communication as they take a combination of lateral acceleration, roll rate, and wheel speed readings to determine the severity and rate at which the vehicle is tilting [24]. Critical thresholds for several variables, such as roll angle, roll rate, wheel speed, wheel lift angle, or lateral acceleration, are set at vehicle startup based on air suspension spring pressures and estimated trailer payloads.

When the system predicts impending roll based on the roll information relative to the critical thresholds, brake pressures are applied at each axle (and the engine retarder for only tractor-based RSC systems) to both safely slow and therefore stabilize the vehicle. By regulating the amount of braking at each tire of the vehicle, directional stability can be maintained. For example, to control roll, braking at the outside wheels is generally applied during cornering. This reduces lateral forces, keeping the inside wheels on the ground and reducing the likelihood of rollover. Another result of controlled braking is the deliberate leaning of the vehicle into corners inward of the vehicle centerline to create a stabilizing roll moment.

Braking capabilities of RSC systems depend on the hardware of the system. Although the controllers and black boxes of systems are highly proprietary and secret operational information, hardware differences between RSC systems are very clear and open to the public. Some RSC systems, for example, can include converter dolly brakes in RSC brake operation. Some systems can incorporate connectivity between the RSC operations at multiple trailers, applying RSC at neighboring trailers after one is activated. One last example are systems that divide axle brake efforts to provide individual wheel braking capabilities. This is done by using multiple brake control modulators to control brake efforts at each side of every axle. Systems that group brake efforts across an axle usually use one modulator and a wheel speed sensor at each wheel, and either wheel can call for system activation. These systems are called 2S1M systems, for two sensors and one modulator. Similarly, 2S2M systems use a wheel speed sensor and a modulator for each wheel on an axle. Figure 2-11 illustrates the two types of systems.

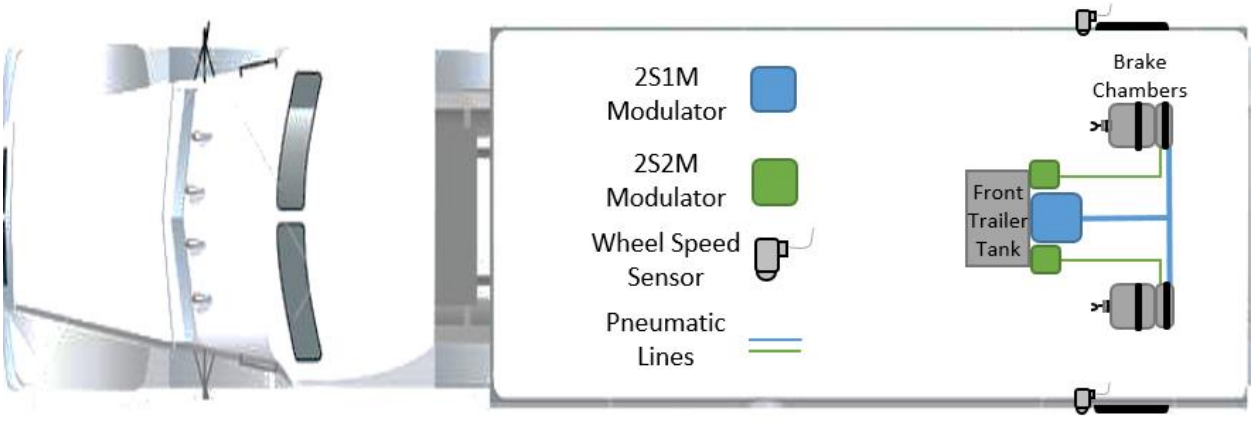

Figure 2-11. 2S1M and 2S2M RSC systems illustration.

An example of an RSC system black box is shown through US Patent 6,263,261 B1 schematic shown in Figure 2-12, indicating the variables from which this specific RSC system gathers information. As always, the algorithms and specifics within the controller are highly proprietary. Figure 2-12 also shows the distribution of braking forces to all tires as four blocks labeled FR, FL, RL, and RR are linked to the brake control block, indicating that this system is a one-modulator system.

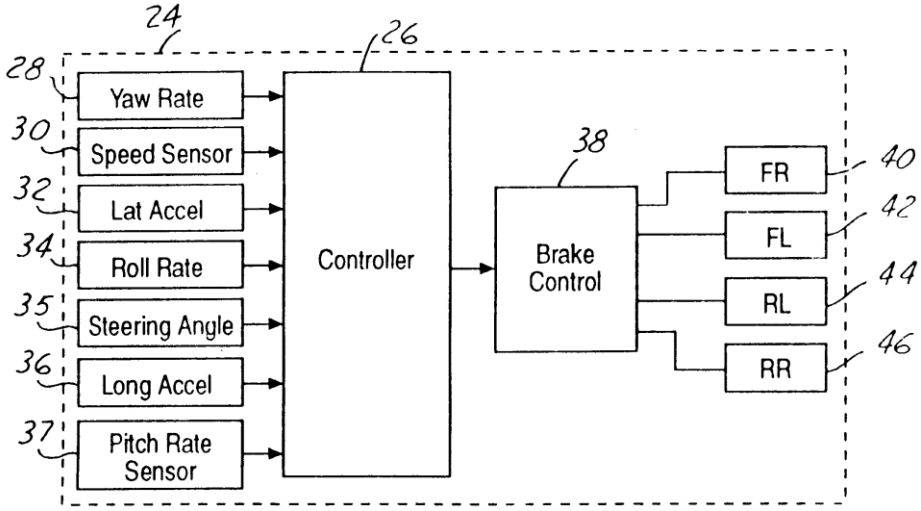

Figure 2-12. Example RSC system schematic showing basic monitoring and operation [26].

RSC manufacturers have their own patented methods of tuning the controller in charge of selecting thresholds and used sensors. For informative purposes, the Roll Stability Control system developed at Ford Motor Company in 2003 will be discussed as an example. Again, controller algorithm modules such as wheel lift detection and brake hydraulics enhancement are highly proprietary, and will not be included. However, a quick summary of the vehicle roll dynamics estimation will be discussed.

Ford's algorithm of identifying roll used several roll plane (a vehicle's *yz*-plane) coordinate systems. The first is used to find the road's angle (for banks); the second is used to determine the relative wheel lift angle; and the third is used for the body angle compared to the vehicle's suspension (for the body frame). This method would always use a relative body roll angle rather than assuming that the road is always flat. Along with these coordinate systems, the RSC system uses a cluster of sensors that includes a roll rate sensors, a yaw rate sensor, a lateral accelerometer, and a longitudinal accelerometer. Imminent body roll and wheel departure estimations were made from the RSC sensor cluster and these coordinate systems, along with significant arithmetic. As is the case for all safety systems in vehicles, maximum latency between system operation and accident occurrence is of utmost priority. Therefore, control strategies are used along with these calculations to supply applied brake pressures to overcome optimal vehicle body roll countering, as well as to overcome brake hydraulics delays that the vehicle may experience.

RSC systems today have refined the calculations, control strategies, and required hardware to deliver the quickest braking response possible. According to NHTSA, RSC systems now only require an electro-pneumatic brake application valve, one lateral accelerometer, and an ECU, making retrofitting quite simple compared to ESC retrofitting. RSC systems, however, continue to measure the same variables as did Ford: wheel speed, wheel lift, lateral acceleration, and suspension pressure. Wheel lift is the first indication of occurring rollover, so wheel departure detection is one of the most significant features of any RSC system. Relative body roll angle, or the angle of the vehicle body to the road surface, remains the most important variable in directly measuring the potential of rollover for a maneuver. Many of the current RSC system manufacturers use lateral acceleration as the key measured variable to do so. As mentioned earlier, starting thresholds for the measured variables are calculated as well, as RSC systems improve performance as vehicle parameters are updated and the system is tuned accordingly. The flowchart in Figure 2-13 explains a general logic usage of RSC system controllers today. An important advantage of current RSC systems is the capability of tuning the controllers for modified performance, such as changing the lateral acceleration threshold for more or less intrusive brake applications. Finding the fine line for lateral acceleration threshold is difficult, and tuning parameters are kept highly secret by manufacturers and are outside the scope of this project.

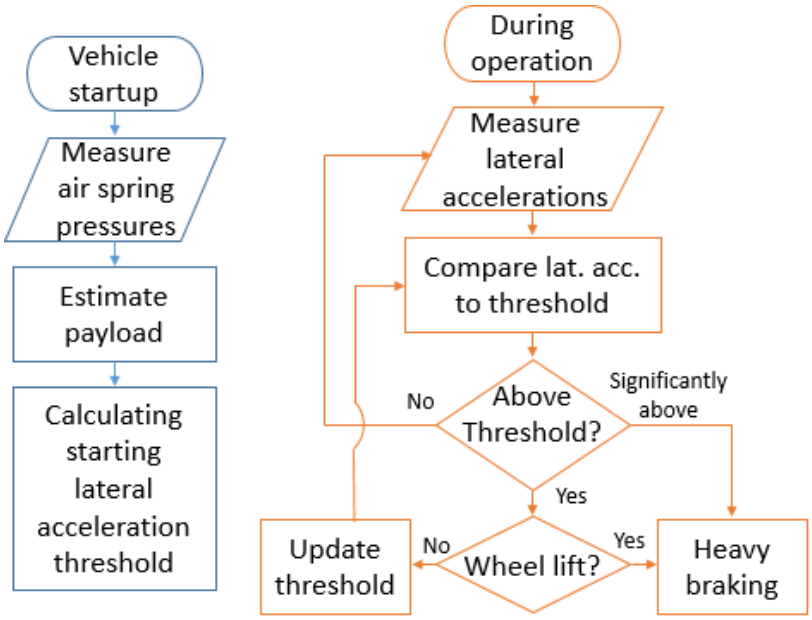

Figure 2-13. General operation flowchart for current trailer-based RSC systems.

2.3.3 Relationship with ABS

It is important to note that RSC systems do not improve or add braking functionality to a vehicle. Instead, RSC systems simply make decisions on when to apply brakes, and therefore RSC system performances are directly related to the vehicle's braking system maintenance and performance. With the introduction of ABS, or anti-lock braking systems, drivers do not need to worry about how to apply brakes, as ABS provides maximum brake force and efficiency by avoiding wheel lock.

ABS is a safety system supplement used in vehicles to prevent wheel slip and wheel lock during braking, and to maintain traction between the road surface and the vehicle's wheels. When the vehicle's brakes are applied too hard (usually in emergency braking situations), the force of the brake pads at the wheel are higher than the forces of the wheel gripping the road, causing the wheel to stop spinning and "lock up." A locked tire is incapable of generating any lateral forces at its contact patch with the ground and therefore loses directional stability. This loss of directional stability can cause understeering and oversteering mentioned earlier in this chapter. Since oversteering occurs with a lack of control at the rear tires, brake systems are almost always designed for wheel lock-up to occur at the front axle. Wheel lock-ups at the front axle cause the vehicle to understeer or plow forward, while wheel lock-ups at the rear axle cause the vehicle to oversteer or spinning out.

Typical ABS systems consist of an ECU, wheel speed sensors, and valves in order to monitor the rotational speed of each of the vehicle's wheels. Upon detecting a wheel rotational speed slower than the speed of the vehicle when braking (a condition indicative of impending wheel lock), the ABS valves release the

pressure at the brakes, allowing the wheel to rotate once more. The ratio between the actual speed of wheel rotation under braking to the free-rolling speed of rotation is called wheel slip. Wheel slip increases as deceleration increases under increased brake pedal application effort. A limit of brake force is eventually met, however, and any additional brake effort past this limit causes wheel lock and wheel skid. The brakes are applied again once the tire is capable of providing the most efficient braking, i.e. the wheel slip falls to the ideal range of between 15-25%. This process can be repeated continuously several times per second. The wheel slip ratio versus brake force plot below can be used to explain why this brake pressure modulation is done. The main function of ABS is to keep the wheel slip ratio in this slip tolerance band of 15-25% wheel slip in order to maximize brake force when decelerating. This range is shaded in gray in Figure 2-14 below. Any braking outside this band is less than optimal and results in increased stopping distances and higher probabilities of losing directional stability.

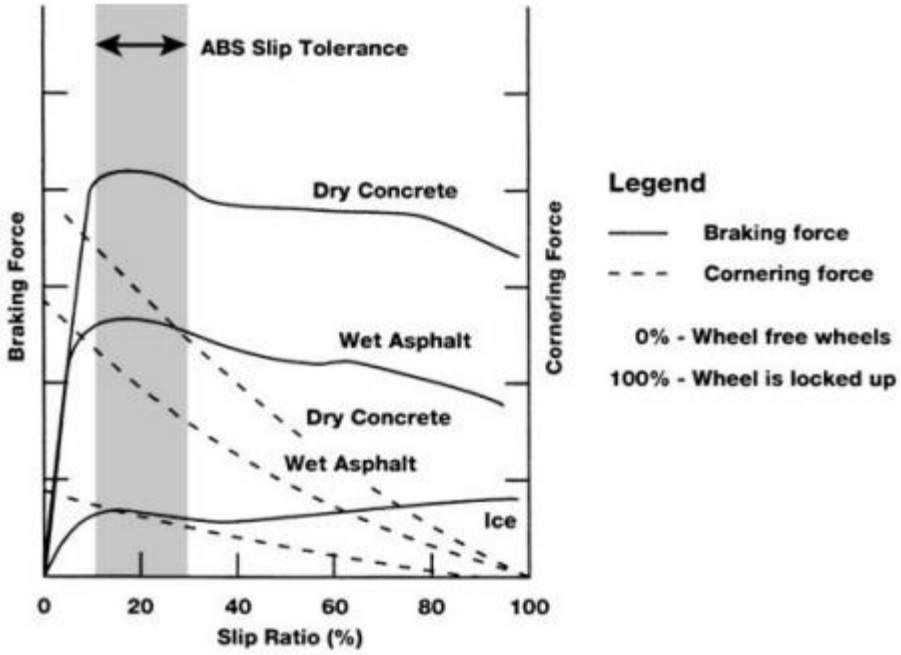

Figure 2-14. Brace force vs. wheel slip percentage [29]. ABS works to keep braking within the gray band.

ABS therefore provides maximum brake performance during braking and emergency events. ABS and stability control systems such as RSC and ESC work hand in hand, delivering maximum brake performance at the right times in order to slow a vehicle and stabilize its heading. ESC and RSC systems can be thought of as extensions to ABS.

2.3.4 Past RSC System Studies

Several studies of the effectiveness of tractor-based RSC systems with heavy vehicles have been conducted already, but few consist of trailer-based RSC systems. Those completed on RSC systems,

however, have rather mixed results, or skip trailer-based RSC testing on vehicles with more than one articulation point (doubles and triples) completely.

Common backing for ESC over both tractor- and trailer-based RSC systems is found, as many organization studies have found RSC systems to be barely beneficial if at all. But almost all of these studies were not conducted on LCVs. For example, the University of Michigan Transportation Research Institute (UMTRI) has stated that ESC systems slightly outperformed RSC systems in preventing rollovers [30] for five-axle tractor semi-trailers only, and did not include benefit estimates for multi-trailer combination vehicles (LCVs). Another example was from NHTSA's latest work on the roll stabilities of heavy vehicles.

NHTSA has been studying heavy vehicle rollover dynamics since the mid-1990s, and active roll stability control systems more recently. NHTSA has recommended ESC and TBRSC over RSC systems in both performance and cost-effectiveness aspects in its FMVSS No. 136 analysis [31]. However, NHTSA used a vehicle cost per equivalent life saved ratio to determine this, while stating that retrofitting trailer-based RSC systems was "extremely costly and not cost effective." This is contradictory to what manufacturers have said in 2017 [32]. Also, NHTSA's study was conducted on a set of test vehicles that did not include a single LCV: two tractors with ESC that were swapped and connected to the same 53' semi-trailer with RSC, and three large buses. As said before, a great deal of evaluation on tractor semi-trailers has been done, as NHTSA additionally tested five baseline tractor semi-trailers as a comparison control in FMVSS 136, while not even mentioning any LCVs. In addition, while it tested several maneuvers within the study, NHTSA used only one maneuver (a 150-foot J-turn) to measure the effectiveness of a trailer-based RSC system, claiming this one maneuver was adequate enough to differentiate the ESC and trailer-based RSC performances. The biggest source of censure to this claim is that rearward amplification depends on the maneuver [20], so only using one maneuver to evaluate an articulated vehicle is flawed. Chapter 4 will provide more explanation as to why several maneuvers are needed, as well as why the J-turn reveals rearward amplification the least. NHTSA used wheel-lift as a qualitative representative of rollover while not quantifying how fast or how much the vehicle actually rolled. It is true that wheel lift is an indicator of rollover, but the two are not synonymous, as wheel lift can happen at numerous axles without vehicle rollover. Finally, it should be noted that NHTS only tested one of the several trailer-based RSC systems available in the market today. In summary, NHTSA's FMVSS 136 mandated ESC on heavy vehicles, but did not properly test trailer-based RSC systems and also ignored LCVs.

Although RSC support among tractor semi-trailer users is partial, other studies have shown a possibility for greater potential in trailer-based RSC performance in LCV applications. Sampson and Cambridge

University modeled a trailer-based active roll control system for LCV roll simulations. Sampson modeled several maneuvers, including steady state cornering, a step steering input, and a double lane change steering input, and successfully studied the effect of rearward amplification on his LCVs, effectively mimicking driving maneuvers experienced on the road. However, due to his RSC system model incorporating elements not normally implemented (anti-roll bars) in the modern RSC industry, his findings of a 27% increase in rollover threshold for his B-double, and 24% for his A-Double [33], should be taken lightly if compared to potential real driving dynamics for LCVs running trailer-based RSC systems only.

Some LCV investigations have even advised against ESC usage without the aid of trailer-based RSC systems [34], and others claim that RSC systems are more practical. The claims of the latter type develop from the fact that LCVs implementing only ESC tend to jackknife more. The dynamics behind this are discussed further in Chapter 3. A rare published study of the roll dynamics of LCVs using a trailer-based RSC system was conducted by Hou and Virginia Tech in 2016. Hou's study involved an A-train double test vehicle instrumented with both ESC at the tractor and RSC at the two trailers, and focused on a comparative benefits/drawbacks study of the performance of the two systems in LCVs. The ESC-only configuration allowed the vehicle to complete the same 150-foot J-turns used by NHTSA at a speed of 12.1% higher than baseline without rollover, and the trailer-based RSC-only configuration produced a slightly smaller improvement at 8.3% [35]. Despite the small improvement in rollover speed threshold, the ESC-only configuration caused the vehicle to oversteer during the J-turn maneuvers. Due to the fear of jackknifing and thus a severe rollover accident, Hou recommended the sole usage of a trailer-based RSC system over that of an ESC system.

Many logistics companies do not hold ownership of both tractors and trailers, but still implement LCVs for their commercial needs through renting. Some, unable to manipulate the tractors they use on their own accord, must solely rely on improving the roll stabilities of their trailers. Based on past studies of modern trailer-based roll stability control, an evaluation of an LCV through vehicle instrumentation and testing would produce a solid conclusion about the performance of trailer-based RSC systems with LCVs. Since A-train doubles are both the most common and the least stable LCV in North America, the test vehicle should be an A-train double.

Lastly, available RSC system manufacturers all implement different operation specifics. There are many areas for unique features, such as interunit communication or additional measured variables. NHTSA's study [13, 31, 36] not only missed testing LCVs with trailer-based RSC systems, but they only used one RSC system. To gain a better, more reliable performance analysis of trailer-based RSC systems, multiple RSC

systems from different manufacturers should be tested. Several maneuvers should be tested as well in order to evaluate trailer-based RSC systems on the effects of rearward amplification on more static and more dynamic movements.

Chapter 3 RSC Braking Suitability for LCVs & A-Doubles

This chapter covers the characteristics of air brake systems used on heavy vehicles: trailer(s) contribution to total vehicle braking effort and brake signal timings. A comparison between an A-Double and a tractor semi-trailer is made to highlight better suitability and performance of trailer-based RSC systems for LCVs as compared with tractor semi-trailers.

3.1 Introduction

Due to several reasons introduced in Chapter 2, adding an active stability control system onto solely the trailers is the only option for many in the trucking industry. The motivation behind the study proposed by this thesis revolves around the hypothetical increase in trailer-based RSC system performance on LCVs such as A-Doubles over that on single-trailer vehicle configurations like tractor semi-trailers. RSC systems use brake application in stabilizing vehicle trailers, and while most passenger cars use hydraulic brakes, this choice is unwise in heavy vehicles due to the length of articulated vehicles. A theoretical RSC performance difference arises from two main aspects of the pneumatic brake systems found in US heavy vehicles. As supplementary trailers are added to a vehicle configuration, both the application and release times of the brakes and the load transfer during deceleration change considerably. This chapter will cover the details regarding both by comparing the characteristics of the two most commonly used combination vehicles: the thoroughly-studied tractor semi-trailer and an A-Double.

3.2 Brake Force Distribution in Heavy Vehicles

This section introduces a simplified science of determining braking force distribution under constant braking conditions, using a braking system analysis which aligns with the largely-adopted UN Braking Regulations 13 and 13H. The fundamental theory behind these analyses assume no lateral variation in the wheel and brake forces acting on the vehicle during braking. They also do not include advanced braking technologies such as ABS and RSC, as they are intended for extreme conditions usage rather than sub-optimal braking system design compensation. Although RSC systems are used for increasing roll stabilities, they do so by simply slowing the vehicle and its trailers to stabilize them. A theorized RSC system performance increase arises from a theoretical increase in trailer brake contribution between a tractor semi-trailer (ST) and an A-Double (AD). A higher trailer brake contribution to that of the entire vehicle would result in better braking by a trailer-based RSC system, and help even more in vehicle stabilization.

It should be noted that this chapter does not cover the full 3D dynamic simulation of a road vehicle during braking, e.g. a multiple degree of freedom model including longitudinal, lateral, and vertical forces and

motions, as the dynamic behavior of articulated vehicles is highly non-linear and complicated. This in-depth look at the dynamics of articulated vehicles during braking is outside the scope of this project. Instead, a rigid vehicle in dynamic equilibrium is presented with a 2D bicycle model and is used to determine the braking contributions made by each axle of heavy vehicles to determine if an additional set of trailer brake axles can affect vehicle braking and therefore vehicle stabilization. No advanced braking technologies, such as ABS and ESC/RSC, are included in the analysis. The equations used to determine the braking distributions for the two free body diagrams are discussed below. Again, these equations are not equations of motion, but rather quasi-static weight transfer equations satisfying Newton's first law of equilibrium and second law of motion.

The primary function of a vehicle braking system is decelerating the vehicle. Under both accelerating and decelerating conditions, a vehicle undergoes weight transfer as rotation about the lateral axis, or pitch, occurs and the vehicle dips or rises between the axles. In the simplified analysis methods presented in this section, this longitudinal weight transfer is modeled as vertical deflections at the axles, causing changes to the dynamic normal reactions at the road surface at each axle, presented in the bicycle models below. In real-world conditions, lateral weight transfer generated by vehicle roll contributes to the normal reactions at the tires when braking along a curved road. Again, due to the complexity of a 3D model for an articulated vehicle, this analysis assumes the vehicle is not cornering during braking to simplify all lateral forces and contributions to be zero.

Braking performances vary directly with the tire mechanics with the road, as they provide the grip between the vehicle and the road. Many factors can affect a tire's ability to provide the proper braking forces. As tire wear accumulates through vehicle operation, braking performance and safety are both compromised. The friction coefficient between the road and the tire can vary because of environmental factors, such as slippery roads due to rain or ice. Fortunately, as will be mentioned in Chapter 4, new tires were installed at the beginning of each RSC testing week, and the weather for the testing days was very similar, so nearly constant tire/road relationship parameters were sustained during actual testing. For the purposes of this analysis, tire mechanics and dynamic forces from the road surface are ignored. The braking weight transfer is simplified and calculated using the rate of braking, the vehicle units' wheelbases, and their centers of gravity heights. A deceleration rate of 0.6 g's was chosen as the rate of braking, which many car manufacturers view as a sensible design target for basic braking system design without ABS [37]. The basic theory behind braking presented in this section starts from the quasi-static approach and assumes no ABS or ESC/RSC operation.

When designing braking systems for an articulated vehicle, each unit is considered separately. The same approach is used in this analysis determining the braking force distribution. Since couplings such as fifth wheels and pintle hitches are shared by two units, two vertical and two horizontal forces are displayed at each in both figures. In general, towing units experience the load of the trailer at the fifth wheel, and trailers experience the supporting normal force of the fifth wheel. Again, under-braked trailers are generally better arrangements for articulated vehicles, so the tractors experience a negative horizontal force at the fifth wheels, and the trailers a positive horizontal force.

Figures 3-1 and 3-2 show the 2D free body diagrams of an ST and an AD, respectively, under simplified dynamic braking conditions. In Figure 3-1, the ST only has two vehicle units while in Figure 3-2, the AD has four, as the dolly was modeled separately. Unit numbers are encircled in red. Both diagrams display color-coded forces, with normal reactions at the tires displayed in blue, braking forces in green, vehicle unit forward momentums in yellow, and vehicle unit weights in orange. A red vertical line in Figure 3-2 is shown to split the vehicle into halves. Each of these vehicle halves is comprised of two vehicle units. Table 3-1 lists the variables found in Figures 3-1 and 3-2, and provides descriptions for them. The parameter values used in this analysis are listed in the Appendix.

As seen in Figure 3-2, the converter dolly is modeled separately from the rear trailer. Although small and seemingly with negligible weight compared to the rest of the vehicle, the converter dolly transfers vertical load to the rear of the first semi-trailer. Since the converter dolly drawbar is short, the resultant load transfer is large enough to significantly load the front trailer's rear axle.

Normal forces at each tire are shown as vertical forces that support the weight and weight transfer during braking. The rear axles of the tractor and semi-trailer are assumed to be close enough to treat the two axles as one, located in between the two tire contact locations. The brake forces at each tire are shown as lateral forces counteracting the momentum of vehicle units. Interunit couplings significantly affect the braking and the braking performance of the vehicle regardless of the type of braking system it is fitted with, so fifth wheels and pintle hitches, both of which allow pitch rotation, are modeled as well. The fifth wheel coupling must be capable of withstanding the lateral forces from accelerating and braking while carrying a portion of the towed trailer weight, and is thus modeled with both horizontal and vertical forces for both units. The drawbar at the pintle hitch connects the two halves of the vehicle and transmits both horizontal and vertical forces between them. Under braking conditions, it is assumed that the drawbar is in compression, meaning the tractor is decelerating more than the attached trailer. Under-braked trailers (relative to the tractor) are generally considered to be the better arrangement [37].

The equations used to determine the braking distributions for the two free body diagrams are discussed below. Again, these equations are not equations of motion, but rather quasi-static weight transfer equations satisfying Newton's first law of equilibrium and second law of motion. The ST in Figure 3-1 will be covered first, followed by the AD in Figure 3-2.

Table 3-1. Free body diagram nomenclature and description.

P, P_{ti}, P_D	Vehicle unit weight of tractor, trailer *i*, or dolly (N)
N_i	Dynamic normal reaction at the road surface of axle *i* under braking conditions (N)
T_i	Brake force at the tire of axle *i* under braking conditions (N)
z	Braking/decelerating rate of the vehicle in terms of *g*'s. Usually quoted as a decimal (g)
L_1	Horizontal distance from the tractor's front axle to the tractor's cg (m)
L_2	Horizontal distance from the tractor's cg to the tractor's rear axle (m)
L_3	Horizontal distance from the front trailer's front axle to its cg (m)
L_4	Horizontal distance from the front trailer's cg to its rear axle (m)
L_5	Horizontal distance from the rear trailer's front axle to its cg (m)
L_6	Horizontal distance from the rear trailer's cg to its rear axle (m)
L_D	Horizontal distance from the dolly's cg to its axle (m)
E_1	Wheelbase of tractor
E_2	Wheelbase of front trailer
E_3	Wheelbase of rear trailer
c_1	Tractor fifth wheel coupling horizontal position relative to its rear axle (m)
c_2	Tow hitch horizontal position relative to front trailer's rear axle (m)
c_3	Tow hitch horizontal position relative to dolly's axle (m)
c_4	Dolly fifth wheel coupling horizontal position relative to its axle (m)
h_1	Tractor cg height (m)
h_2	Tractor fifth wheel height (m)
h_3	Front trailer cg height (m)
h_4	Tow hitch height (m)
h_5	Dolly fifth wheel height (m)
h_6	Rear trailer cg height (m)
h_D	Dolly cg height (m)

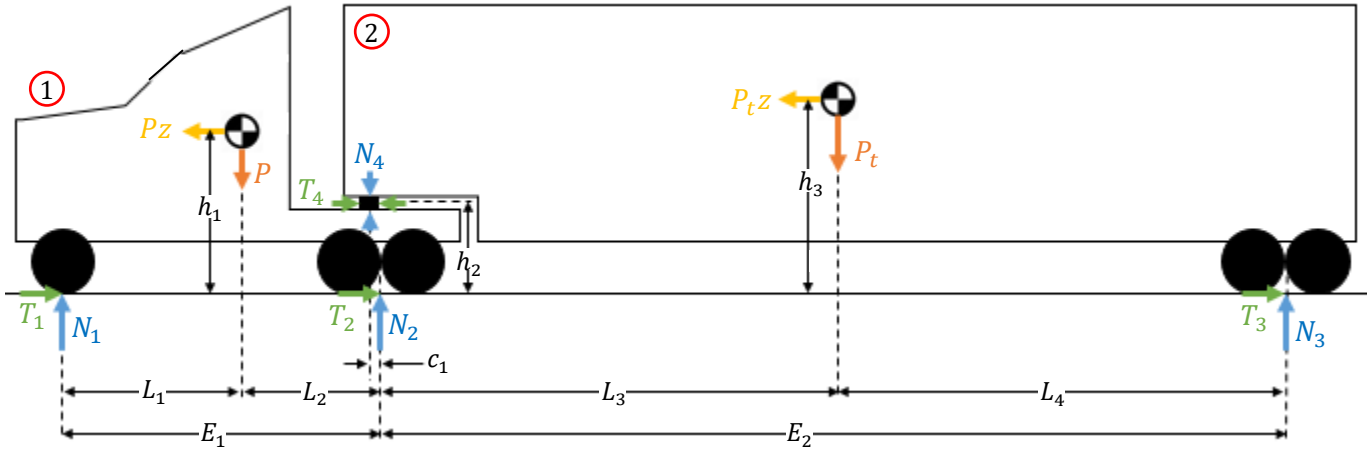

Figure 3-1. Brake distribution FBD for an ST under constant braking.

Considering the tractor part (unit 1) of the ST free body diagram (FBD) shown in Figure 3-1 as a separate unit from the trailer (unit 2), the summation of vertical and horizontal forces are shown in Equation 3-1 and 3-2 below:

$$N_1 - P + N_2 - N_4 = 0 \tag{3-1}$$

$$T_1 + T_2 - Pz - T_4 = 0 \tag{3-2}$$

Taking the moments about the contact point between the front wheels and the road determines Equation 3-3:

$$N_4(E + c_1) + PL_1 - N_2E - Pzh - T_4h_3 = 0 \tag{3-3}$$

Doing the same for the trailer, but taking the moments about the fifth wheel coupling, provides the following equations:

$$N_4 + N_3 - P_t = 0 \tag{3-4}$$

$$T_4 + T_3 - P_tz = 0 \tag{3-5}$$

$$P_ta_2 - N_3E_2 - T_3h_3 - P_tz(h_3 - h_2) = 0 \tag{3-6}$$

Brake system designs for articulated vehicles are complicated since the towing units must be designed to operate with and without the towed trailers, while still having braking systems that are as efficient as possible. Due to the vertical and horizontal forces transmitted between vehicle units during braking, some sort of variable braking distribution would be required to avoid braking system performance degradation of the tractor with the addition of towed trailers. Instead, a fixed braking ratio system is upheld under the assumption of optimum braking distribution, or when the braking on each axle is proportional to the normal load supported by the axle [37]. This means that the braking efficiency is 1, which can only occur at one braking rate, which is specified as $z = z_1$. These assumptions yield the following equations used to determine the braking forces at each tire for both the ST and the AD, where *i* is axle *i*:

$$\frac{T_1}{N_1} = \frac{T_2}{N_2} = \frac{T_3}{N_3} = \cdots = \frac{T_i}{N_i} = z_1 \tag{3-7}$$

$$\sum_i^n X_i = 1 \tag{3-8}$$

The braking force distribution can then be determined for a specific rate of deceleration, z, and a brake system can be designed around a preferred deceleration rate for the less stable and more dangerous

vehicle configuration with the trailer(s). As mentioned above, a *z* value of 0.6 g's was chosen, which many car manufacturers view as a sensible design target for basic braking system design without ABS [6, 37].

Equations 3-1, 3-2, 3-3, 3-4, 3-6, and 3-7 (split into equations for T_1, T_2, and T_3) were used with vehicle parameters available in the Appendix to determine the braking force distribution for a conventional WD-64 tractor semi-trailer vehicle decelerating at 0.6 *g*'s. The same process was completed for producing brake force distribution analysis equations for the conventional A-Double vehicle shown in Figure 3-2.

Resolving forces both vertically and horizontally for the AD tractor yields the following two equations:

$$N_1 - P + N_2 - N_4 = 0 \tag{3-9}$$

$$T_1 + T_2 - Pz - T_4 = 0 \tag{3-10}$$

Taking the moments about the contact between the front wheels and the road determines Eq. 3-11:

$$N_4(E_1 + c_1) + PL_1 - N_2E_1 - Pzh_1 - T_4h_2 = 0 \tag{3-11}$$

Doing the same for the trailer, but taking the moments about the fifth wheel coupling, provides the following equations:

$$N_4 + N_3 - P_{t1} - N_5 = 0 \tag{3-12}$$

$$T_4 + T_3 - T_5 - P_{t1}z = 0 \tag{3-13}$$

$$P_{t1}(L_3 - c_1) - N_3(E_2 - c_1) - T_3h_2 - P_{t1}z(h_3 - h_2) + N_5(E_2 + c_2 - c_1) = 0 \tag{3-14}$$

Unit 3 (converter dolly) equations were completed in the same fashion, with the moment equation taken about the pintle hitch location, and are listed below as Equations 3-15 to 3-17. Unit 4 (the rear trailer) equations were created in the same fashion as Unit 2 equations, and are listed below as Eq. 3-18 to 3-20.

$$N_6 - P_D + N_5 - N_8 = 0 \tag{3-15}$$

$$T_5 - T_8 + T_6 - P_Dz = 0 \tag{3-16}$$

$$T_8(h_5 - h_4) + P_Dz(h_4 - h_D) - T_6h_4 + P_D(c_3 - L_D) + N_8(c_3 + c_4) - N_6c_3 = 0 \tag{3-17}$$

$$N_8 + N_7 - P_{t2} = 0 \tag{3-18}$$

$$T_8 + T_7 - P_{t2} = 0 \tag{3-19}$$

$$P_{t2}L_5 - P_{t2}z(h_6 - h_5) - T_7h_5 - N_7E_3 = 0 \tag{3-20}$$

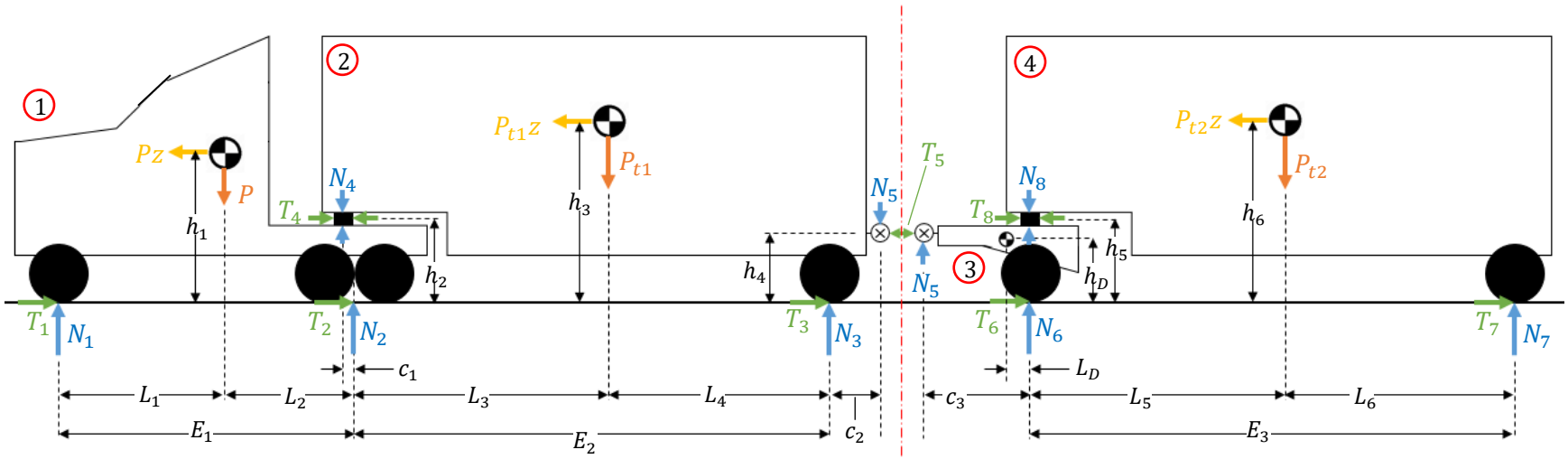

Figure 3-2. Brake force distribution FBD for an AD under constant braking.

The used parameters are available in the Appendix. The same tractor was used for both the ST and the AD; the weights for the trailers for the AD were measured using a scale, while the ST's trailer was determined from the difference between the max GWVR of a WD-64 semi-trailer truck of 80,000 lbs. This approach was used since STs are usually loaded to maximum GWVR, while ADs are loaded to maximum trailer volume rather than weight.

Using the calculated brake forces at each axle, the braking force distribution throughout the vehicle can be determined by taking the ratio of the brake force at each axle to the combined normal reactions of all the axles, or the total weight of the vehicle. This agrees with Equation 3-8, where the summation of the braking force distributions is equal to one. Equations 3-21 and 3-22 below display the calculations for the braking distributions at each axle *i*, X_i, for the ST and the AD, respectively. Table 3-2 shows the results for both the ST and the AD under constant braking at 0.6 *g*'s.

$$X_i = \frac{T_i}{P+P_t} \tag{3-21}$$

$$X_i = \frac{T_i}{P+P_{t1}+P_{t2}+P_D} \tag{3-22}$$

Table 3-2. Brake distribution for each axle in a ST and AD with the same tractor at 0.6 *g* deceleration.

Brake Distribution	Tractor Semi-trailer	A-Double	
X_1	.1946	.2498	
X_2	.4553	.3129	
X_3	.3501	.1548	
X_6		.1815	
X_7		.1072	
Tractor	.6499	.5565	**Difference**
Trailers	.3501	.4435	.0934 or 9.34%

Table 3-2 shows that the trailers of the AD contribute more to the total vehicle braking effort under constant deceleration, as the trailer brake axles contribute around 44.4% of the braking compared to the 35.0% found at the ST trailer axle. This indicates higher vehicle decelerations when using trailer-based RSC systems and therefore applying brakes only at the trailers in ADs than in STs. Table 3-3 presents the trailer distribution results for different constant deceleration rates of both vehicles, and shows the general conclusion to be the same. Harder braking, and therefore higher decelerations, cause more weight transfer to the tractor, calling for higher tractor braking contribution and lower trailer braking

contribution. Table 3-3 shows an increase in trailer braking contribution as the deceleration rate is increased, implying an even larger trailer-based RSC influence difference between an ST and AD during emergency braking.

Adding trailer and trailer brakes decreases tractor contribution and distributes the total vehicle brake effort more along the vehicle. Trailer-based RSC systems may therefore contribute more in ADs than they do in STs, as higher trailer-brake decelerations can yield higher vehicle stability.

Table 3-3. Trailer brake contributions under different constant deceleration rates for both ST and AD.

Deceleration (*g*)	ST Trailers	AD Trailers	Difference	Dolly Contribution
0.2	.3915	.4728	.0813	.1760
0.3	.3809	.4653	.0844	.1776
0.4	.3705	.4580	.0875	.1790
0.5	.3602	.4507	.0905	.1803
0.6	.3501	.4435	.0934	.1815
0.7	.3402	.4364	.0962	.1826
0.8	.3304	.4294	.0990	.1836
0.9	.3208	.4225	.1017	.1844
1	.3114	.4157	.1043	.1852
2	.2246	.3521	.1275	.1903

The analysis produced an interesting observation regarding the braking contributions made by the dolly's axle: as braking efforts and deceleration rate increase, the dolly braking contribution increases. The dolly contributions are included in the last column of Table 3-3 above. This draws weight towards testing an RSC system that includes the dolly brakes in the vehicle's RSC braking application.

3.3 Brake Timing Benefits

3.3.1 Air Brakes Basics

Pneumatic brake systems largely originated from application on railway vehicles in order to decrease the high number of train crashes back in 1869, and were invented by George Westinghouse, the founder of the Westinghouse Air Brake Company, or WABCO. The basic operation of the pneumatic system called for charged air to be sent down pipelines to initiate the brake system and release the brakes using the charged air signal. This system was essentially fail-safe, and became the basis for the modern air brake system

used by heavy vehicles today. Their ease of installation and fail-safety were key reasons for pneumatic brake systems to be used with heavy vehicles over hydraulic brake systems.

Compressed air brake systems are now commonly used on heavy trucks and buses and consist of many parts and valves in order to complete different functions and fail-safety. Past studies have shown that the response times typically exhibited by air brake systems are good enough to provide sufficient braking performance in these heavy commercial vehicles, both in deceleration rates and vehicle stopping distances. Figure 3-3 displays the stopping distance results from a study performed by Day when comparing hydraulic and air brake systems on typical trucks when braking is initiated at 60 mph on a dry road. It should be noted that hydraulically-braked vehicles still perform better due to primarily higher torque at the front brakes, which also attribute to better braking force distribution under empty trailer conditions [37]. It is known, however, that the increased stopping distances over hydraulic brake systems is largely due to the braking application and release timing lags in air brake systems.

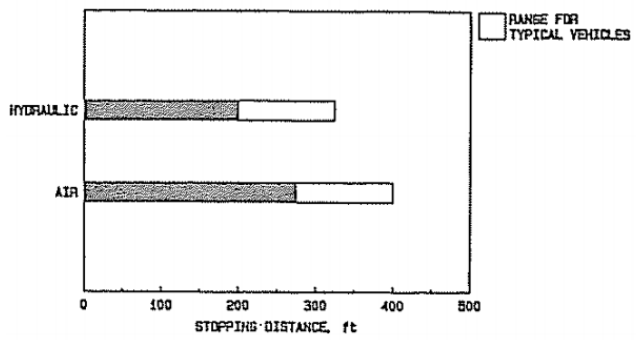

Figure 3-3. Stopping distances for typical trucks at 60 mph on dry road [38].

The basic operation of an air brake system largely consists of compressed air in tanks, the brake pedal, and two separate pneumatic circuits called the supply circuit and the control circuit. A heavily simplified diagram of the air brake system found in an articulated vehicle is shown in Figure 3-4. The red lines symbolize the control circuit, while the blue represents the supply circuit. The supply system has the main responsibility of compressing, storing, and supplying high-pressure air to the brakes as well as the control system, as Figure 3-4 displays the beginning of the control system sprouting from the primary and secondary tanks. The control system is responsible for sending a brake application signal initiated by the brake pedal. The brake pedal is also called the foot valve. The amount of air pressure applied at the brakes depends on the brake pedal application force, as harder pedal presses cause higher air pressures and vice versa. The compressor replenishes the supply reservoirs as well as the tanks located throughout the vehicle.

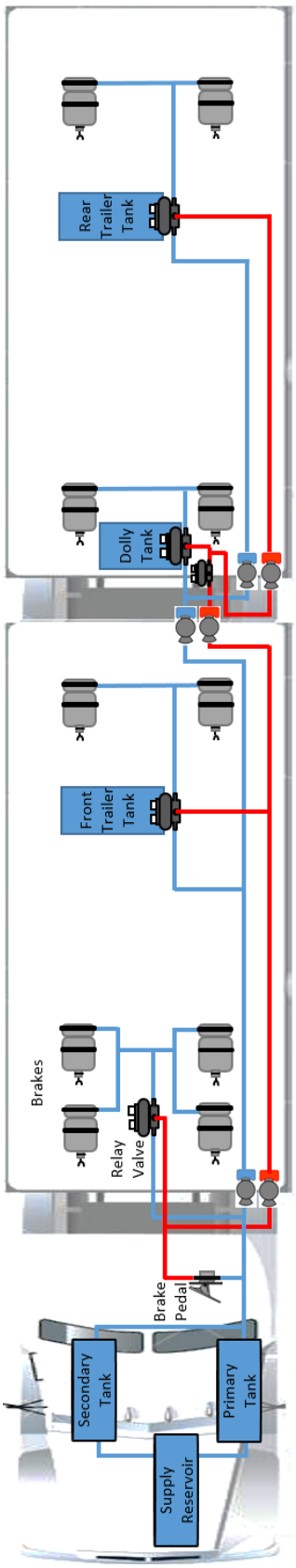

Figure 3-4. Simplified brake system for an A-Double.

Air brake systems consist of many different parts such as double check valves and safety valves, and involve busy tubing systems; the system shown in Figure 3-4 is highly simplified. This simplification was made since the focus of Figure 3-4 is demonstrating the length of tubing required for a pneumatic signal sent through the control circuit by the brake pedal to reach the front and rear trailers. It is important to know that other factors, such as the use of valves, coiled tubing, and tractor brake adjustment levels, also add to the tractor and trailer brake lags. It has been predicted, due to the large volumes of air that need to be moved through the system, that LCVs such as an AD will have considerably longer brake application and release times than an ST.

3.3.2 Brake Application and Release Times

FMVSS 121 provided pneumatic timing requirements for brake application and release for heavy vehicles. However, these timings covered the times between the registration of the service signal at the brake valves and when a specified psi was reached within the brake chamber, rather than the times between brake pedal application and the registration of the service signal at different parts of the vehicle. Both types of timings contribute to brake application time and will be covered in this chapter, although a direct comparison between an AD and an ST is only available in the first type: brake application and release times in accordance to FMVSS 121 by NHTSA.

NHTSA tested brake timings for 24 tractor semi-trailer combinations and 7 double trailer combinations. Gladhand timing of all towing vehicles were connected to a test rig to evaluated to measure the apply and release times of brakes for different attached trailers. Unfortunately, it was found that the FMVSS 121 trailer test rig was much faster than actual tractors in providing a control signal to attached trailers. Therefore, the timing results of trailers with the test rig are not representative of actual tractors in real world conditions. The test rig was reported to apply a control line pressure four times faster than, and released twice as fast as, the fastest tractor evaluated.

Still, comparisons between semi-trailer combinations and double trailer combinations using similar length and diameter pneumatic tubing and the same tractor are still valid using NHTSA's results. It was determined from their testing that doubles combinations have relatively slow brake timings, as the sheer length of pneumatic tubing through which the control signal much flow is must longer than that in a semi-trailer combination. Interestingly, test results for an ST and an AD using the same tractor and same front trailer produced different average application and release times at the front trailer measured from the first movement of the brake pedal [39]. The application and release times for the ST trailer were faster

than those exhibited by the AD. Although the actual results are inapplicable to real world timings, it is safe to assume that the trends remain the same under comparable conditions.

3.3.3 Brake Signal Registration Timing Differences between Driver Braking and RSC Braking

Brake response time is defined as the time between brake pedal activation to a certain "level of effectiveness" [40]. For pneumatic brake systems, brake response time is measured as the time between brake pedal application to the instant when a certain pressure level is reached in the brake chamber. The analysis presented in this section differs slightly, as a brake registration time is measured from the instant of brake pedal application to any pressure experienced at the brake chambers, as the brake chamber pressure for any significant braking is unknown or unspecified for the test vehicle, and cannot be measured without torque sensors at each braked wheel.

The following plots in Figure 3-5, 3-6, and 3-7 show the significant differences in time in brake registration when comparing pedal-application braking and RSC-application braking in a conventional A-Double. Figure 3-5 presents the brake chamber pressures at the driver and passenger side brakes for both the front and rear trailer during braking initiated by brake pedal application. The black dashed line in the plot represents the time during which the brake pedal was pressed by the driver. Figures 3-6 and 3-7 show the driver and passenger side brake chamber pressures at the front trailer and rear trailer, respectively, during braking with RSC system activations. The dashed black line here represents RSC activation, and the pink line is an event flag for one of the tests conducted in this study.

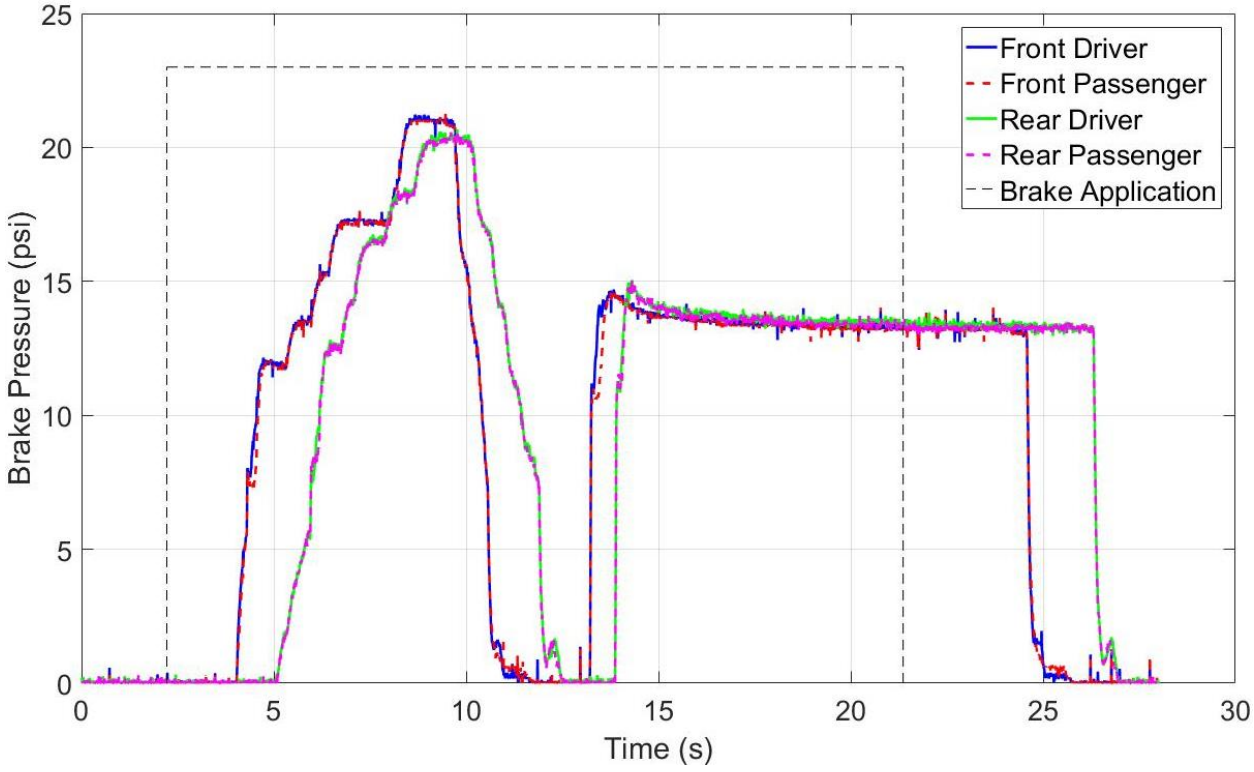

Figure 3-5. Brake chamber pressures during driver-operated braking in an A-Double.

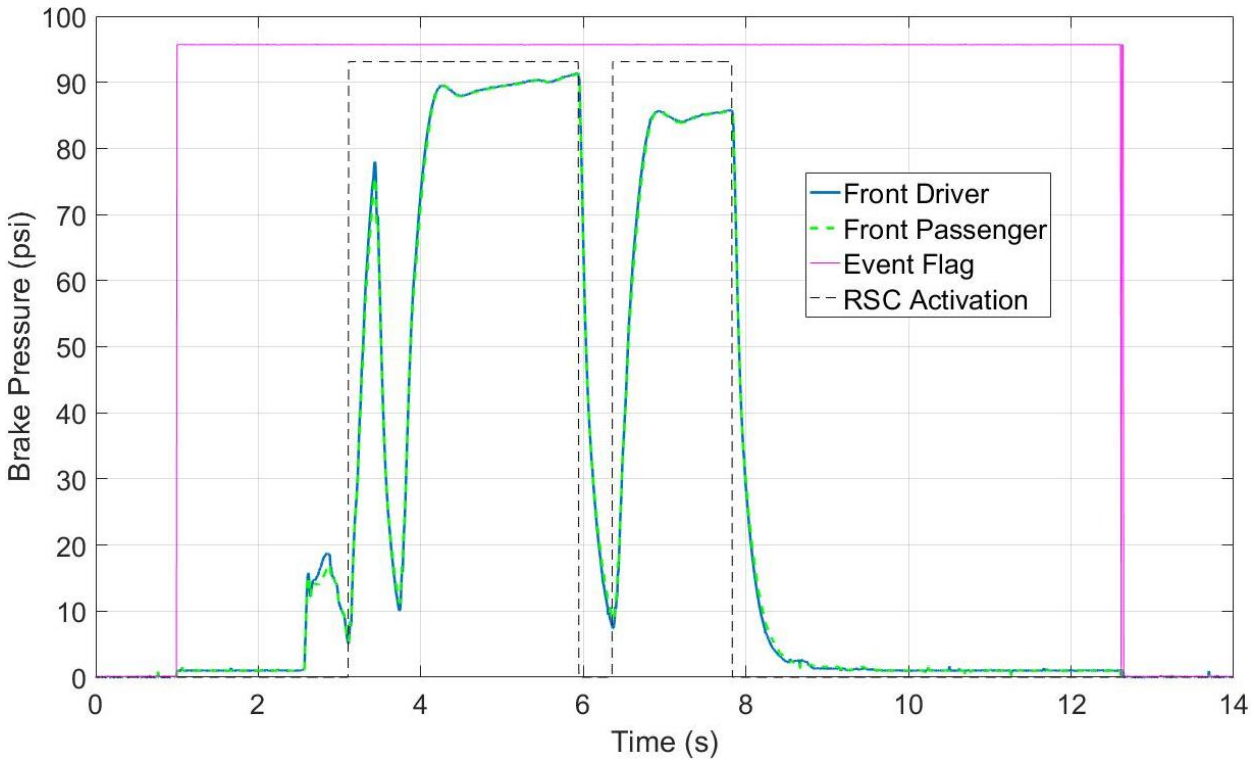

Figure 3-6. Brake chamber pressures at the front trailer during RSC-operated braking in an A-Double.

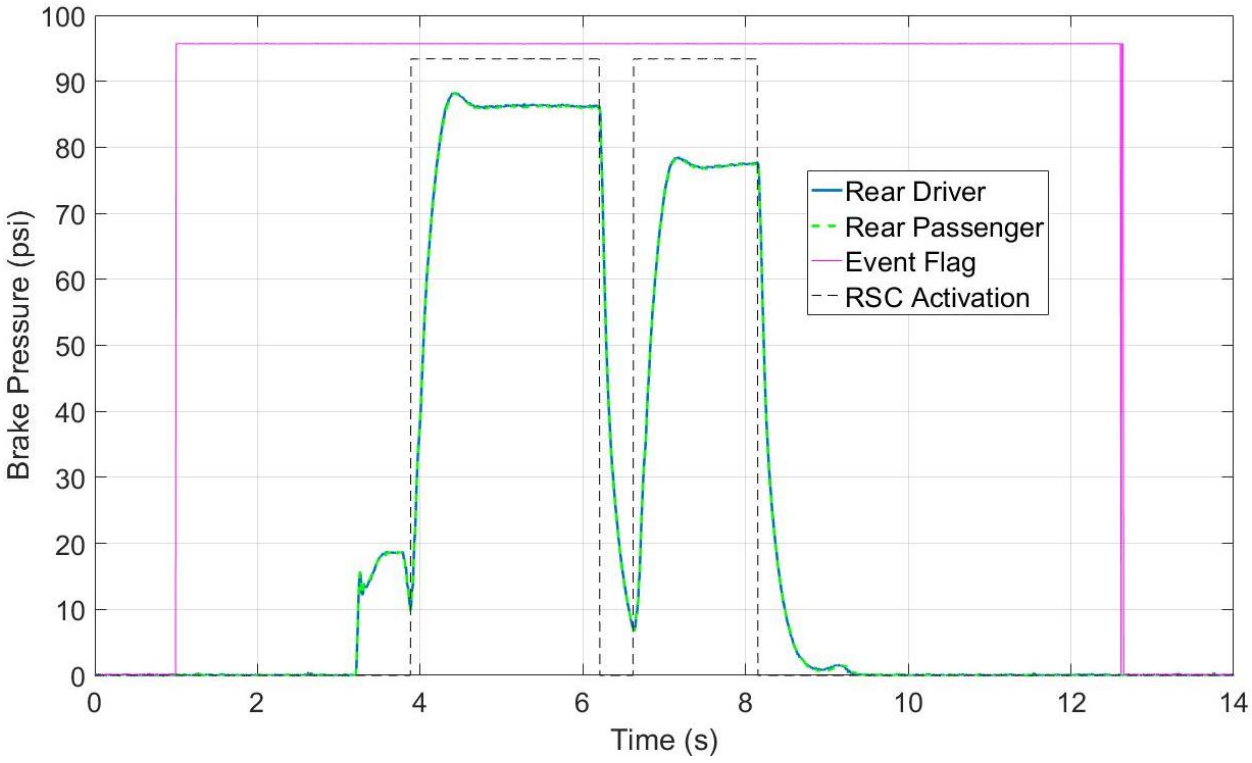

Figure 3-7. Brake chamber pressures at the rear trailer during RSC-operated braking in an A-Double.

It can be seen that RSC systems, upon determining imminent rollover, apply a brake signal to the respective trailers on which they are installed, and thus instantaneously deliver braking force using the trailer's air tank. On the other hand, pedal-application braking delivers a pneumatic signal that must travel through the vehicle lines before applying brake pressures. Although this application pressure is released immediately, the time that the pneumatic signal takes to travel the length of the vehicle is simply too large for evasive or emergency situations, especially on the highway. As seen in Figure 3-5, the braking of the rear trailer (+3 seconds after brake pedal application) lags behind that of the front trailer (+2 seconds after brake pedal application), as logically it takes longer for the rear trailer to receive a pneumatic signal than for the front trailer. Since rearward amplification affects the rear trailer further, this brake lag experienced at the last trailer is even worse than it seems.

Brake release times are an important aspect of brake registration time as well, and again, RSC systems show instantaneous brake release times. Longer lags than those seen in brake application times are present for the pedal-applied braking, as the front trailer takes around 3.5 seconds and the rear trailer takes 5 seconds to release their brakes after the pedal is released.

It should be noted that the dip in brake chamber pressures at 10-14 seconds in Figure 3-5 occurs from the driver releasing the brake pedal enough to not reach the necessary threshold to apply brake pressure, while technically still applying the brake pedal. Regardless, lags in the front and rear trailer brake chamber pressures are still visible within that time period. A sudden spike is seen in the RSC-activated brake chamber pressures at the front trailer at 3-4 seconds in Figure 3-6. This spike occurs due to ABS releasing pressure in a predicted wheel lockup case, only for the ABS action to be canceled upon further calculations. Small jumps in pressure are seen right before the first RSC activations in Figures 3-6 and 3-7. These are test pulses sent by the RSC modulators as they check the vehicle's roll conditions.

Unfortunately, a similar approach in determining the brake registration lag for an ST is unavailable due to a lack of a semi-trailer. It is also unavailable through literature despite a comprehensive review of brake timing studies. However, it is fair to assume that the brake registration lag of an ST is lower than those shown in an AD in consideration of two facts: NHTSA's study results showing ST valves and glad hands reacting faster than those in the AD, and the longer vehicle length and therefore longer pneumatic line length of an air brake system in an AD over that found in an ST.

In conclusion, trailer-based RSC systems will have a larger influence on the braking timings of an AD than on an ST since brake pedal signals must travel longer distances in an AD under driver-operated braking. This is especially true for the rear trailer of an AD, as rearward amplification also affects it more than the front trailer. Although the differences between the brake application and release times of driver braking and RSC braking on an AD seem minimal, the additional 2-3 seconds in lag are invaluable time during emergency or evasive maneuvers.

3.4 Summary

Although past studies on tractor semi-trailers indicate that RSC systems are not effective as a tractor-based stability control system such as ESC, it is predicted through the presented analyses in this chapter that trailer-based RSC systems can achieve higher efficiencies on trucks with multiple trailers, such as A-Doubles, than on tractor semi-trailers. Both the trailer braking contribution to the total vehicle braking effort and the timing improvements found in RSC usage over driver-operated brake lag show that RSC systems are more suitable for ADs than they are for STs. It is therefore necessary to evaluate RSC systems on LCVs, such as a double, due to the combination of the analyses in this chapter and the low number of related studies regarding RSC performance on LCVs. In addition, as mentioned in Chapter 2, trailer-based systems can reduce the likelihood of jackknifing when braking [35].

The braking analysis in this chapter consisted of highly simplified modeling and constant decelerations on straight roads, as the high non-linearity found in LCV dynamics in a 3D braking model was outside the scope of this project. However, field testing is applied to directly evaluate the performance of trailer-based RSC systems in several braking applications. Brake contribution from the dolly increased with deceleration rate, so there is some motivation behind evaluating an RSC system that includes dolly brakes.

Chapter 4 Track Testing with 28 foot A-Double

This chapter discusses the entirety of the preparation for track testing an experimental 28' A-Double, otherwise known as a western double. There were six main points to the vehicle instrumentation: the anti-jackknifing systems, safety outriggers, load frames, trailer reinforcement beams, the steering robot, and the data acquisition system. This includes both the mechanical and electrical vehicle instrumentation completed in order to prepare the vehicle for testing. The chapter ends with a summary and description of the test maneuvers run during testing, as well as the reasoning behind the test maneuvers chosen.

4.1 Mechanical Preparations

The majority of the efforts undertaken on the mechanical side of vehicle instrumentation were made for safety concerns and vehicle preservation during testing, and were implemented by a team of five members. Five of the six main instrumentations will be covered in Section 4.1: the safety outriggers, the load frames, the trailer reinforcement beams, the anti-jackknifing systems, the steering robot, and the data acquisition system. The anti-jackknifing system involved a series of ropes and chains to keep the vehicle units from reaching articulation angles indicative of jackknifing. The steering robot was essential in providing repeatable testing maneuvers and therefore reliable data via the DAQ system and sensors. The outriggers were used to determine if the vehicle had rolled during a maneuver while keeping the vehicle upright. The load frame adjusted the two semi-trailers to simulate a realistic center of gravity and weight distribution during testing. Finally, the reinforcement beams strengthened the trailer bodies to withstand forces exerted by load frame and outriggers during roll. Figure 4-1 shows these key instrumentations. Each of these five will be detailed in the following sections and then the section will conclude with other preparations made to the vehicle for testing.

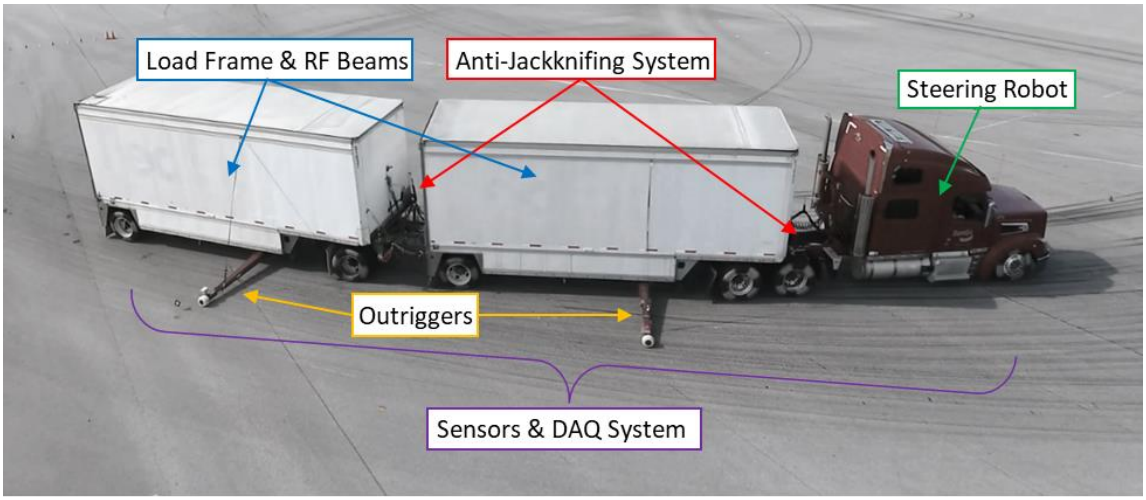

Figure 4-1. Vehicle instrumentation.

4.1.1 Outriggers

The testing conducted for this study was obviously aimed at evaluating the roll stability of the test vehicle. Considering the proposed test objective, outriggers to prevent the vehicle from rolling over while still allowing all indicative signs of rollover were necessary. Outriggers, or projecting structures on a vehicle that usually aid its lateral stability, would protect the vehicle, its passengers, and the custom installation work done on it. A thorough literature review was conducted on outrigger designs used in prior roll stability projects in the particular area of designing outriggers that met all of the following specifications:

- The outriggers needed to provide sufficient enough rigidity and strength to save and support a conventional 28' A-Double from rollover in extensive testing.
- The outrigger contact wheels needed to be strong enough to survive countless hits of various force magnitudes while being light enough to provide a negligible stabilizing moment.
- The outriggers needed to be collapsible in order to transport the test vehicle from its instrumentation location at CVeSS to the testing facility via highway travel.
- The outriggers needed to provide enough sprung mass roll angle to determine that roll was imminent while also keeping the vehicle upright before lateral accelerations grew too great.
- The outrigger wheel heights needed to be adjustable in order for quick changes for conducting tests with different objectives.
- The outriggers and their weight needed to generate the minimum possible effects on trailer rotational inertia.
- The loads experienced by the outrigger contact wheels needed to be distributed evenly onto the trailer frames.
- The outriggers needed to supply enough ground clearance to allow passage under the vehicle.

Considerable design work was done by CVeSS due to the fact that the previous outrigger designs did not meet all of the comprehensive specifications listed above. Figure 4-2 displays the final design of the outriggers, which were designed to be mounted to the underside of the two trailers with collapsible capabilities. As seen in Figure 4-2, the outrigger assembly is made of three main parts: two outboard beams containing the contact wheel, and the inboard beam used to attach the assembly to the bottom of each trailer. The outriggers also feature a hinge at the connections of the outboard beams to the inboard beam to allow for adjustable outrigger wheel heights. Two rows of bolt holes are used to mount the assembly to the laterally running trailer frame rails under the body.

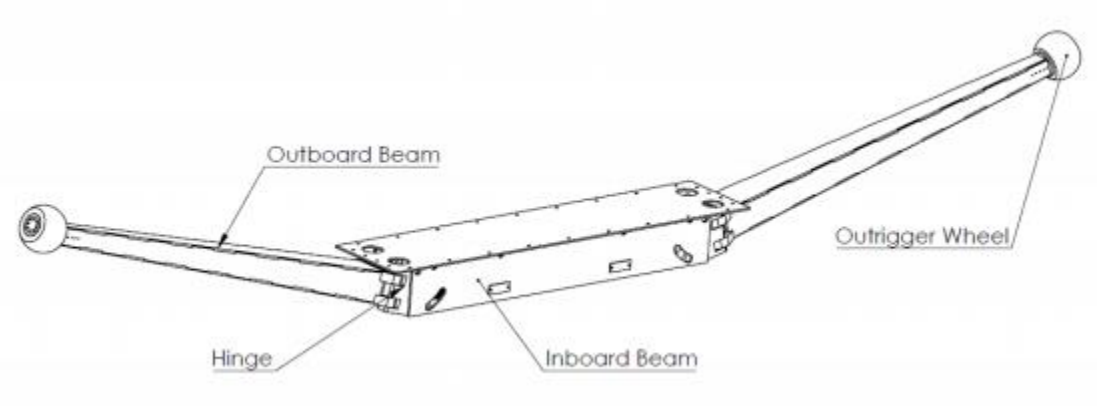

Figure 4-2. CVeSS outrigger schematic.

The CVeSS outrigger design was largely inspired by the latest generation of NHTSA's safety outriggers [41], which were used as guidelines and standards. NHTSA's Class 8 trailer outriggers also feature foldable outboard beams, adjustable contact wheel heights, and a light but strong contact wheel. CVeSS adopted these contact wheels made of a high density polyethylene compound which was strong enough to resist massive contact forces during rollover, and light enough to be negligible even when extended seven feet laterally out from the trailer walls. After extensive setup testing completed prior to actual track testing, the wheel height, or the distance between the bottom of the outrigger wheel at seven feet out to the ground, was set at nine inches, as shown in Figure 4-3. This height was chosen because outrigger contact meant initial wheel lift at the other side of the vehicle. Figure 4-3 also shows a latch used to secure the outrigger wheel from reaching heights under 9" during operation unintentionally due to vibrations or structural fatigue.

Figure 4-3. Outrigger wheel height.

The largest difference between the CVeSS outrigger design and that of NHTSA's (as well as all other trailer outrigger designs) is the added feature of contact force measuring at the contact wheel. This was done as an effort to use a novel method in quantifying rollover events instead of simply identifying them with wheel lift as NHTSA has done in the past. Two large-scale load cells were mounted within the outrigger inboard beam for this capability, as shown in Figure 4-4. NHTSA designed for and documented a load rating of 11,000 lb_f for their outboard beam due to the massive weight of Class 8 trailer in motion, and a simple statics analysis determined the necessary load cell measurement range of 0 – 200,000 lb_f. These potential enormous contact forces can be safely measured and evenly distributed to the trailer frames. The electrical work required for instrumenting and using the load cells calls for the ground clearance requirement previously mentioned. Figure 4-4 also shows many parts, namely the threaded rod, which are used to adjust the wheel height and transfer load from the wheel to the high-capacity tension load cell.

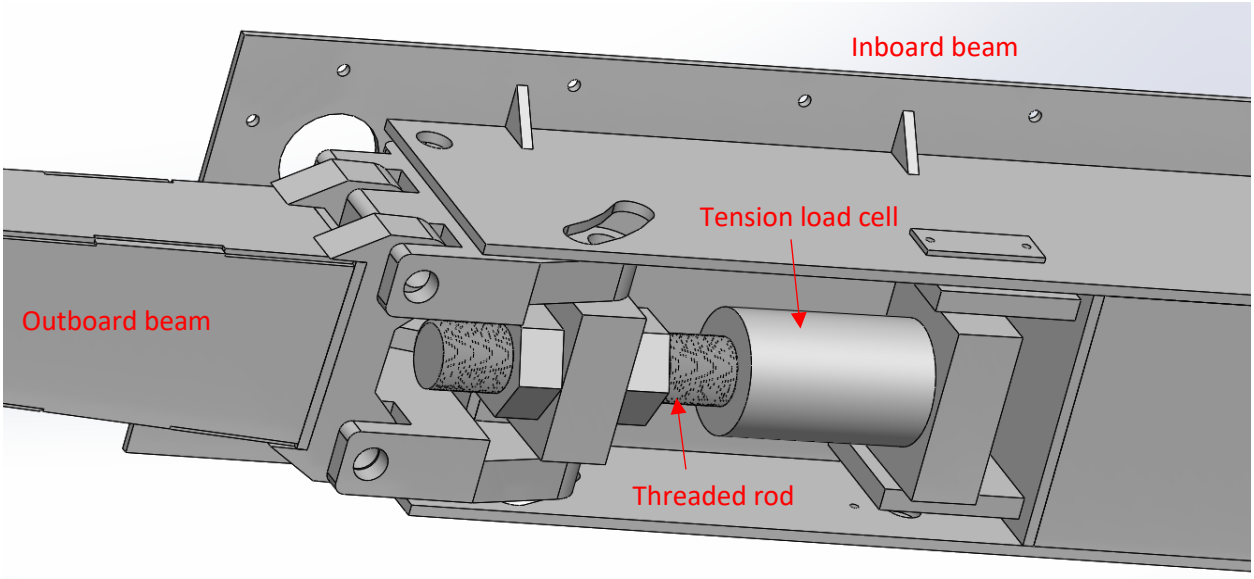

Figure 4-4. Load cell in outriggers.

4.1.2 Anti-Jackknifing System

Although the scope of this study does not involve jackknifing, it was still a major concern for the test vehicle during track testing. A large effort was taken to prevent any anti-jackknifing for safety precautions for, again, the vehicle as well as the humans in it. Since the roll and yaw motions are coupled, especially in aggressive maneuvers, stabilizing the yaw at each of the two articulation points of the test vehicle without affecting the roll dynamics during maneuvers is difficult. However, a support for the vehicle's yaw instability is needed just as the outriggers are needed for its roll instabilities. To accomplish this, CVeSS

used an arrangement of heavy-duty ropes and chains at both articulation points to simply constrain the maximum articulation angles allowed between adjacent vehicle units.

The primary feature of this anti-jackknifing system, or AJS, is the kinetic energy ropes used with its metal chains. The ropes absorb kinetic energy when elongated as the articulation angle exceeds a designed threshold length. This dissipation of yaw inertia is more gradual than other active anti-jackknifing control systems. The metal chains are used as a backup to the ropes for situations when they are overloaded or are not quick enough to absorb energy during severe instability, and are accordingly installed in parallel with the ropes. Contrary to the ropes, the chain only engages at the maximum allowed articulation angle and therefore when the ropes reach their maximum allowed lengths as well. Additional pintle hooks are mounted to the corners of both units involved in the two articulation points in order to connect AJS. A schematic of the AJS installed at both articulation points is shown in Figure 4-5.

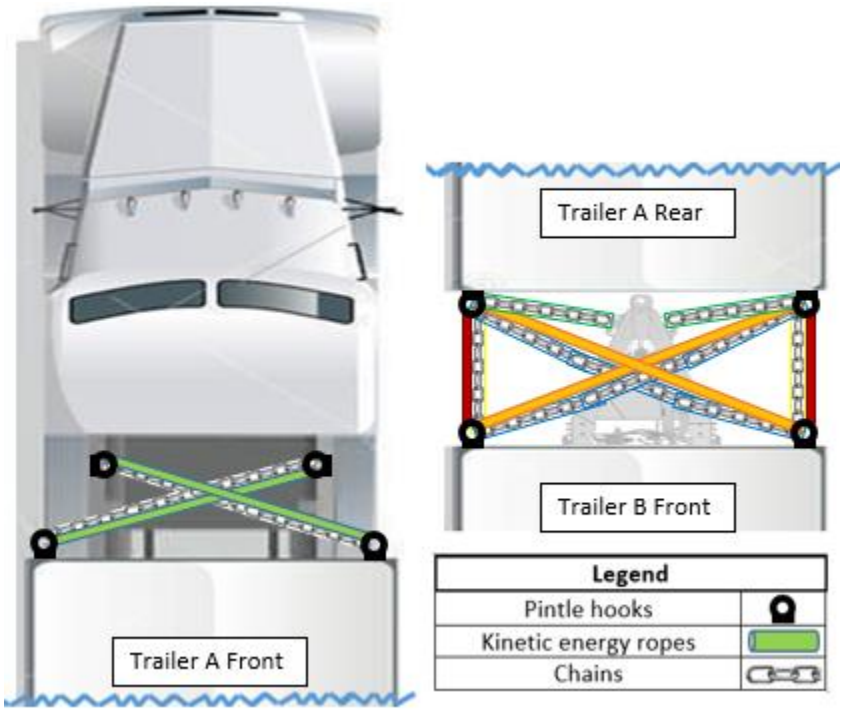

Figure 4-5. Anti-jackknifing system (AJS) ropes and chains diagram.

Simple 3-D geometry and math calculations were completed to determine the starting lengths of the rope and chains after some TruckSIM simulation studies for Case 1 (shown in Figure 4-6) running maneuvers discussed later in this chapter. If the ropes are too long, both scenarios of jackknifing, as well as trailer-to-trailer contact, are allowed to happen. If the ropes are too short, the vehicle would no longer act as an A-Double, but rather a B-double in the manner that Trailer B followed Trailer A's path seemingly without an

articulation point at the dolly. Because of the behavior predicted in the latter, the ropes were included in the TruckSIM model as springs with high stiffnesses. Variables under consideration were the maximum articulation angles between two units, as well as yaw inertia moments to purchase the correct strength rope. Pre-testing experimental trial and error was used to check and adjust lengths when either not enough vehicle maneuverability was demonstrated, or when too much articulation during test maneuvers was reached.

As seen in Figure 4-5, there are several more ropes and chains at the dolly than there are at the tractor end. This is done because there are two degrees of freedom (DoF) at the dolly due to its pintle hitch and fifth wheel, while the articulation point at the tractor and Trailer A only has one Dof at the fifth wheel. Two types of jackknifing can arise due to the two DoFs: trailer and dolly jackknifing. Examples of both types of jackknifing are shown in Figure 4-6, which shows the importance of the longitudinal set of ropes and chains (colored red in Figure 4-5) and the cross set (yellow ropes and blue chains) in prohibiting these two jackknifing scenarios between Trailer A and Trailer B.

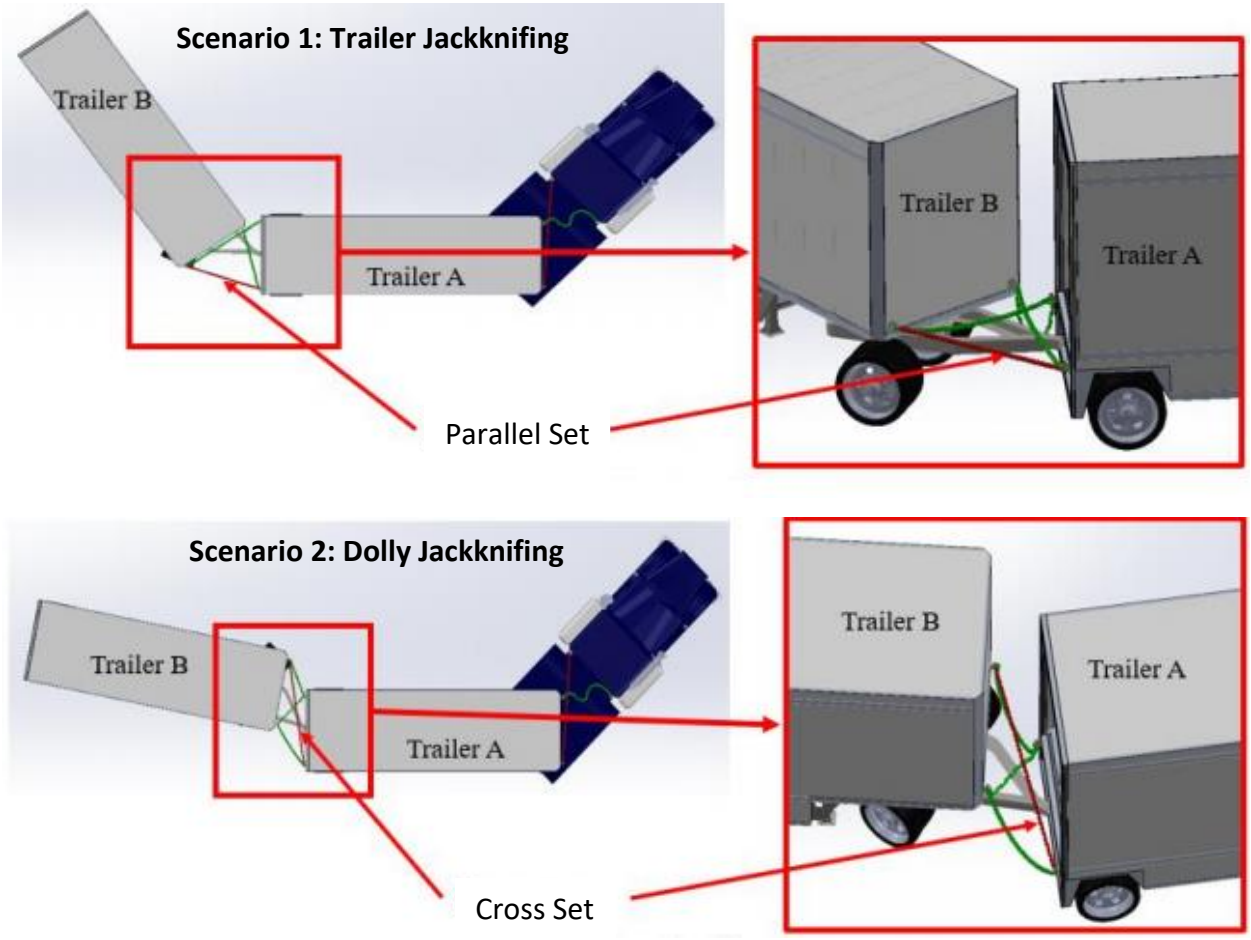

Figure 4-6. Two jackknifing scenarios between Trailers A and B.

The set of chains (green) are used to restrain the dolly for rotating during dolly jackknifing. There are no ropes installed with this set of dolly chains, as ropes are only used for trailers. These additional dolly chains were added as an extra precaution, as a third type of jackknifing that combines the two (shown in Figure 4-6) can occur in which the main concern is the trailer-to-trailer contact. By restricting dolly rotation with respect to Trailer A to 12.5^{o}, any risk of the third jackknifing event, which only occurs when the dolly follows Trailer B rather than Trailer A in a maneuver (such as when the vehicle is in reverse) is diminished. Figure 4-7 shows a picture of the dolly chains, as well as the rest of the AJS at the dolly. In order to quickly determine if any jackknifing had occurred, color-coded zip-ties used to restrict chain usage were checked. Some of these zip-ties are shown at the bottom of Figure 4-7, encircled in red.

Figure 4-7. AJS at dolly.

4.1.3 Trailer Reinforcement Beams

With the vehicle instrumented with support for roll and yaw instabilities, it needed to be fitted with the capability of handling the roll and yaw interties dissipated or transmitted by the outriggers and AJSs. As mentioned in Section 4.1.1, the outrigger contact forces are distributed into the trailer frames, but since

the semi-trailers are not designed to handle these loads, they can be severely damaged. Also, although the pintle hooks, ropes, and chains were durable enough to withstand trailer yaw moments, the trailer walls they were mounted to were not. Because of the need for structural strengthening for the scope of the study, roll and yaw reinforcement structures were created.

Figure 4-8 shows two views of a Solidworks CAD model of a semi-trailer with the complete reinforcement beam structure that was installed onto each of the two trailers in red. These structures were assembled using 4 in square steel rectangular beams along with steel gusset plates and SAE Grade 8 bolts, nuts, and washers. By mounting these structures to the trailer frame rails, force transfer from the outrigger wheels and anti-jackknifing systems was carried to the frame rails. The weight of these structures was considered in the calculation and design of the trailer cg, which is covered in the next subsection. A closer look at the roll reinforcement structure assembly (RRS) is labeled in Figure 4-8 and is shown in Figure 4-9.

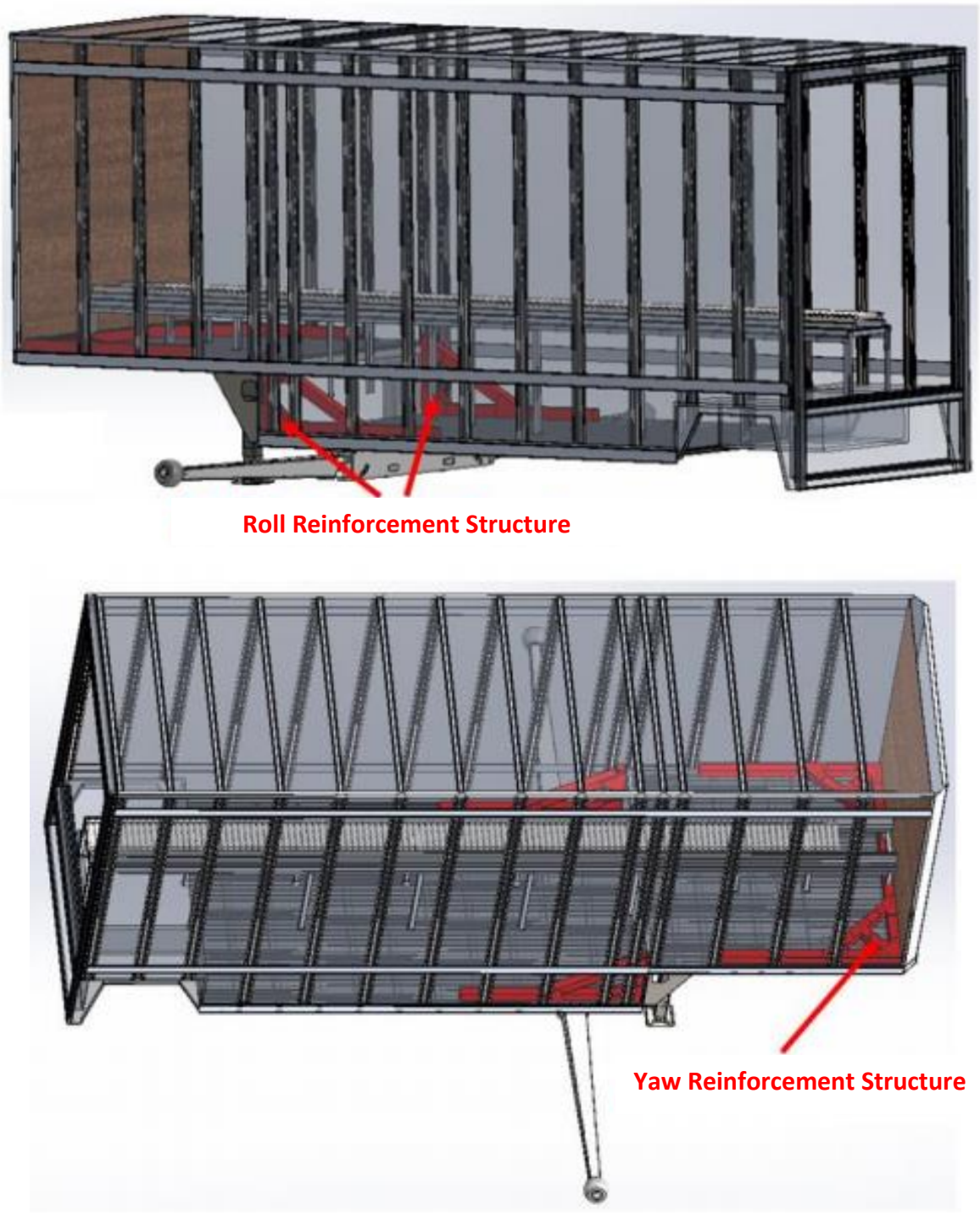

Figure 4-8. Reinforcement beam structures and placement in trailer.

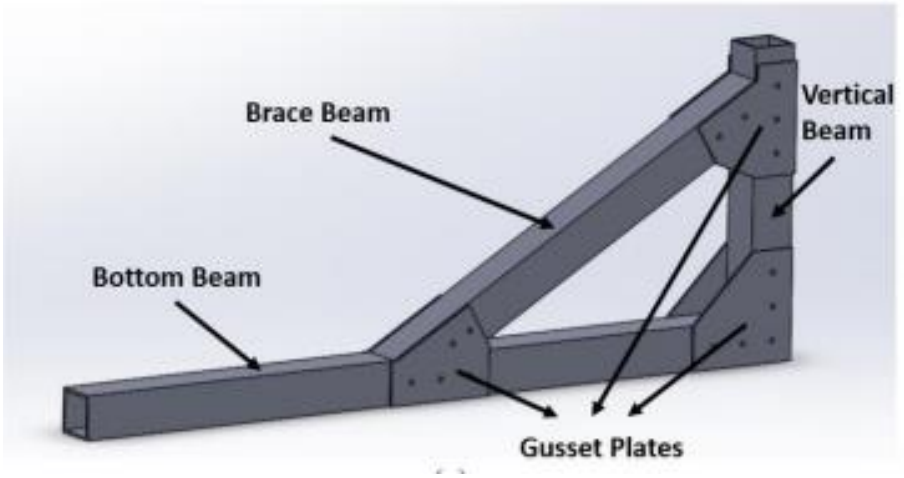

Figure 4-9. Design of roll reinforcement beams.

As seen in Figure 4-8, two of these structures are installed at the inside bottom corners of the larger compartment of the trailers. Not only was this area right above the outrigger mounting locations, but it also provided a vertical area to use to secure the RRS. This additional mounting method led to the design shown in Figure 4-9. The designed length of the bottom beam allows enough distribution of the contact forces transmitted from the outrigger assembly to the trailer frame rails without affecting the longitudinal cg location. This was important, as the total weight of both RSS was around 285 lbs. The vertical beam allows additional securing with longitudinal bolts to aid the vertical bolts along the bottom beam. The gusset plates and brace beam are used to strengthen the assembly.

The same design was used creating yaw reinforcement structures (YRS), which are shown in the bottom view of Figure 4-8. The one glaring difference between the two is that the two YRS assemblies are actually combined by the front beam, labeled in Figure 4-10. A front beam running across the entire lateral dimension inside the trailer was necessary for the trailer wall reinforcement plate used for AJS pintle hook mounting at the bottom of the bulkhead of both trailers. The entire YRS is shown in Figure 4-10.

The impact forces dissipated from the AJS to the pintle hooks during yaw would ultimately be transmitted to the trailer body as yaw inertia. Distributing these forces with long side beams of the YRS applies the same principle as the use of the bottom beams of the RRS assemblies. The 380 lbs. that the YRS added to the trailer weight was distributed through the lengths of the beams. Again, both longitudinal and vertical bolting allowed for structural rigidity.

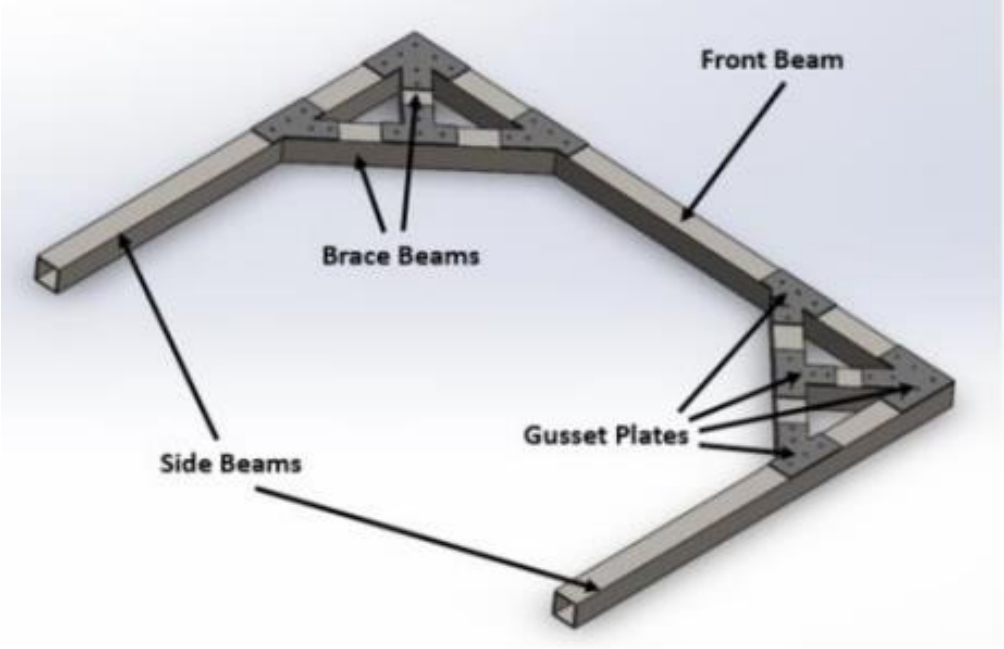

Figure 4-10. Yaw reinforcement structure.

4.1.4 Load Frame

In order to provide the most realistic study possible, properly loaded trailers are needed. Therefore, ideally, a typical loading configuration found in highway-used 28' drop-frame trailers was also used for the testing in this project. These drop-frame trailers are frequently employed in the trucking industry for their improved volumetric spacing, allowing greater logistic efficiency as shipped packages usually carry more volume than mass. A model of a drop-frame trailer is shown in Figure 4-11.

Also shown in Figure 4-11 is a red mass inside the trailer, which is representative of a typical loading configuration (according to management within a large trucking industry company) of a drop-frame trailer: 6,000 lbs. distributed across 75% of the available volume within the trailer. Table 4-1 displays the numbers behind this typical load, including cg position. The variables presented in Table 4-1, most importantly the cg location, needed to be replicated in order to simulate the empty test trailers as trailers with the dynamic characteristics as they are usually loaded.

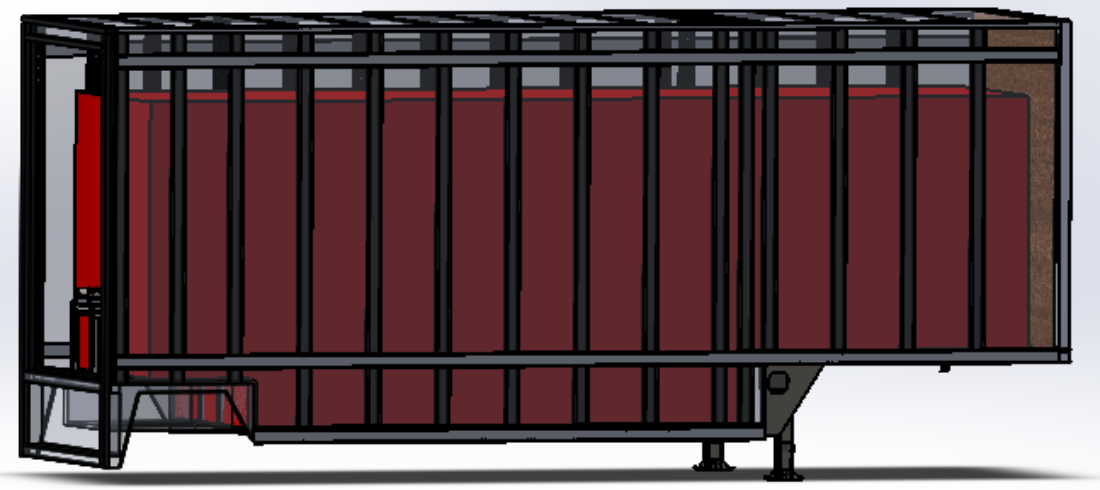

Figure 4-11. Drop frame trailer and typical loading configuration.

Table 4-1. Typical load properties for 28’ drop frame trailer.

	Typical Loading Configuration
Total weight	6,000 lbs.
CG height from ground	74.8 in.
CG longitudinal distance from bulkhead	170.66 in.
Roll inertia at ground	117839173 $lb \cdot in^2$
Pitch inertia at ground	235916591 $lb \cdot in^2$
Yaw inertia at fifth wheel	450541787.02 $lb \cdot in^2$

A load frame designed by CVeSS was created for this purpose. A double-layered pallet-rack structure holding sandbags was chosen as the suitable design with the following listed capabilities:

- Compensate for the effects of outriggers and reinforcement structures on cg height and moments of inertia,
- Withstand outrigger wheel impact forces and the resulting accelerations from cornering and braking, and
- Take advantage of the vertical volume available in the trailer while circumventing the rolling table situated in the middle.

The load frame structure allowed for these extra capabilities due to its design, such as the ability to adjust the height of the pallets and adjust the weight by removing or adding sandbags. These sandbags made up the remaining weight needed to mimic a loaded trailer.

Four I-beams and pallet rack loading beams were used to create the structure of the assembly, and the I-beams were fixed to the floor and to each other. Several measures were taken in order to secure the load frames securely, as they would roll with the trailer collectively. L-brackets were used to secure the I-beams to the rolling table, and steel cables from the four bottom corners of the trailer were used to fix the load frame further. Another load-supporting frame structure that ran two lateral support racks to back the two pallet racks was added for further support against rollover.

FEA on the load frame design was done using SOLIDWORKS, and the results are shown in Figure 4-12. As seen in the figure, the maximum stress of approximately 20,000 lb. from a uniformly-applied 2,500 lb. and 1,259 lb. vertical and lateral force, respectively, is much lower than the yield strength of the assembly (approximately 36,000 psi).

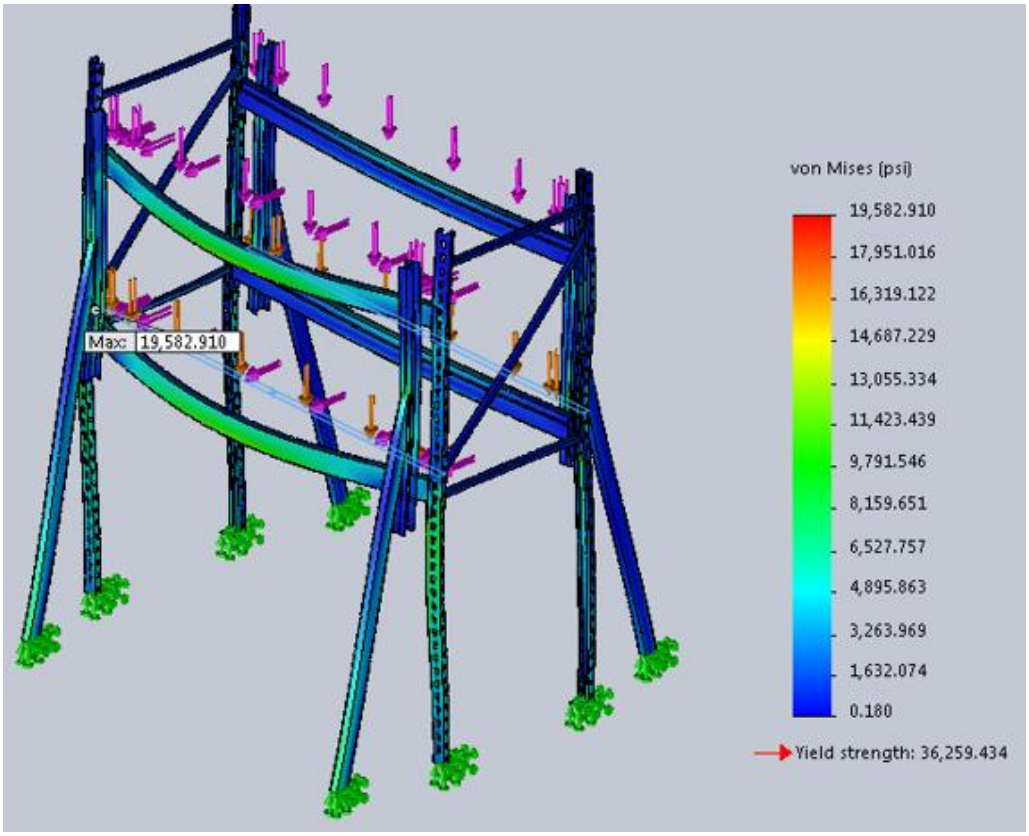

Figure 4-12. SOLIDWORKS FEA analysis on load frame.

The design for the CVeSS load frame is shown in Figure 4-13. It should be noted that this 3D model does not include the lateral load supporting frame, securing steel cables, and the 50-lb. sandbags used to make

up the rest of the weight. Instead, Figure 4-14 shows the entire side of Trailer B and displays the entire load frame system.

Figure 4-13. Model of load frame within a trailer.

The total weight of the outriggers, load frame, and reinforcing structure systems was approximately 2,600 lbs. The rest of the 3,400 lbs. were added by sandbags, with 34 in each pallet. Once loaded, the double-bagged sandbags are secured down within the pallets using wood beams and ratchet straps. The correct weight and distribution of this load is the second most important need in this study, and the results of the load frame implementation on both are shown in Table 4-2. These results were considered acceptably within the range of desired values by the test team.

Table 4-2. Trailer load characteristics.

	Typical Loading Configuration	**Instrumented Trailer Loading**	**% Difference**
Total weight	6,000 lbs.	5,980 lbs.	-0.002%
CG height from ground	74.8 in.	73.68 in.	-1.5%
CG longitudinal distance from bulkhead	170.66 in.	167.2 in.	-2%
Roll inertia at ground	117839173 $lb \cdot in^2$	129415570.94	+9.8%
Pitch inertia at ground	235916591 $lb \cdot in^2$	215165643.01	-8.8%
Yaw inertia at fifth wheel	450541787.02 $lb \cdot in^2$	399924978.36	-11.2%

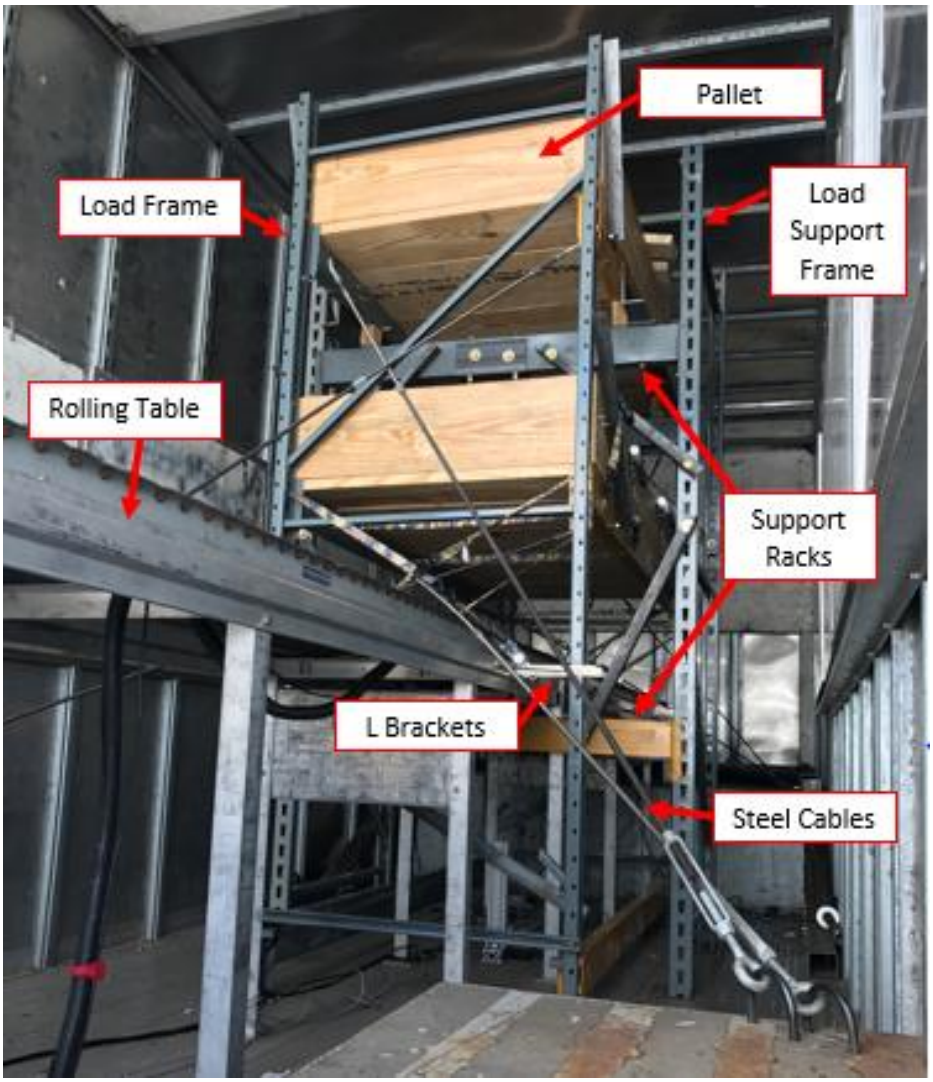

Figure 4-14. Entire Load frame system.

4.1.5 Steering Robot

The single most important aspect of test preparation was the creation of a steering robot. Without several testing constants, such as tire and road conditions, trailer loading configuration, suspension characteristics, etc., RSC system comparisons would not be valid. Among these needed constants, steering input for the same maneuver is absolutely crucial. Having a steering robot to handle steering brings about several advantages over having a professional driver. Some standard test maneuvers require precise steering inputs, and the more identical each test run is the better. Also, since both the number of tests planned is massive and test track availability is limited, testing must be completed over several weeks. The difference in repeatability found in machines over humans is even larger when the testing is over several weeks. Obviously there is less error in maneuvering during valuable test track time as well.

Most commercially available steering robots for Class 8 tractors regulate the vehicle speed during operation and also cost nearly $200,000. The steering robot made at CVeSS does neither. The hardware for the robot is installed in the engine bay and operates by applying a coded steering input directly at the steering column. A clamp design around the steering column means that this steering robot could be installed on any steering column of 1.5 in diameter with enough space in the engine bay to accommodate the hardware shown in Figure 4-15. The steering robot module includes a motor/gearbox/controller unit, a roller chain to link the motor to the steering column, split spherical roller bearings, and a torque reaction mount. A disadvantage along with the inability to automate vehicle speed is the need for an additional operator during vehicle operation to run, control, and modify the robot or steering inputs.

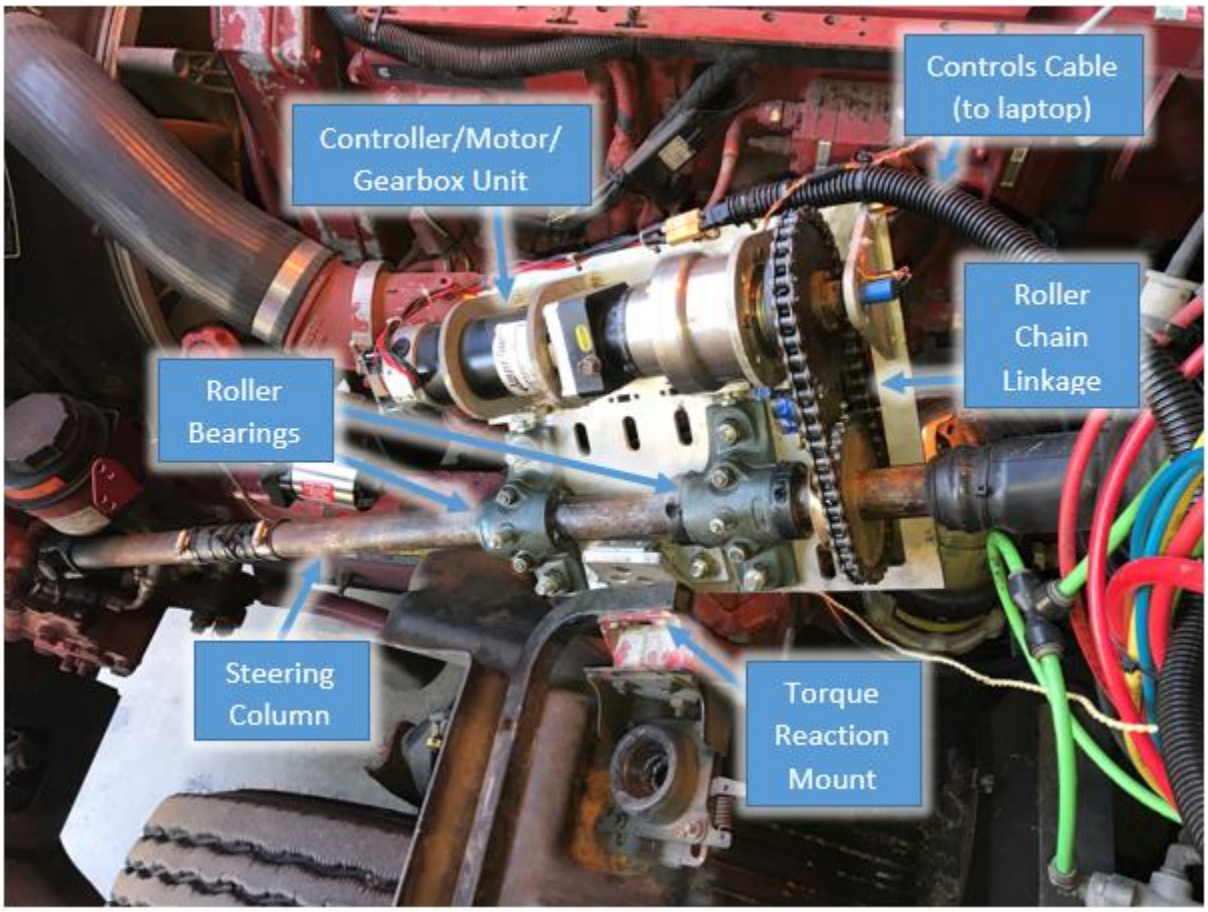

Figure 4-15. Steering robot hardware in engine bay.

For safety, the steering robot engages via control by a Deadman's switch. At all times when the Deadman's switch is not on, the driver has full control of the vehicle. The steering input for every test must be pre-loaded into the controller with the laptop and appropriate software. Operation of the steering robot therefore requires another passenger within the cab. As explained before, the CVeSS steering robot does

not control the vehicle speed, so the driver is always in control of the throttle, brakes, and gear changes during vehicle operation. An emergency stop switch was mounted on top of the dashboard to terminate any undesired, dangerous steering results.

Most of the effort done to install an operational steering robot required extensive controls work and knowledge. Some electronic discussion regarding the steering robot and data acquisition system will be discussed in Section 4.2. The controls behind the steering robot will not be covered in this paper.

4.1.6 Other Hardware Setups

Several other preparations were made to the vehicle in preparation for testing, the most important of which was the painting of the vehicle wheels. All axle tires were painted white so that wheel lift and wheel lock were more easily discernible in testing and in video recording during post analysis. This is shown in Figure 4-16.

Also shown in Figure 4-16 is one of the outriggers. The outrigger wheels were taped with yellow and black warning tape for the same purpose of ease of visibility during testing and post analysis of outrigger hits. Taping of the vehicle wheels was repeated for each set of new tires installed at the beginning of every test week. New tires ensured similar tire dynamics week to week, allowing valid RSC performance comparisons. The figure shows a clean central portion of the outrigger wheel, which occurs when enough rollovers have happened and the tape is ripped off.

Figure 4-16. Outrigger wheel and vehicle wheel preparation.

Several other hardware implementations were undertaken for installing the necessary sensors, and will be covered in Section 4.2.

4.2 Data Acquisition System

This section covers the sensor and data acquisition system instrumentation for the vehicle used for this study. There were a total of 31 sensors that were calibrated, installed, and used on the vehicle at first, but only a certain number of them were used for main evaluation of RSC performances. Based on the nature of RSC systems, it was found that the most important sensors for this study were the trailer pressure sensors, load cells, steering wheel angle sensor, and accelerometers. The other sensors, such as the LIDAR sensors (from LEDDAR) and string potentiometers, were found to be more important for collecting information regarding the vehicle dynamics and suspension. The following sections will cover the details regarding the installation and purposes of the pressure, load cells, steering wheel angle, and accelerometer sensors, as well as the data acquisition system used with them – the National Instrument CompactRIO.

A total of 31 sensors were installed on the vehicle, and even though only four types of sensors were used for RSC performance gauging, the others were still used to gain valuable information regarding the dynamics of the vehicle for future analyses. The tractor and trailer suspension information can be used to model the vehicle in TruckSim to simulate even more configurations than were professionally tested. The following sections cover both the sensors used for measuring RSC performances.

The overall sensor list and setup are shown in Table 4-3 and Figure 4-17, respectively. Figure 4-17 shows the general area of the sensors on the vehicle, as well as the LED lights and GoPro cameras. Figure 4-17 also shows how the multiple sensors are powered and managed by junction boxes. These junction boxes are denoted as JB1 and JB2 for Trailer A and Trailer B, respectively. A third “Power” box is found in the cab with the data acquisition unit and several sensors. Table 4-3 consists of the sensor type, brand, model, measurement range, necessary supply voltage, output data format, sensor label, and application. The sensors detailed in this section are highlighted in blue.

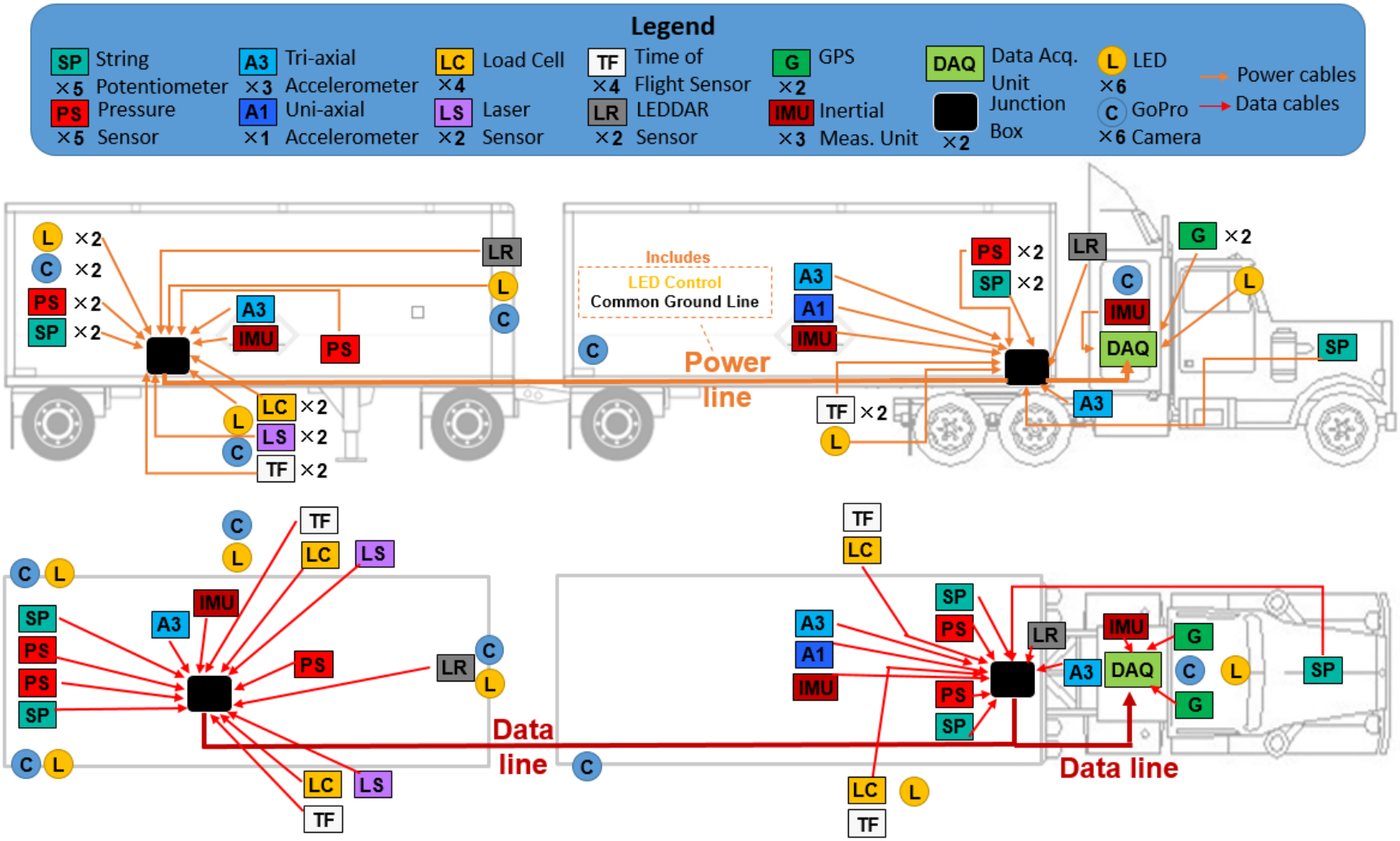

Figure 4-17. Overall sensor schematic. A total of 30 sensors in total are used.

Table 4-3. Overall sensor list and details.

	Sensor Type	Brand and Model	Measurement Range	Supply Voltage	Output Type	Label	Application
1	String potentiometer	Uni Measure – VP510-10-NJC	0 – 10 in.	25 V Max.	Analog	SP-3	Suspension travel on driver's side – rear trailer
2	String potentiometer	Uni Measure – VP510-10-NJC	0 – 10 in.	25 V Max.	Analog	SP-4	Suspension travel on passenger's side – rear trailer
3	String potentiometer	Uni Measure – VP510-10-NJC	0 – 10 in.	25 V Max.	Analog	SP-5	Suspension travel on driver's side – tractor
4	String potentiometer	Uni Measure – VP510-10-NJC	0 – 10 in.	25 Volts Max.	Analog	SP-6	Suspension travel on passenger's side – tractor
5	String potentiometer	Uni Measure – HX-P510-15-NJC-N6-L3M	0 – 15 in.	4.9 – 30 VDC	Analog	SP-S	Steering wheel angle
6	Pressure transducer	OMEGA – PX329-200G5V	0 – 200 psi	9 – 30 VDC	Analog	PS-1	Air tank pressure – rear trailer
7	Pressure transducer	OMEGA – PX329-200G5V	0 – 200 psi	9 – 30 VDC	Analog	PS-2	Airbag pressure on driver's side – rear trailer
8	Pressure transducer	OMEGA – PX329-200G5V	0 – 200 psi	9 – 30 VDC	Analog	PS-3	Airbag pressure on passenger's side – rear trailer
9	Pressure transducer	OMEGA – PX329-200G5V	0 – 200 psi	9 – 30 VDC	Analog	PS-4	Airbag pressure on driver's side - tractor
10	Pressure transducer	OMEGA – PX329-200G5V	0 – 200 psi	9 – 30 VDC	Analog	PS-5	Airbag pressure on passenger's side - tractor
11	Load cell	OMEGA – LC714	0 – 200,000 lb.	10 VDC (15 VDC max.)	Analog	LC-1	Outrigger contact force on driver's side – rear trailer
12	Load cell	OMEGA – LC714	0 – 200,000 lb.	10 VDC (15 VDC max.)	Analog	LC-2	Outrigger contact force on passenger's side – rear trailer
13	Load cell	OMEGA – LC714	0 – 200,000 lb.	10 VDC (15 VDC max.)	Analog	LC-3	Outrigger contact force on driver's side – front trailer
14	Load cell	OMEGA – LC714	0 – 200,000 lb.	10 VDC (15 VDC max.)	Analog	LC-4	Outrigger contact force on passenger's side – front trailer
15	Laser sensor	Omron ZX1-LD600A86	200 – 1,000 mm (7.87 – 39.37 in.)	30 VDC max.	Analog	LS-1	Outrigger distance to the ground on driver's side – rear trailer

16	Laser sensor	Omron ZX1-LD600A86	200 – 1,000 mm (7.87 – 39.37 in.)	30 VDC max.	Analog	LS-1	Outrigger distance to the ground on passenger's side – rear trailer
17	Accelerometer	PCB 3713D1FD3G	0 – 3G	6 – 30 VDC	Analog	A3-3-1	Longitudinal, lateral, and vertical acceleration – tractor frame
18	Accelerometer	PCB 3713E1150G	0 – 50G	6 – 30 VDC	Analog	A3-50-2	Longitudinal, lateral, and vertical acceleration – front trailer
19	Accelerometer	PCB 3713D1FD3G	0 – 3G	6 – 30 VDC	Analog	A3-3-2	Longitudinal, lateral, and vertical acceleration – rear trailer
20	Accelerometer	PCB 3741D4HB10G	0-10G	6 – 30 VDC	Analog	A1-4273	Lateral acceleration – front trailer
21	LIDAR sensor	LeddarTech M16	0 – 25 m (0 – 85 ft)	12 – 24 VDC	Digital	LD-1	Articulation angle between the tractor and the front trailer
22	LIDAR sensor	LeddarTech M16	0 – 25 m (0 – 85 ft)	12 – 24 VDC	Digital	LD-2	Articulation angle between the front trailer and the rear trailer
23	GPS	Garmin GPS 18x-5Hz	N/A	5 VDC	Digital	N/A	Tractor travelling speed and path
24	GPS	Chang Hong Information GPS Magnetic Antenna	N/A	2.3 – 5.5 VDC	Digital	N/A	Tractor traveling speed and path
25	IMU	SparkFun Electronics LSM9DS1	0 – 8G	1.9 – 3.6 VDC	Digital	IMU-T	Accelerations and angular rates in 3D – tractor cab
26	IMU	SparkFun Electronics LSM9DS1	0 – 8G	1.9 – 3.6 VDC	Digital	IMU-A	Accelerations and angular rates in 3D – front trailer
27	IMU	SparkFun Electronics LSM9DS1	0 – 8G	1.9 – 3.6 VDC	Digital	IMU-B	Accelerations and angular rates in 3D – rear trailer
28	Time of Flight Sensor	ST Microelectronics VL53l0X	0 – 2 m	2.6 – 3.5 VDC	Digital	TF1	Outrigger distance to the ground on driver's side – front trailer
29	Time of Flight Sensor	ST Microelectronics VL53l0X	0 – 2 m	2.6 – 3.5 VDC	Digital	TF2	Outrigger distance to the ground on passenger's side – front trailer
30	Time of Flight Sensor	ST Microelectronics VL53l0X	0 – 2 m	2.6 – 3.5 VDC	Digital	TF3	Outrigger distance to the ground on driver's side – rear trailer
31	Time of Flight Sensor	ST Microelectronics VL53l0X	0 – 2 m	2.6 – 3.5 VDC	Digital	TF4	Outrigger distance to the ground on passenger's side – rear trailer

4.2.1 Tractor Hardware

There are a total of ten total sensors located on the tractor, four of which are located in or on the cab. This list includes two GPS units, one string potentiometer (steering wheel angle sensor), and an inertial measurement unit (IMU). There are also a "Power Box" and data acquisition system (LabVIEW CompactRIO, or cRIO), which are mounted to the cab table at the back seats. The electronics behind the steering robot will be briefly covered as well.

The Power Box supplies power to all vehicle sensors in conjunction with the two junction boxes in the trailers. The Power Box is made up of a breadboard circuited with 5V voltage regulators, and supplies a constant 13V supply, a constant 5V supply, and a switched 13V supply. The three different circuits are separated in an efficient manner via electric binding posts and ring terminals, as shown in Figure 4-18. A breadboard is also used to change the original 13V circuit to 5V circuit. Figure 4-18 shows a picture of the Power Box with binding posts and labels for the three different supply circuits. Several different appliances are connected to the Power Box. Figure 4-18 also shows two bus bars – one for power and one for ground – that help clean up the connections for the number of connected appliances. A power output port for a "Power" cable made up of male-to-male BNC coaxial cable to transfer battery power from the Power box to the junction box in Trailer A was created. A binding post adapter was used on both ends of the Power cable as shown in Figure 4-18. The switch used to control the switched 13V power circuit is shown in Figure 4-19; this circuit is primarily used for LEDs.

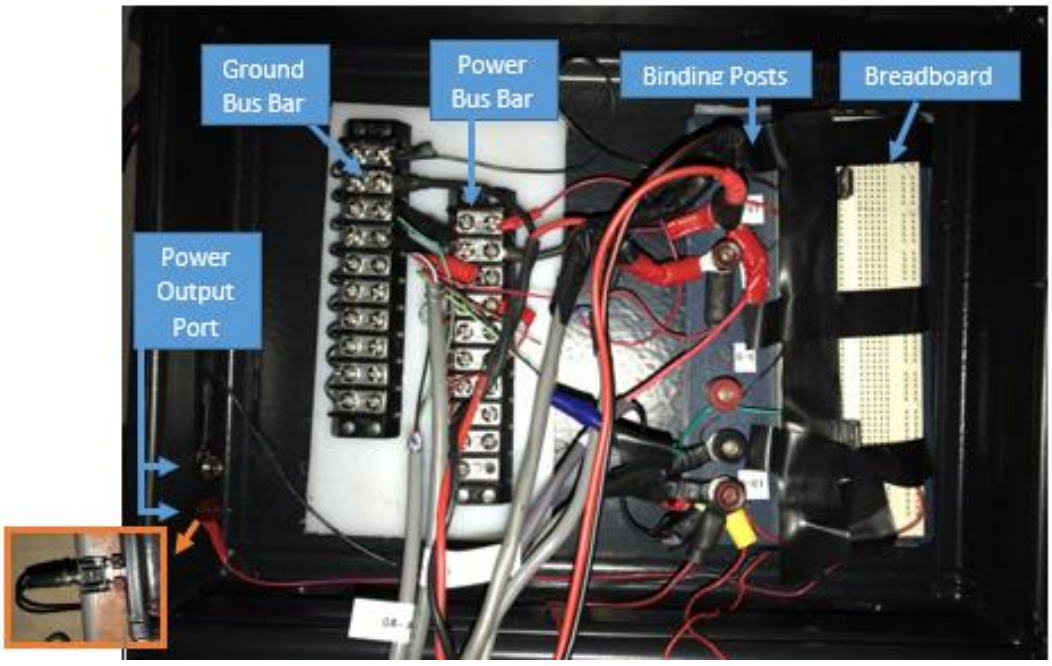

Figure 4-18. Power Box in tractor.

The data acquisition system, or the cRIO, is placed next to the Power Box. It is powered by the constant 13V circuit in the Power Box and is connected to the laptop with an Ethernet cord for data access. The 13V power source is supplied by four Lithium-Ion battery cells connected in series with a charging port connector and a power output connector as well. The cables used to connect a battery to the respective junction box have a fuse soldered for the safety of the data acquisition system. This is shown later in Figure 4-24. The layout for the Control Desk in the tractor is shown in Figure 4-19. More about the cRIO is available in Appendix B.

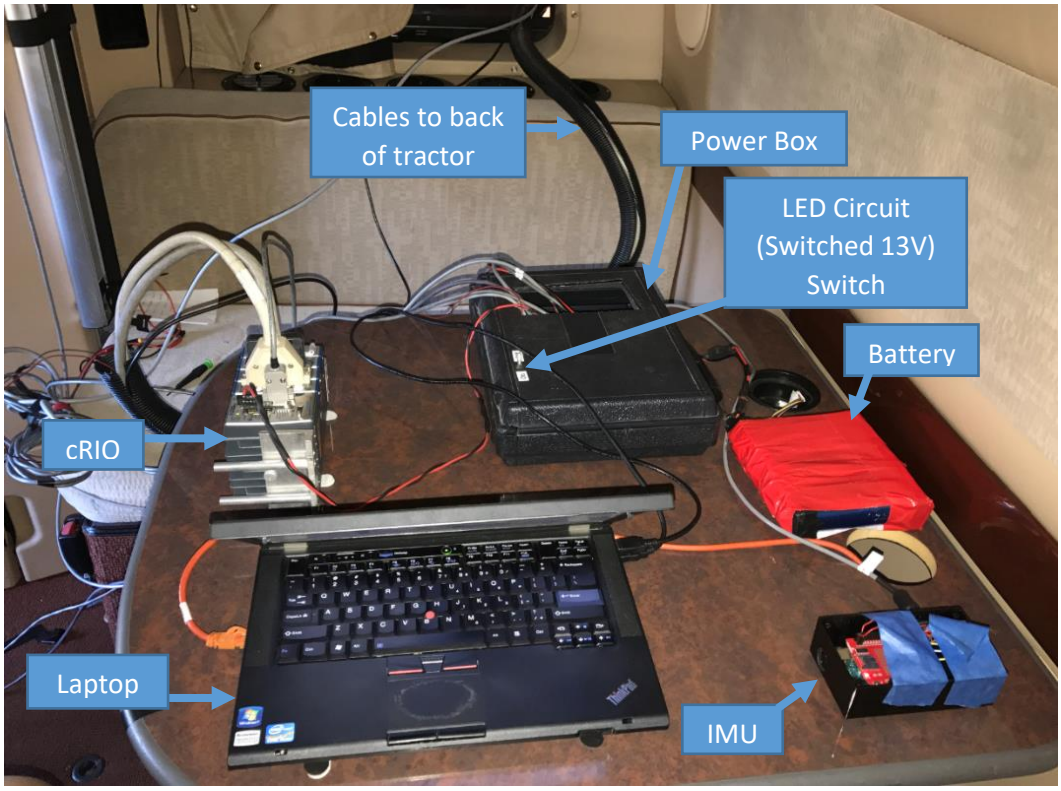

Figure 4-19. Control Desk in tractor.

Among the several sensors and appliances installed in the cab or around the tractor, the GPS units, the tractor accelerometer, the steering wheel angle sensor, and the cab LED are directly used for RSC evaluation. The two GPS units and LED are routed under the passenger seat and up the passenger door pillar, as the GPS units are actually mounted outside on the hood, and the LED is mounted under the sun visor for easy camera vision. The GPS units are used to record the speed and tracking of the tractor during operation, since the steering robot does not automate vehicle speed. The LEDs on the vehicle are all within a camera's view, and are used to synchronize the cameras and data together. More about LED and camera usage is available in Section 4.2.5.

It should be noted that the steering wheel angle sensor is not directly connected to the Power Box, but will be covered in this section. The steering wheel angle sensor is actually a string potentiometer that is wrapped around the steering column. As the steering column rotates, any retraction or extension of the string potentiometer is used with the circumference of the 1.5 in diameter steering column and the tractor's steering ratio to determine the steering wheel angle. A steering wheel angle sensor is a clean method of determining whether the steering robot had operated correctly for each test. The mounting of the steering wheel string potentiometer is shown in Figure 4-20. The steering wheel string potentiometer is mounted orthogonally to the steering column at the same height as the top of the column. The string potentiometer wire was then wrapped around the steering column, wrapped in rubber and secured with zipties, and then calibrated. The cabling for this sensor is routed under the tractor along the chassis and into Trailer A's junction box, JBA, through the bulkhead.

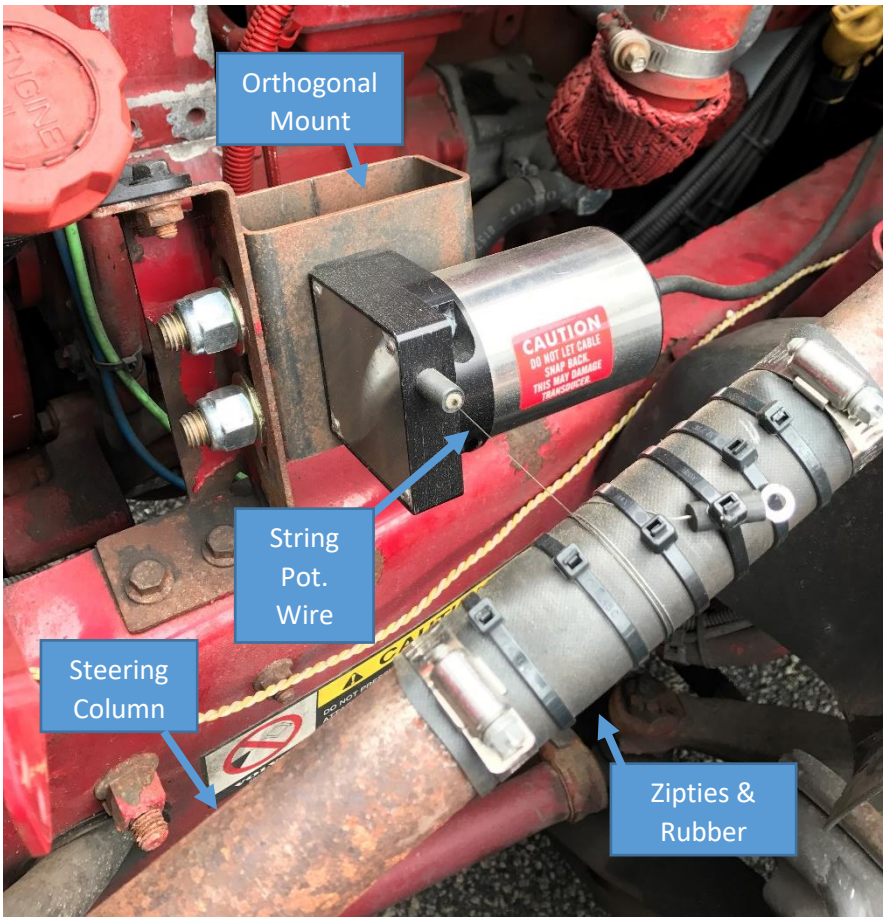

Figure 4-20. Steering wheel string potentiometer installation.

The cab frame accelerometer is connected to the junction box in Trailer A, and it is mounted using a previous bolt hole on a convenient previously-existing yet unused bracket. Although more emphasis is

placed on the lateral accelerations at the trailers, a reference tractor lateral acceleration is needed for comparison. These accelerometers must be placed near the cg of the vehicle unit on which they are mounted, and this holds true for those on Trailer A and Trailer B, as will be discussed.

Lastly, the steering robot hardware covered in Section 4.1.5 is controlled by a laptop and electronics in a suitcase kept in the cab. Again, this document does not provide information regarding the electronics used in the control scheme, or the control scheme itself. General operation information, however, is covered. The aforementioned Deadman's switch was wired together with the LED circuit, or the switched 13V circuit from the Power Box. By doing so, the LEDs flag whenever the steering robot is on via the Deadman's switch, and thus whenever testing is underway.

4.2.2 Trailer Hardware

This section will cover the installations for the pertinent sensors on both trailers, and will include the load cells, the LEDS, and the accelerometers. A closer look at the load cells is provided first, because while a model was shown in Section 4.1.1, no information regarding their installation was given. A picture of the load cell within the outrigger assembly is shown in Figure 4-21. The figure shows the order of installation for the parts within the outrigger assembly when observed from left to right: a height adjustment cube, the Omega load cell, the threaded rod, a height adjustment nut, the second height adjustment cube, and the second height adjustment nut to finish. It should be noted that installation of the load cell was not as easy as described, as there was no indication or mechanical design to show at what position the load cell should be placed in order to point its data cable port in a desirable position with enough ground clearance. Figure 4-21 shows a configuration in which there is barely enough ground clearance, as the data cable connector and cable need additional space to bend the cable back up towards the trailer. Small holes were drilled into the center of both trailers near the outrigger locations where the load cell cables were routed to their respective junction boxes. Ideally, the load cells would be installed before the outriggers, but due to a lead time of up to two months, this option was unavailable for the team.

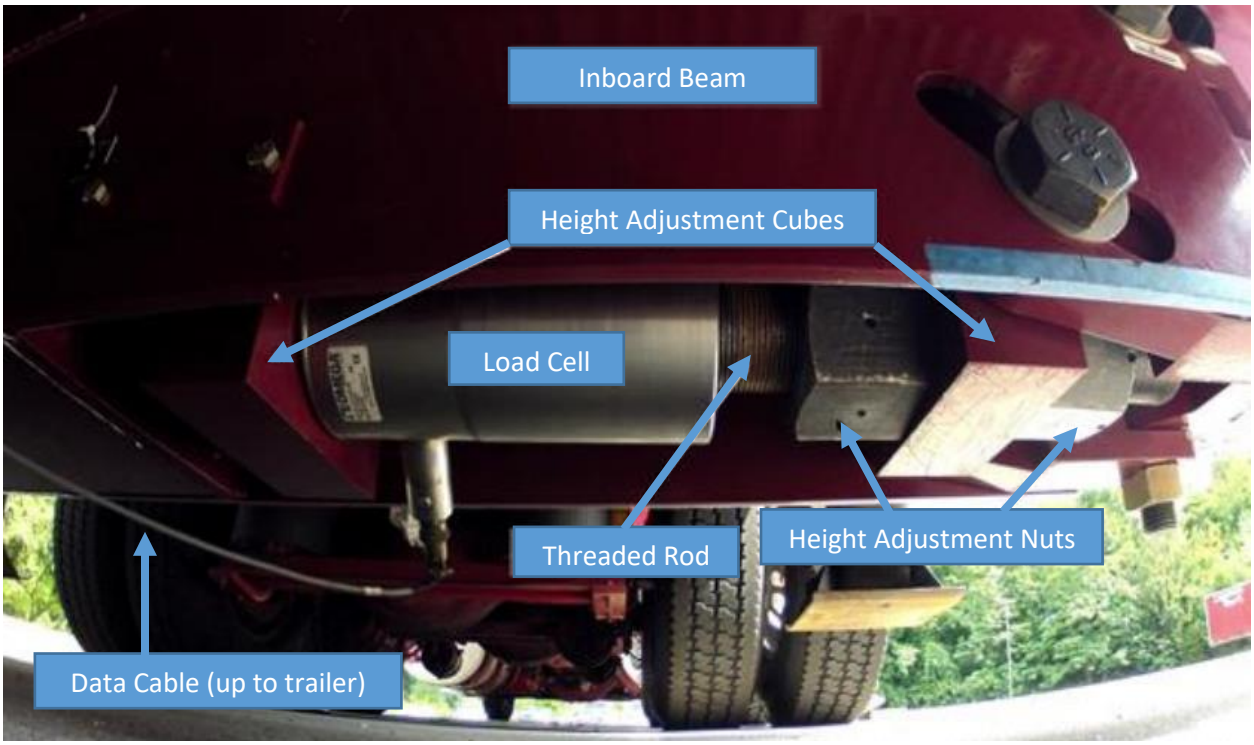

Figure 4-21. Load cell within outrigger.

One tri-axial accelerometer was placed on each vehicle unit, and one IMU unit was installed near those on the trailers for additional lateral acceleration readings for high accuracy measurements. The resolution of the tri-axial accelerometers is lower than that of the uni-axial accelerometers, so while the tri-axial accelerometer was mounted in the correct vertical cg height at 1.25 ft from the trailer floor, the uni-axial accelerometer was not. A mounting assembly made of three L-brackets and two pieces of 8020 structure were used as a simple method of securing the tri-axial accelerometer. Bolt holes were drilled through the bottom of the trailer to fix the 8020 structure. The same method of mounting accelerometers was used at both trailers. A uni-axial accelerometer at Trailer A was installed due to the resolution of the 50g range tri-axial accelerometer used there. It was simply duct-taped to the 8020 structure at the lateral cg location as it was only installed as a backup measure on the fly. The IMUs were attached under the same circumstance.

4.2.3 Junction Box A

As mentioned previously, several of the tractor sensors are actually powered by the junction box in Trailer A, JBA, due to the proximity of JBA to these sensors. A 3.5 in hole was drilled through the front wall in order to route the cables and wires from the tractor sensors. Figure 4-22 shows the final design of the box in its entirety, with labels for each part of the box. As seen in Figure 4-22, there are two bar buses that

supply 13V to anything connected to them when their circuit is switched on. The switched 13V supply comes from the LED wire from the Power Box mentioned in the prior section. There is one power and one ground bar bus, and these are generally used for the LEDs mounted on Trailer A due their switch-based activation. A second, smaller breadboard is seen next to the green DB-37 breakout board. The Trailer A Data Cable is connected to this breakout board and uses a DB-37 connector. This smaller breadboard is used for two reasons: (1) to supply a constant 5V and (2) to feedback a 5V pulse synced with the LED 5V switch circuit to the data acquisition system. The cRIO is only capable of reading channels of 0 – 10 volts, so the 13V supply voltage from the batteries connected to the Power Box must be regulated down. Finally, a third bus bar can be found above the breakout board in Figure 4.9. This bus bar was not used for general data acquisition, but was instead added for a specific RSC system which required additional relays for each trailer to determine activations. All components of the junction boxes are screwed down, with additional double-sided tape under the Power Board to protect the solders at the underside.

Figure 4-22 shows the sensor ports, which safely and quickly connect or disconnect sensors to the data acquisition system via a breakout board and breadboard supplying power, or Power Board. By using both breakout boards and Power Boards, the data acquisition system is made modular, allowing quick modifications to both the number of sensors and types of sensors. The Power Board voltage is supplied by power and ground binding posts and the Power Cable, which extends from the Power Box circuit supplied by the batteries, and provides the same circuit to all soldered sensor ports. The systematic organization of the sensor ports and custom-made sensor cables allow sensors to use any port. This is shown in Figure 4-23.

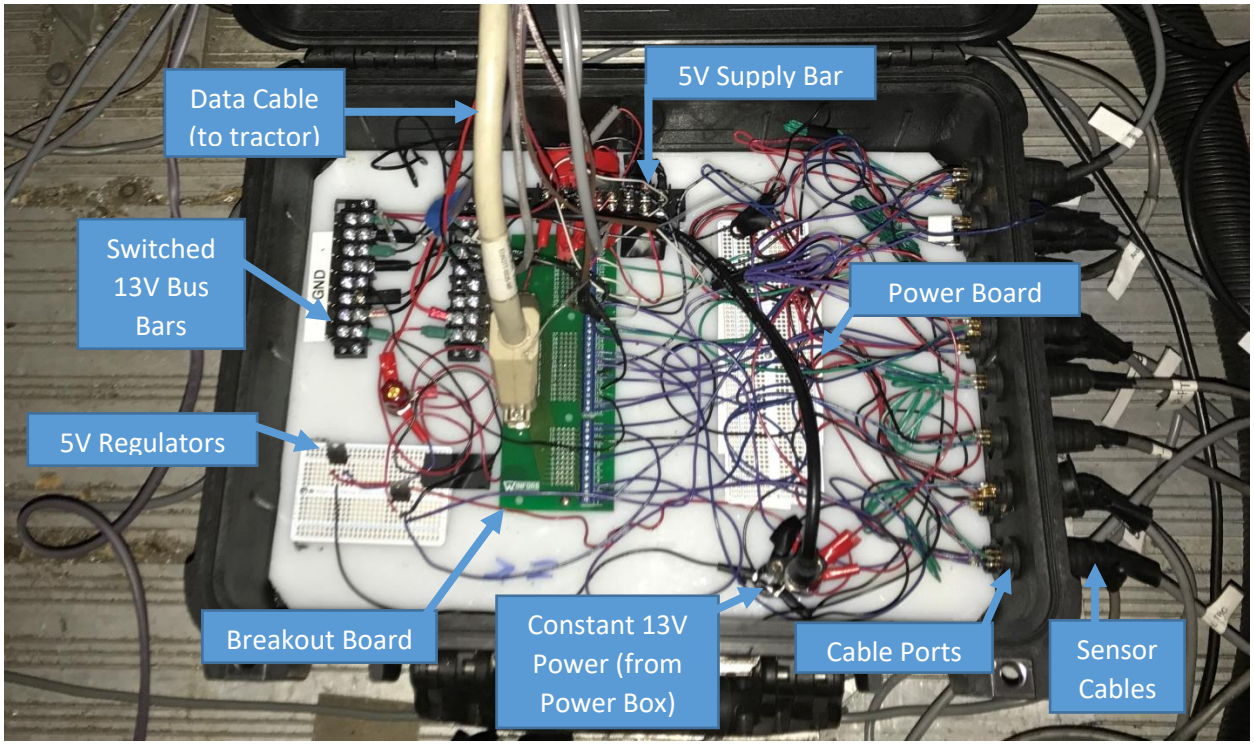

Figure 4-22. Junction Box A (JBA) and its components.

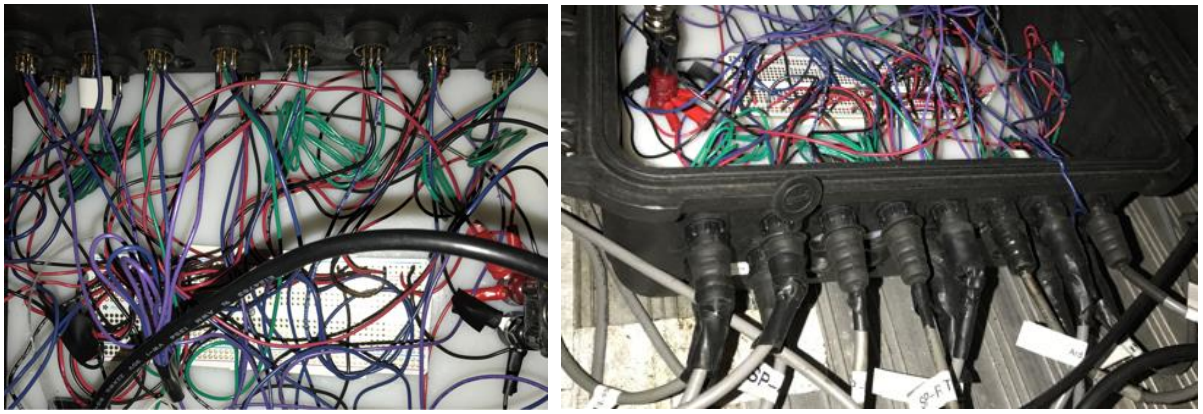

Figure 4-23. Closer look at JBA's sensor ports and receptacles.

4.2.4 Junction Box B

Junction Box B (JBB) is quite similar to JBA, but differs somewhat due to power and sensor configuration requirements. As for JBA, only the final design/arrangement for JBB will be discussed. Figure 4-24 shows the box, and the rest of this section will describe the uses of each labeled portion of the box.

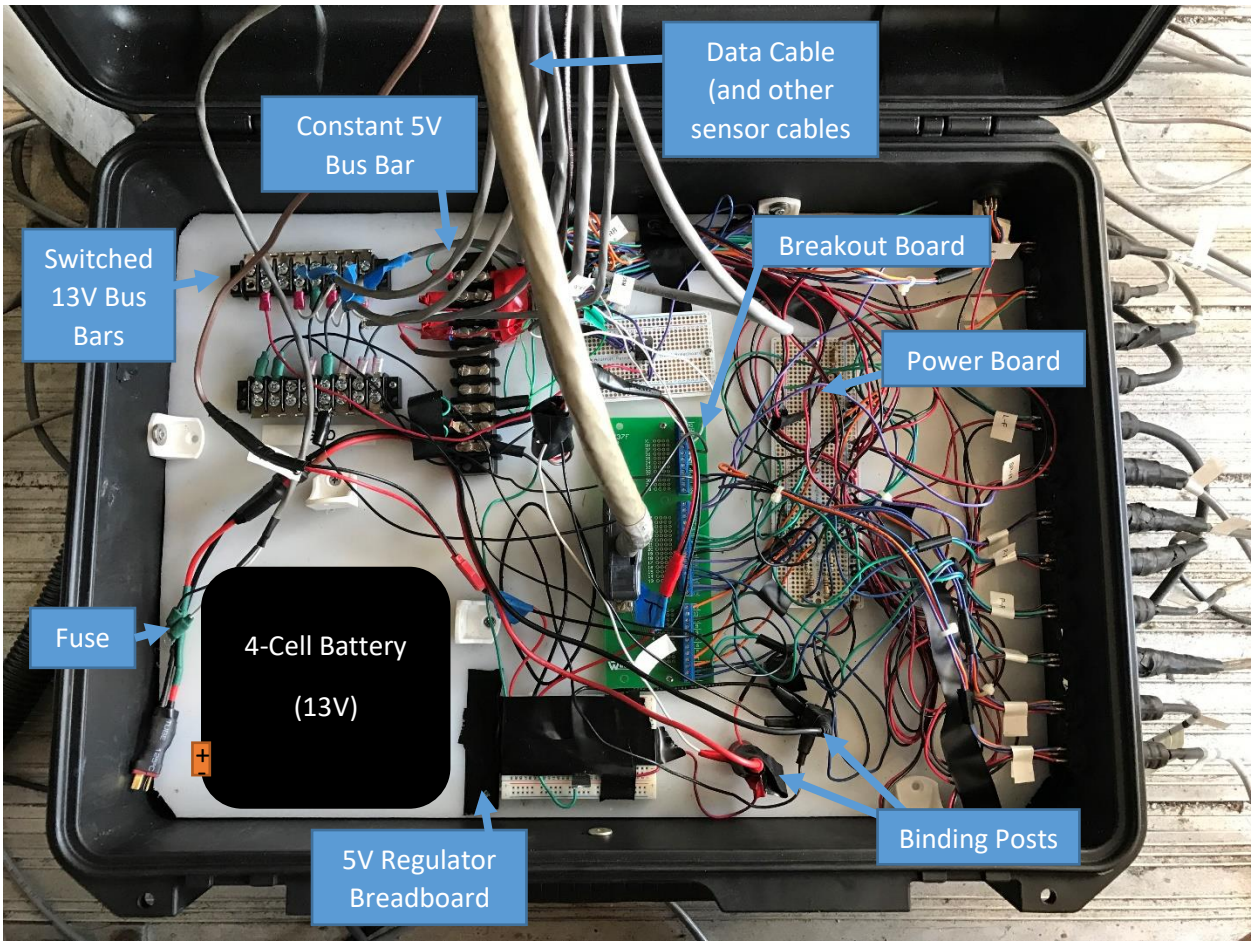

Figure 4-24. JBB and its components.

Another 13V 4-cell battery is used with and located in JBB. JBA's location at the front of Trailer A was close enough to use the Power Box's power circuit, while JBB's location made it necessary to supply it with its own power supply. A common ground was run through both junction boxes, however, to counteract any common ground issues between the two batteries. Several stoppers drilled into the plastic bottom were used to secure the battery from interfering with any wiring and breadboards. Positive and ground terminals suppling the battery's power and ground were used to connect all the electrical utilities in the box, which are discussed next. The cable used to connect the battery to the junction box again has a fuse soldered in it.

Several different circuits were needed within JBB due to both different sensor power requirements, as well as different types of electrical appliances. Multiple breadboards were used to supply these different powers to numerous targets in a simplified manner. The first breadboard is the main sensor breadboard located on the right in Figure 4-24. Similar to that in JBA, the main breadboard was connected by soldered

wires and by spade connectors at the power and ground terminals. Solder bridges were fashioned between the sets of five pins to connect the entire rows for power and ground rows. Receptacle port pins were then connected at these power and ground rows by soldered wires at both ends. The outputs of these receptacle port output pins were connected to the DB37 breakout board found in the middle of JBB. The data from the Trailer B sensors are transmitted to the cRIO at the tractor via a 120-ft DB37 cable. More information about the receptacle ports and breakout board pinout is available in later sections of this chapter.

The remaining two smaller breadboards were both used to create and provide 5V circuits using 5V voltage regulators. There were many additions made to JBB that required 5V circuits, so originally only the bottom mini-breadboard was used to supply that power. As more needs for 5V power were implemented into the DAQ system, the third bus bar was added to install more applications in a more secure and safer manner than inserting wires into a breadboard.

The mini-breadboard at the top was used to supply the two Arduino systems with a 5V flag used to sync up independently gathered data from several Arduino systems in post-processing. A 5V flag was necessary, as the 13V switchable circuit that the LEDs used was too high for Arduinos to process. At the end of the project, the time-of-flight sensors used with the Arduino systems were deemed not accurate enough and were not used. The flag was supplied by the two LED bus bars that actually do not use JBB battery, but the LED power circuit from the power box. This connection is made by a LED control cable that connected the JBA bus bar set to the JBB bus bar set. Figure 4-19 serves as a diagram for the connections of the data acquisition system.

4.2.5 Cameras

Cameras were the final hardware used on the truck during testing. Video not only clarifies uncertainties within data, but also allows easier understanding and analysis of test results. Seven cameras were used to supplement the analog data acquisition system, six of which were mounted on the vehicle body, with one camcorder set aside along the test track. These six cameras were placed near and captured views of inside the cab, in between the two trailers, at Trailer A's passenger side, at Trailer B's driver and passenger sides, and at the dolly's driver side. LEDs are taped in view of the cameras, and activation timings are used to synchronize the six cameras and their flags to the analog data using timing offsets. Figure 4-25 displays the cameras locations and their points of views, and Figure 4-26 displays the synchronization process. A drone was brought in to take aerial shots of the vehicle during each maneuver, with the sole purpose of ease of understanding each maneuver.

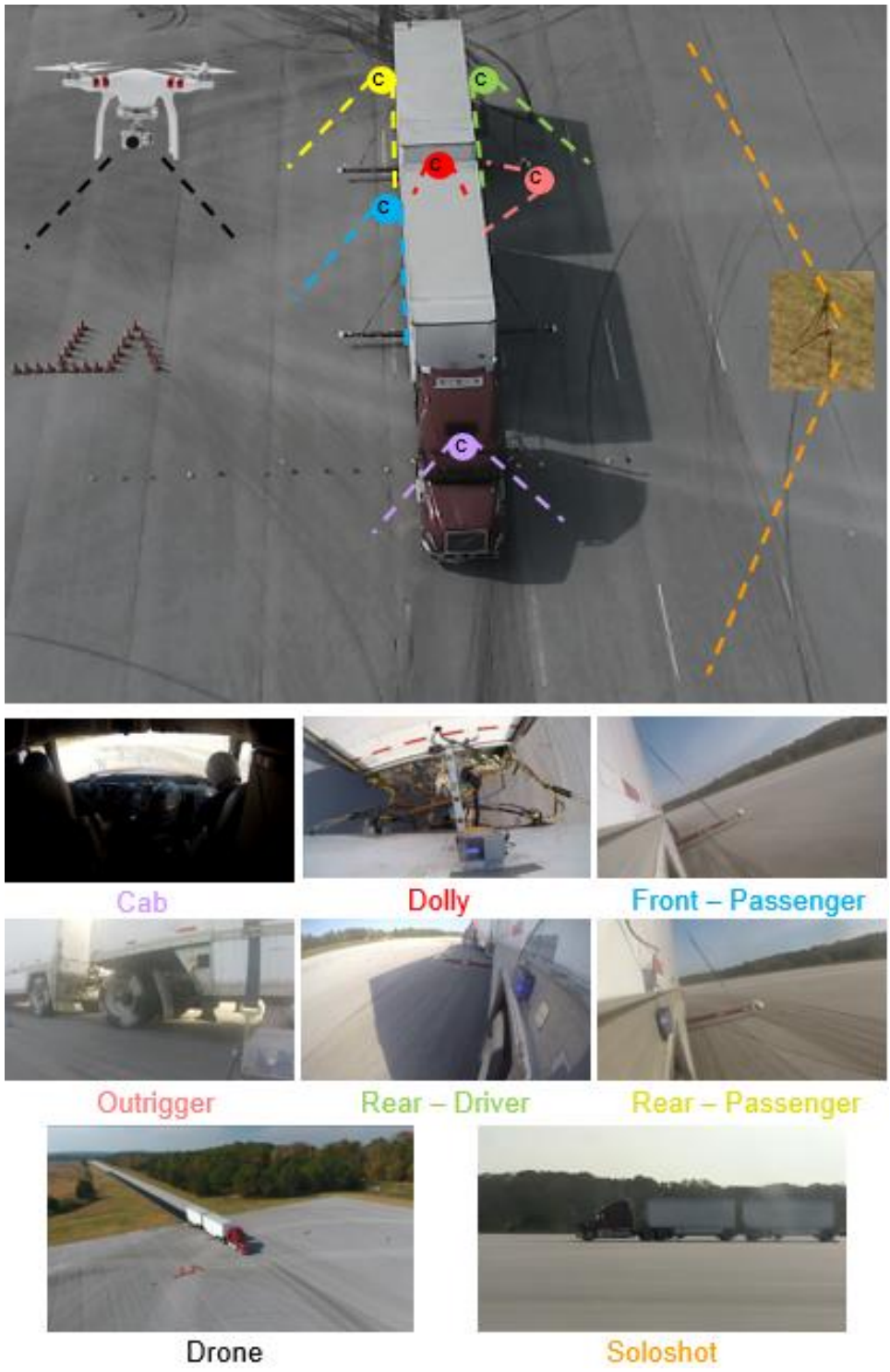

Figure 4-25. Cameras and views, and LED usage.

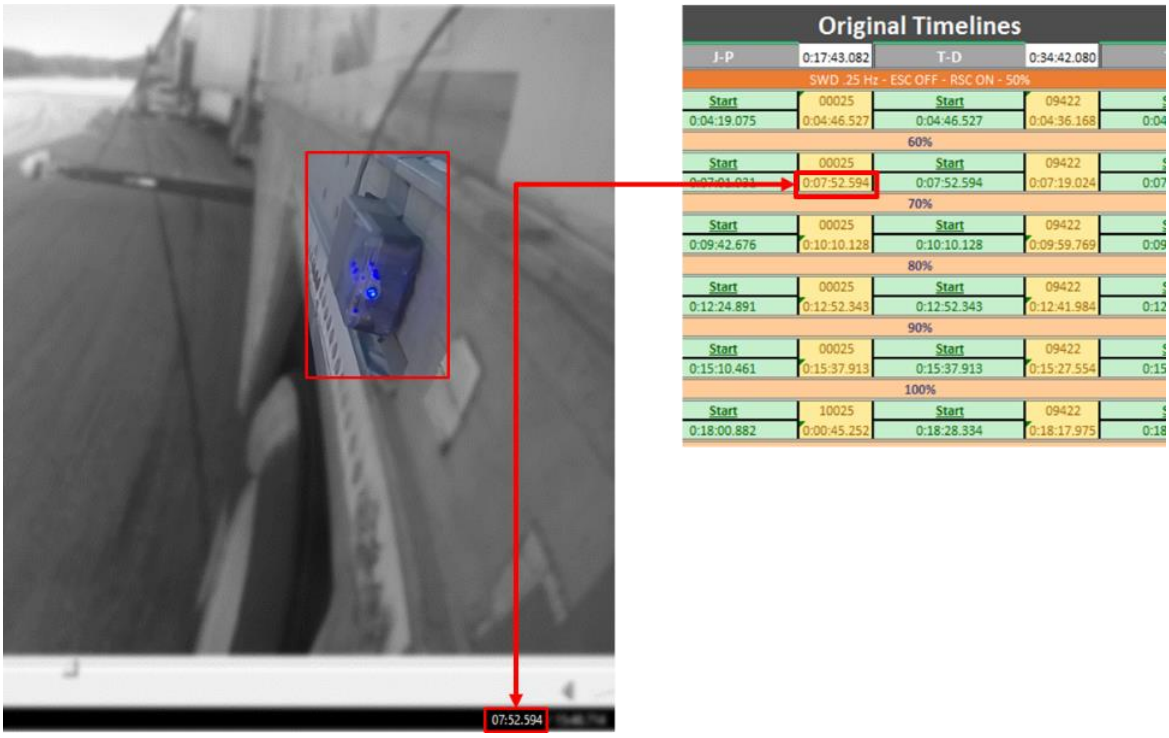

Figure 4-26. LED activation timing used for synchronize cameras with offsets.

A video of every test from each of the cameras is available for aid in data analysis. Each test's starting time was logged to Excel to bookkeep the massive number of tests. With these videos, uncertain results, such as outrigger forces used to determine rollover, could be validated or disproved. Making video data clearer was the reason behind painting the vehicle tires and taping the outrigger wheels.

4.3 Testing Overview

A thorough test procedure for studying the stabilities of an articulated truck must involve different maneuvers, as rearward amplification plays a pivotal role in the dynamics of the vehicle. The selection of the correct maneuvers to test is of utmost importance. Comprehensive review of potential test maneuvers to use during track testing of an LCV was completed first, as a combination of NHTSA and the National Transportation Research Center (NTRC) standards were used. A set of maneuvers thought to collectively exhibit the gamut of dynamics of LCVs was chosen. These maneuvers are summarized in Table 4-4 and discussed in detail in the remainder of Section 4.3.

Table 4-4. Summary of proposed test maneuvers.

Maneuver	Replicated Scenario	Description	Visual
150 ft. J-turn	Entry or exit ramp	Straight entry with dropped throttle around a 150 ft. radius 180° turn	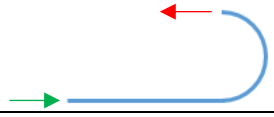
Double lane change (DLC)	Lane change at high speeds/ Obstacle avoidance on straight road	Straight entry with dropped throttle while move to left lane, then back again over 340 ft.	
0.25 Hz Sine-with-Dwell (SWD)	Obstacle avoidance onto curved road	Straight entry with dropped throttle with a sinusoidal steering input interrupted by a dwell	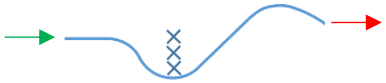

4.3.1 Maneuver 1: J-Turn

Directly taken from NHTSA's tractor semi-trailer testing in 2011 [36] is the J-turn maneuver. This maneuver calls for a constant radius turn of 150 ft. with a straight entry and dropped throttle once the turning has begun. This maneuver replicates the curvature of a curved portion on a highway, which is what most vehicles in the trucking industry use for travel. NHTSA used both a 150-ft. and 200-ft. radius J-turn, but only the 150-ft. variation was used as it called for more steering wheel angle during the turn and therefore more lateral accelerations. The inside and outside radii were marked by cones, and a lane width of 12 ft. was set to match conventional highway lane width. Contrary to NHTSA's methods, no test termination conditions were placed, so rollovers denoted by outrigger contacts did not end the test run. However, any off-tracking resulted in a bad run, as cones would be knocked over.

J-turns are driver-operated maneuvers that are largely static, as a theoretically constant steering wheel input is used to rotate the vehicle leftward, and roll dynamics can be studied without yaw. Since there is driver feedback, roll dynamics are not entirely detached.

4.3.2 Maneuver 2: RSM

Both the driver and the steering robot were capable of completing J-turn tests, but the steering robot's path had a slight deviation from the J-turn described above, as driver feedback is absent. Instead of path-following efforts, the steering robot completes J-turns by using a constant steering wheel input. This led to a variation of the J-turn referred to as a ramp steering maneuver, or RSM. Figure 4-27 displays the steering input for all speeds.

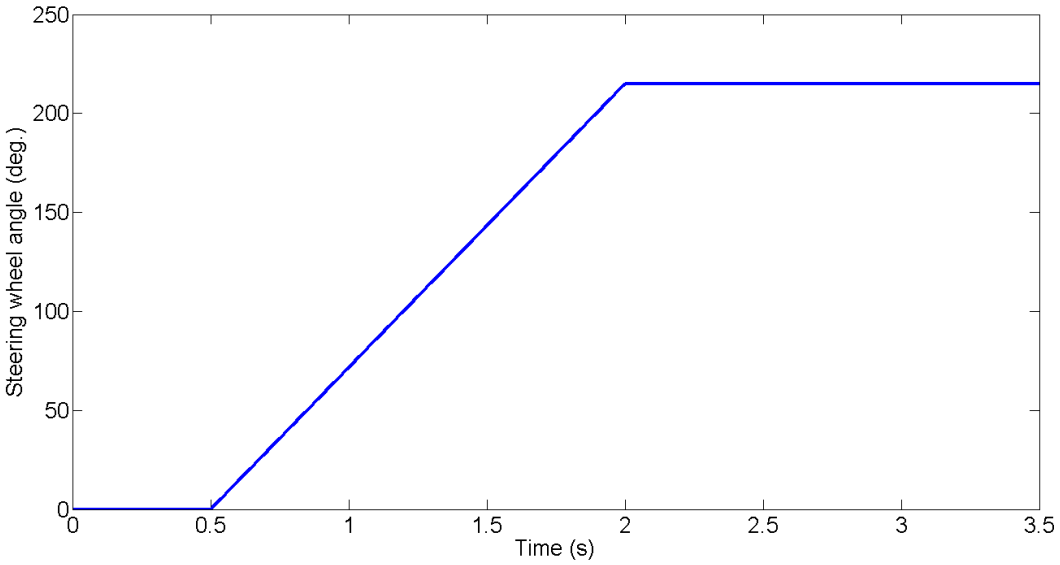

Figure 4-27. Steering input for the robot J-turn, or RSM.

Both driver- and robot-conducted J-turn test sets started at a speed of around 30 mph and increased by one-mph increments until failure of the evaluated RSC system occurred, marked by severe roll. This method was repeated for each of the RSC systems under evaluation. Any errors in path-following during the cornering called for a rerun for that particular speed. The robot J-turns, or the RSMs, obviously failed to follow the laid path, but as long as the robot was started at the beginning of the J-turn path, no reruns were called for. Timing references were created for each test maneuver to ensure similar activation locations.

4.3.3 Maneuver 3: DLC

The proposed double lane change maneuver is also taken directly from NHTSA's testing of a tractor semi-trailer; it simulates an evasive maneuver into the adjacent lane and back, and was to be completed by a human driver only. The maneuver specifics are shown in Figure 4-28. Cones are denoted by black squares, and the dimensions shown have been adapted for LCVs. Again, this maneuver called for a straight vehicle entry followed by a throttle drop. The dotted line in Figure 4-28 demonstrates the vehicle path. Test runs were considered successful if the vehicle had followed this path and cleared all cones. Any failures resulted in a rerun. Again, no terminating conditions were set for this test. The DLC maneuver was chosen, as it is the clearest presentation and exhibition of rearward amplification, and is a standard performance maneuver for evaluating RA in combination vehicles due to a sufficient vehicle excitation.

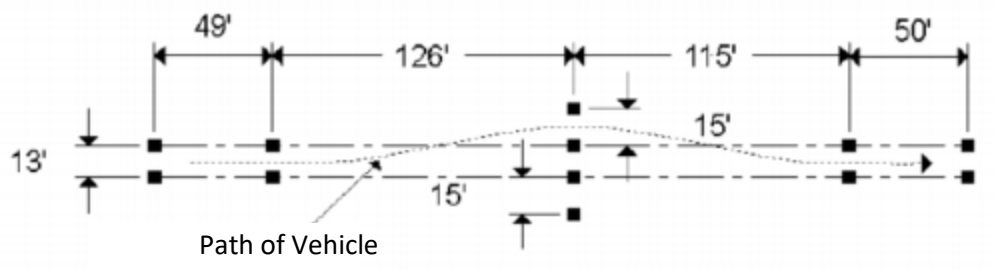

Figure 4-28. Diagram of DLC adapted for long combination vehicles [36].

DLC tests were another set of maneuvers that steadily increased the speed in which the vehicle was run after every successful test. The entering speed generally started at 48 mph and increased in one- or two-mph increments until severe rollover occurred based on the judgement of the test team. This method was repeated for each of the RSC systems under evaluation.

4.3.4 Maneuver 4: SWD

The sine-with-dwell maneuver was actually designed by NHTSA as a maneuver for studying the yaw stability of Class 8 trucks. Although it is still a highly dynamic and roll-inducing maneuver, SWD maneuvers were still included in this study as yaw instability indirectly affects roll instability. A sine-with-dwell, or SWD, maneuver consists of a sinusoidal steering input with a pause, or dwell, of 1 second after the third quarter-cycle of the sinusoid is completed. A visual representation is available in Figure 4-29, which shows the steering input over the full duration of the maneuver. It is important to note that this figure is not a plot of the vehicle path. This steering maneuver is only completed by the steering robot, as a SWD maneuver is a prime example of the repeatability and reproducibility found in using a steering robot over a human driver, no matter the training, due to its complicated design.

NHTSA's design of the SWD test originated from the results of a slowly increasing steer, or SIS, maneuver in their tractor semi-trailer testing. The amplitude of the steering input of the SWD is based on the result of SIS tests when a 0.5 g lateral acceleration was experienced at the tractor. NHTSA's SWD calls for a 0.5 Hz sinusoidal steering input. The SWD used in this study has been modified to one that uses a 0.25 Hz sinusoidal steering input instead, with a pause of two seconds instead of one. This change was made in efforts to adapt NHTSA's test maneuver for one more suitable for LCVs, as a lower frequency steering input can sufficiently excite the rear trailer in an A-Double configuration. Unlike other maneuvers, the 0.25 Hz SWD uses an entry speed of 45 mph for all tests. The independent variable for this maneuver is the ratio of the maximum steering input that is used. The first tests are generally run with increments of 10% until 100% is reached. This 100% refers to the steering input amplitude of $\pm\ 250°$ from the SIS results aforementioned. Figure 4-29 shows the steering wheel angle inputs for 50%-100%.

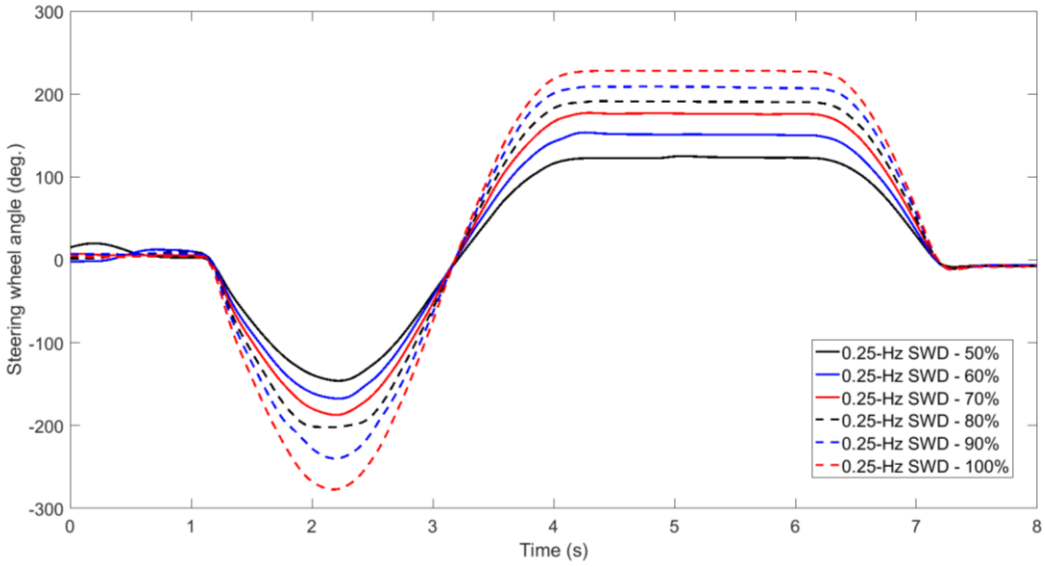

Figure 4-29. 0.25 Hz SWD steering inputs for 50-100%.

4.3.5 Maneuver Summary

Table 4-5 summarizes the four maneuvers and provides ratings for characteristics such as trailer loading, steering frequency, and repeatability. The stars indicate the maneuvers' ratings for each characteristic, as one star means low and five stars mean high. The maneuver's situational equivalent, steering operation, effects on both front and rear trailers, steering input rate, repeatability, and overall severity can be found, and each of the characteristics is explained below.

A maneuver's situational equivalent indicates which real-world situation best relates to the tested maneuver, and is usually the reason why the maneuver was chosen for the study. As discussed in each individual maneuver subsection above, the four maneuvers are either operated by a subjective professional driver or by a steering robot (in which the speed of the vehicle is still controlled by a human driver). Rearward amplification plays different roles for different steering actions, and its effects can be noted by the rear trailer's excitation for each maneuver (Table 4-5). There are maneuvers in which the front trailer is more prone to rollover as well, as shown by the front trailer excitation marks in the table. The steering input rate shows how quickly a steering input changes throughout the test. For example, the RSM maneuvers hold a steady steering input, while the DLC maneuver incorporates three quick and consecutive steering actions to direct the vehicle through the cones, as shown in Figure 4-28. The repeatability found in conducting the tests is also shown in Table 4-5 and shows driver operated pathing was difficult to keep constant for the J-turn and DLC due to human error and degree of steering difficulty. The SWD and RSM tests are considered to be the more reliable tests and test results shown in Chapter 5 can be seen as more conclusive. Finally, the overall severity in terms of rollover propensity for each

maneuver is provided. All maneuvers were run under the assumption of having a symmetric response if the tests were run in a mirror fashion relative to the descriptions provided above.

Table 4-5. Maneuver characteristics comparison.

	J-Turn	Double Lane Change (DLC)	Ramp Steering Maneuver (RSM)	0.25 Hz Sine-with-Dwell (SWD)
Situational Equivalent	Curved road	Passing on highway, obstacle avoidance	Exit off-ramp	Near missed exit
Operator	Driver	Driver	Robot	Robot
Front Trailer Excitation	★★★★	★	★★★★★	★ ★
Rear Trailer Excitation	★ ★	★★★★★	★	★★★★
Steering Input Rate	★ ★	★★★★★	★	★★★
Repeatability	★★★	★	★★★★★	★★★★
Overall Severity	★★★	★	★★★	★★★★★

4.3.6 Test Environment

The three proposed maneuvers will be used to track test the A-Double test vehicle at the Michelin Lauren's Proving Ground, or MLPG, in Laurens, SC. The testing behind the study was spread out over six weeks, with the schedule detailed in Table 4-6. The first two weeks were used for pre-testing setup, as tuning of the vehicle instrumentation was completed. Actions completed included outrigger wheel height setup, steering robot tuning, and AJS rope and chain length determination. The last three weeks focused on RSC system evaluations, as each week focused on one RSC manufacturer. A total of five RSC systems were tested during these three weeks (Weeks 3-5).

Table 4-6. Testing schedule at MLPG for this study.

Test set	Date (All 2016)	Objective
1	Sept. 12 – Sept. 16	Testing setup
2	Sept. 19 – Sept. 23	Testing setup
3	Oct. 24 – Oct. 28	RSC Systems 1 & 2
4	Nov. 7 – Nov. 11	RSC System 3
5	Nov. 28 – Dec. 2	RSC Systems 4 & 5

Test track "Track 8" at MLPG was used to conduct all tests for this RSC evaluation study on A-Double roll stability. Track 8 consists of a two-mile loop through a rectangular test section with the area of 400 ft. by 1400 ft. called the Vehicle Dynamic Assessment (VDA) pad. This course was able to accomodate all

proposed maneuvers and was a perfect test environment. Fortunately, the testing days throughout the three RSC weeks (3, 4, and 5) had consistently sunny weather of nearly the same temperature. This is important to rule out possible different tire/ground dynamics every week in combination with new sets of tires every week. A photo from Google Earth of the track is shown in Figure 4-30. Table 4-7 shows the forecast for the testing days from the RSC weeks. The test procedure for each of the days generally focused on one or two maneuvers, and followed the general maneuver procedures detailed in Sections 4.3.1, 4.3.2, and 4.3.3.

Figure 4-30. Track 8 at Michelin Laurens Proving Ground via Google Earth.

Table 4-7. Forecast of testing days from RSC weeks.

Week	Date (All 2016)	Weather	Temperature	Precipitation	Wind Speed
Week 3	Oct. 26	Sunny	71°/37°	0.00 in.	3 mph
Week 3	Oct. 27	Sunny	77°/46°	0.00 in.	4 mph
Week 3	Oct. 28	Sunny	82°/55°	0.00 in.	4 mph
Week 4	Nov. 9	Sunny	69°/44°	0.00 in.	4 mph
Week 4	Nov. 10	Sunny	68°/33°	0.00 in.	2 mph
Week 4	Nov. 11	Sunny	69°/35°	0.00 in.	4 mph
Week 5	Nov. 30	Sunny	69°/59°	0.51 in.	10 mph
Week 5	Dec. 1	Sunny	60°/41°	0.00 in.	7 mph
Week 5	Dec. 2	Sunny	59°/32°	0.00 in.	2 mph

4.4 Summary

This chapter provided a general description of the instrumentation done on the test vehicle prior to track testing. The key preparations included:

- Safety outriggers: instrumented with load cells and used to quantify rollover occurrence and severance and keep the vehicle upright
- Anti-Jackknifing Systems (AJSs): a series of ropes and chains to dissipate yaw inertia and prohibit potential jackknifing when needed
- Trailer reinforcement beam structures: installed to increase trailer structure strength and ability to withstand outrigger contact and AJS forces
- Trailer load frames: used to replicate a typical 28 ft. trailer loading configuration (total weight, cg location, and rotational inertias)
- CVeSS steering robot: provided repeatability in steering inputs during testing not found with human drivers
- Data acquisition system and sensor instrumentation: gathered and logged data for analysis

This was followed by a description of the maneuvers chosen for RSC evaluation, and of the environment during the test days at MLPG. Some perceptive over why the proposed maneuvers were selected was also provided. The four used maneuvers are summarized in Table 4-4 and are as follows: (1) J-turn, (2) RSM, or robot-operated J-turn, (3) DLC, and (4) 0.25 Hz SWD.

Chapter 5 Roll Stability System Evaluation

This chapter provides analysis of the gathered data from track testing as a means of evaluating the performance of the RSC systems on roll stability of an A-Double. Both images from the cameras and analog data from the data acquisition system were used in describing the efficacy of a total of five systems compared to a baseline A-Double vehicle. The chapter starts with a description of the selection process of data from properly run tests as the first stage of data analysis. The rest of the chapter is split into separate sections, as results for each of the three conducted studies are discussed by maneuver in detail. The chapter ends with a summary of the findings.

Three separate studies were conducted in an effort to evaluate RSC systems: a single channel (2S1M) RSC systems evaluation, an assessment of the significance of dolly brake usage in RSC systems, and a single channel and dual channel (2S2M) RSC system comparison. As mentioned in Chapter 2, trailer-based RSC systems can incorporate different hardware, and an example of that was the number of brake modulators involved at each axle. Two-modulator systems (2S2M) are capable of splitting brake responsibilities at each axle to individual tires, and an evaluation of the benefits (if any) of 2S2M systems over 2S1M systems will be completed. Chapter 3 introduced brake contributions for each axle, and it was found that the converter dolly axle had increasing contributions with deceleration rate. The third study regarding the benefits (if any) of including dolly brakes in RSC systems will also be conducted.

Three systems will be analyzed during the first study, as similar 2S1M RSC systems from three different manufacturers will be tested individually, with their individual results compared to the results from the baseline vehicle's tests. These systems are System A, B, and C. Two systems will be analyzed in the second study of dolly significance, as System A will be compared to another of Manufacturer A's products: System A-D. System A-D is essentially System A, but with the dolly axle included in the controlled brake applications by the RSC system. Finally, in the third study of modulator significance, System C will be compared to System C-2, which is also another product made by Manufacturer C. System C-2 is a 2S2M version counterpart of System C.

5.1 Bases of Evaluation

The objective of the testing completed was to evaluate the performance of five different RSC systems. All systems used trailer-based RSC systems at both trailers, and the same ABS system. The test week consisted of two preparation days and three testing days. No major issues occurred during testing.

A total of 136 tests were conducted at Track 8. Additional testing was conducted for most of the maneuvers, as both robot- and driver-operated steering held inconsistencies. The J-turn and DLC tests needed constant retesting, due to the difficulty of the maneuver even with a professional test driver, as maneuver entry speed, path following, and driver feedback proved to be the three largest sources of discrepancy between tests and weeks. The RSM and SWD tests also needed retesting as robot activation times and maneuver entry speed needed to be as constant as possible. The availability of Track 8 and the same professional driver each test week demanded a flexible schedule, so the amount of testing and retesting was quite limited. The best performed tests were selected for evaluation with the help of GPS speed, GPS path, cameras, and steering wheel angle data.

There are proprietary and disclosure considerations seen in the data revealed in this chapter and document, so not all numbers are revealed. This is also the reason why a deeper look at RSC operation such as braking operation and efficiencies and lateral accelerations throughout tests, are not covered in this document. The sponsor for this project is to remain unacknowledged.

The following variables were selected for data analysis to display the efficiency of each RSC system: outrigger contact forces, RSC activation times, and RSC warning times. The outrigger contact forces were used to qualify rollover and quantify the severity of it, and the RSC activation and warning times were used to describe how reactive each system was. Activation time refers to the time between maneuver start to the activation of the RSC system, and warning time refers to the time between the RSC activation to the time of outrigger (OR) contact. Figure 5-1 displays a timeline that shows the definition of activation and warning time.

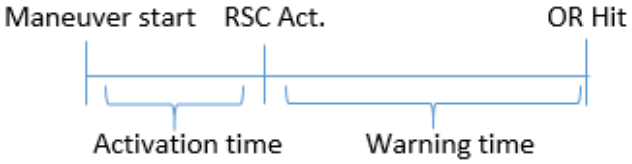

Figure 5-1. Activation time and warning time definitions.

5.1.1 Example Evaluation

This section will cover an example evaluation of the variables listed above: outrigger contact, activation time, and warning time. This process was repeated for each RSC system, for the selected tests in all four maneuvers. Figure 5-2 displays the three variables in a single plot. The blue event flag line denotes the start of the test whether it was driver or robot operated. The green event flag line indicates RSC activation through relay activation. The black plot line represents the outrigger contact force read by the load cell at a particular outrigger. The maximum outrigger contact force reading was taken at each of the four load

cells to measure the severity of the experienced rollover during the specific test. The presented outrigger forces are the equivalent force exhibited on the edge of the trailers instead of at the outrigger itself. The activation time and warning time of a particular test use the first outrigger contact rather than the highest.

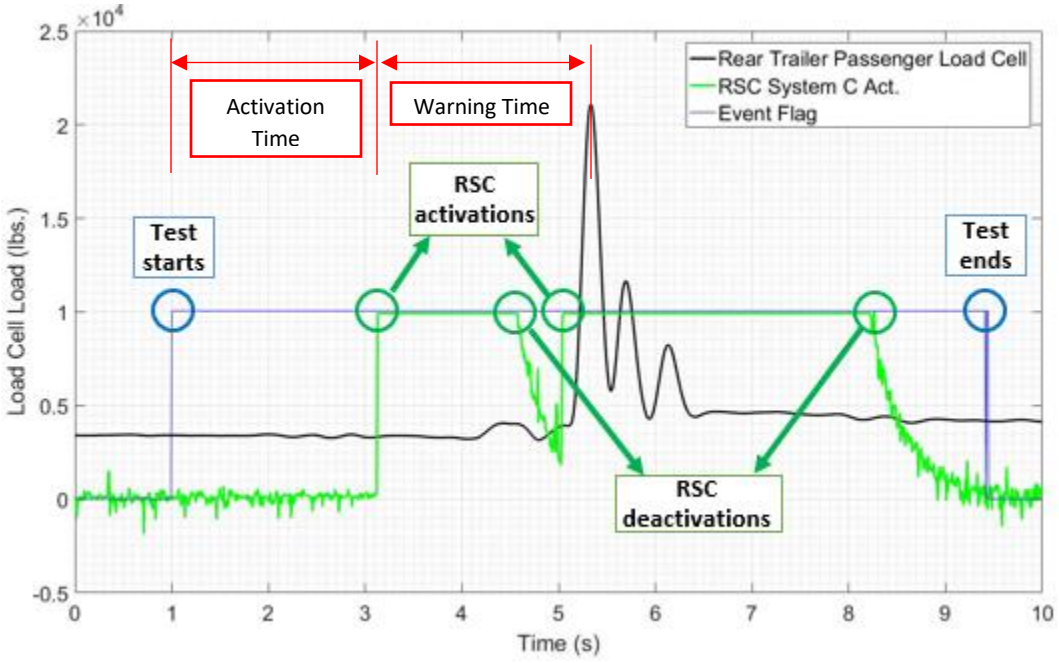

Figure 5-2. Plot of example data for RSC evaluation.

The data collected are analyzed in this manner, and presented in this document with multiple datasets starting from the baseline vehicle's rollover speed (J-turn, RSM, and DLC) or rollover steering (SWD), both of which will be hereafter referred to as the OERS. In efforts to mask the numbers, figures in this chapter will use x-axis labeling relative to the OERS, such as in the example outrigger contact force during J-turns shown in Figure 5-3. No result tables will be included in this thesis, neither in the documentation nor in the appendix. This chapter will continue to use the color scheme for the different RSC systems seen in Figure 5-3, as well as a light orange for RSC System A-D, and a purple for RSC System C-2. Both will be introduced in later sections of this chapter. Also included in Figure 5-3 is the pattern scheme shown in the legend framed in red, which is also continued throughout this chapter. Graphs such as that shown in Figure 5-3 show four datasets, and will show two sets of overlapped bars. The left side of a vehicle configuration section is for the front trailer, and the right side is for the rear trailer. Often, these graphs are followed by graphs that split up the front and rear trailer data. In figures showing specific trailer data, a solid bar denotes the driver side, and the diagonal striped bar denotes the passenger side. This is apparent in Figure 5-3 as well. Notes regarding the absence of data are present too, as some tests were not conducted for a specific configuration as seen below.

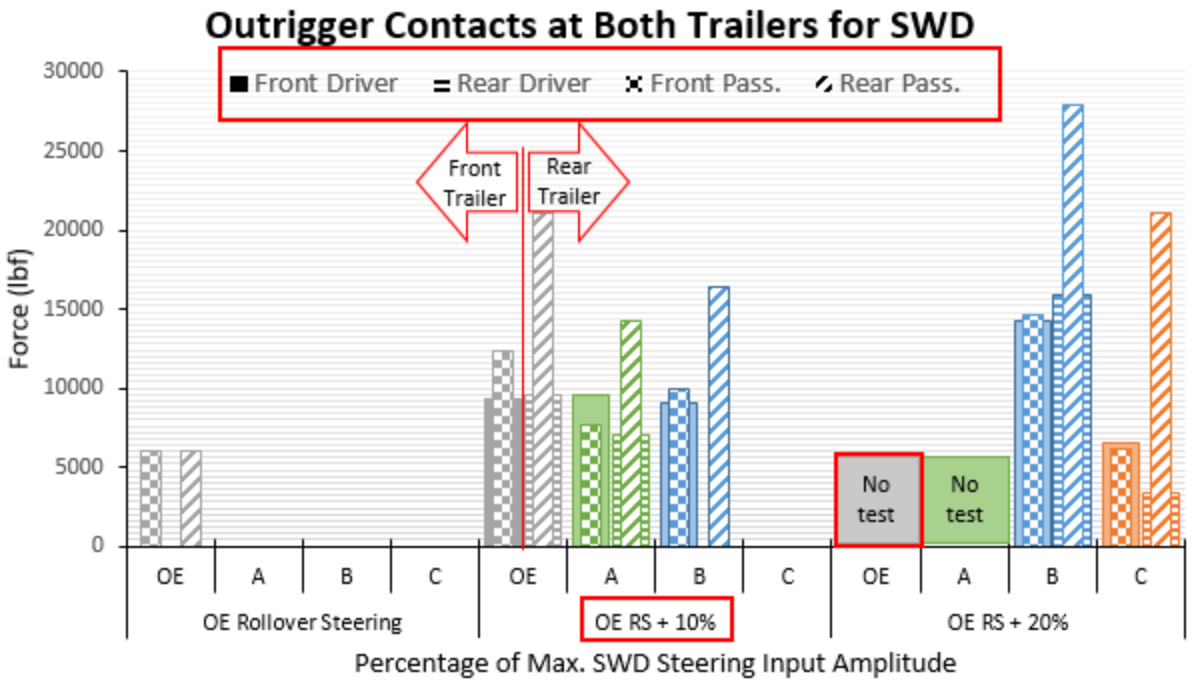

Figure 5-3. Example multiple dataset figure.

5.2 Single Channel RSC System Performance Study (A vs. B vs. C Study)

There were four total maneuvers at MLPG, two of which were conducted with a professional driver and two that are conducted with the steering robot. The two driver-operated maneuvers were the J-turn and the DLC, and the results of both are covered in this section.

An evaluation of the performances of the single channel, or 2S1M, RSC systems across multiple maneuvers is the primary objective of this document. It should be noted that the results of the multiple RSC systems are held relative to those of the baseline A-Double configuration, and a side-by-side comparison of the RSC systems is provided to demonstrate that RSC performance can largely differ among commercially available RSC systems, as well as from maneuver to maneuver for an individual system. Each maneuver subsection provides an outrigger contacts discussion first, followed by activation time and warning time. A conclusive performance increase or decrease for each of the RSC systems is provided for each maneuver.

5.2.1 J-turn Results

The first maneuver discussed is the J-turn. The results focus on the front trailer, as it experiences earlier and more severe roll than does the rear trailer. This occurs most likely due to the design of the test itself, as both trailers would theoretically roll one after another. However, the speed drop caused by the brakes stops the rear trailer from following the first trailer's roll. Since the steering is completely directed to the

driver side of the vehicle, analysis efforts focus on the passenger side of the vehicle. Although the rear trailer exhibited a much lower number of rollovers, it cannot be concluded with certainty that the rear trailer would not have rolled as often as the front trailer. The lateral momentum of the vehicle could have largely been dissipated through outrigger contacts.

Figure 5-4 shows that System B experienced the lowest outrigger contact forces, while System C demonstrated the single highest outrigger force during all J-turn tests. All systems demonstrated rollover at a speed 2.6% faster than the baseline rollover speed, or OERS. No J-turns with the baseline vehicle were conducted at a speed 10.5% faster than the OERS, as the vehicle underwent severe roll and yaw dynamics at OERS+5.3%. It should be noted that usage of all RSC systems led to an improvement in roll severity. It should be noted that an outrigger contact force threshold of 300 lb_f qualified vehicle rollover, and forces under the rollover contact force threshold did not qualify imminent rollover, but still indicated a high likelihood for it. This threshold is hereafter shown on all outrigger plots. Tests conducted at OERS+2.6% were not completed for baseline, System A, or System B, and were consequently left out. Unfortunately, System A was not tested with J-turns at all and is therefore disregarded in this maneuver study. Figures 5-5 and 5-6 split the outrigger contact data into a graph of the front trailer and rear trailer, respectively. Figure 5-6 shows that RSC systems heavily mitigated rollover at the rear trailer.

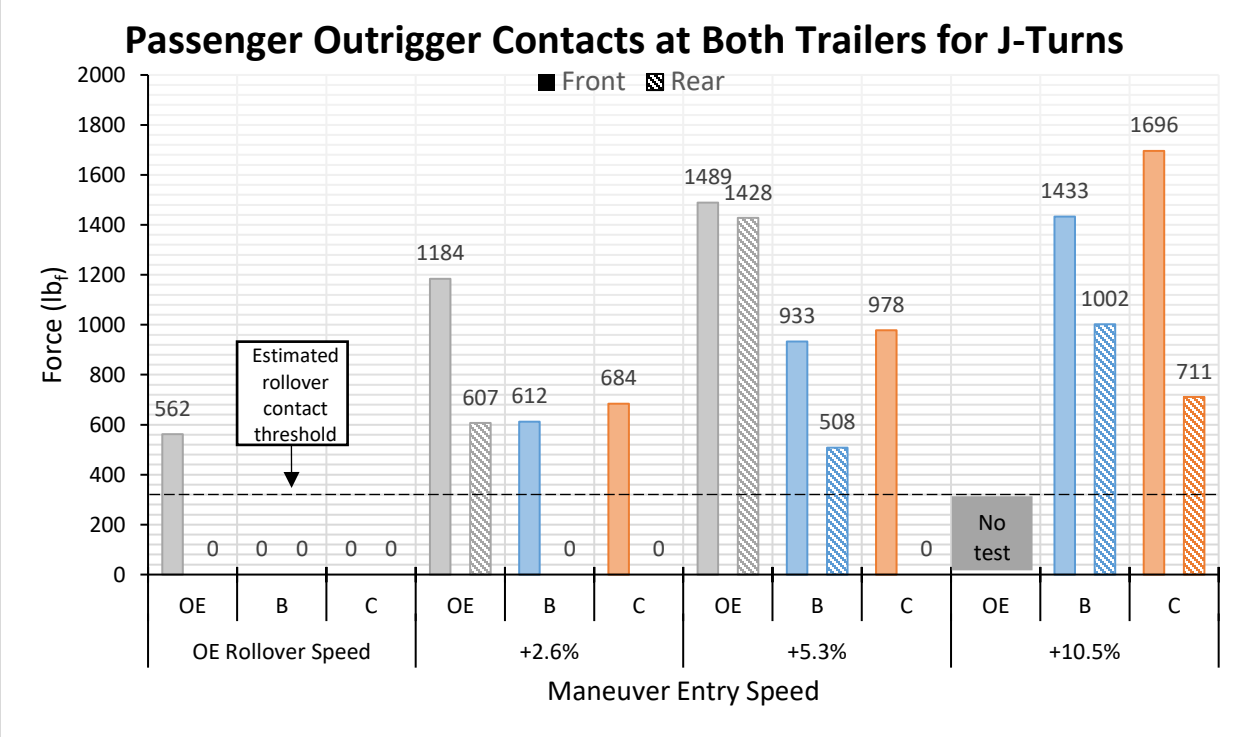

Figure 5-4. Passenger side outrigger contacts at both trailers during J-turns in 2S1M study, from OERS to +10.5% mph.

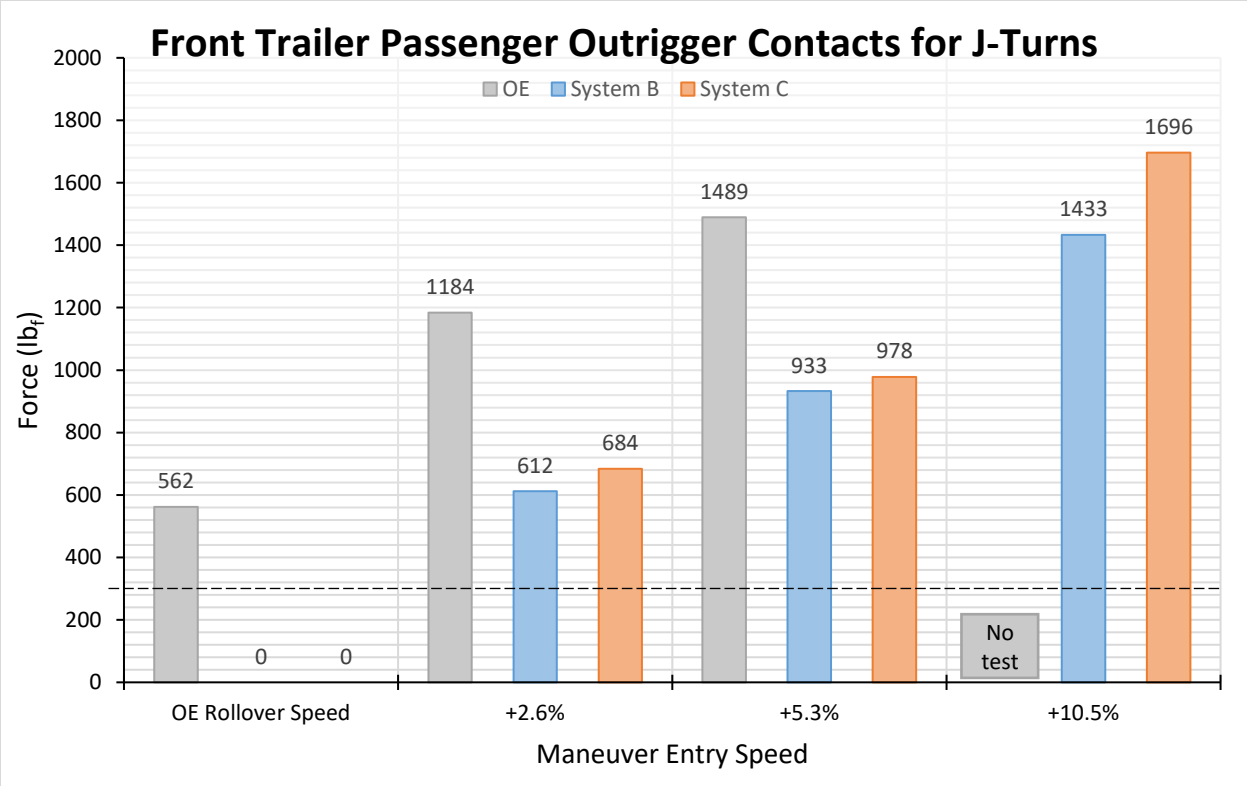

Figure 5-5. Front trailer passenger outrigger contacts during J-turns in 2S1M study, from OERS to +10.5% mph.

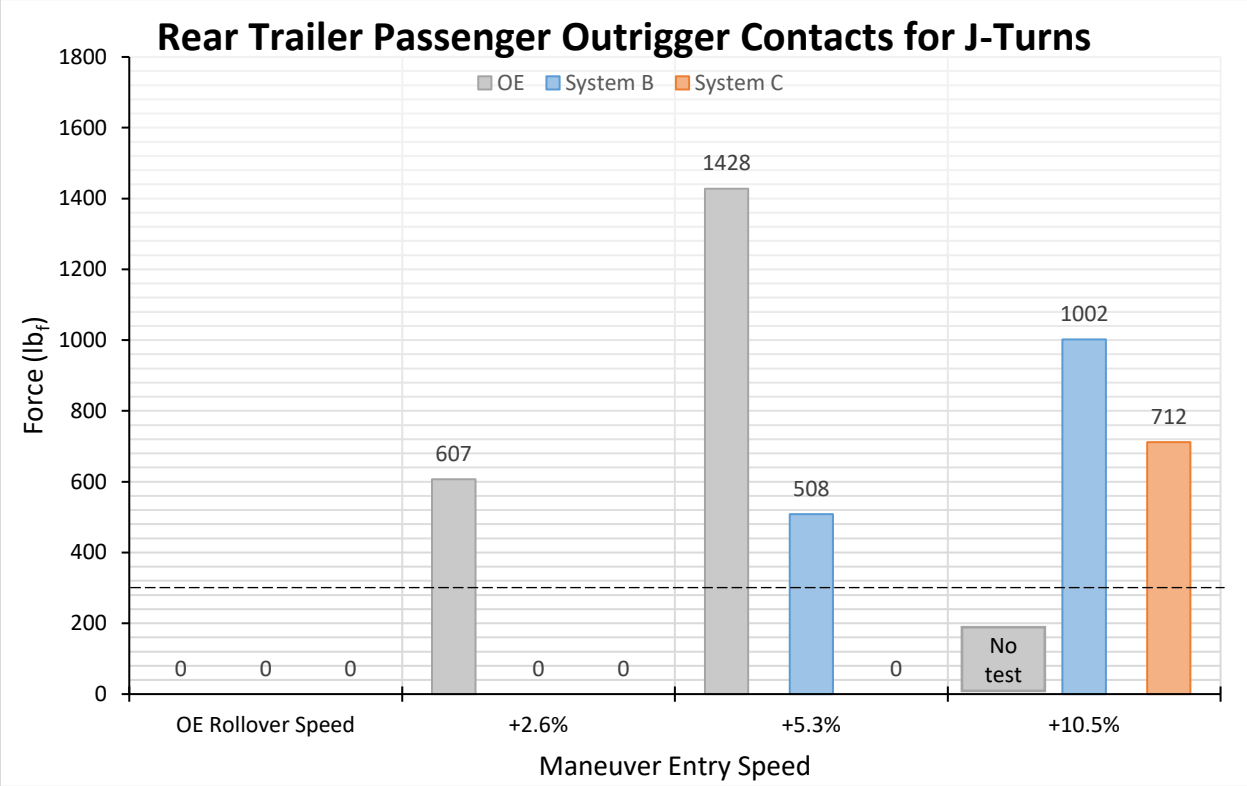

Figure 5-6. Rear trailer passenger outrigger contacts during J-turns in 2S1M study, from OERS to +10.5% mph.

Activation time and warning time results for the front trailer are shown below for multiple maneuver entry speeds in Figure 5-7 and 5-8, respectively. These variables only apply to RSC systems, so no baseline vehicle data is included in graphs that covered them. System B had the lowest outrigger forces, but rather high activation times. Higher activation times imply longer rollover recognition times, but do not necessarily relate to rollover performance, as System B had the least severe rollovers. Rollover recognitions highly depend on the sensor system and algorithm used at the black box, but again due to proprietary reasons, no details regarding these system modules will be discussed. It is therefore difficult, if not impossible, to explain the trends in both activation time and warning time. Nevertheless, it is clear that System C has the smallest activation time standard deviation through the test speed range at only 33.3 ms, and reacted an average 9.87% quicker than System B.

Figure 5-8 shows the warning times for the same entry speeds. Warning time indicates the time between RSC activation and inevitable rollover in which the driver can prevent roll via correct braking and steering measures. Standard human reaction is around 0.3 seconds, and applying the brakes takes about another 0.1 seconds. Therefore, a brake activation time of 0.4 seconds is included in all warning plots. System C demonstrated the highest warning times throughout the majority of the testing, as shown in Figure 5-8. The largest difference between the warning times of the two systems was 29.46% at OERS+5.3%.

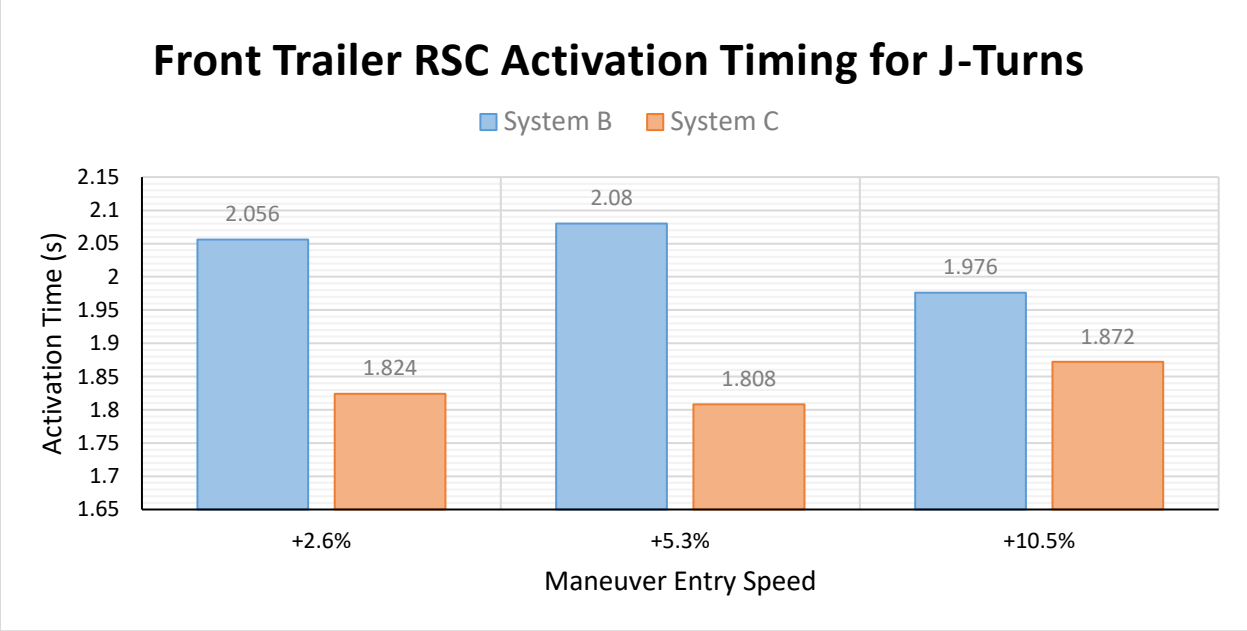

Figure 5-7. RSC activation times at the front trailer for J-turns in 2S1M study, from OERS + 2.6% to +10.5% mph.

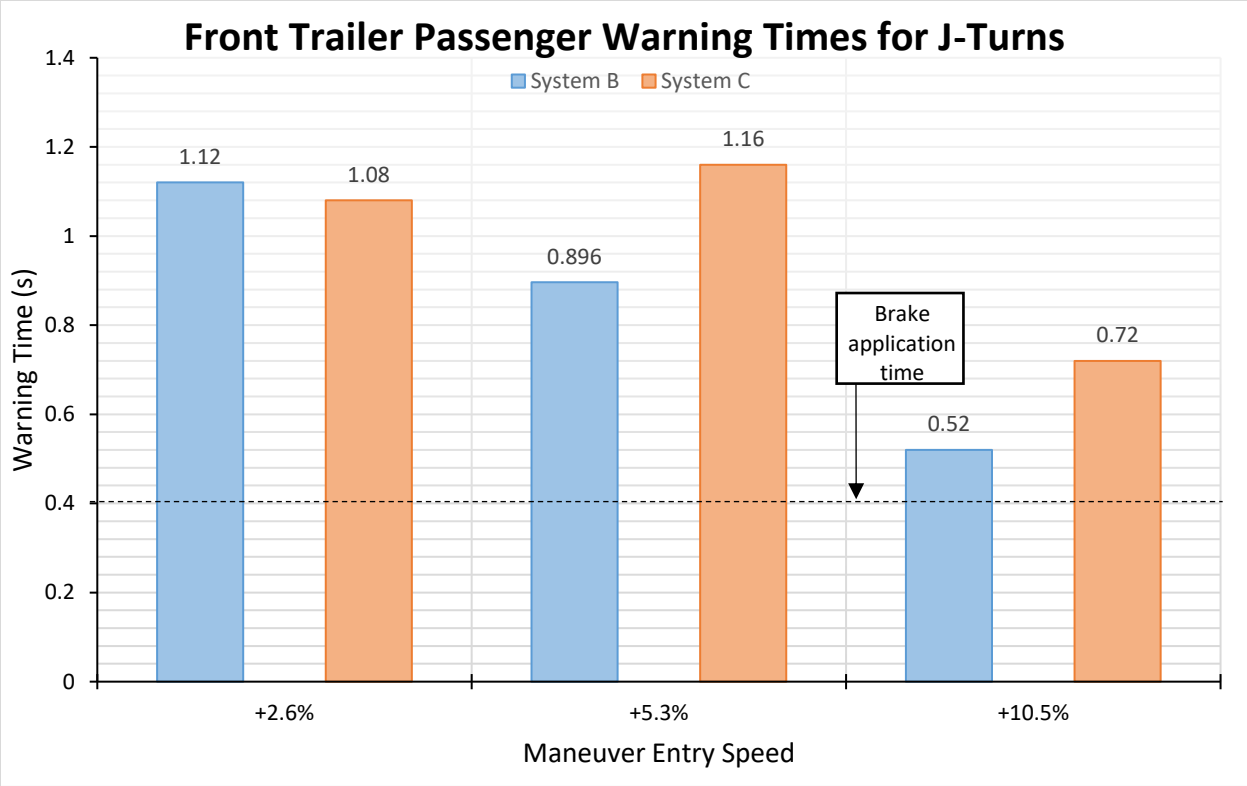

Figure 5-8. Front trailer passenger warning times during J-turns in 2S1M study, from OERS + 2.6% to +10.5% mph..

5.2.1.1 J-Turn Conclusion

In conclusion, RSC Systems B and C provided maximum front trailer passenger outrigger contact improvements of 48.35% and 42.27%, respectively, and a difference of 6.08% between the two at +2.6% speed. This difference translates to an outrigger force difference of nearly 72 lb_f. This force is of slight significance in the grand scheme of the forces exhibited on the vehicle body, but is enough (+20% of the rollover threshold) to cause rollover from situation to situation. The difference of 45 lb_f at +5.3% speed, however, is not enough (<20%) and is more likely to cause wheel lift without rollover. This minimum significance was decided subjectively by the team. The contact improvements for different speeds are shown in Figure 5-9.

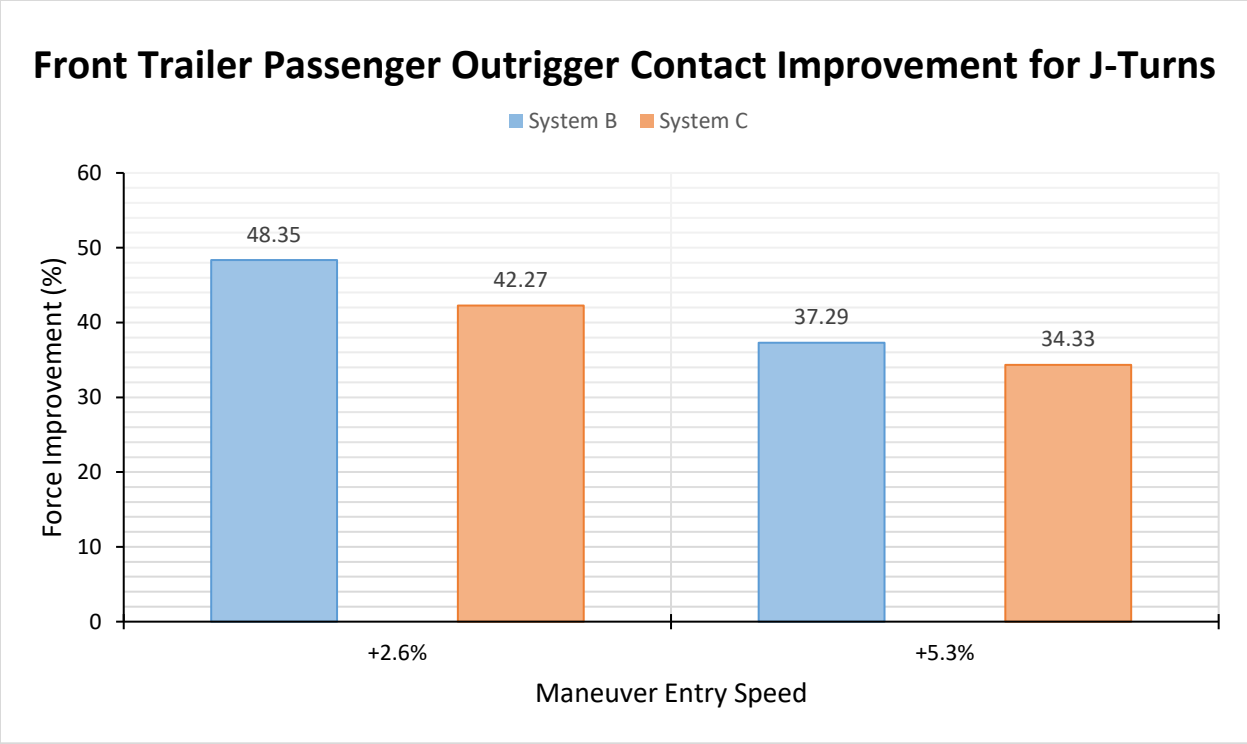

Figure 5-9. Front trailer passenger outrigger contact improvement during J-turns in 2S1M study, from OERS + 2.6% to +10.5% mph.

The rollover speed improvements over baseline for both the front and rear trailers found in using the two RSC systems are shown in Figure 5-10. Since a rollover at either trailer qualified vehicle rollover, there was no difference in rollover speed improvement between the two, and the improvment over the baseline configuration was miniscule.

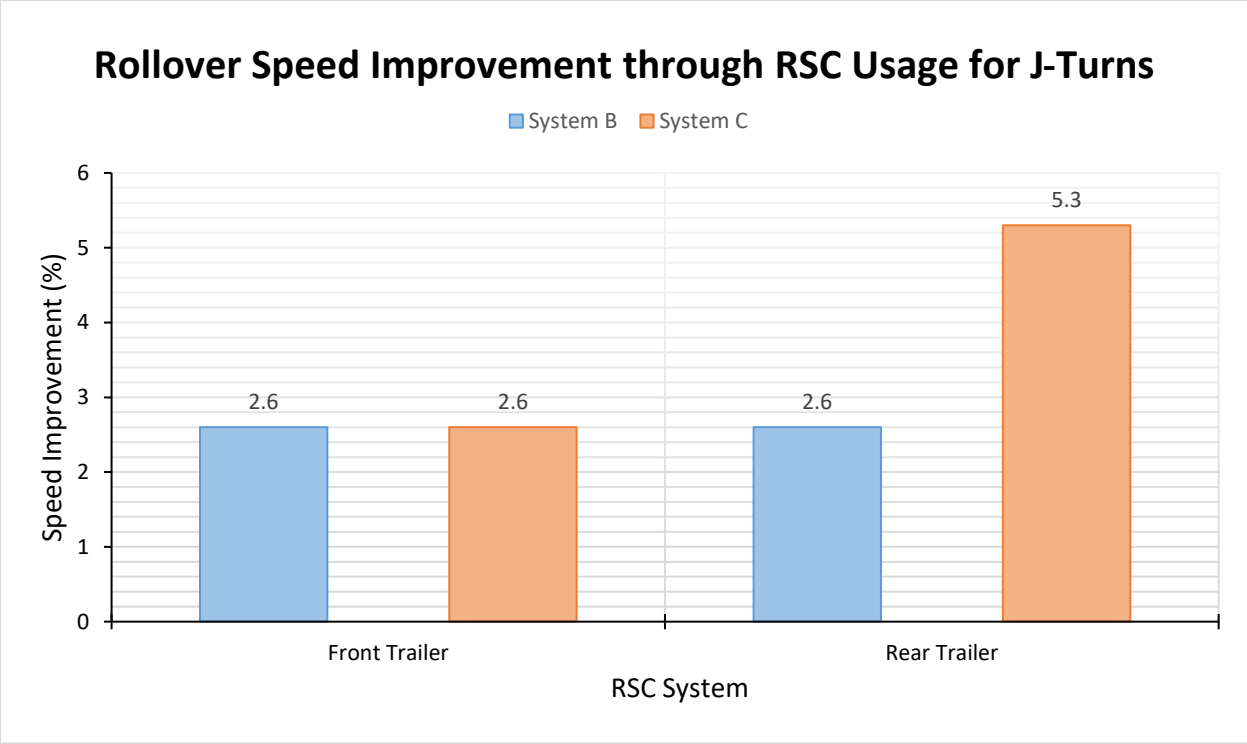

Figure 5-10. Rollover speed threshold improvement over baseline for both trailers during J-turns in 2S1M study.

5.2.2 RSM Results

The RSM maneuver provides an even more gradual approach to trailer rollover than do J-turns, as it eliminates any driver feedback and uses a constant steering wheel angle input with no dedication to path following. This maneuver therefore requires its own section, as results differ from those of the closed-loop J-turn maneuvers. As shown in Figure 5-11, System C was the only system tested at OERS+15% after not exhibiting any rollover to lower speeds, while the rollover speeds for baseline, System A, and System B were OERS, OERS+2.5%, and OERS+5%, respectively. System A had the lowest rollover speed, as well as the highest contact forces recorded among the RSC systems. There were no recorded outrigger contacts at the rear trailers for the speeds run for any of the systems, so there will be no rear trailer discussion in this section.

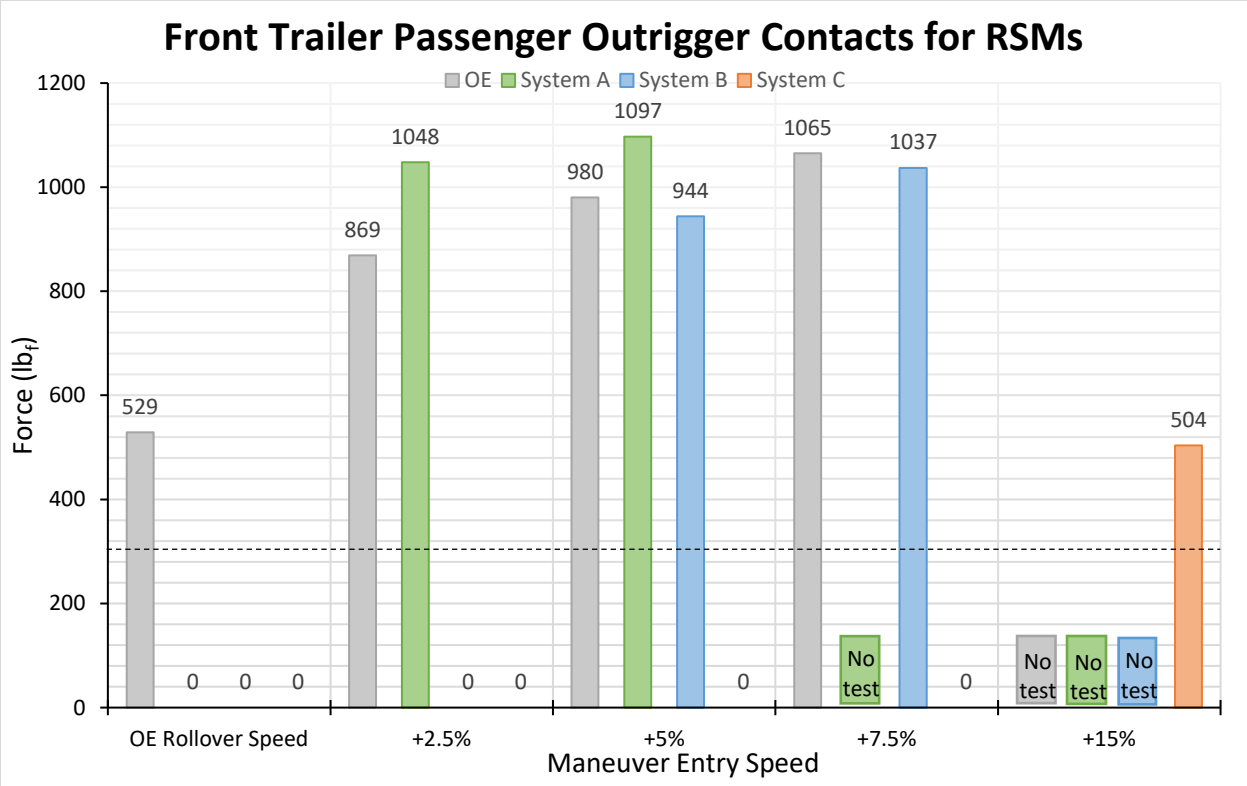

Figure 5-11. Front trailer passenger outrigger contacts during ramp steer maneuvers in 2S1M study, from OERS to +15% mph.

The three systems had more consistent activation times through OERS and OERS+5% in the RSM compared to the J-turn, demonstrating the significance that driver feedback has on rollover detection by the systems. This maneuver has more useful activation and warning time comparisons than that of the J-turn. The pattern remains the same, however, as System C has the lowest activation times and reacts more quickly and more proactively. The largest difference in activation times among the three systems was 0.818 s between System A and System C, as seen in Figure 5-12, and the two also had the largest outrigger contact force difference as well. At the speed of OERS+7.5%, a difference of 0.448 s was enough for System B to experience a large contact, and for System C to not rollover at all.

Again, due to a lack of information regarding the specific operation of the systems included in this study, only a correlation can be made from the activation and warning time results. This means that lower activation times can either indicate the system has a lower lateral acceleration threshold or reacts quicker to calculations. An analysis of the brake pressures used by each system is not provided due to a potential proprietary information leak regarding brake operation and braking efficiency of each system. System C

also exhibited the longest warning time among the activations that occurred from OERS to OERS+15, shown in Figure 5-13, even when System C only activated at a higher speed than that of the other systems.

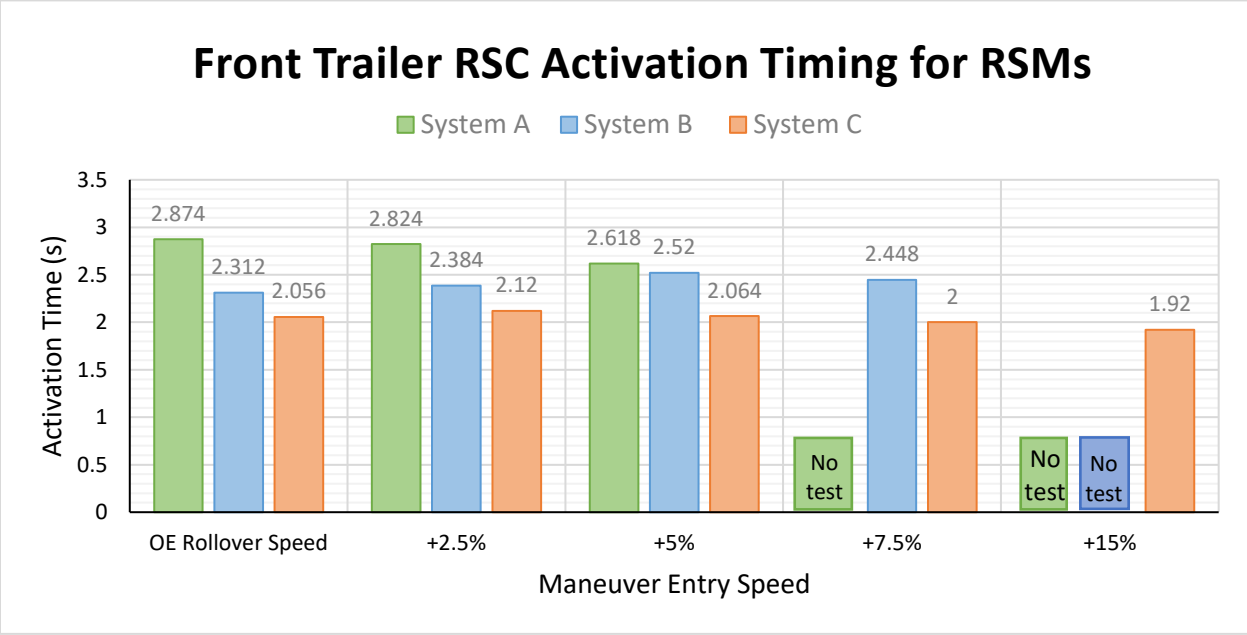

Figure 5-12. RSC activation times at the front trailer during ramp steer maneuvers in 2S1M study, from OERS to +15% mph.

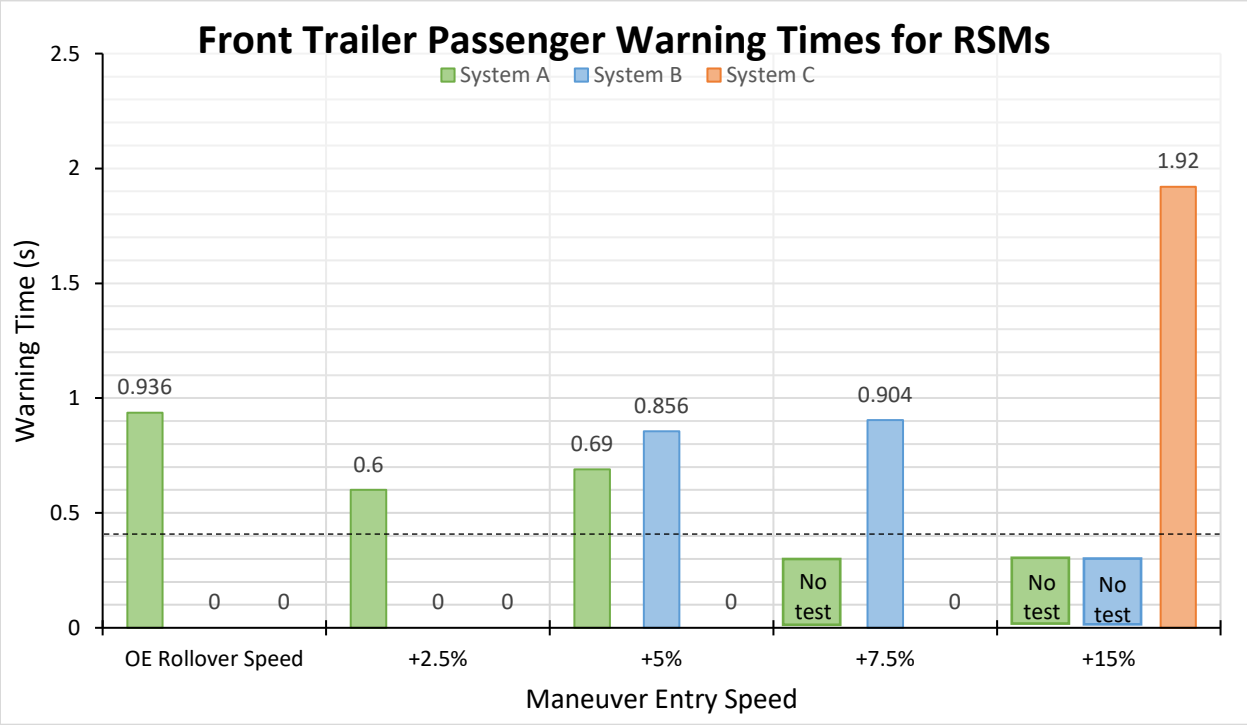

Figure 5-13. Front trailer passenger warning times during ramp steer maneuvers in 2S1M study, from OERS to +15% mph.

5.2.2.1 RSM Conclusion

In conclusion, RSC Systems B and C provided a maximum front trailer passenger outrigger contact improvement of 100%, meaning the vehicle did not roll at a speed at which did baseline. A maximum difference of 120.64% (seen in Figure 5-14) between systems at OERS+2.5% represents the massive performance difference that two RSC systems can have. This performance difference caused nearly a 5 mph improvement in rollover speed threshold, as seen in Figure 5-15. The lowest performing system only provided 1 mph improvement, showing diminutive stability gains. Using the rollover speed of System A rather than the rollover speed of System C can easily destroy any case advocating RSC usage when, in fact, the benefits of RSC can be quite helpful.

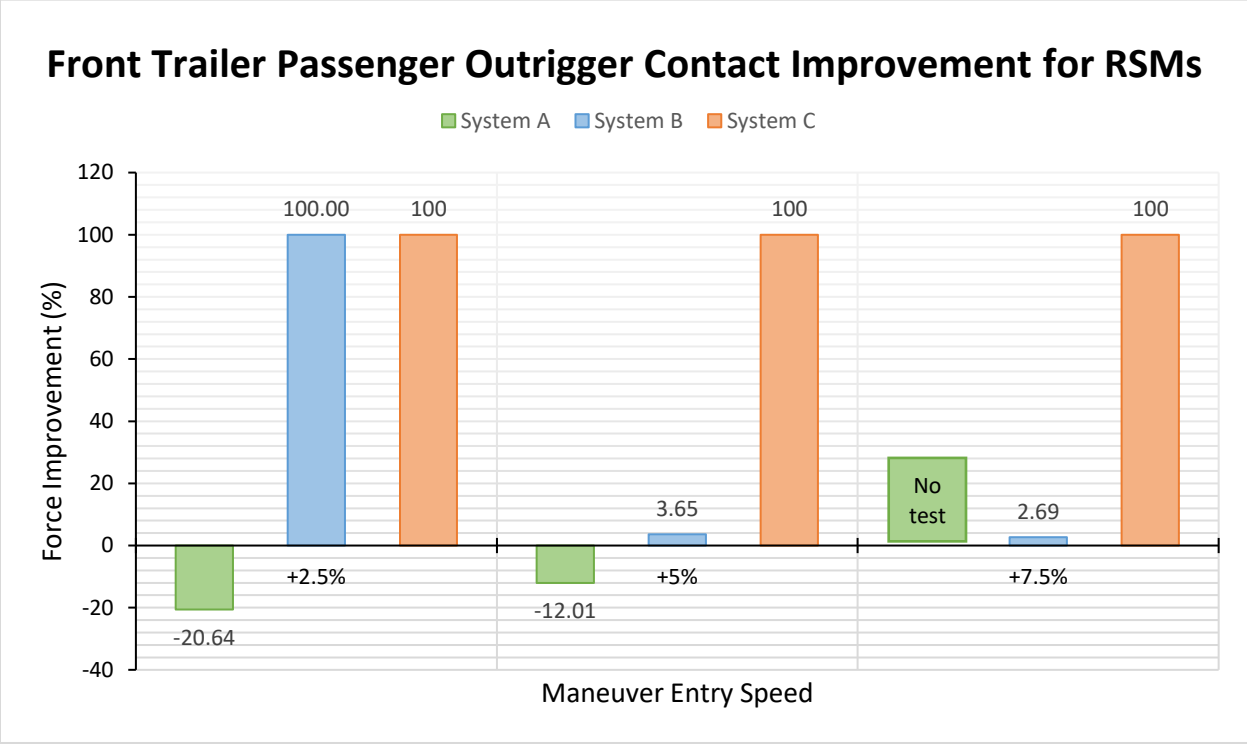

Figure 5-14. Front trailer passenger outrigger contact improvement during ramp steer maneuvers in 2S1M study, from OERS + 2.5% to +7.5% mph.

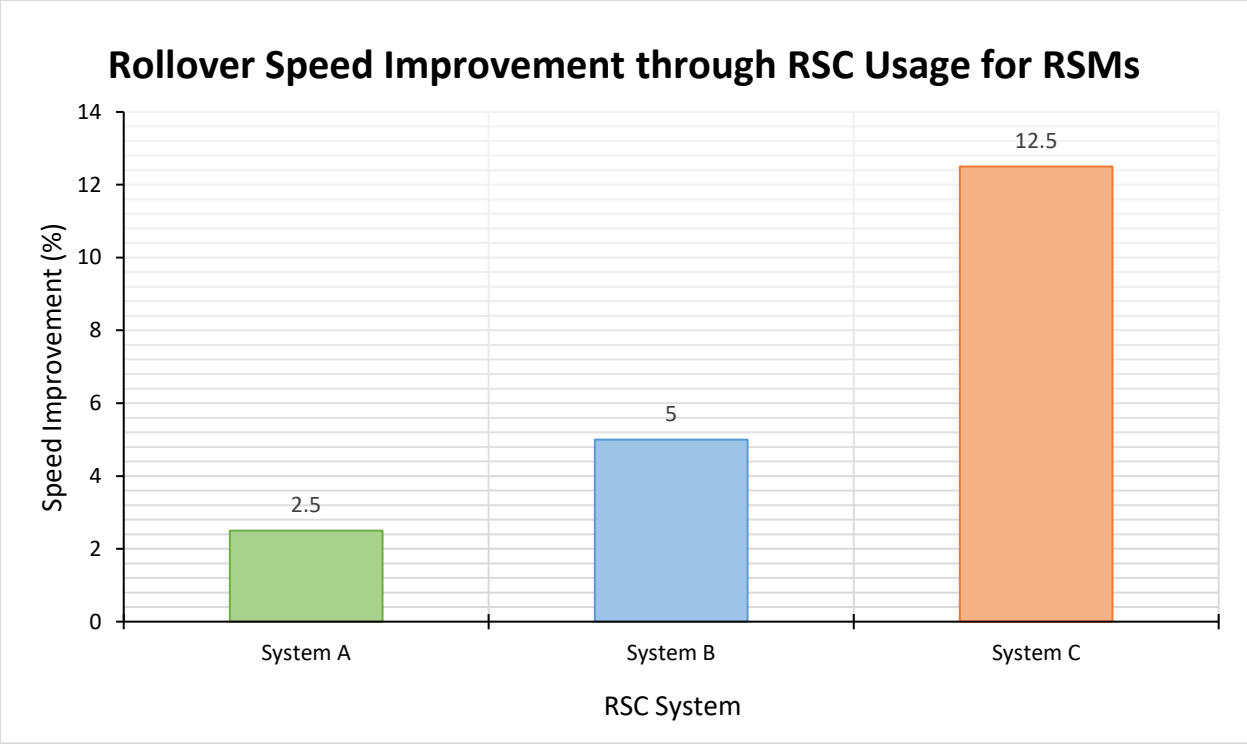

Figure 5-15. RSC system rollover speed threshold improvement over baseline during ramp steer maneuvers in 2S1M study.

5.2.3 SWD Results

SWD maneuvers involve leftward and rightward-directed paths as indicated in Figure 5-16, which shows the GPS results of a 90% SWD test. There are both driver- and passenger-side outrigger hits at both trailers because of this, as this was the most dynamic maneuver used in this study. The driver-side outrigger contacts occur during the first steering to the right, and the passenger-side contacts during the second. Outrigger contact data indicates that System C is the most reactive to the sudden change of direction during the second steering, and this is later supported by the activation time plots. The tests were run at the same speed while incrementing the maximum steering amplitude as the dependent variable. Therefore, SWD results are summarized by improvements in maneuverability rather than in speed.

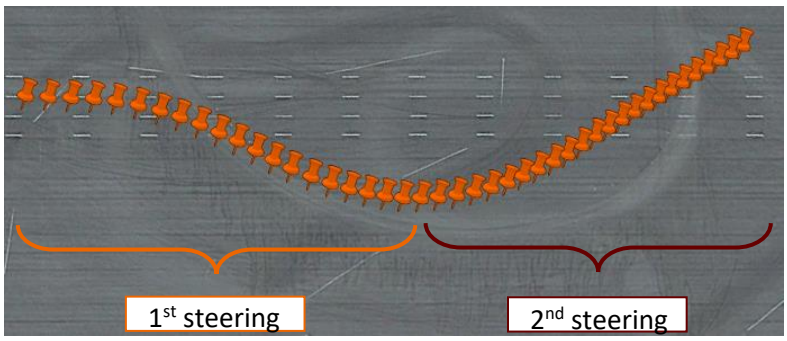

Figure 5-16. GPS results of a 90% sine-with-dwell test via Google Earth. There are two steering actions in a SWD.

As seen in Figure 5-17, the rollover steering amplitude of the baseline vehicle is referred to as the OERS. OERS for SWD tests refers to one of the certain ratios of the maximum steering input mentioned in Chapter 4 and shown in Figure 4-29. The 100% SWD was too dangerous for the baseline vehicle and System A. There was a noticeable difference between the RSC during these tests, with large improvements in the contacts at the front driver, front passenger, and rear driver side outriggers. The rear passenger outrigger constantly recorded the largest force, as a result of rearward amplification for a maneuver that swung the vehicle to the passenger side. Figures 5-18 and 5-19 break down the information provided in Figure 5-17 into front and rear trailer outrigger contacts.

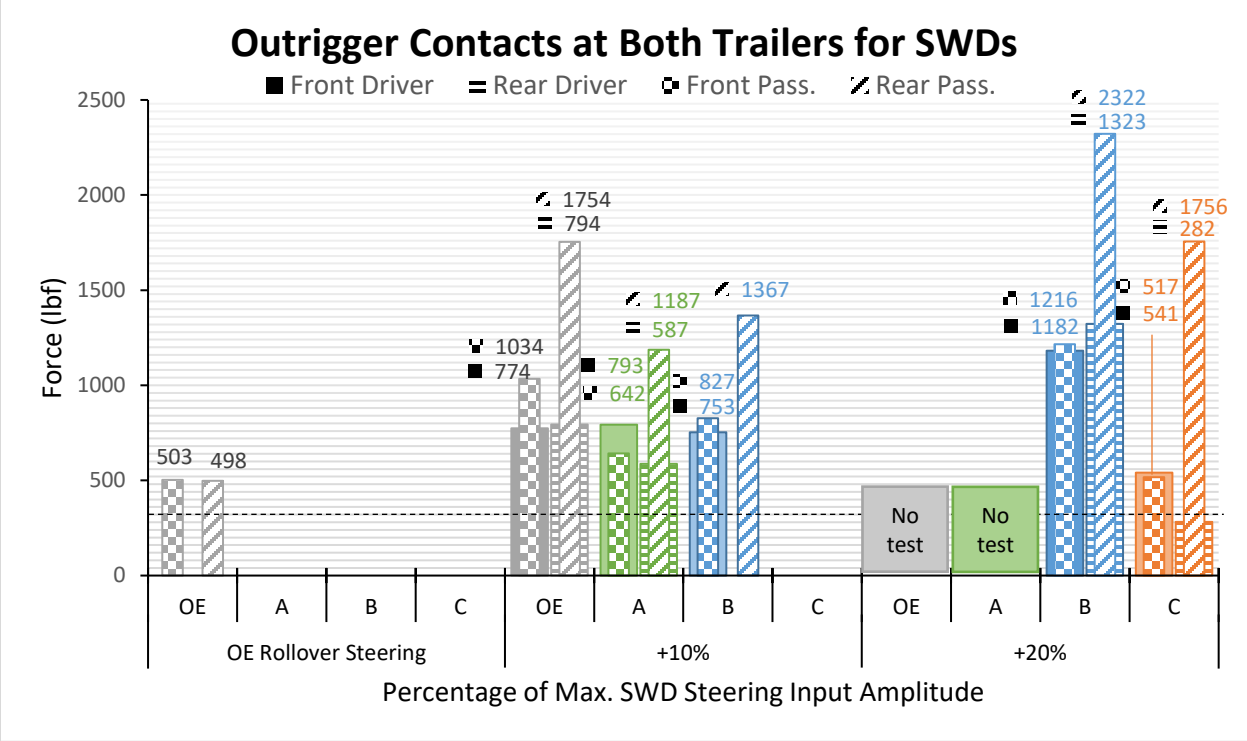

Figure 5-17. Outrigger contacts at both trailers during sine-with-dwells in 2S1M study, from OERS to +20% steering.

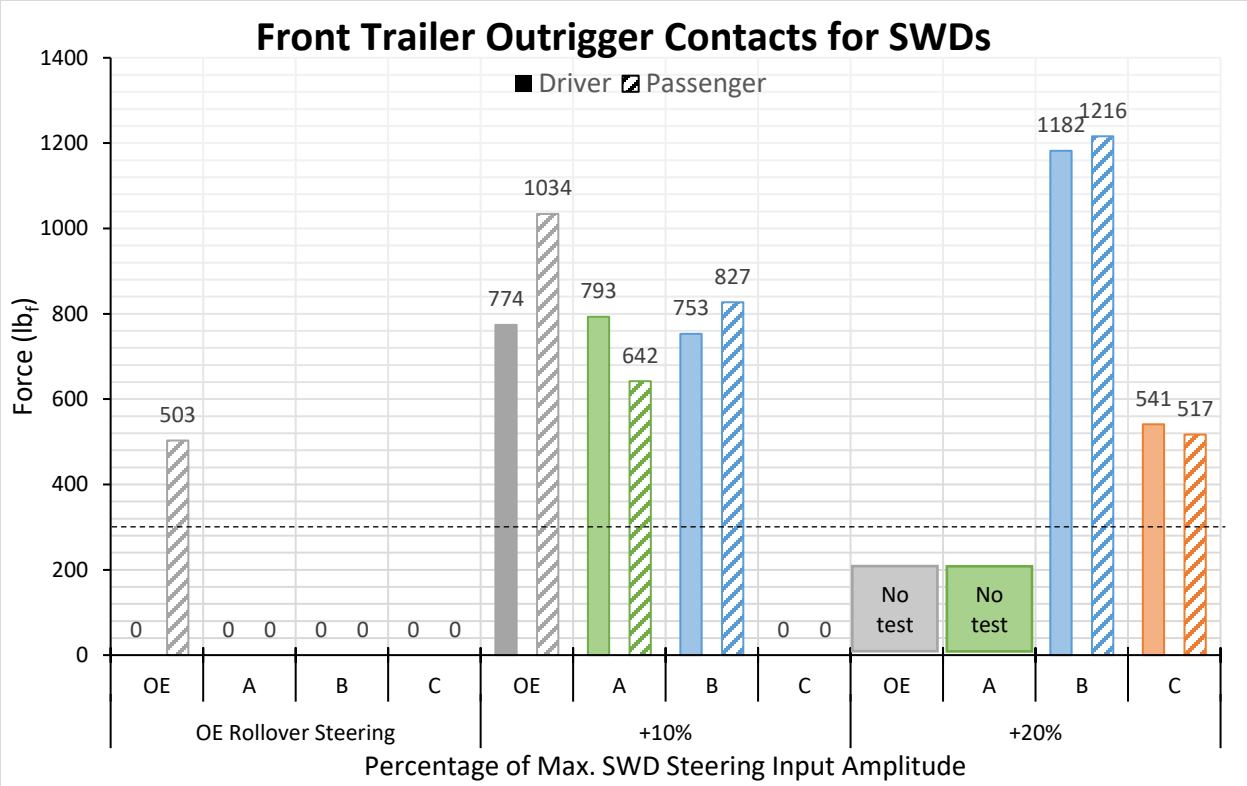

Figure 5-18. Front trailer outrigger contacts during sine-with-dwells in 2S1M study, from OERS to +20% steering.

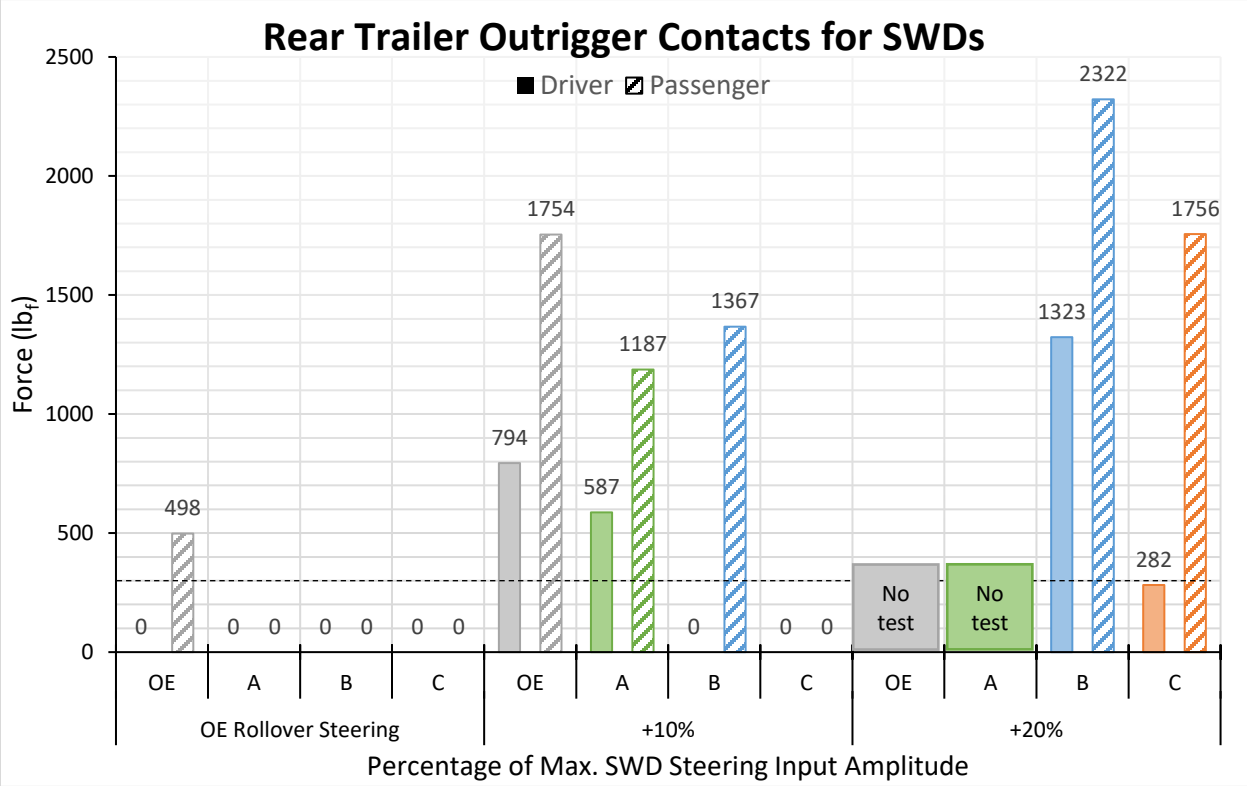

Figure 5-19. Rear trailer outrigger contacts during sine-with-dwells in 2S1M study, from OERS to +20% steering.

The activation times for this maneuver were partitioned to a first, or rightward-directed, steering, and a second, or leftward-directed, steering, as shown in Figures 5-20 and 5-21. Both driver- and passenger-side warning times were therefore considered using these results. Figures 5-20 and 5-21 show six datasets for the three SWD maneuvers discussed: System A's front and rear trailers, System B's front and rear trailers, and System C's front and rear trailers. The first steering is heavily inclined to rear trailer activations, while the second steering brought all four outriggers to contact regularly. System B stood out, as it held high activation times in the OERS+10% and OERS+20% tests, only activating after the entire maneuver was finished. In fact, Figure 5-22 presents negative warning times for System B, as the system would activate after the outrigger had contacted and roll had initiated. System B, and any other system that fails to detect roll when needed, was nothing but a baseline vehicle in those tests. System C, meanwhile, produced a positive warning time for a maneuver considered to be the most dynamic and strenuous on the vehicle.

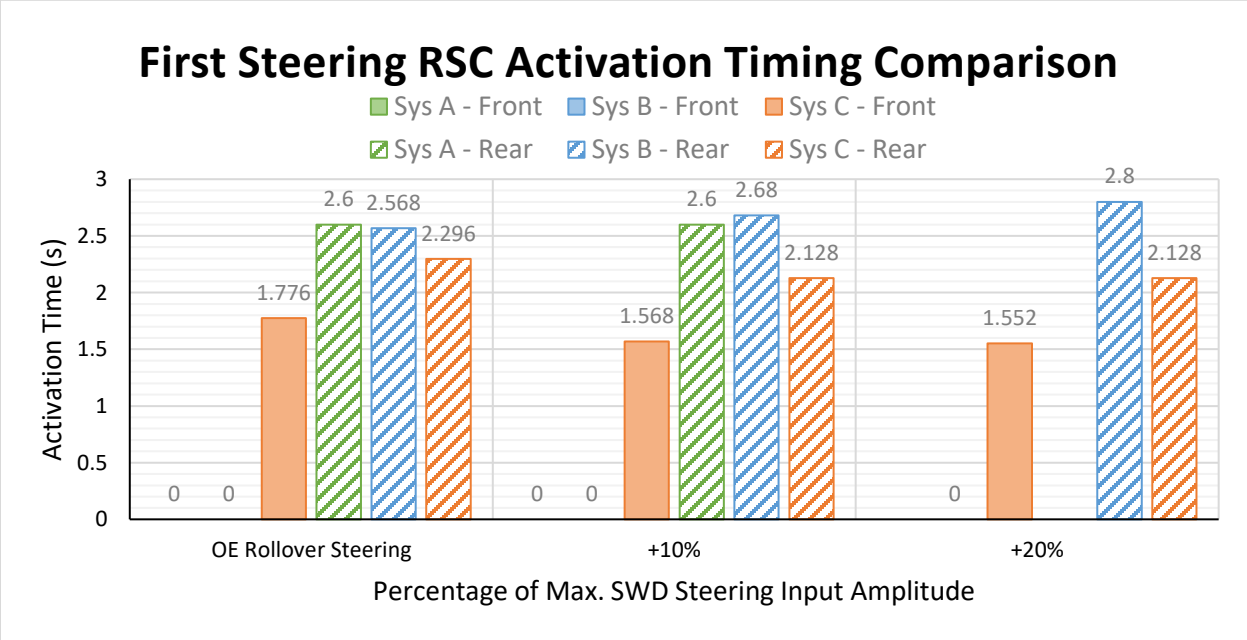

Figure 5-20. RSC activations at both trailers during first steering of sine-with-dwells in 2S1M study, from OERS to +20% steering.

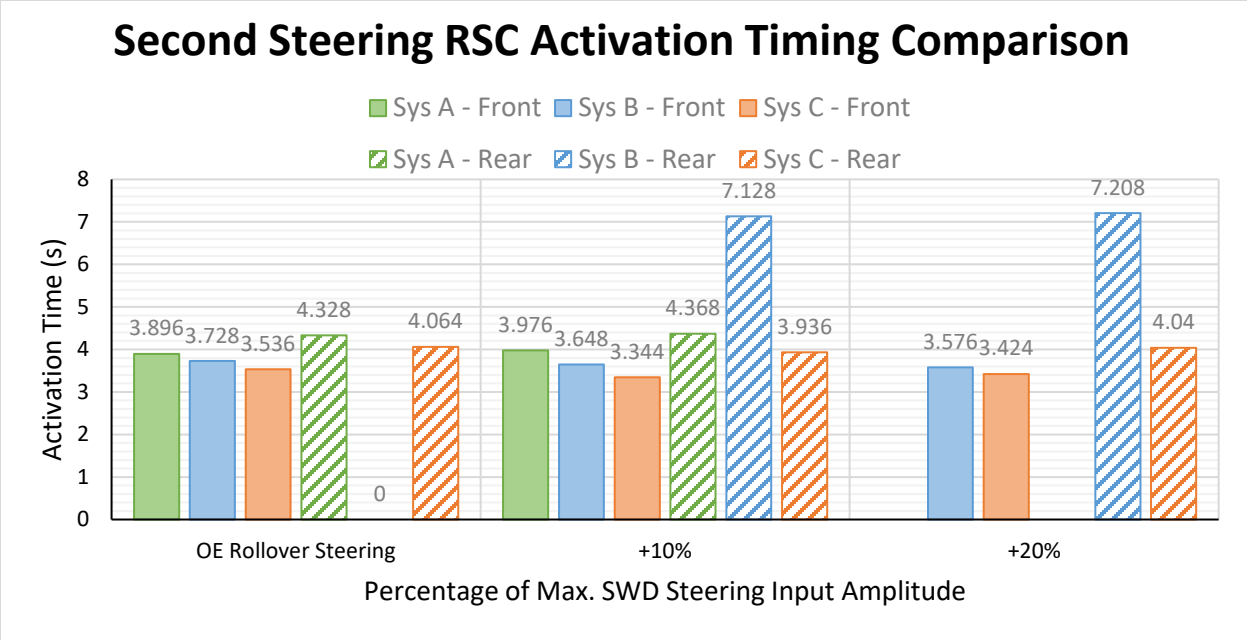

Figure 5-21. RSC activations at both trailers during second steering of sine-with-dwells in 2S1M study, from OERS to +20% steering.

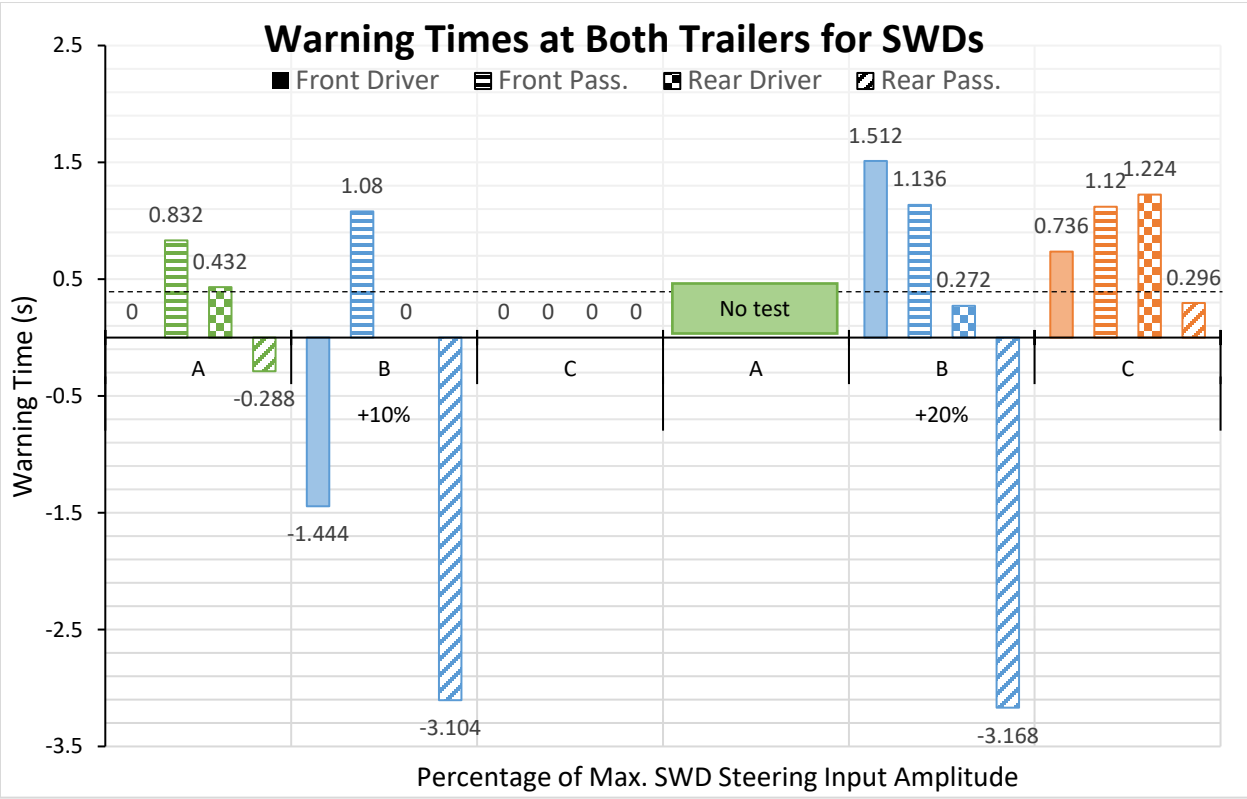

Figure 5-22. Warning times at both trailers during sine-with-dwells in 2S1M study, from OERS + 10% to +20% steering.

The objective of the vehicle in SWD tests is to stay upright while successfully evading an obstacle. In order to check the latter, cones were set up, as shown in Figure 5-23, every four feet laterally at a distance of 200 ft. where the vehicle's maximum lateral traveled distance occurred during the maneuver. A total of 17 cones were placed to mark a lateral distance of 64 ft. By logging the number of cones hit for each SWD test, the amount of inward tracking by each system was recorded, and the differences at respective rollover speeds were used to determine maneuverability improvements. This loss of maneuverability when braking is an important aspect of RSC system performance in gauging the ability of a vehicle to successfully avoid an obstacle without rolling over.

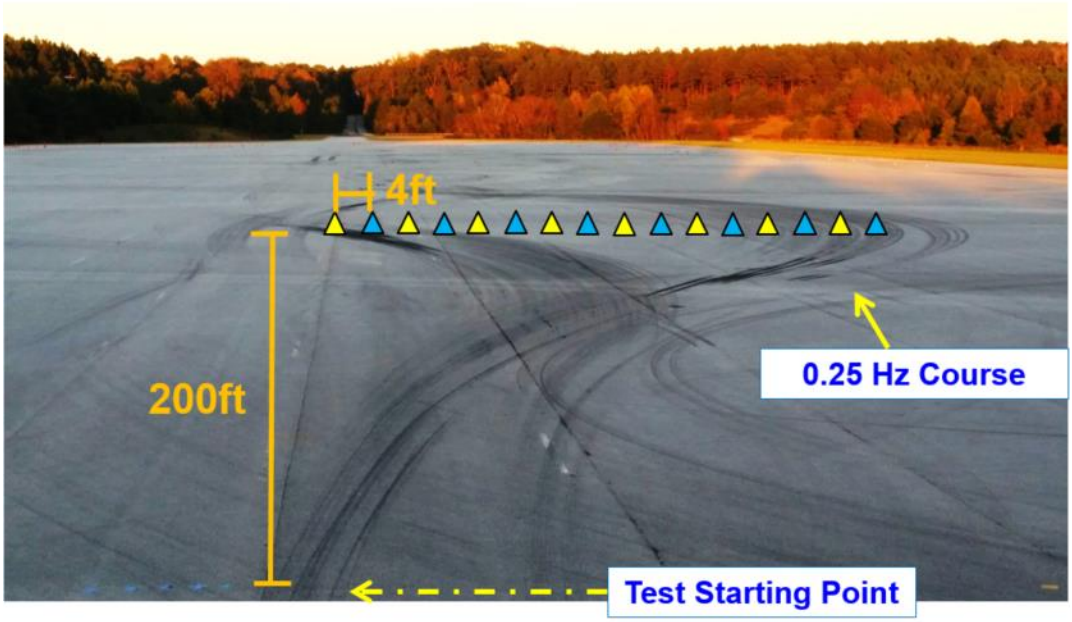

Figure 5-23. SWD course cones used to measure inward tracking. Understeer measured by number of cones hit.

Data of hit cones also shows that the tested RSC systems do not cause much inward tracking relative to the baseline vehicle's path. It is important to note that the activation times show that only System C applied brakes before reaching the cones, so only System C can be treated as a potential comparison between stock and RSC-using A-Doubles, but there was no difference between baseline and System C, as shown in Figure 5-24. In fact, for the OERS+10% steering, System C performed better at evading cones than did the baseline vehicle.

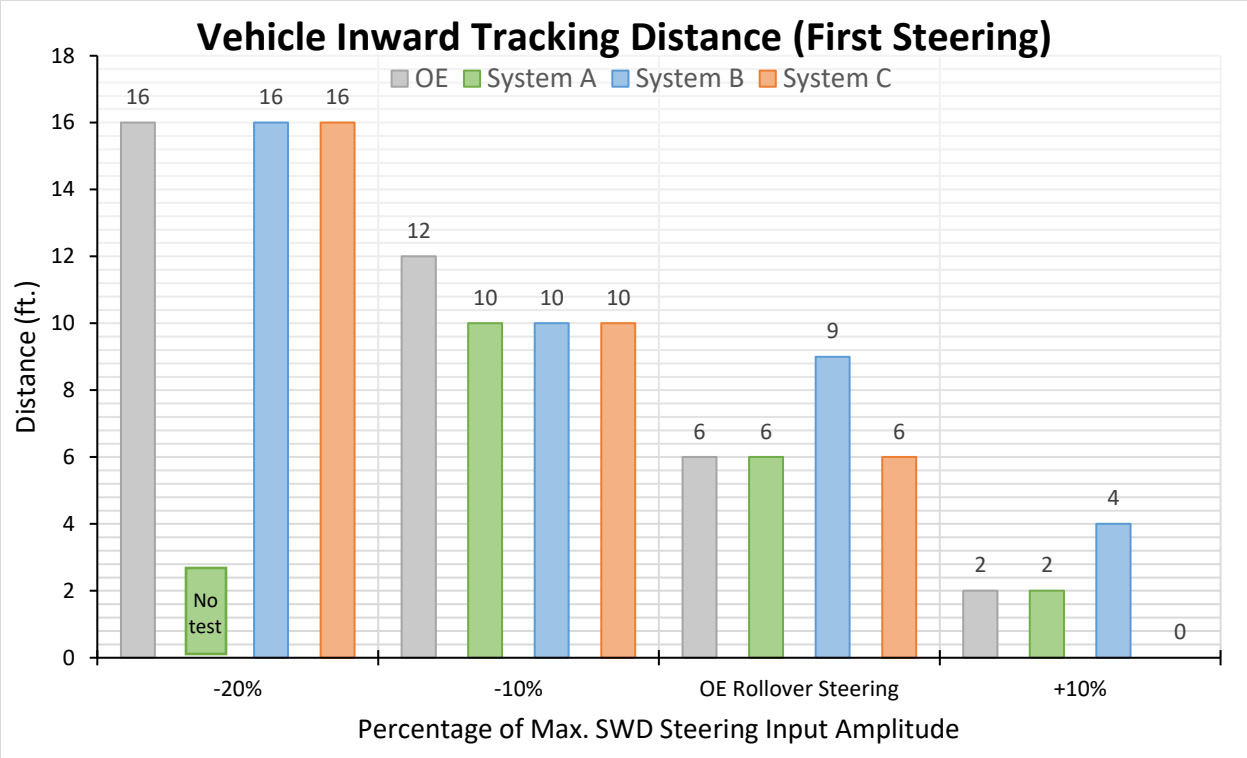

Figure 5-24. Vehicle inward tracking distance during sine-with-dwells in 2S1M study, from OERS - 20% to +10% steering.

5.2.3.1 SWD Conclusion

To conclude, RSC System C provided outrigger contact improvements of up to 100% at the steering of OERS+10%, as no outriggers contacted. Meanwhile, Systems A and B provided an average improvement of 24.93% and 36.21%, respectively, at all outriggers at the same steering. The maximum difference between two systems was 102.37% at the front trailer driver-side outrigger, and more importantly, the difference between outrigger contact forces at the rear trailer passenger-side outrigger was 77.94%. This large difference between System B and System C arose from the additional 3.192 s that System C worked with from an earlier activation time. Figure 5-25 shows the outrigger contact force improvements for all four outriggers at OERS+10% steering.

The outrigger force improvements resulted in a maximum maneuverability of 20.63% before rollover and a minimum of 9.53%, showing the efficacy of RSC systems in general for wide steering maneuvers, and potentially large performance differences between RSC systems. Figure 5-26 displays the rollover steering threshold improvements for the three RSC systems at OERS+10% steering.

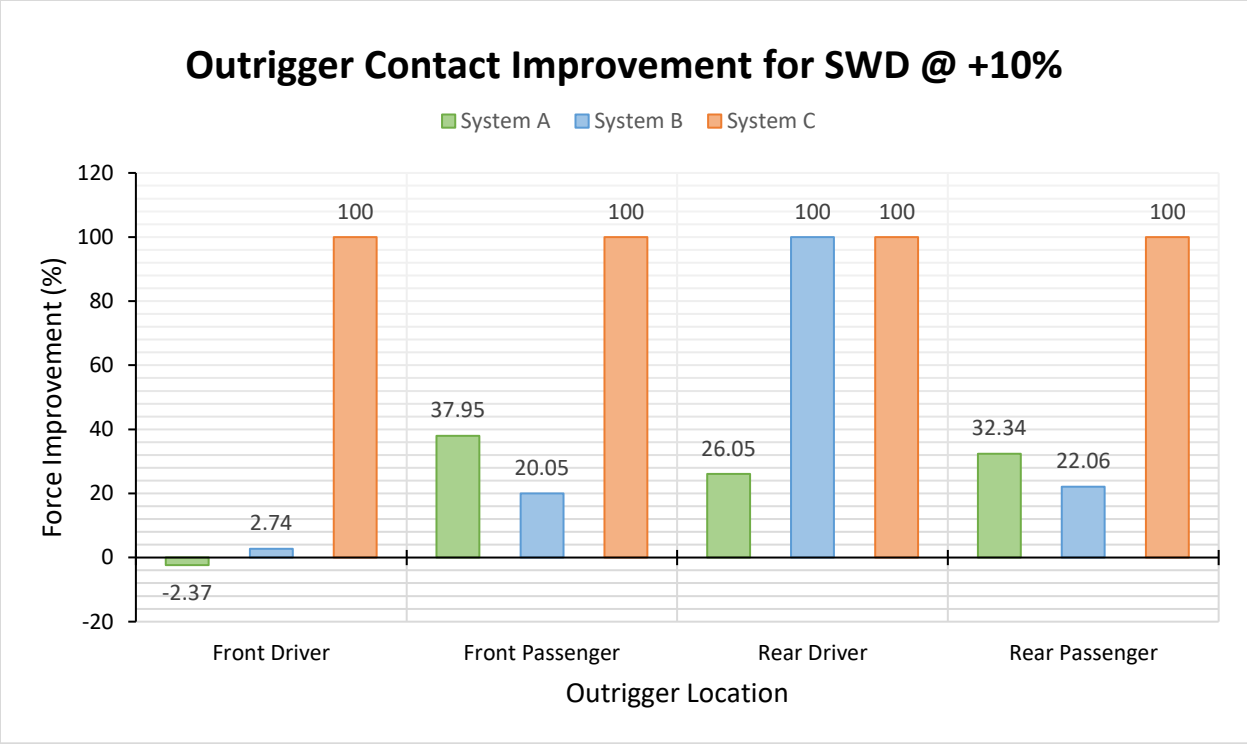

Figure 5-25. RSC system outrigger contact improvement for OERS+10 % steering sine-with-dwell test.

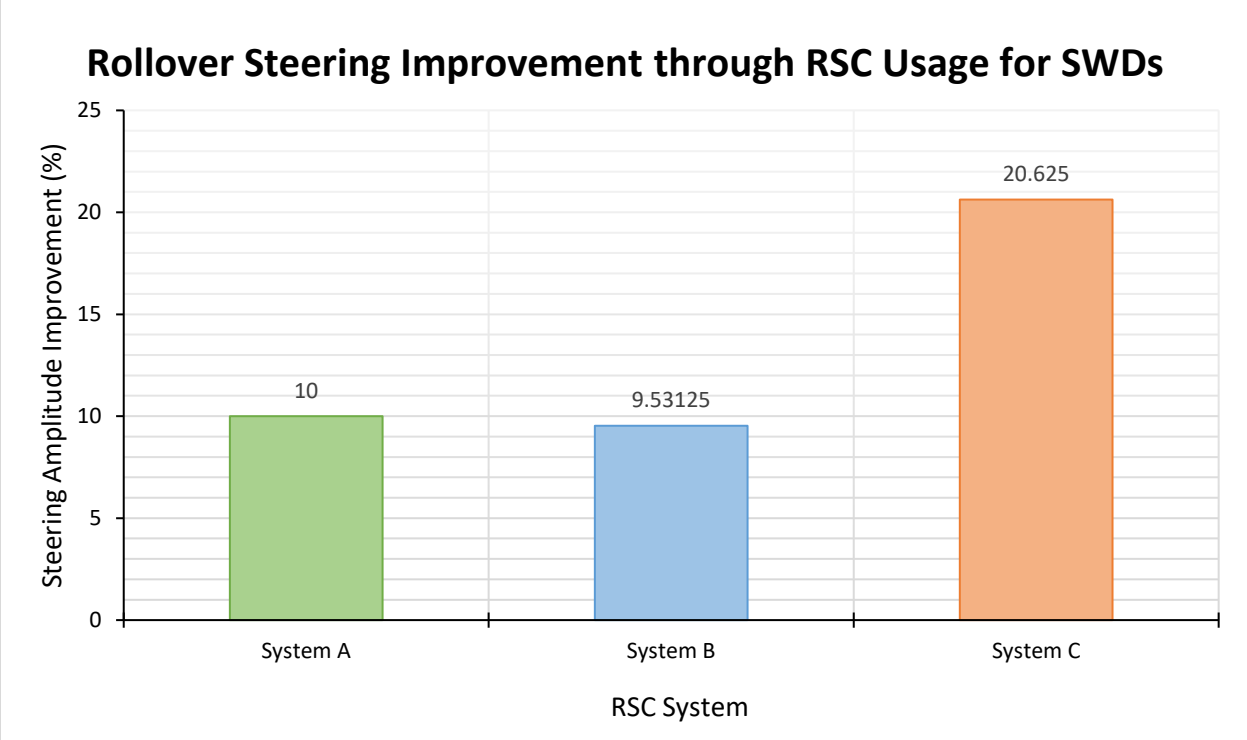

Figure 5-26. RSC system rollover steering threshold improvement over baseline during sine-with-dwell tests.

5.2.4 DLC Results

Figure 5-27 displays the outrigger contacts at both trailers for DLC maneuvers held at OERS to OERS+3.7%. System A did not have any DLC testing. The baseline vehicle exhibited harsh roll both at OERS mph and OERS+1.9%, and was withheld from any OERS+3.7% testing. Severe yaw dynamics usually accompanies maneuvers in which outrigger contacts are present at both sides of a trailer, especially when both contacts are of high magnitude, such as in the baseline OERS+1.9% test. The double lane change maneuver is highly dynamic, as rearward amplification plays a pivotal role in the dynamics of the rear trailer. This is evident in Figure 5-27, as the rear passenger outrigger experiences the highest contact forces as a result of a left-right-left DLC maneuver.

DLC outrigger contact force results appear to be inconclusive, as severe yaw and roll occur with System C at OERS and OERS+1.9%, but not at OERS+3.7%. The results also show that there was no rollover speed threshold improvement, as the rollover speed of the baseline, System B, and System C were the same. A closer look at Figure 5-27 will expose the fact that System C experienced the only front trailer roll out of any configuration, and also experienced rear driver outrigger contact at the three speeds. There seems to be large yaw stability differences between RSC systems, as System B exhibits no front trailer roll in any test, unlike System C. A closer look at the outrigger contacts at the rear trailer is shown in Figure 5-28.

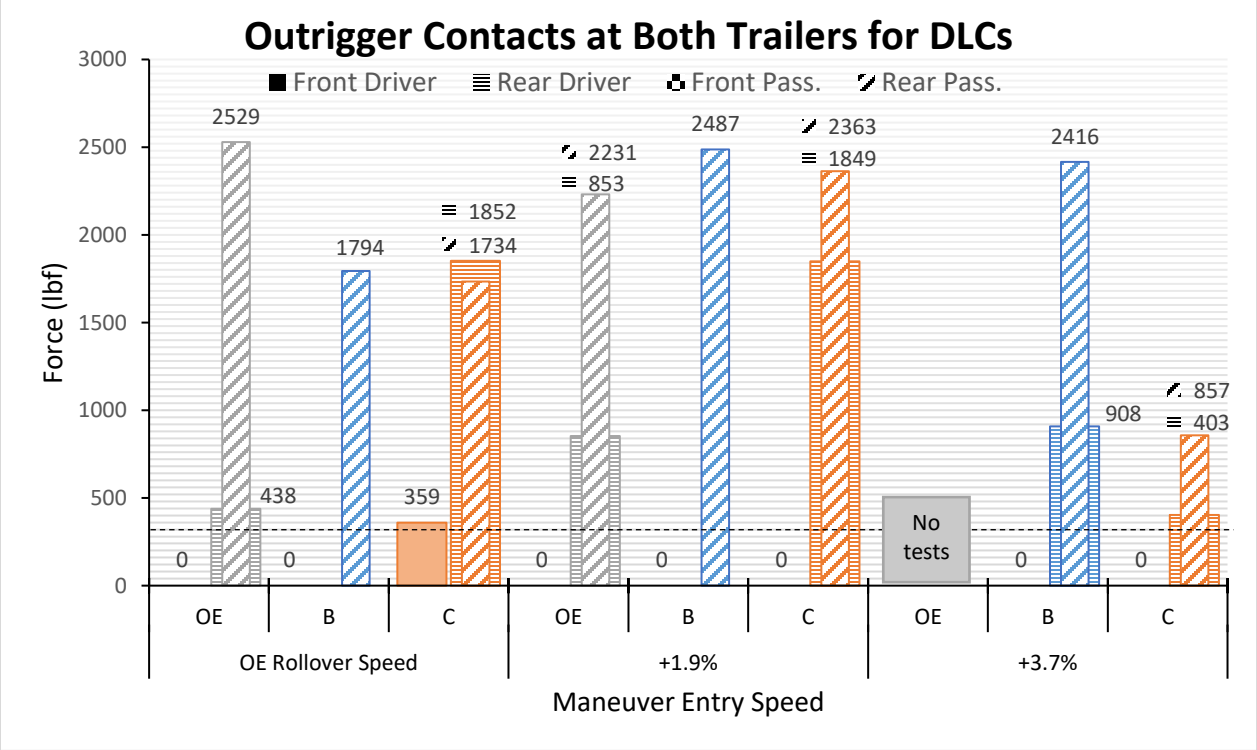

Figure 5-27. Outrigger contacts at both trailers during double lane changes in 2S1M study, from OERS to +3.7% mph.

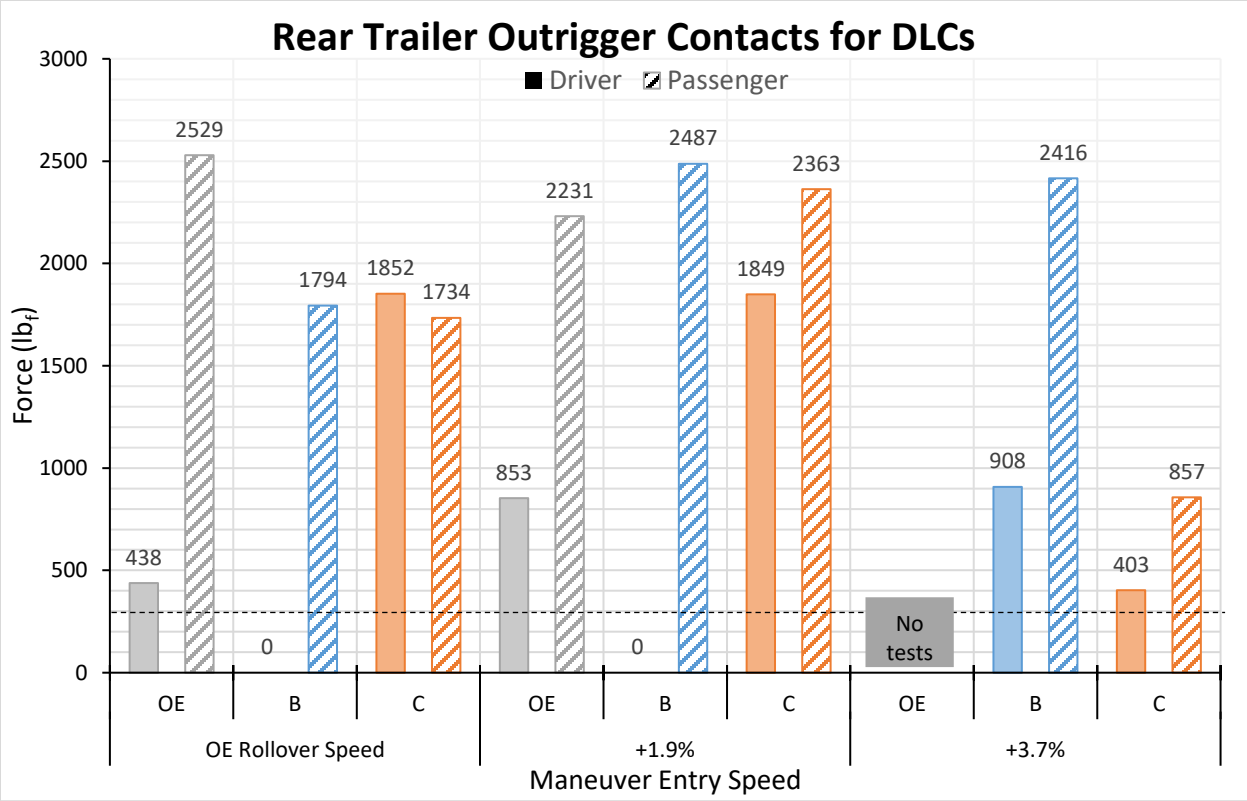

Figure 5-28. Rear trailer outrigger contacts during double lane changes in 2S1M study, from OERS to +3.7% mph.

Similar to the SWD maneuver, DLCs can be split into three separate steerings (Figure 5-29) which shows the GPS results for a 55-mph DLC baseline test. The activation times for the two tested RSC systems for both trailers are shown in Figures 5-30, 5-31 and 5-32, which show the first, second, and third steerings of a DLC maneuver, respectively. Figure 5-30 shows that System C activated, while System B had not, implying a more reactive (and possibly more intrusive) RSC system. Figures 5-31 and 5-32 display quite similar trends in both RSC systems tested, with System C demonstrating shorter activation times. These differences in activation time again play a large role in the warning times of the systems, as System B activated too late while System C had operated but not with sufficient time for brake application (Figure 5-33).

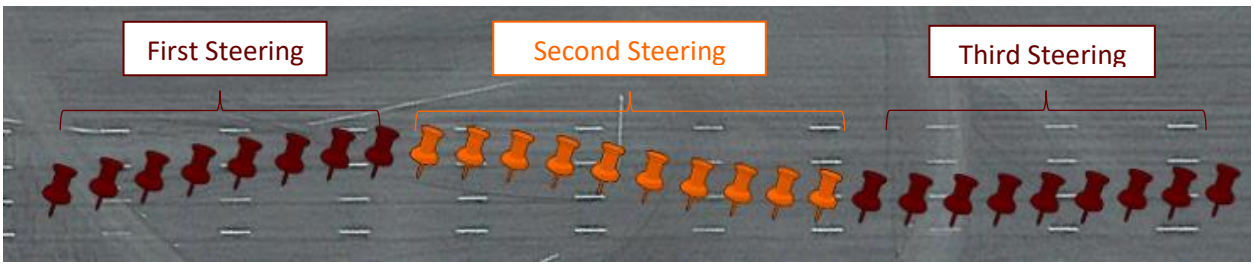

Figure 5-29. GPS results for a double lane change test via Google Earth. There are three steering actions in a DLC.

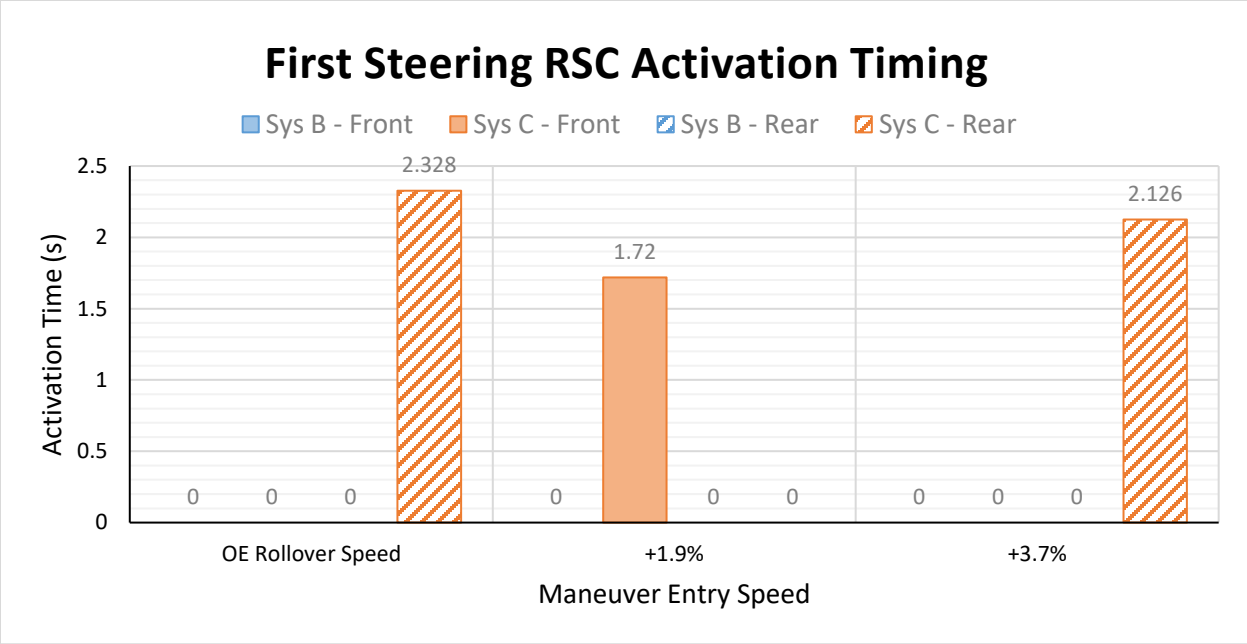

Figure 5-30. RSC activation times during the first steering of double lane changes in 2S1M study, from OERS to +3.7% mph.

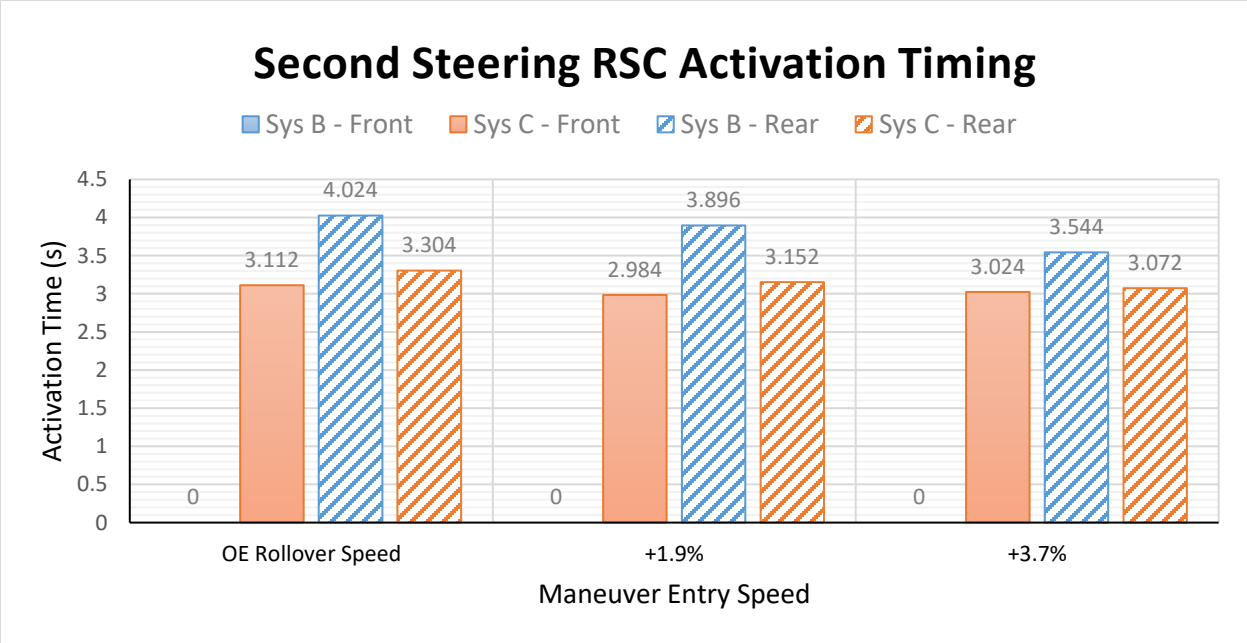

Figure 5-31. RSC activation times during the second steering of double lane changes in 2S1M study, from OERS to +3.7% mph.

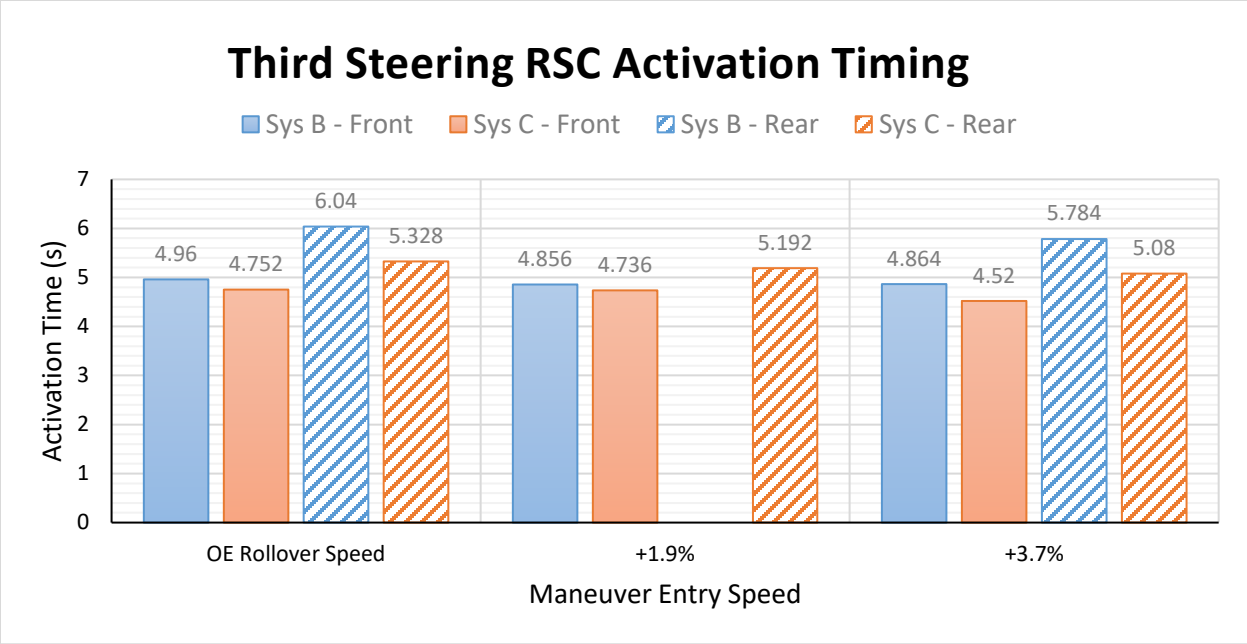

Figure 5-32. RSC activation times during third steering of double lane changes in 2S1M study, from OERS to +3.7% mph.

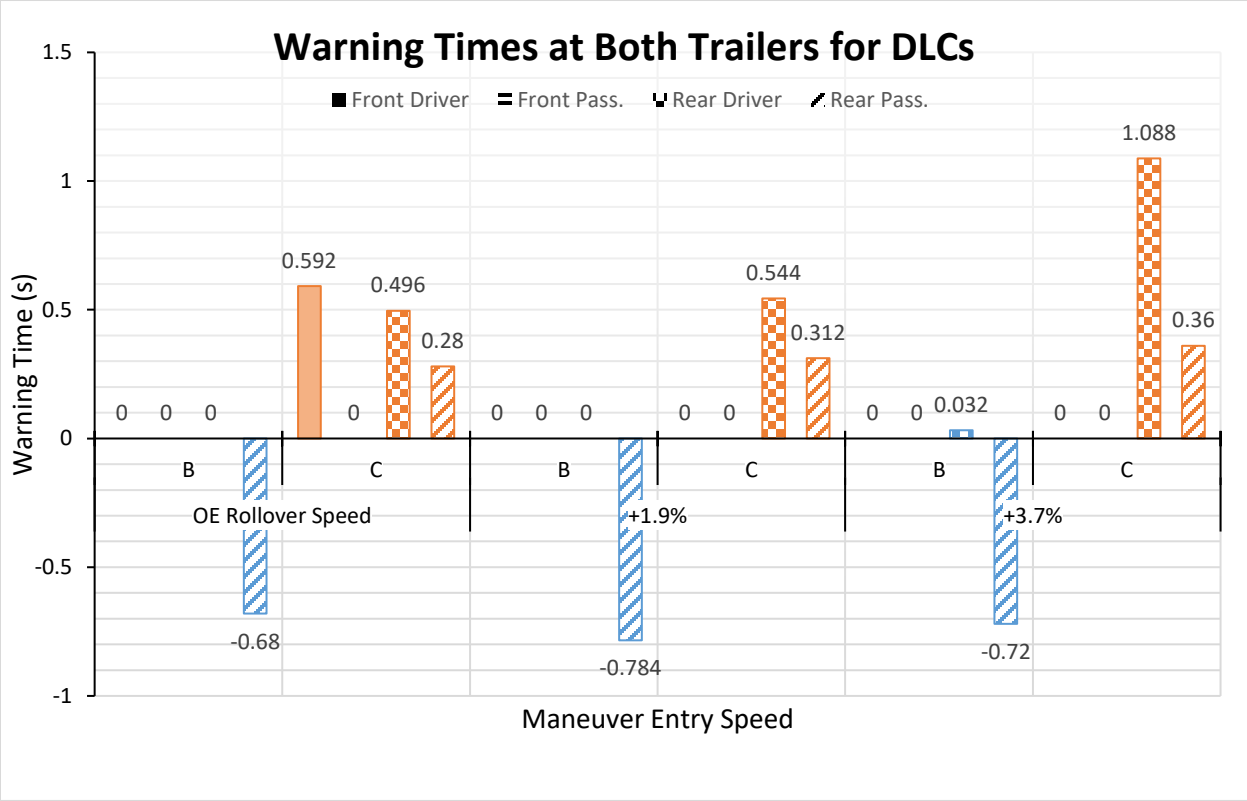

Figure 5-33. Warning times of both trailers during double lane changes in 2S1M study, from OERS to +3.7% mph.

5.2.4.1 DLC Conclusion

The lack of a clear conclusion from this study could be the result of driver operation, as both driver feedback and driver error varied through each test and retest. With the number of total tests completed for this maneuver, it would not be surprising to see an increase in driver performance in later tests, and therefore less rollover at higher speeds than would be otherwise predicted. Repeatability was a large issue in this test maneuver, as repeats at the same speeds saw different outriggers hit, as well as a different number of outriggers hit. It is possible that the energy dissipated with each outrigger hit had a significant effect on the dynamics of the vehicle, causing almost unrepeatable results.

Outrigger contact improvements for all four outriggers are shown in Figure 5-34. It can be seen that System C, which worked well in the SWD testing performed significantly worse than the baseline vehicle, as System C's rear driver outrigger contacted an average of 219.60% harder than that of the baseline. The opposite is true for System B, as it prevented roll at the rear driver side outrigger at both OERS and OERS+1.9%, while the baseline and System C rolled. However, System C yielded 54.17% and 44.32% rear driver and rear passenger outrigger contacts, respectively, during the OERS+3.7% testing over System B. In addition to the fact that System C was the only system that saw front driver roll, the DLC study generated wildly inconclusive results that did not show the same general performance improvements or trends as did the previous three maneuvers. No rollover speed threshold improvement was found among the two tested RCs systems for this maneuver.

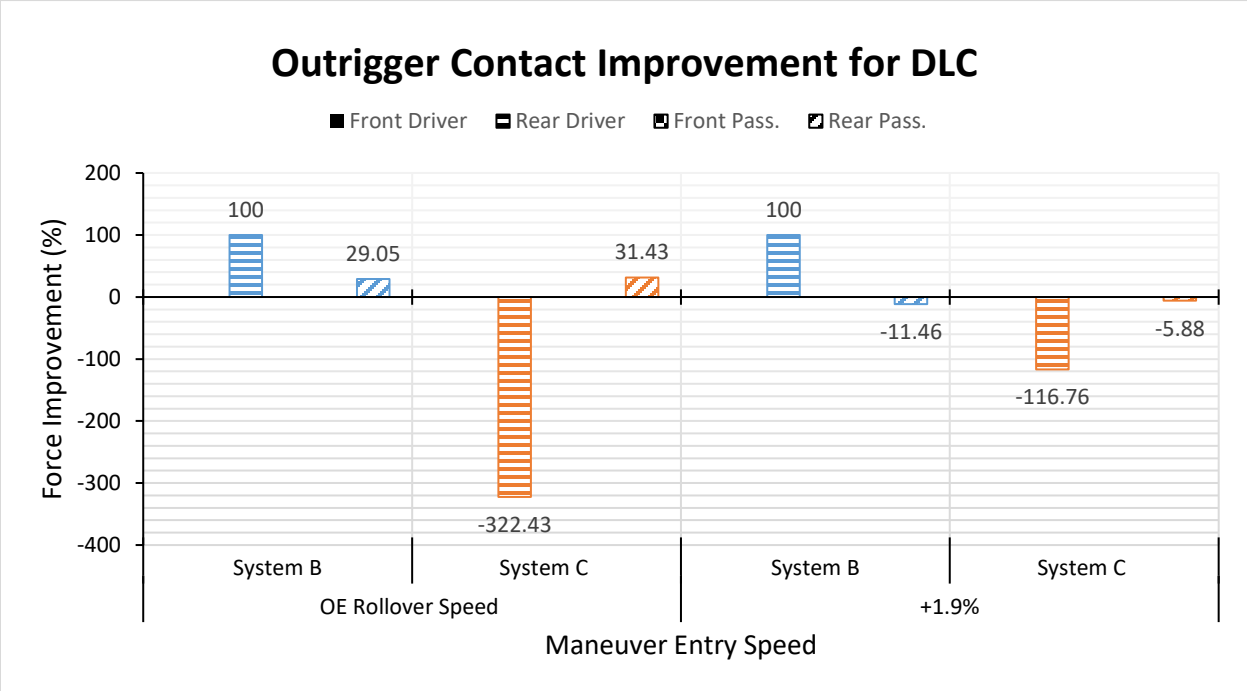

Figure 5-34. Outrigger contact improvement for OERS and OERS + 1.9% steering double lane changes.

5.2.5 Summary (A vs. B vs. C)

In summary of the single channel RSC system performance study, the following figures have been generated. Four maneuvers were used to evaluate three different RSC systems, and outrigger contact forces were used to quantify the roll severity for every rollover. The increase in rollover speed, or steering for the SWD tests, are the main measure of determining the benefits of RSC systems in general, as well as those of each specific RSC system tested. The differences between the RSC systems is calculated to support the notion that there are measureable differences between the efficacies of different commercially available RSC systems. Figure 5-35 shows the outrigger contact improvements for all three RSC systems for all four maneuvers at a speed or steering one increment past the OERS. The outriggers under consideration are the focus for each maneuver, so the J-turn and RSM tests concern the front passenger side outrigger while the SWD and DLC look at the rear passenger side outrigger.

It can also be seen that although System C generally performed better than System A and System B, the latter two performed better at different maneuvers. System B brought about a 100% increase (or prevented roll completely) during the OERS+2.5% RSM, yet provided the worst improvement at 22.06% for the OERS+10% SWD. System A actually worsened the front passenger-side outrigger contact force by 20.64% during RSM, but yielded a larger improvement over System B for SWD. Even System C, which dominated SWD improvement results with a 20.63% maneuverability improvement, performed worse than System B at J-turns. This data shows that RSC system algorithms can be geared towards certain maneuvers more than others, and that RSC systems' performances vary from situation to situation. The OERS threshold improvements are shown in Figure 5-36. Steering improvements are shown on the right-side axis, and speed improvements are shown on the left-side axis.

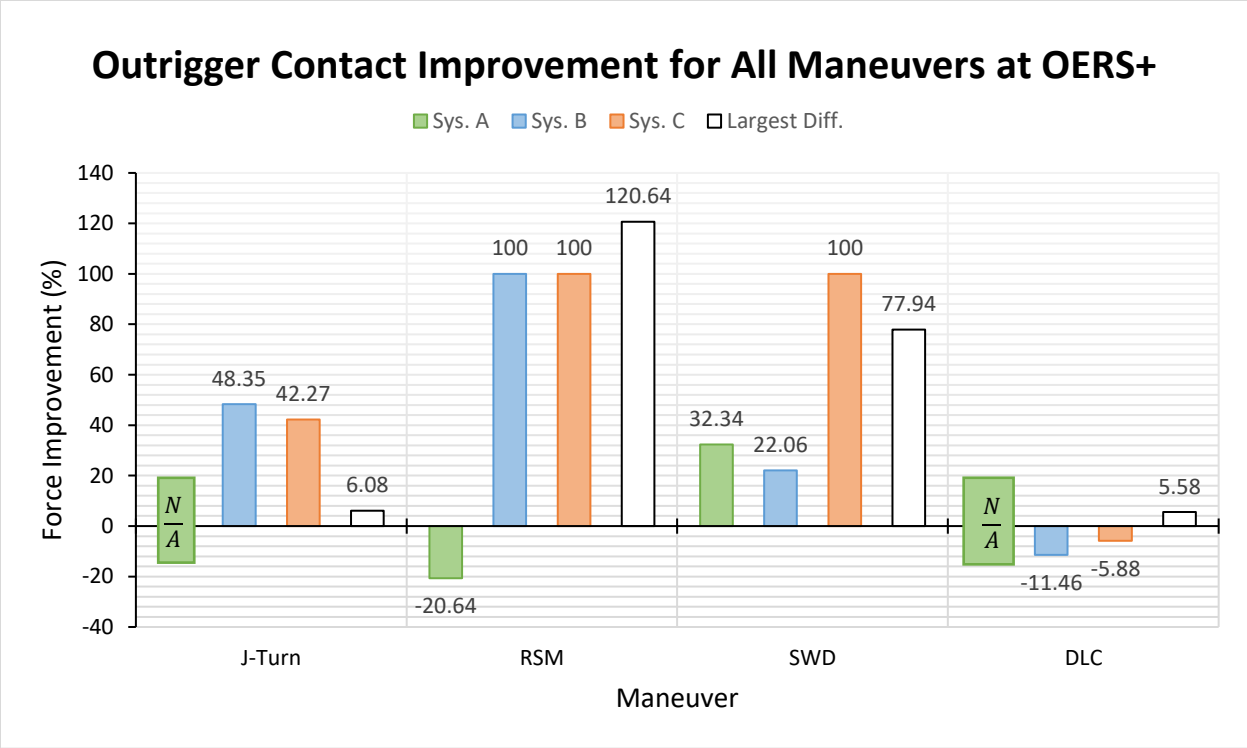

Figure 5-35. Outrigger contact improvements of all systems for all maneuvers at a speed or steering one increment past the OERS.

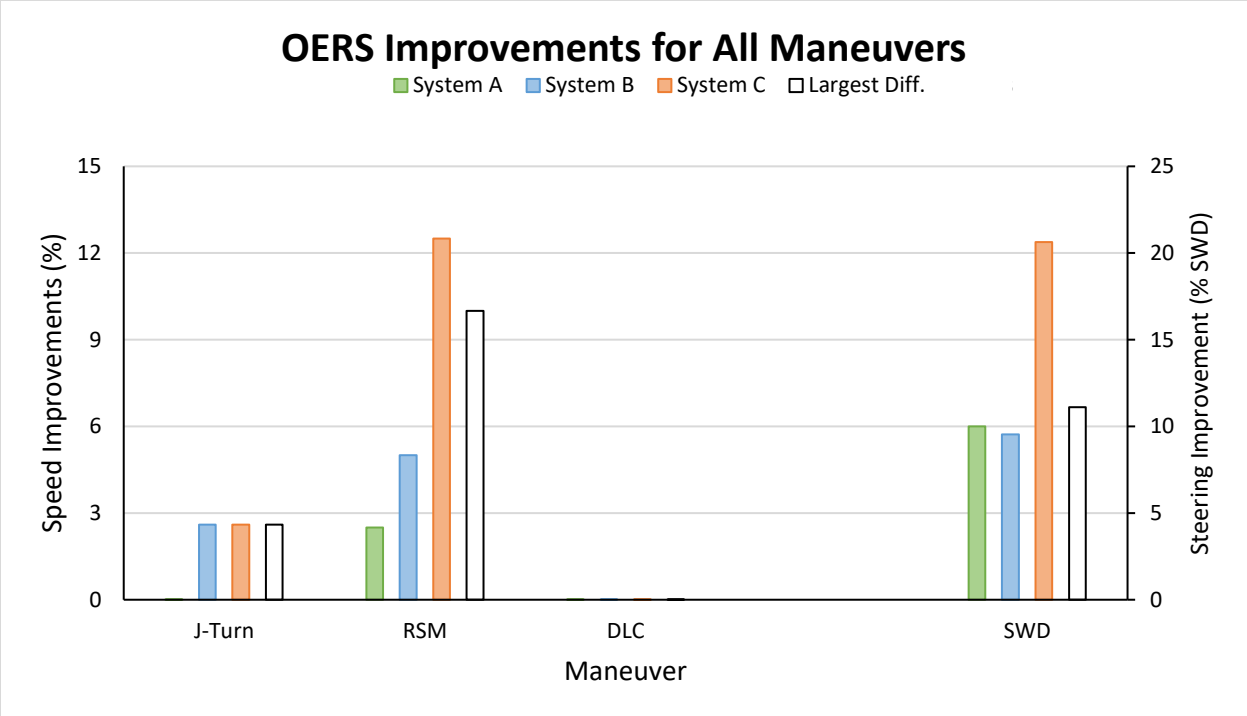

Figure 5-36. OERS threshold improvements of all systems for all maneuvers.

5.3 Dolly RSC Significance Study (A vs. A-D Study)

As mentioned earlier, RSC operation differs depending on the software within the black box and the hardware used with it. One option is to add an RSC system to the A-Dolly in addition to the two trailers, adding another set of brakes to control the vehicle. The idea here is to minimize the rotational freedom between the dolly to both the front and rear trailers by decelerating the three units together. An ancillary exploration into whether a dolly RSC could affect RSC system performance, and whether an addition of dolly RSC gears the system towards a type of certain maneuver, is covered in this section.

The following graphs will provide an analysis of System A and System A with dolly RSC, hereby referred to as System A-D. Since System A was not tested with J-turns and DLC, a comparison between the two systems will made only through RSM and SWD results.

5.3.1 RSM Results

Figure 5-37 displays the outrigger contact forces at the front trailer for RSM tests at OERS to OERS+5%. As noted before, System A's rollover speed, or RS, for RSM was OERS+2.5%, while Figure 5-37 shows that System A-D's RS is at OERS. System A-D has a 24% lower contact force at the front trailer than the baseline vehicle exhibited. Both System A and System A-D experienced harder rolls for OERS+2.5% and OERS+5% RSM tests, while System A-D provided both more roll stability at OERS+2.5%, and less at OERS+5%. The average difference between the two systems is only 157 lb_f in favor of System A.

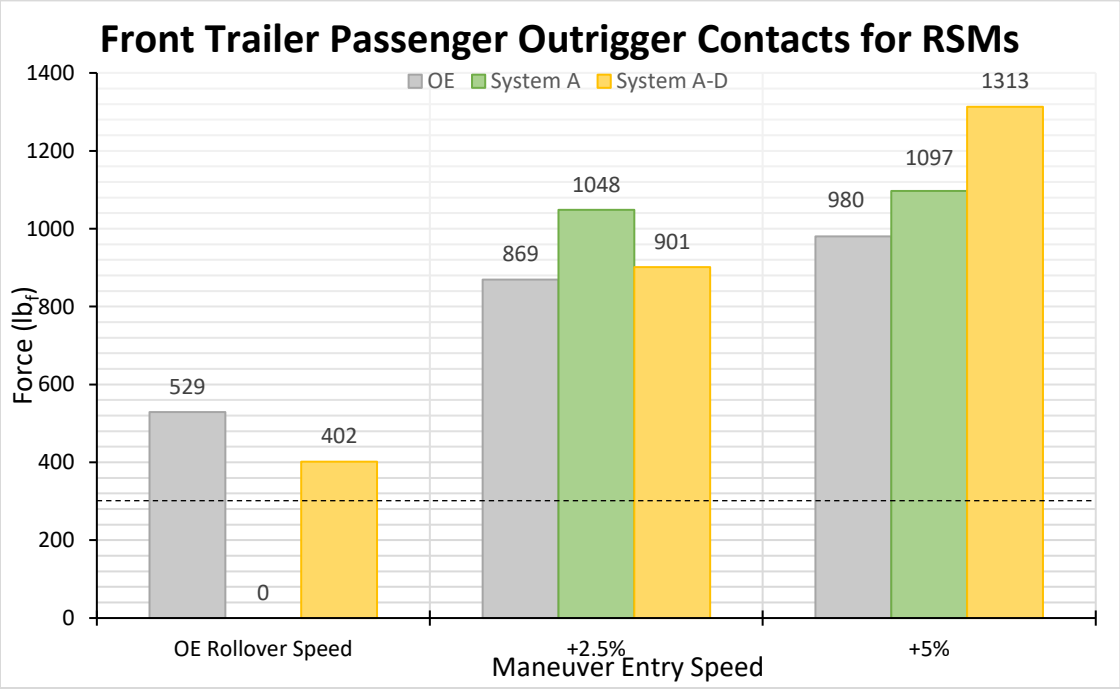

Figure 5-37. Front passenger outrigger contacts during ramp steer maneuvers in dolly study, from OERS to +5% mph.

Figure 5-38 shows a puzzling trend in the System A front trailer activation time, while the System A-D activations trend towards a naturally quicker activation as the maneuver entry speed increases. More importantly, however, is the fact that, ultimately, the difference between the system activations becomes small. Quite inconclusive warning time results are shown in Figure 5-39.

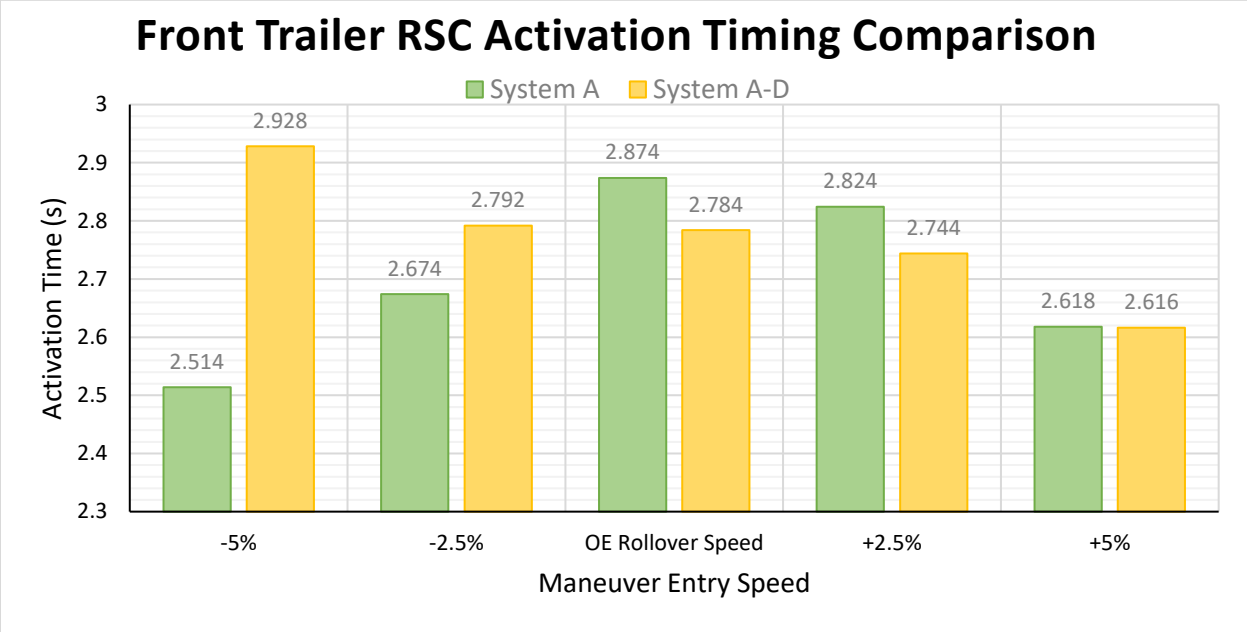

Figure 5-38. Front trailer activation times during ramp steer maneuvers in dolly study, from OERS to +5% mph.

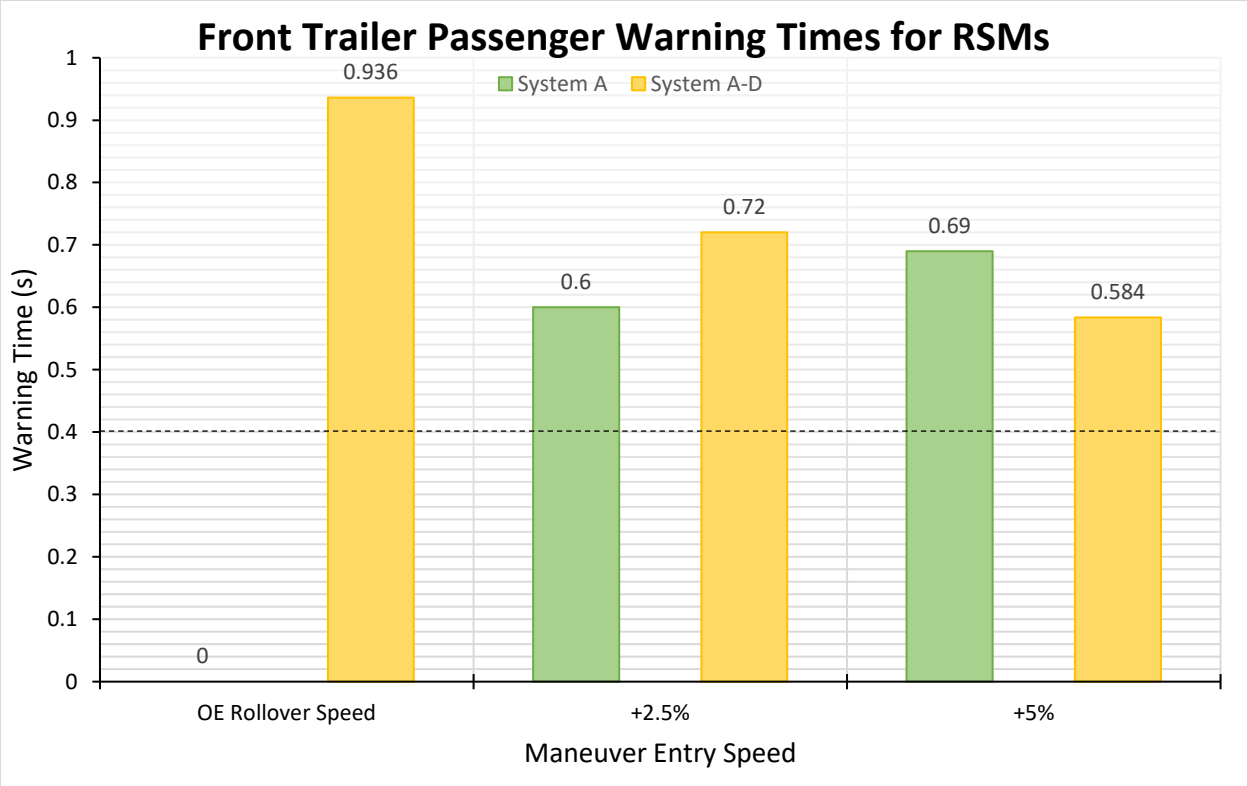

Figure 5-39. Front trailer warning times during ramp steer maneuvers in dolly study, from OERS to +5% mph.

5.3.1.1 RSM Conclusion (A vs. A-D)

Outrigger contact, activation data, and warning time data showed small differences between Systems A and A-D. The only visible difference lay in the fact that System A-D rolled at OERS, one mph earlier than System A, while activating earlier. This OERS yielded the largest front trailer passenger outrigger contact improvement of 75.92%, but the average difference through two speeds in which both rolled was only 2.51% in favor of System A. Figure 5-40 shows these outrigger contact improvements. A very small rollover speed improvement difference is shown in Figure 5-41.

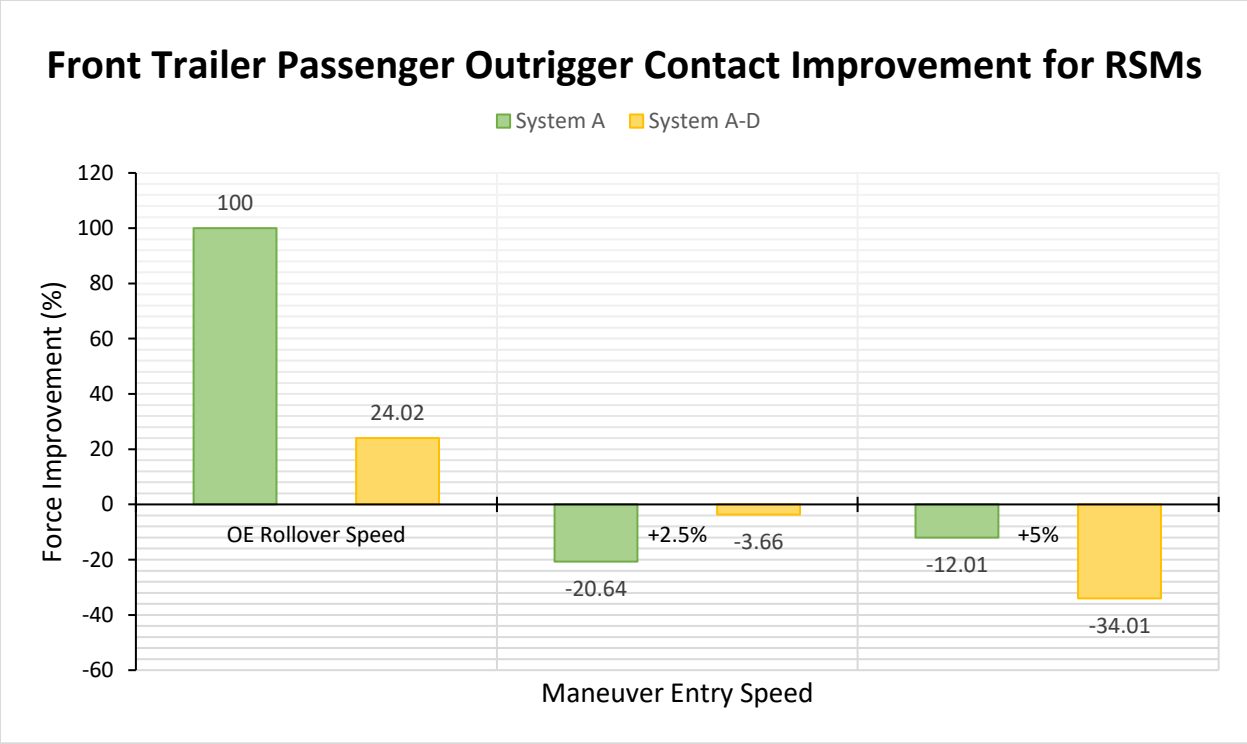

Figure 5-40. System A and A-D front trailer passenger outrigger contact improvements for ramp steer maneuvers in dolly study, from OERS to +5% mph.

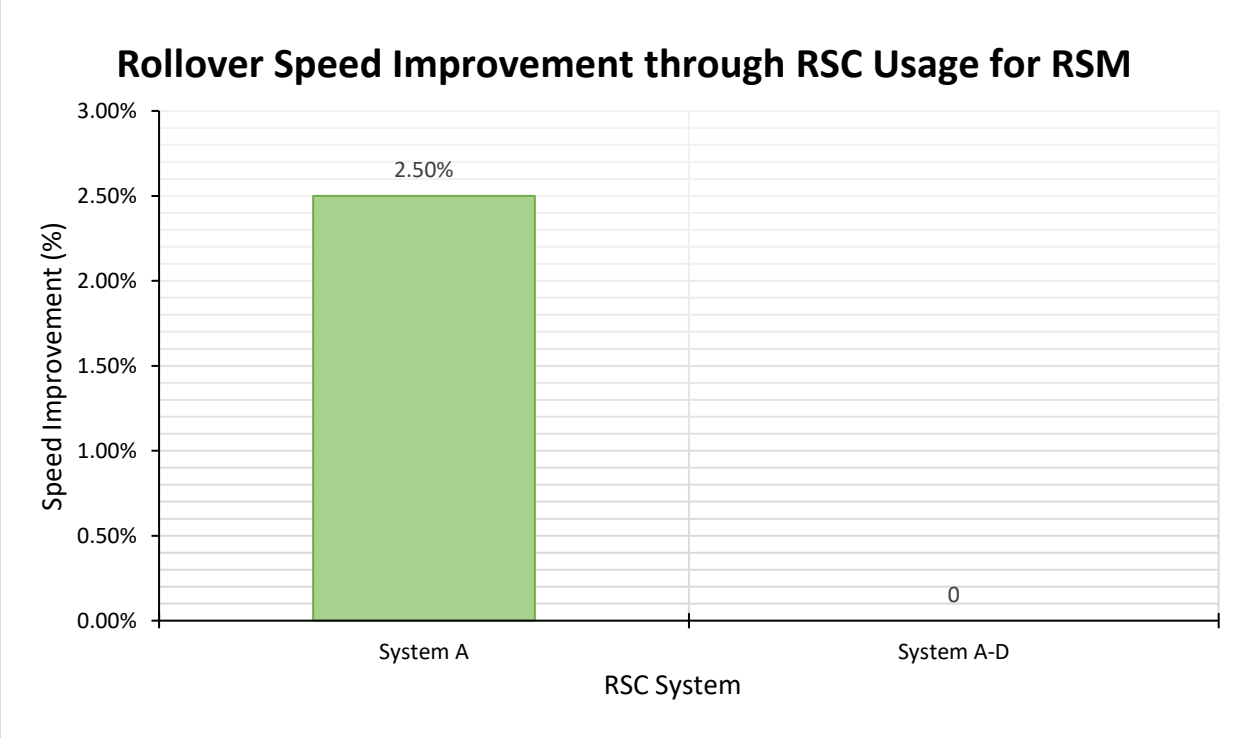

Figure 5-41. System A and A-D rollover speed threshold improvement over baseline for ramp steer maneuvers in dolly study.

5.3.2 SWD Results

The next several graphs cover the test results from SWD maneuvers. Figure 5-42 shows the outrigger contact forces at the front trailer for SWD tests at OERS and OERS+10% steering amplitude. As seen in all other SWD tests, the rear passenger side outrigger experiences the highest contact forces. System A-D sees improvement over all four outrigger contacts at OERS+10%, which is the rollover steering for both systems in this test set. Both System A and System A-D decrease all four outrigger contacts, mostly the front passenger outrigger contact of 32.34% and 59.45%, respectively. Systems A and A-D perform quite similarly, as seen in the closer looks at the front and rear trailer outrigger contacts for the second test shown in Figure 5-42, with small improvements found in System A-D. The front trailer is shown in Figure 5-43 and the rear trailer is shown in Figure 5-44.

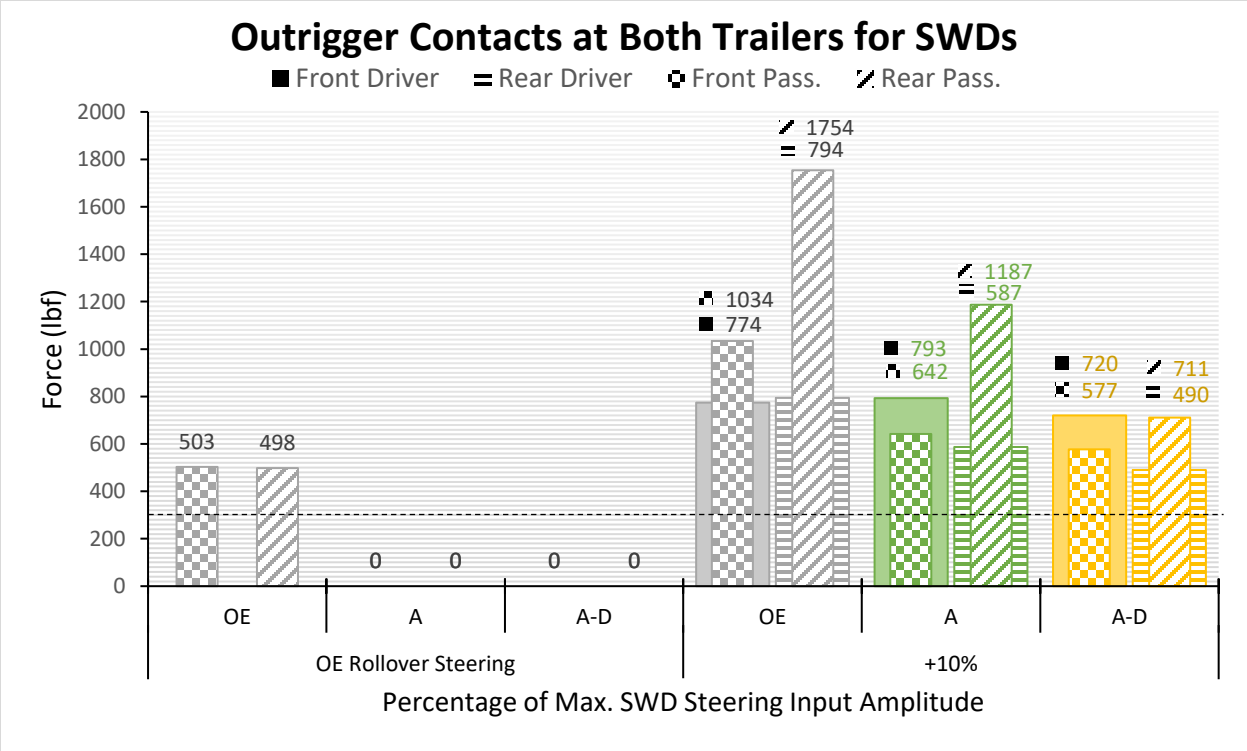

Figure 5-42. Outrigger contacts at both trailers for sine-with-dwells in dolly study, from OERS to +10% steering.

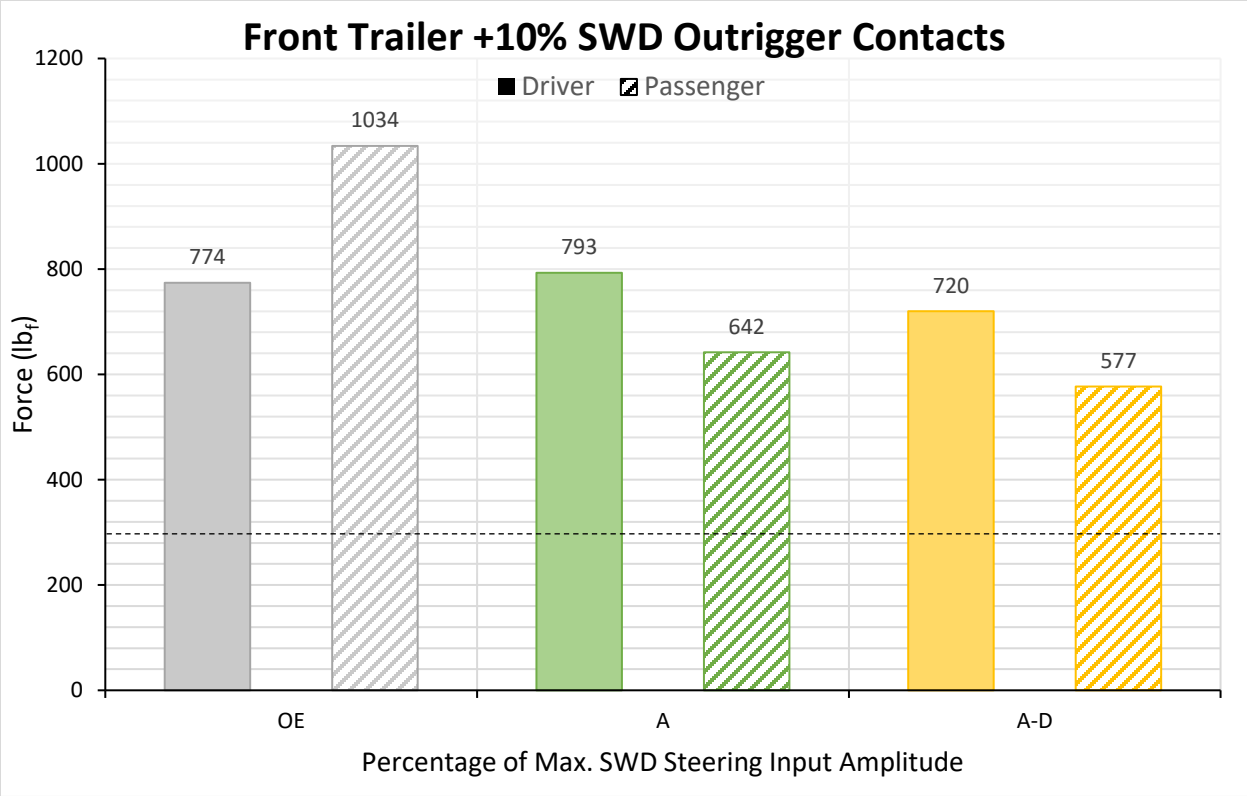

Figure 5-43. Outrigger contacts at front trailer during OERS +10% steering sine-with-dwell in dolly study.

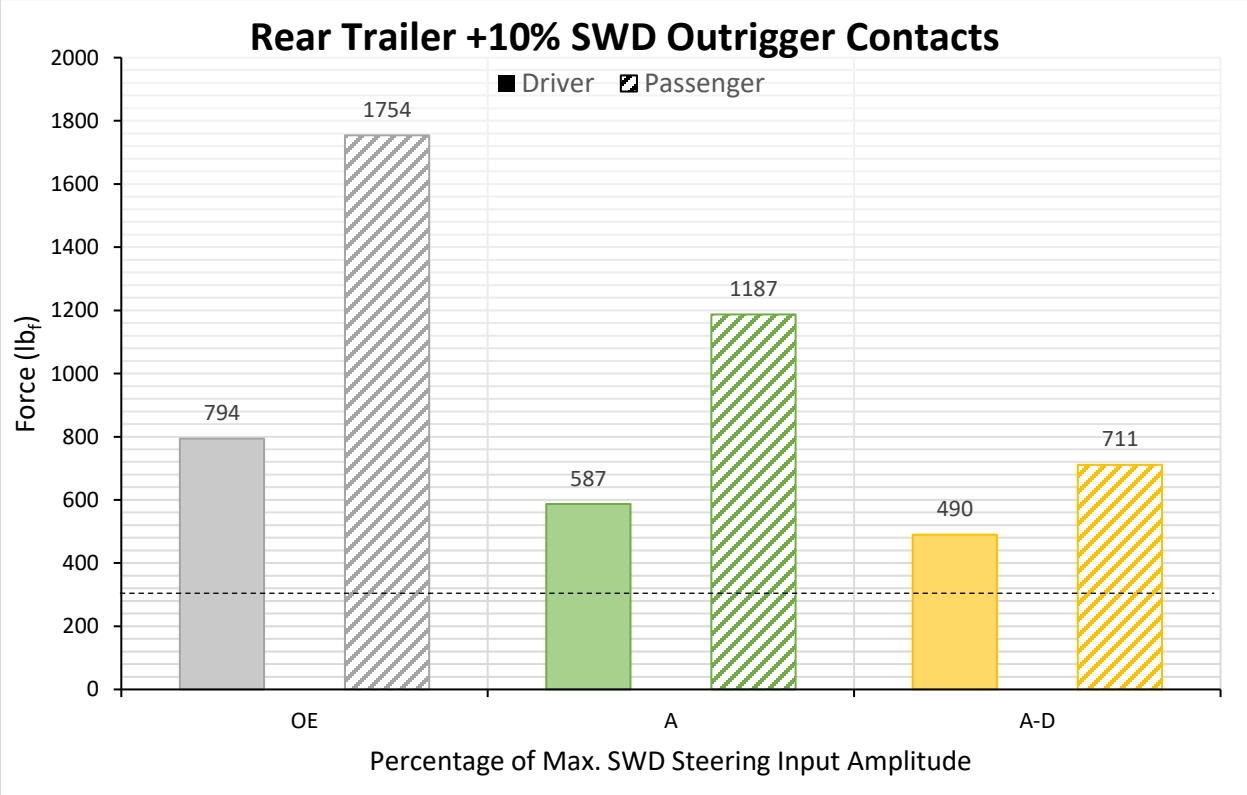

Figure 5-44. Outrigger contacts at rear trailer during OERS +10% steering sine-with-dwell in dolly study.

Activation times and warning times show just how similarly the two perform. As it holds for any SWD test, activation times are split into the first and second steerings of the maneuver. Figure 5-45 shows the first steering activation times, and Figure 5-46 shows the second steering activation times. The minimal improvements of one system over the other provide negligible differences in real-life rollovers of such heavy and large vehicles. Figure 5-47 displays the similar warning times of the two systems at +10% SWD.

An argument for inward tracking differences as a measure of performance was again valid for this study as both systems activated brakes before reaching the cones in SWD tests. The amount of vehicle understeer is shown in Figure 5-48. There was no significant difference between the inward tracking between System A and System A-D.

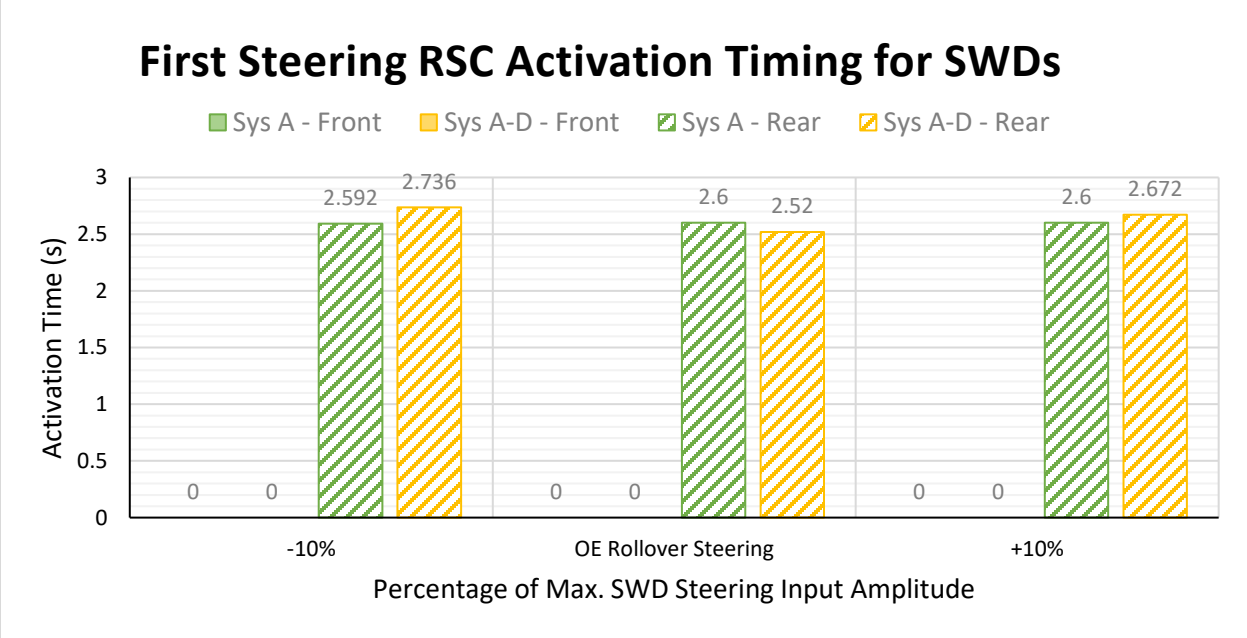

Figure 5-45. RSC activation times during first steering of sine-with-dwells in dolly study, from OERS -10% to +10% steering.

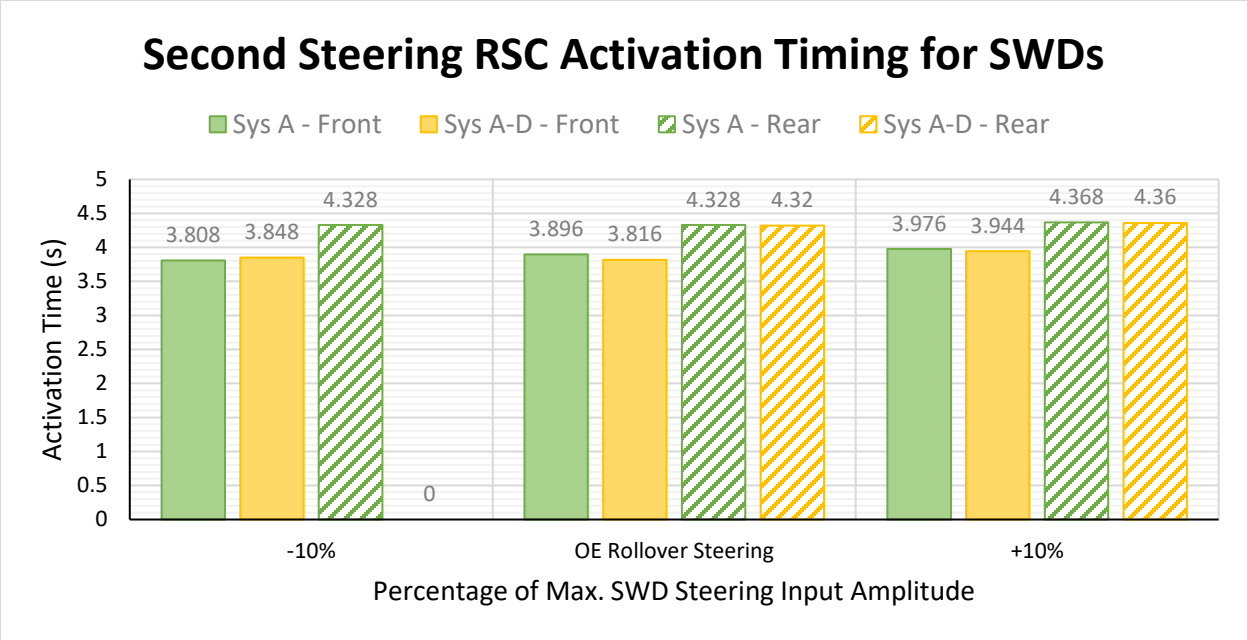

Figure 5-46. RSC activation times during second steering of sine-with-dwells in dolly study, from OERS -10% to +10% steering.

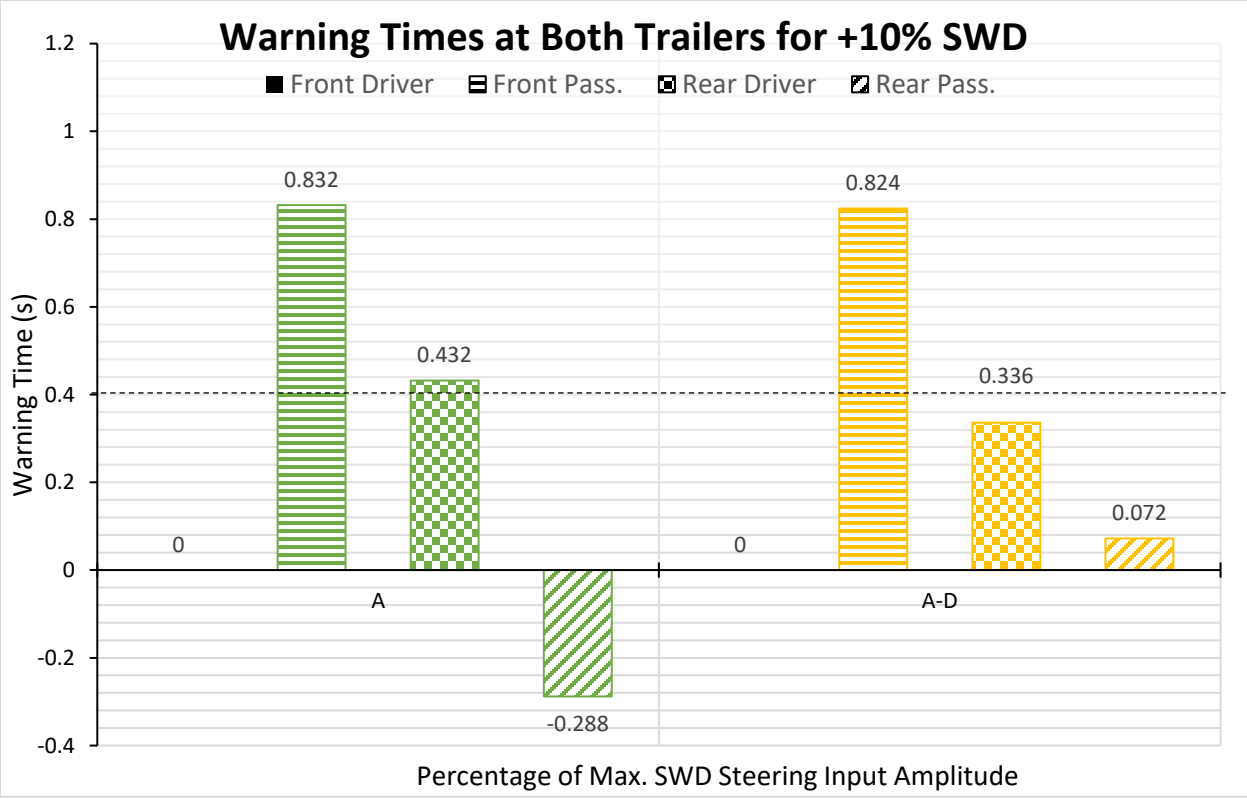

Figure 5-47. Warning time for both trailers during OERS +10% steering sine-with-dwell in dolly study.

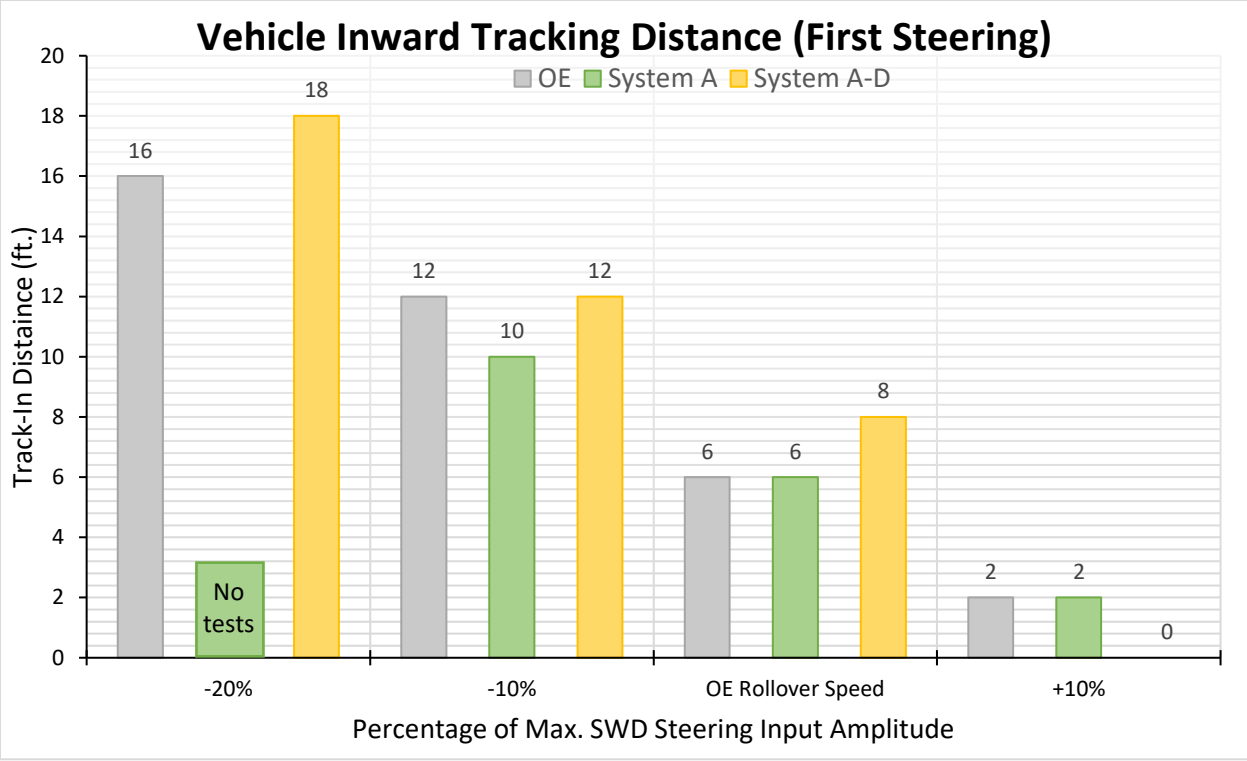

Figure 5-48. Vehicle inward tracking distance during OERS +10% steering sine-with-dwell in dolly study.

5.3.2.1 SWD Conclusion (A vs. A-D)

As seen in the RSM results for the two systems, there were small differences between the two systems found in the SWD results. Figure 5-49 presents the outrigger contact improvement for SWD at OERS+10% steering, and shows the similar performance of the two systems. Figure 5-49 shows all four outriggers for the OERS+10% steering, and the most important is again the rear passenger side outrigger. The difference between the two systems there was 27.11%, while the average of the differences at the other outriggers was a measly 9.30%, with System A-D outperforming System A. This is not enough to create any measurable differences in roll stability. This holds true for the small maneuverability difference seen between the two, which is shown in Figure 5-50.

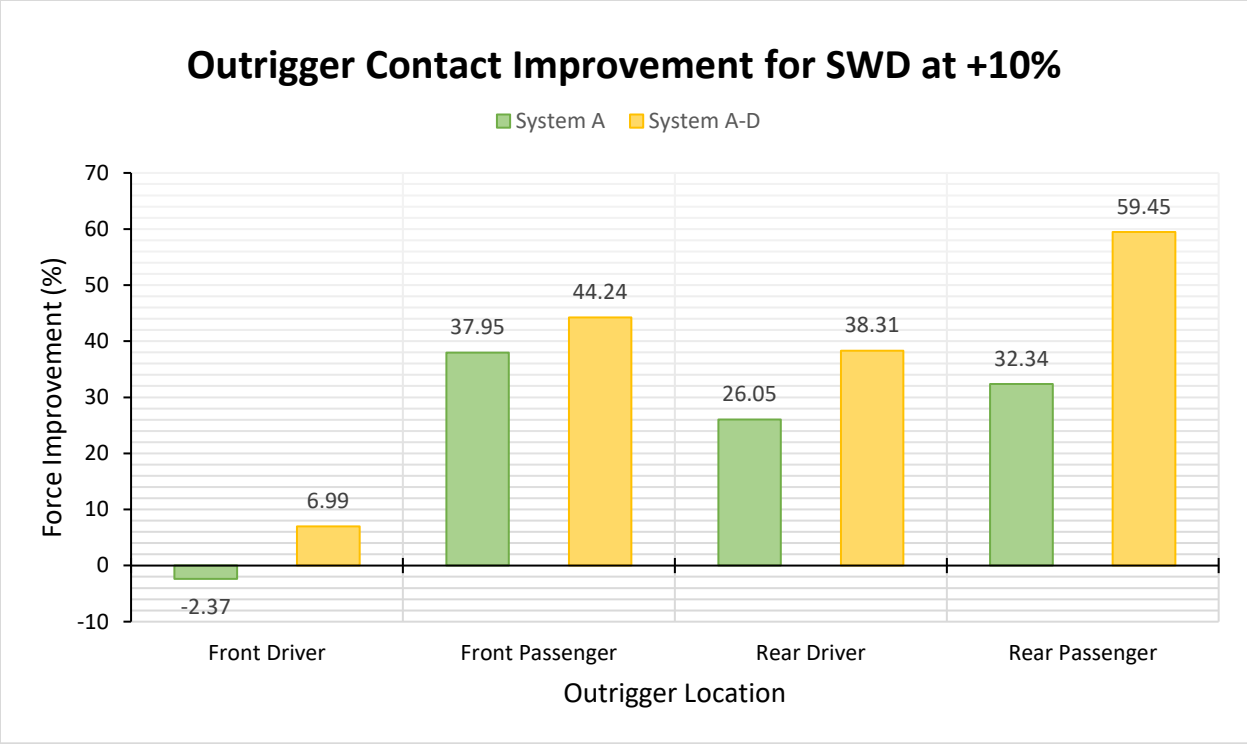

Figure 5-49. System A and A-D outrigger contact improvement for OERS + 10% steering sine-with-dwell.

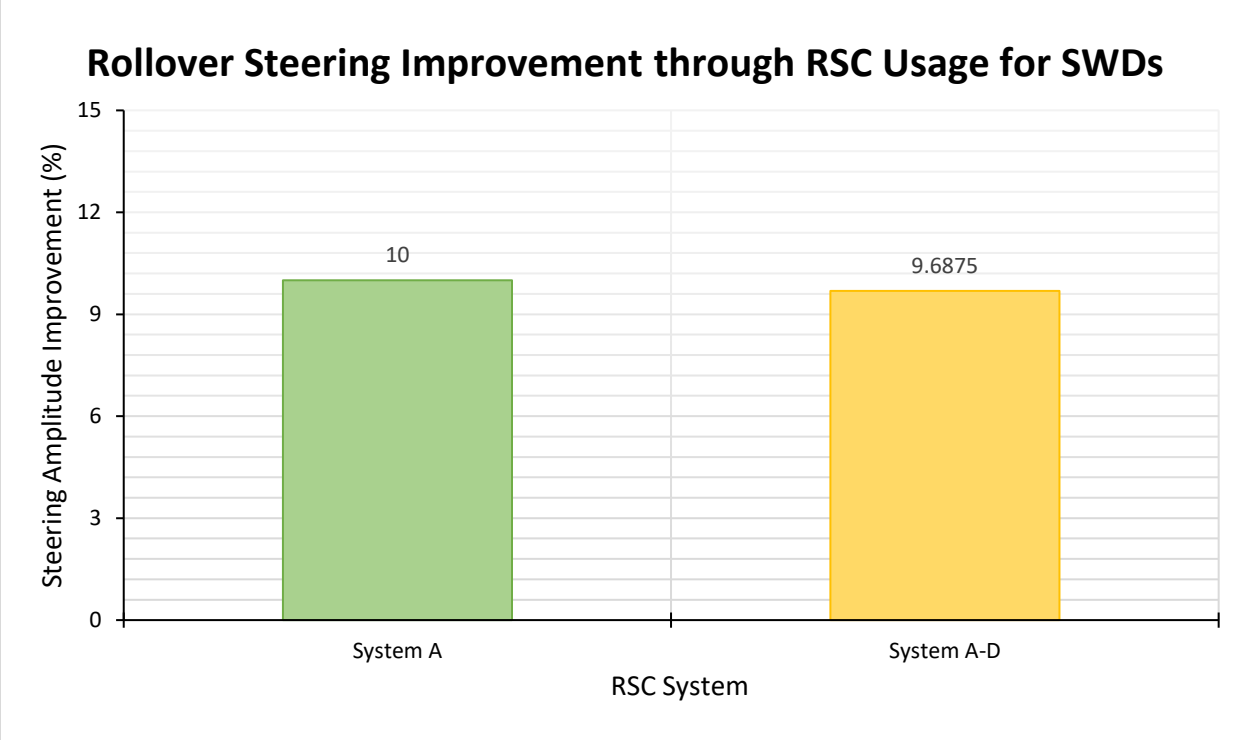

Figure 5-50. System A and A-D rollover steering threshold improvement over baseline during sine-with-dwells.

5.3.3 Summary (A vs. A-D)

The study of dolly RSC significance was taken as a secondary study to evaluate the potential performance differences between those RSC systems that included dolly brakes and those that did not. The following figures have been generated in summary of the study of dolly RSC significance. Only two maneuvers were used to evaluate Systems A and A-D, as no tests for System A were completed with J-turns and DLCs. Similar to Section 5.2.5, the outrigger contact improvements for the two RSC systems for RSM and SWD at a speed or steering one increment past the OERS is provided. Figure 5-51 shows this information. Again, the outriggers under consideration are those of focus for each maneuver, so the RSM tests use front passenger side outrigger data, while the SWD tests use rear passenger side outrigger data.

Figure 5-51 shows that there is a small performance improvement gained from adding dolly RSC through the numbers. System A-D outperforms System A in both a static maneuver found in RSMs, and in a more dynamic one in SWDs. From these findings, it can be concluded that dolly inclusion to an RSC system does not change or alter the types of maneuvers the system favors or works better with. However, such small reported differences rarely mean any practical performance upgrade when dealing with LCVs, which is best illustrated using Figure 5-52. Figure 5-52 displays the OERS threshold improvements in both RSM and SWD maneuvers, and the difference between the two systems is miniscule. The RSM results are shown on the left axis, and the SWD results are on the right. In conclusion, RSC installation on the dolly has minimal effect on the performance of an RSC system, and a decision regarding whether this upgrade is cost-effective is not within the scope of this thesis.

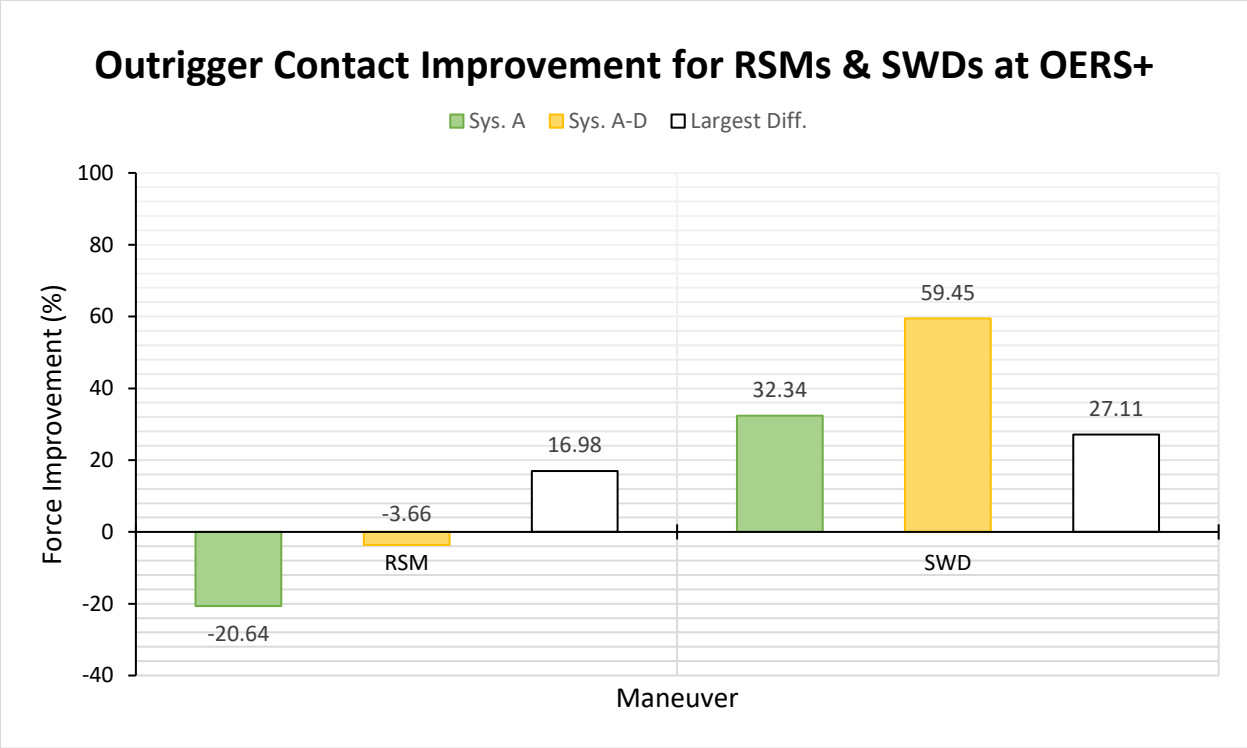

Figure 5-51. Outrigger contact improvements of Systems A & A-D for ramp steer maneuvers and sine-with-dwells at a speed or steering one increment past the OERS.

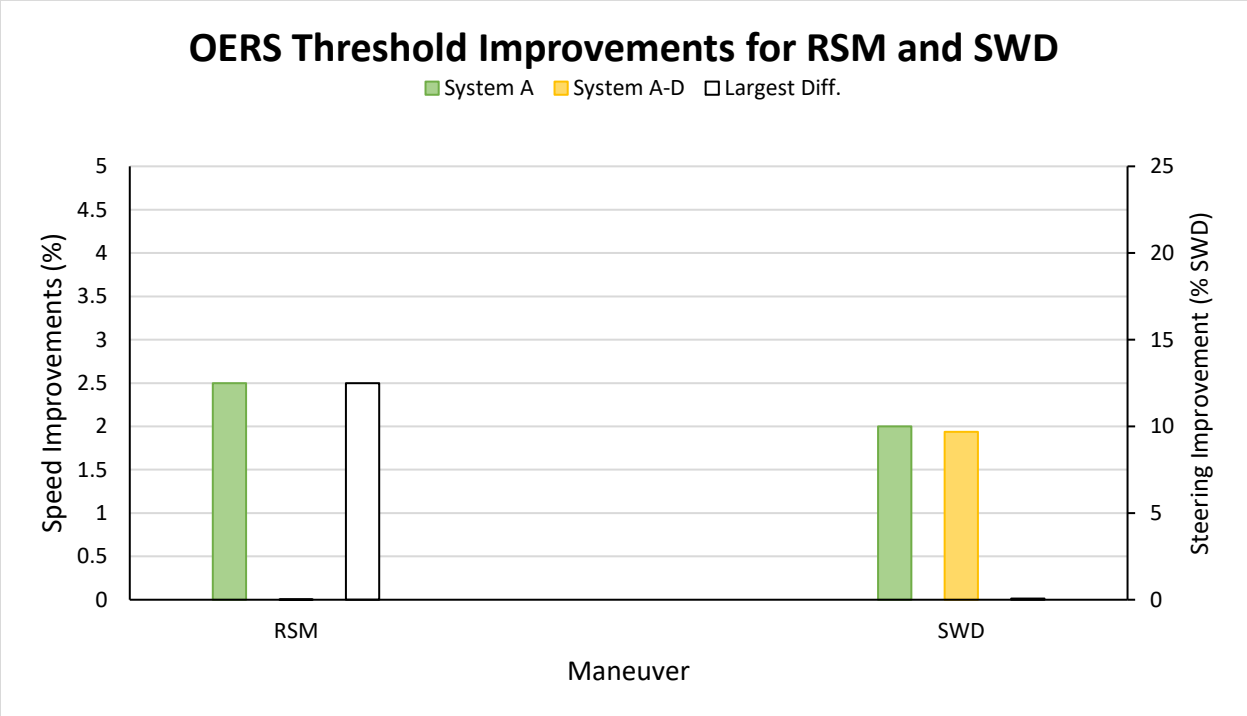

Figure 5-52. OERS threshold improvements of Systems A & A-D for ramp steer maneuvers and sine-with-dwells.

5.4 Single vs. Dual Channel System Performance Study (C vs. C-2 Study)

Another option to differentiate RSC operation from one system to another is to change the number of ABS modulator valves used for braking. For example, the three single-channel RSC systems evaluated earlier are of a 2S1M configuration, which includes two wheel sensors (one for each wheel), and one ABS modulator. A 2S2M system allows for distinct control of either side of a trailer and thus individual braking at each wheel. Figure 2-11 in Chapter 2 shows a simple diagram of the difference between a 2S1M and a 2S2M RSC system. Another key difference between the two systems is the number of activation steps used. A 2S1M system (RSC System C) has one activation step, while the 2S2M system (RSC System C-2) has two. Due to the proprietary nature of the operation of the systems, a more detailed description of the two systems is not provided. This section of this chapter will cover the performance comparison between a 2S1M system (RSC System C) and an equivalent 2S2M system (RSC System C-2) for all four maneuvers.

5.4.1 J-turn Results

Figure 5-53 shows the passenger outrigger contacts at both trailers in J-turns from OERS to OERS+10.5%. The baseline vehicle was not tested past OERS+5.3% mph due to roll severity at that speed. System C-2 performed with a 20.22% average improvement from System C over the four speeds in which roll occurred. Also, while System C displayed rear trailer roll, System C-2 never did. Figures 5-54 and 5-55 show the front and rear trailer outrigger contacts. Vast performance differences between the two systems can be noted.

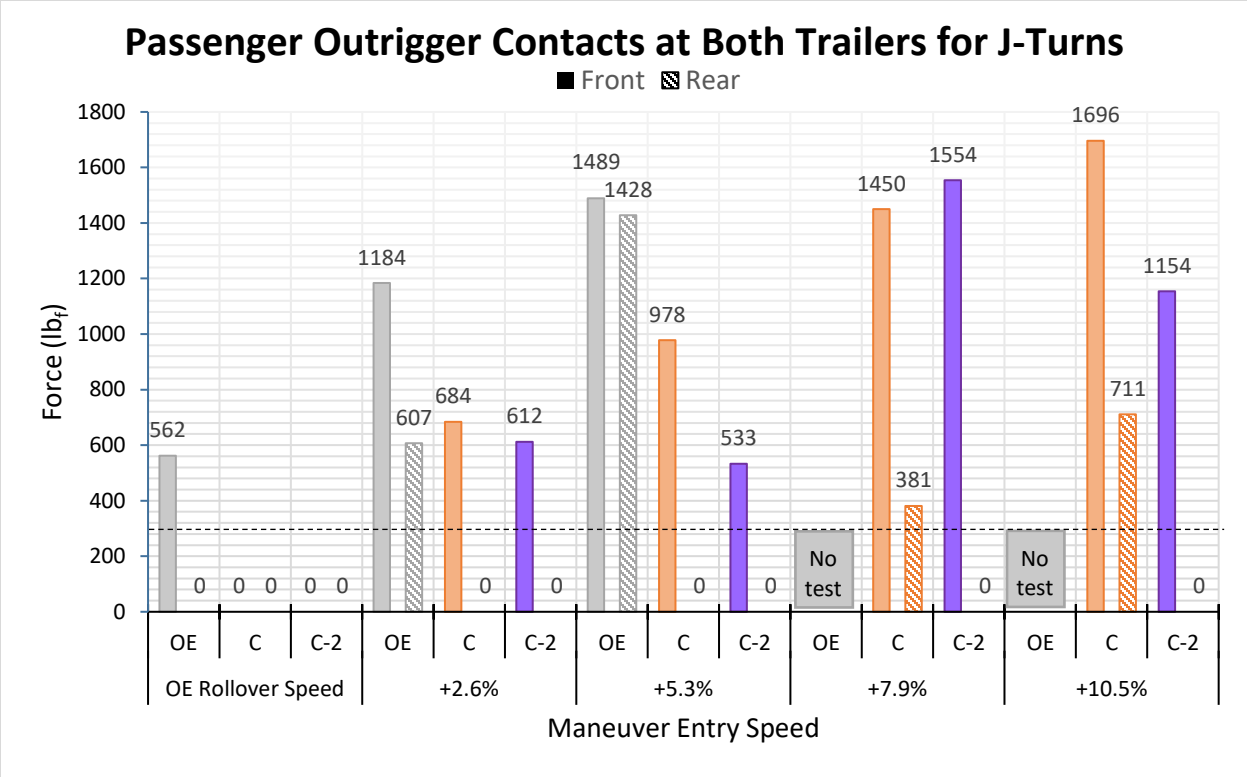

Figure 5-53. Passenger outrigger contacts at both trailers for J-turns in 2S2M study, from OERS to +10.5% mph.

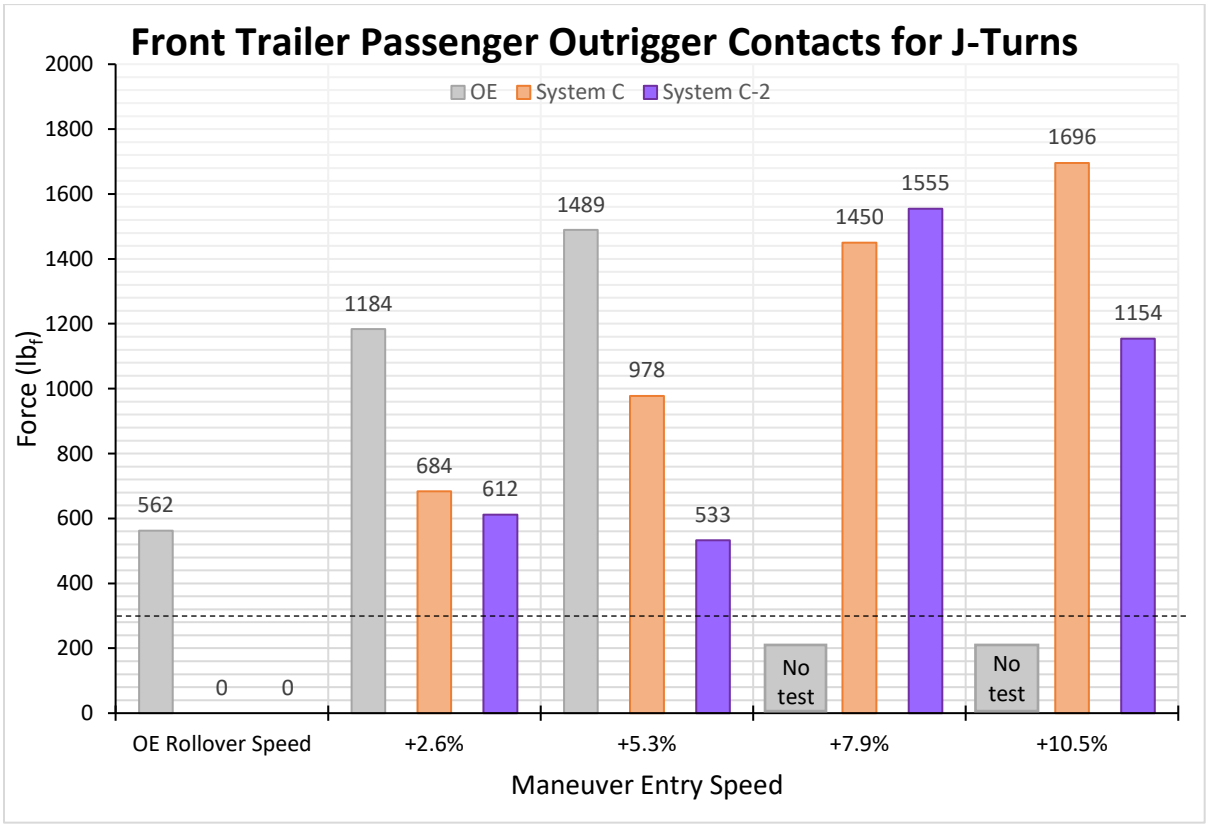

Figure 5-54. Passenger outrigger contacts at front trailer during J-Turns in 2S2M study, from OERS to +10.5% mph.

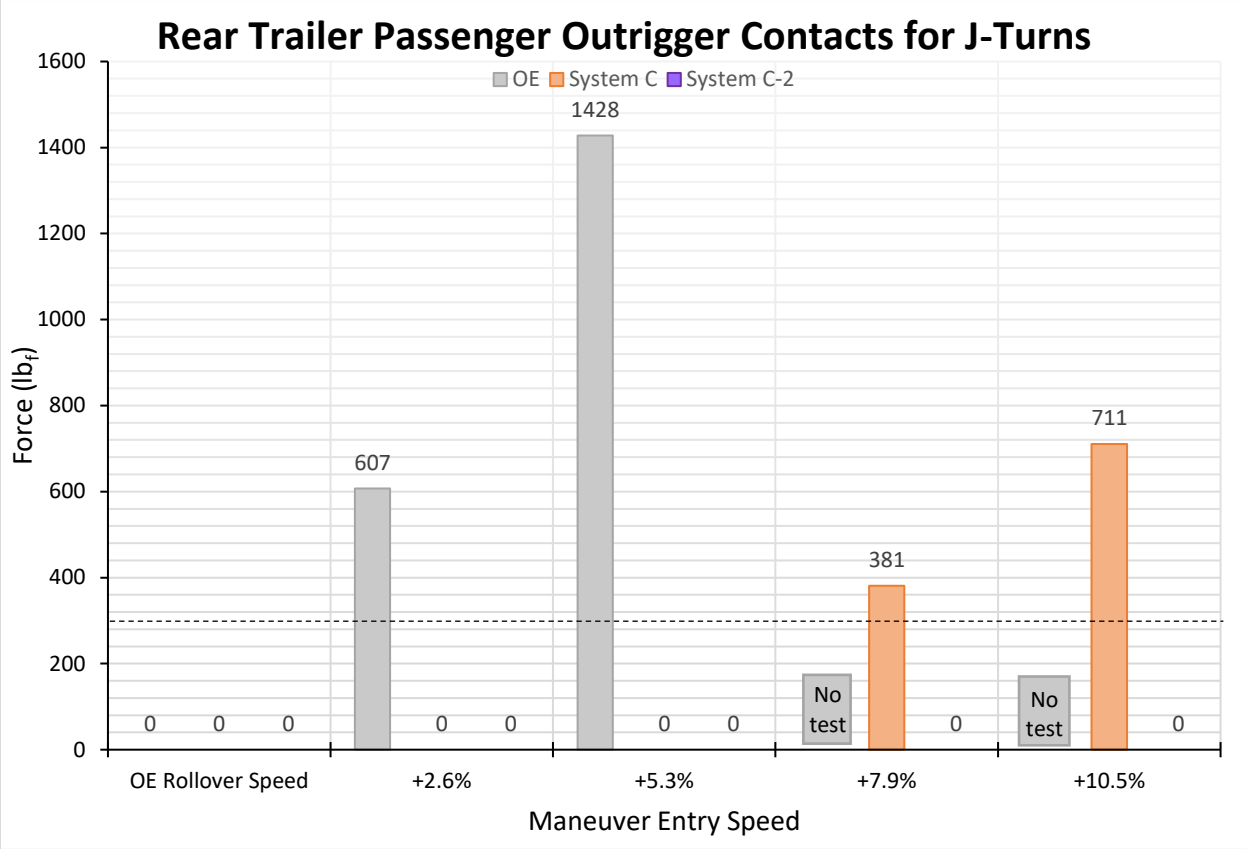

Figure 5-55. Passenger outrigger contacts at the rear trailer during J-turns in 2S2M study, from OERS to +10.5% mph.

Figures 5-56 and 5-57 display the activation time and warning time comparisons of System C and C-2. System C-2 continues to show improved performance over its single-channel/single-modulator counterpart, displaying averages of 22.51% and 46.37% improvement in activation timing and warning time, respectively, over four speeds. By outperforming System C, System C-2 has even larger performance differences between itself and Systems A, A-D, and B as well.

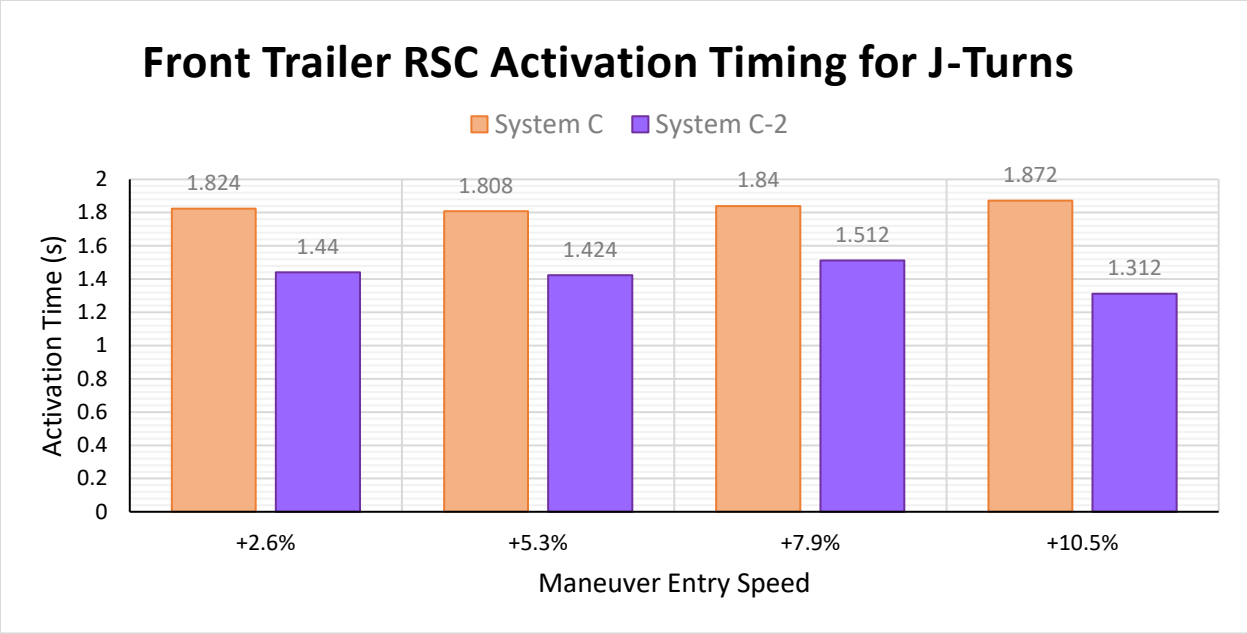

Figure 5-56. RSC activation times at the front trailer during J-turns in 2S2M study, from OERS to +10.5% mph.

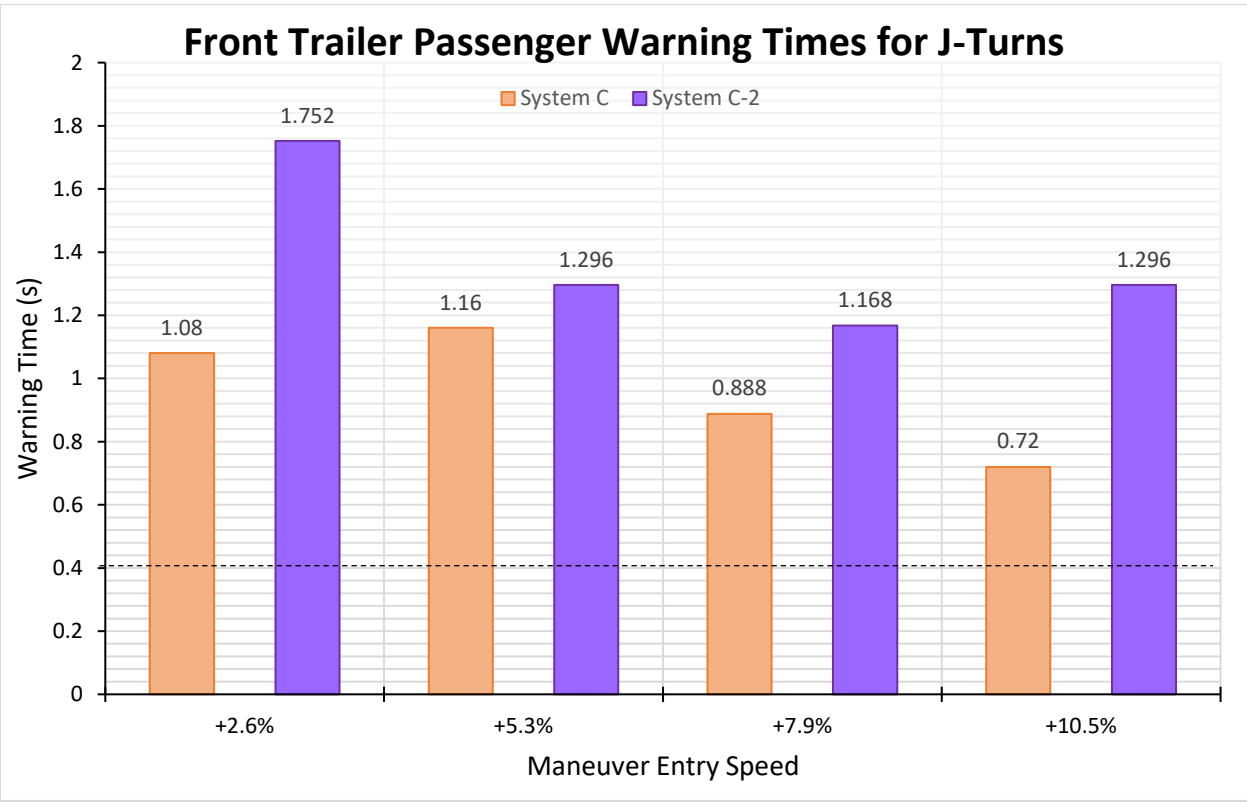

Figure 5-57. Passenger warning times at the front trailer during J-turns in 2S2M study, from OERS to +10.5% mph.

5.4.1.1 J-Turn Conclusion (C vs. C-2)

RSC System C-2 largely outperformed its single-channel counterpart System C, yielding a peak outrigger contact force improvement difference of 29.89% between the two systems. The front trailer passenger outrigger contact improvements for two speeds are shown in Figure 5-58. It is important to note that System C-2 provided a massive improvement at the rear passenger side outrigger, as a contact force of 711 lb_f with System C was decreased to zero (no roll) at OERS+10.5%.

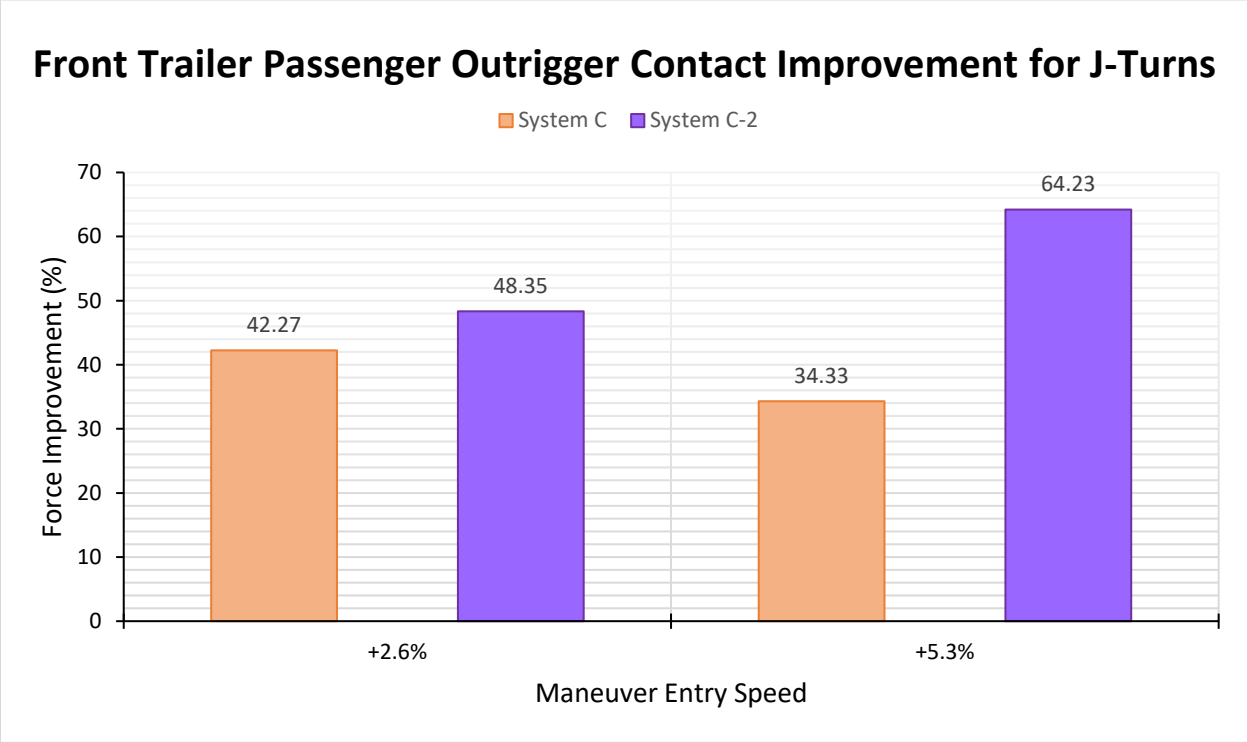

Figure 5-58. Front passenger side outrigger contact improvements of Systems C and C-2 over baseline during J-turns in 2S2M study, from OERS + 2.6% to +5.3% mph.

The rollover speed improvements over baseline for both the front and rear trailers found in using the two RSC systems are shown in Figure 5-59. Although the RS improvement at the rear trailer is significant, the there is none at the front trailer for either of the two systems. Since speed improvements were calculated using roll at either trailer, there is no speed improvement between the two systems. Again, driver feedback can play a large role in the test results.

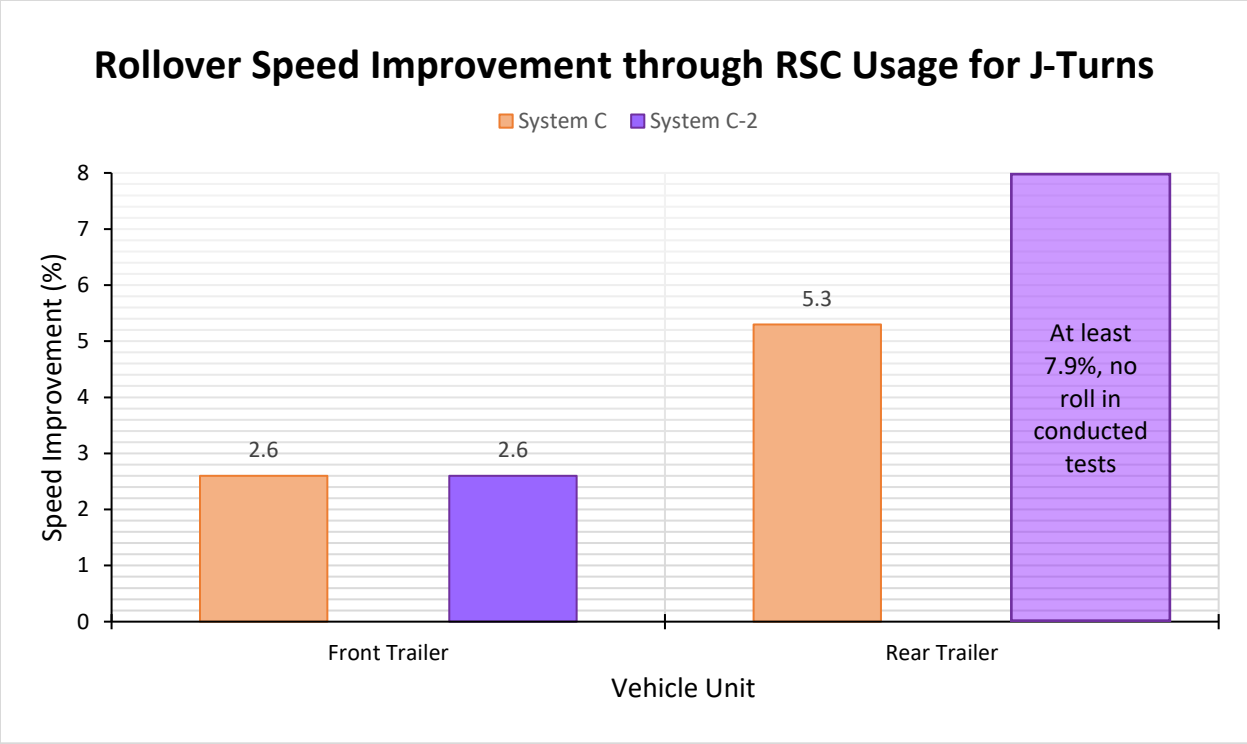

Figure 5-59. Rollover speed improvement of Systems C and C-2 during J-turns in 2S2M study.

5.4.2 RSM Results

Figure 5-60 displays the results for RSM testing done at higher speeds than were previously used in RSM testing. This was directly due to the superiority of Systems C and C-2, as a maximum speed of OERS+15% was tested. The baseline vehicle was not tested past OERS+7.5% due to roll severity. System C-2 shows mixed results relative to System C, with a 21.11% average improvement between the two in the two speeds where roll occurred. The performance trends shown in Figure 5-60 aren't as clear as those shown in the driver-operated J-turn results. However, a visible improvement over System C is again reinforced through activation and warning time analyses in Figures 5-61 and 5-62. A maximum difference occurred between the warning times of 0.68 s, or a 58.22% increase over System C at the same speed. This is a significant amount of time in which a seasoned driver can stop any rollovers that RSC systems would not be able to prevent through brake application alone. Both the activation and warning times for the J-turn and RSM found in System C and System C-2 give a driver sufficient time to use corrective steering. It should be noted that a vehicle with System C-2 would not roll over during a OERS+12.5% RSM test since the outrigger contact was less than the rollover threshold force of 300 lb_f. Realistically, the vehicle would have exhibited wheel lift, but would have come right back down and not rolled over.

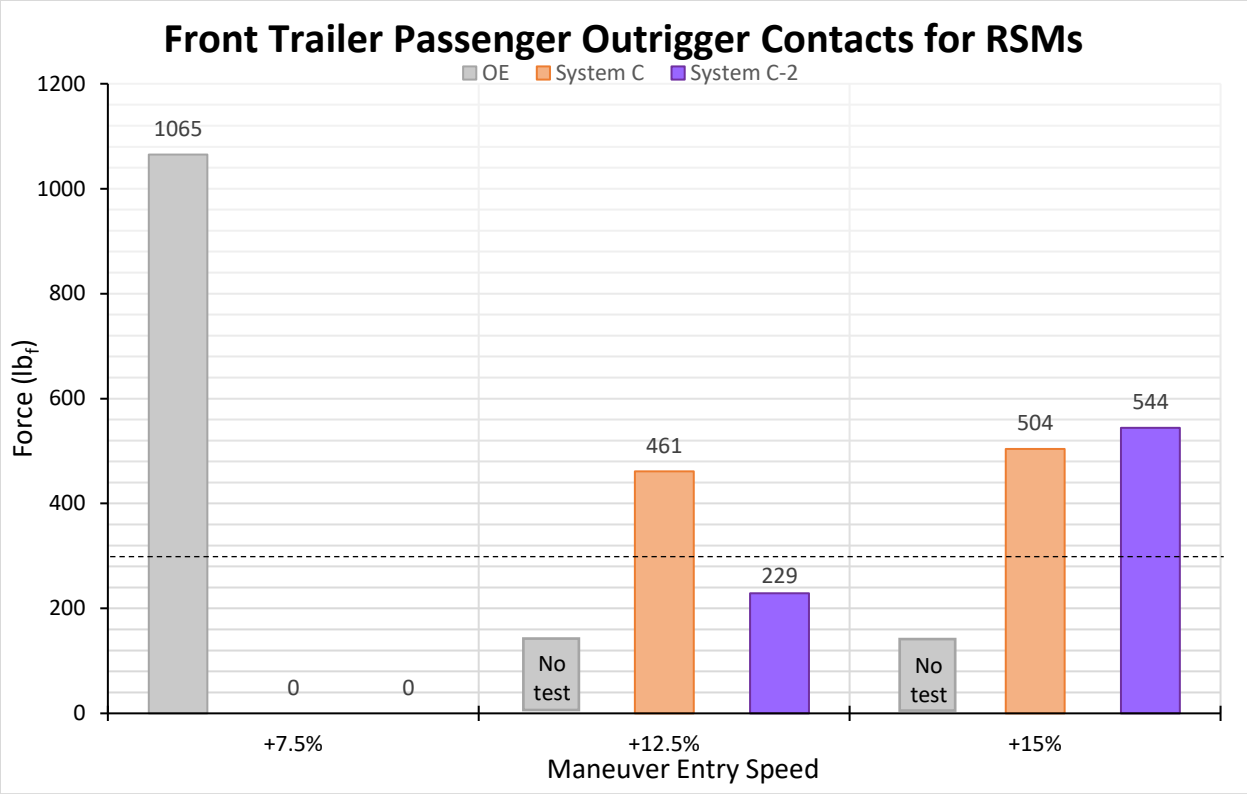

Figure 5-60. Passenger outrigger contacts at the front trailer during ramp steer maneuvers in 2S2M study, from OERS + 7.5% to +15% mph.

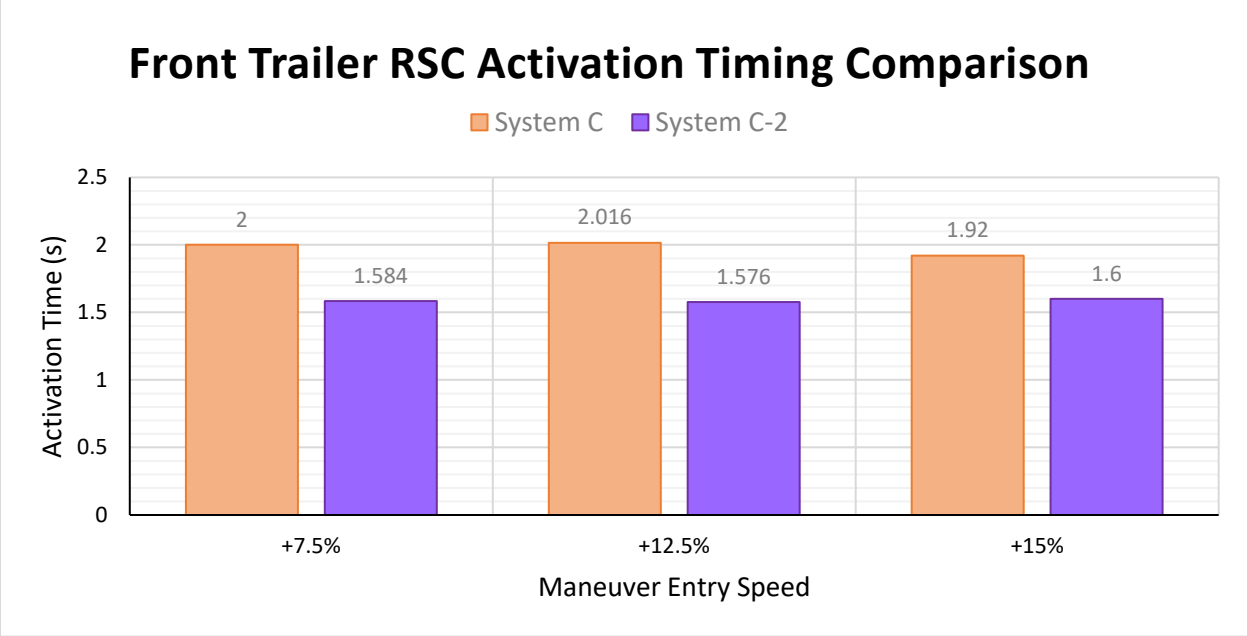

Figure 5-61. RSC activation times at the front trailer during ramp steer maneuvers in 2S2M study, from OERS + 7.5% to +15% mph.

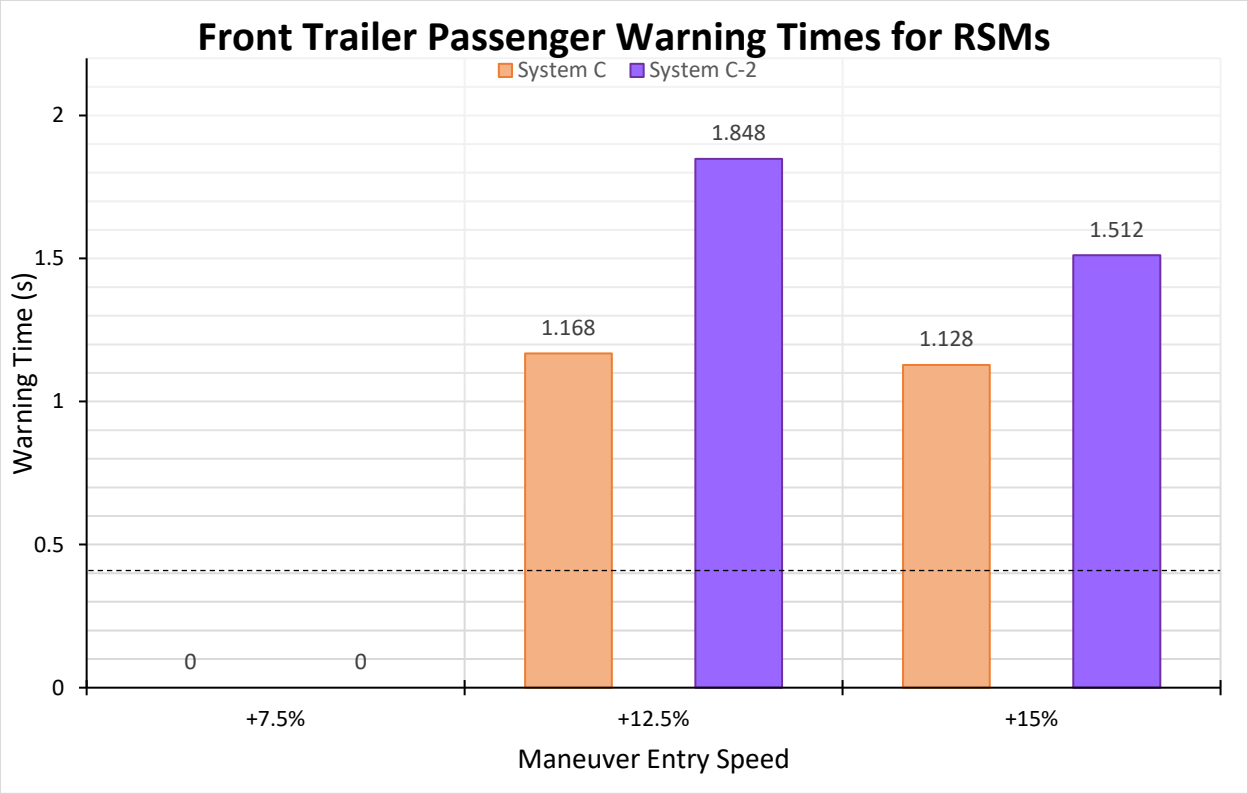

Figure 5-62. Passenger warning times at the front trailer during ramp steer maneuvers in 2S2M study, from OERS + 7.5% to +15% mph.

5.4.2.1 RSM Conclusion (C vs. C-2)

The RSM results from this study are difficult to analyze simply due to the sheer roll stability advantages of the two systems at hand. Both Systems C and C-2 were tested to OERS+15%, and rolled at OERS+12.5% in RSM tests, two speeds at which neither the baseline vehicle nor other RSC systems were tested. The only reference points to compare these two systems in this maneuver are themselves, and a comparison between the two has been discussed above. It is clear that neither system rolled at either OERS or OERS+7.5%. These were the last two speeds tested with the baseline configuration.

The performance increase from System C in RSM is less than that seen for J-turns, which saw no rise in rollover speed threshold. The same holds true for RSM results, as both System C and System C-2 yielded a 5 mph rollover speed threshold. Even though there were no measurable differences between the rollover speed improvement of System C and System C-2, clear differences between the warning times of the two systems are present. These differences could definitely produce larger rollover speed differences, as drivers have more time to react and prevent rollover when the RSC systems themselves cannot.

5.4.3 SWD Results

A comparison of SWD results for Systems C and C-2 are shown below. Figure 5-63 displays the outrigger contact forces at the front trailer for SWD tests at OERS, OERS+10%, and OERS+20% steering amplitude. Again, the rear passenger side outrigger experiences the highest contact forces. System C-2 rolls earlier at OERS+10% than does System C, yielding a higher maneuverability improvement for the latter over the former. System C-2 does not roll at the front driver side however, due to earlier first steering activation times, which are shown in Figure 5-64. On the other hand, System C-2 has a harder contact at the front passenger side outrigger. The driver side outriggers contact during the first steering of a SWD, which is quite quasi-static, and the passenger side outriggers contact as the vehicle whips back towards the left. This initially generated the theory that System C would be better at dealing with dynamic maneuvers, while System C-2 would perform better for more static maneuvers such as the J-turn and RSM. This theory is supported further in Figures 5-64 and 5-65, which show the first and second steering activation times. The differences in activation time between the two systems diminishes from the first and second steerings.

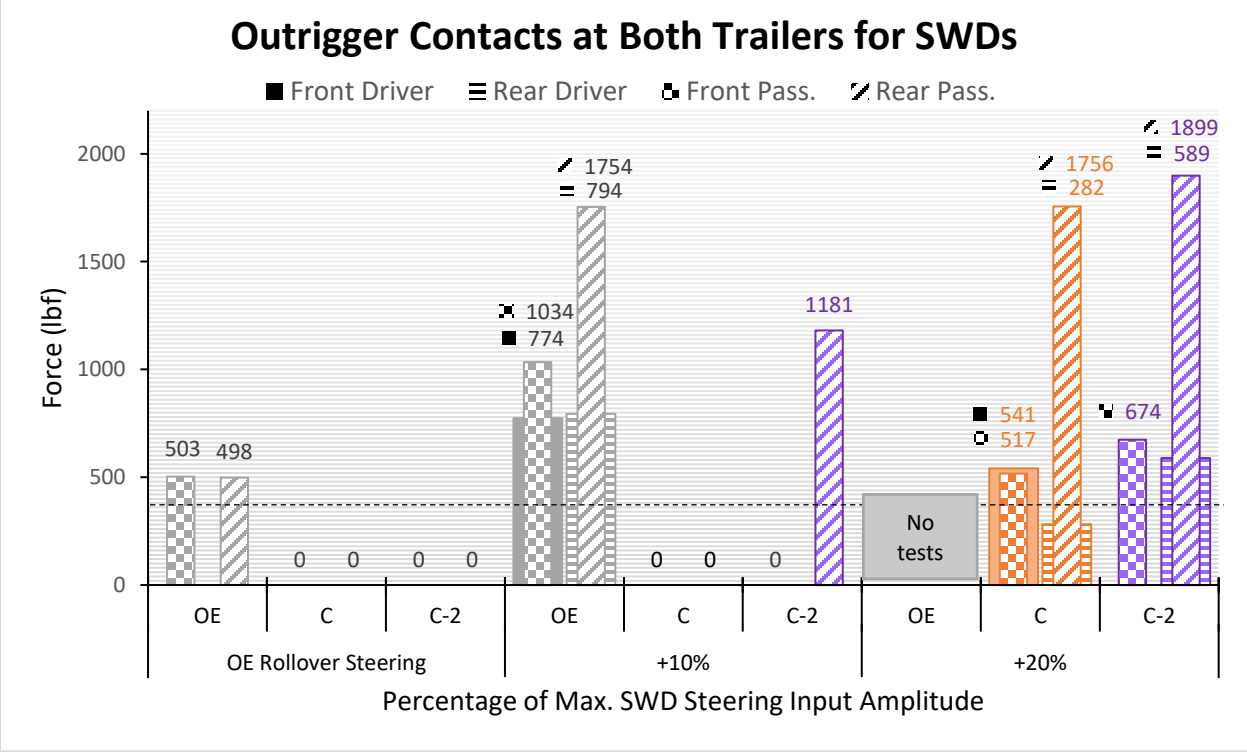

Figure 5-63. Outrigger contacts at both trailers during sine-with-dwells in 2S2M study, from OERS to +20% steering.

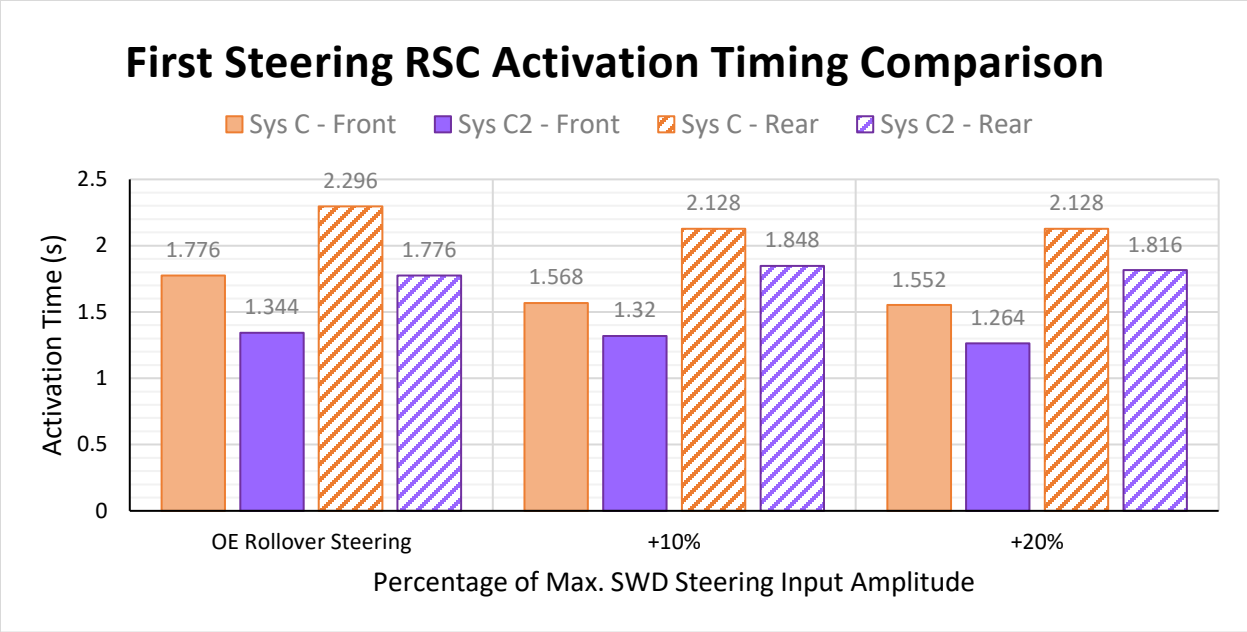

Figure 5-64. RSC activations at both trailers during first steering of sine-with-dwells in 2S2M study, from OERS to +20% steering.

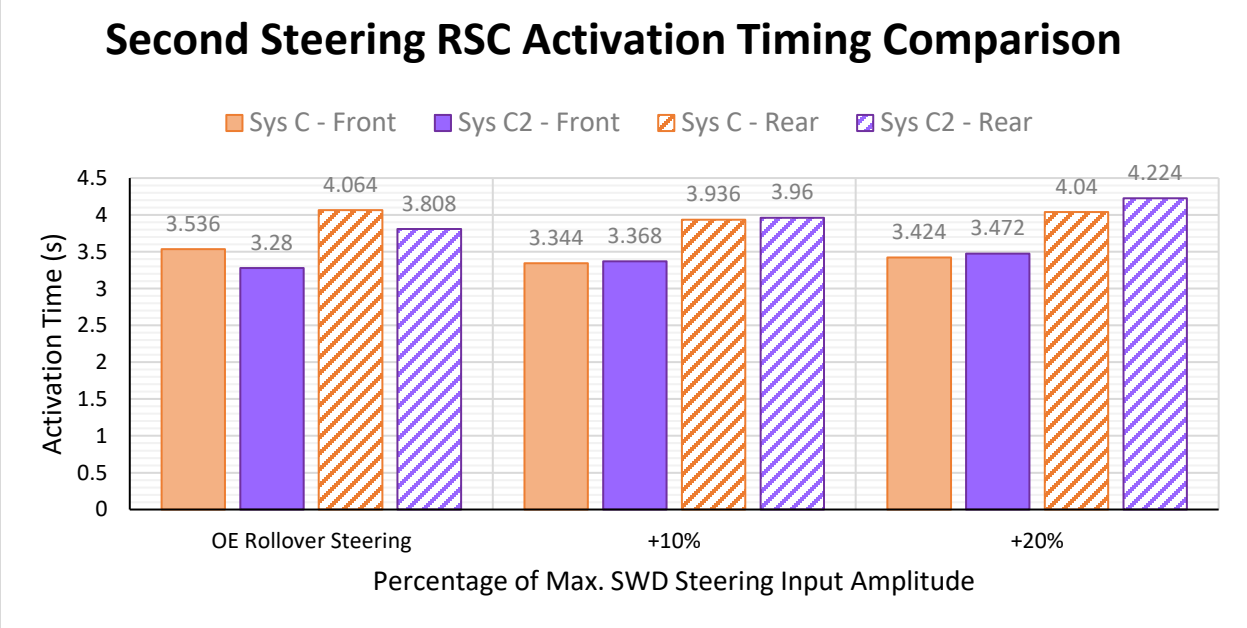

Figure 5-65. RSC activation at both trailers during second steering of sine-with-dwells in 2S2M study, from OERS to +20% steering.

Figure 5-66 shows the largest recorded warning time exhibited by System C-2 at the rear passenger outrigger, even though it had the largest contact. With driver feedback, this contact may have been decreased considerably. The higher warning times found in System C-2 J-turn and RSM tests are gone in SWD tests, except for at the rear driver side outrigger. Since the first steering of the SWD is similar to a

static, constant steering such as in J-turns and RSMs, this large warning time occurs. Figure 5-66 shows the warning times for both trailers at OERS+10% and OERS+20% steering results for Systems C and C-2.

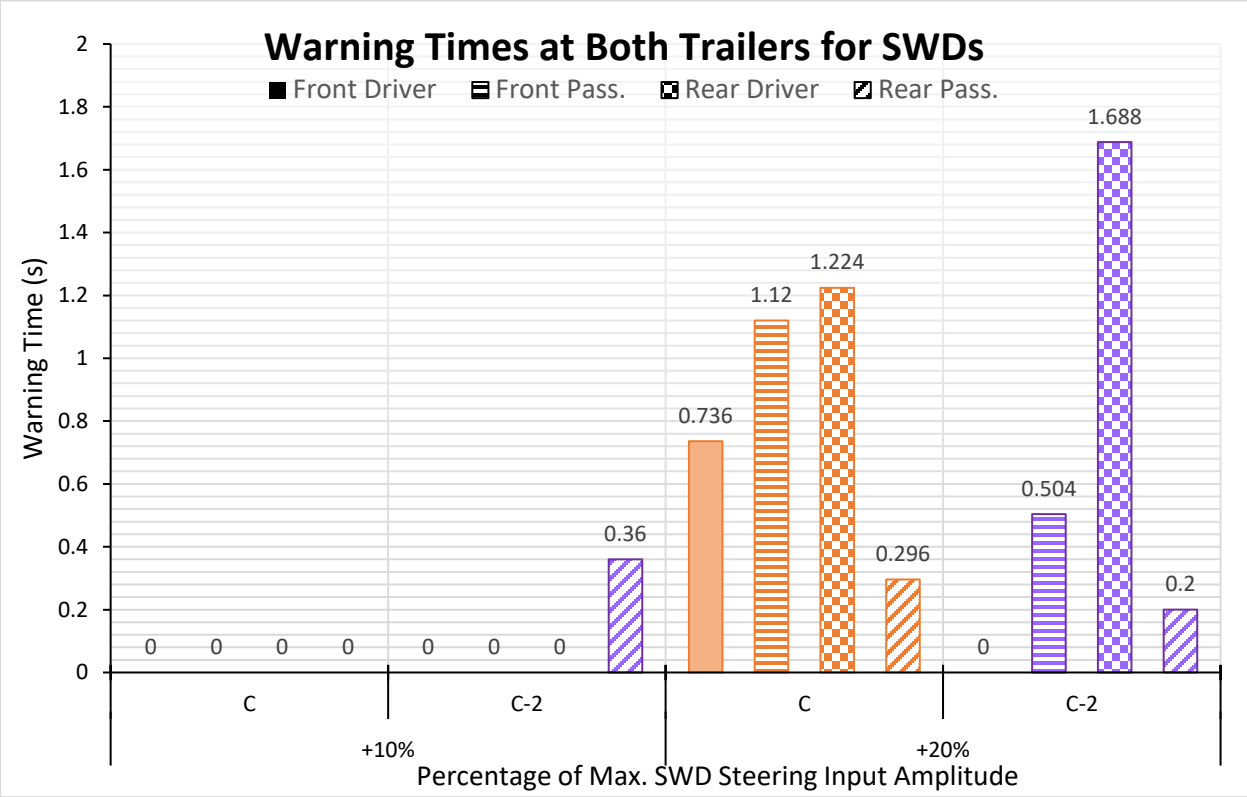

Figure 5-66. Warning time at both trailers during sine-with-dwells in 2S2M study, from OERS + 10% to +20% steering.

System C-2 activates more quickly in SWD maneuvers than any other RSC system included in this entire study, giving the biggest chance for brake application to cause understeer in the SWD. Yet there is still no evidence that inward tracking during evasive maneuvers occurs due to RSC usage (Figure 5-67). Again, it should be noted that this conclusion was reached for the systems tested, and not for all RSC systems.

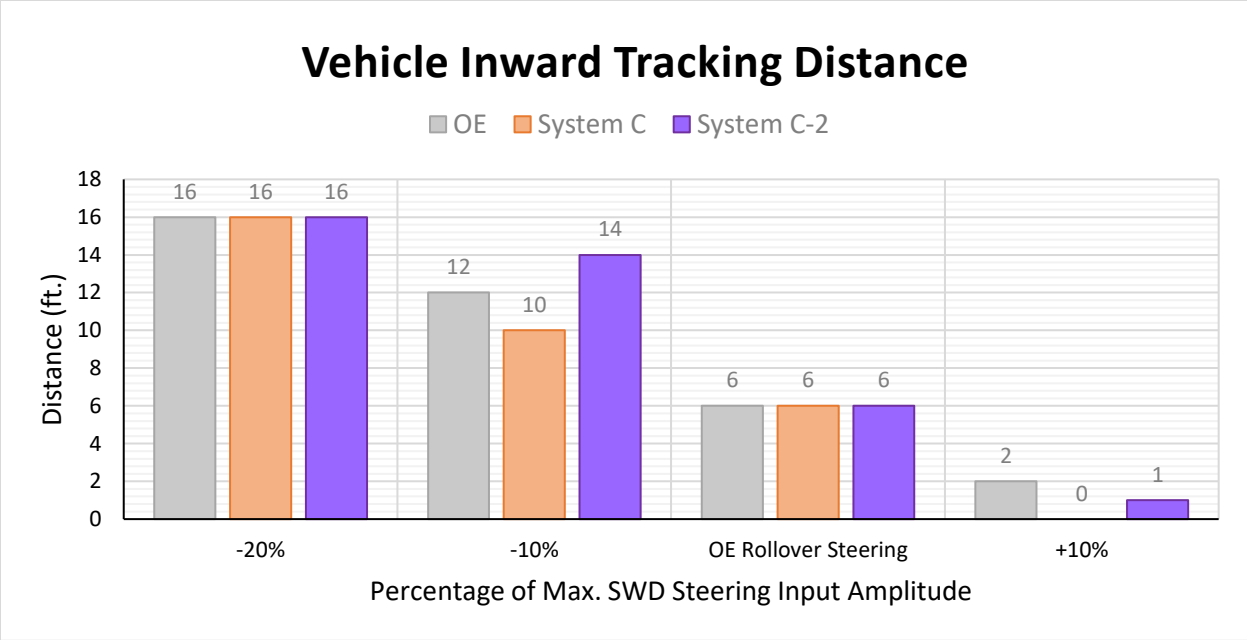

Figure 5-67. Vehicle inward tracking distance during sine-with-dwells in 2S2M study, from OERS -20% to +20% steering.

5.4.3.1 SWD Conclusion (C vs. C-2)

At OERS+10% steering, all four outriggers of the baseline vehicle contacted while none of the System C vehicle configuration did so. System C-2 showed a 32.69% decrease in outrigger contact force at the rear trailer passenger side outrigger at this speed, meaning that System C-2 sees a lower maneuverability improvement than does System C, as seen in Figure 5-68.

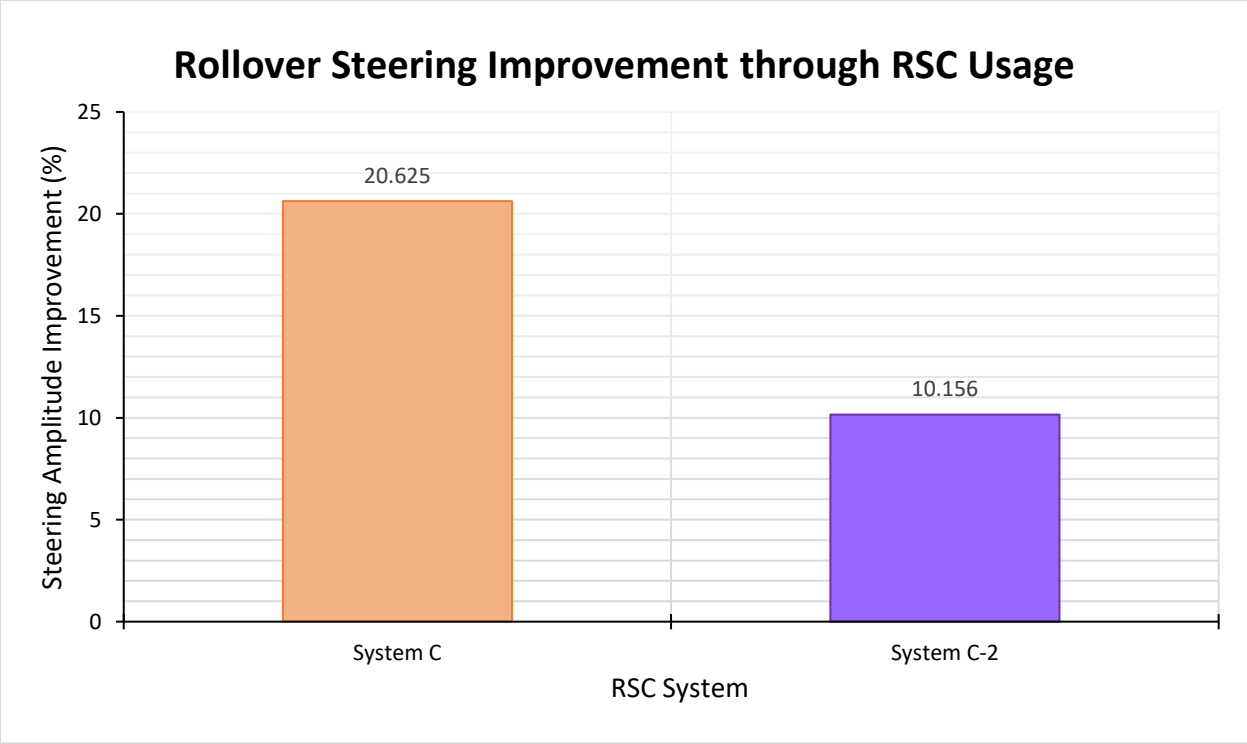

Figure 5-68. Rollover steering improvements of Systems C and C-2 for sine-with-dwells.

5.4.4 DLC Results

Figures 5-69 to 5-73 present the results between Systems C and C-2 for DLC maneuvers at OERS to OERS+3.7%. Although the DLCs results in the first study were largely inconclusive, System C-2 quite handedly outperformed System C. Figure 5-69 shows there was no roll for System C-2 for the completed tests. No further testing was done due to time limitations at the test track, as well as rollovers at lower speeds, which were discounted after maneuver validity analysis. Again, since these are driver-operated tests, driver performance as the tests are conducted may be a significant factor, especially as System C-2 tests were conducted after System C tests.

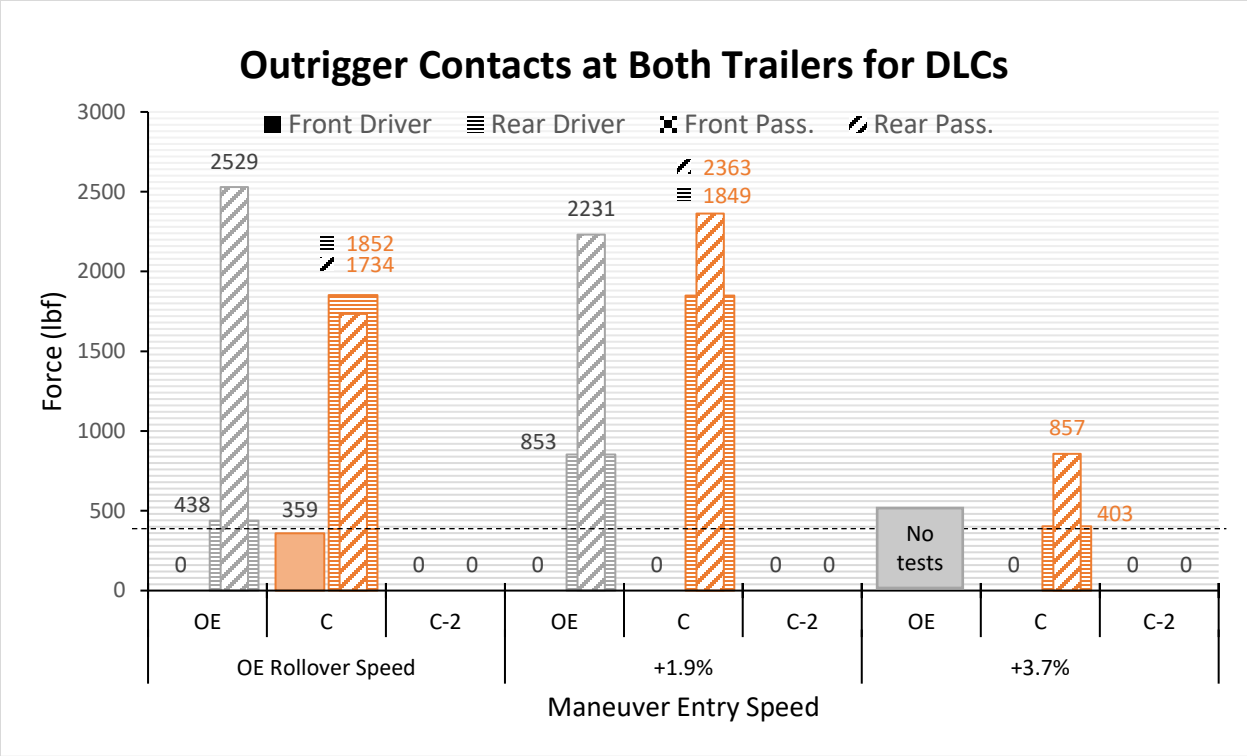

Figure 5-69. Outrigger contacts at both trailers during double lane changes in 2S2M study, from OERS to +3.7% mph.

Figures 5-70, 5-71, and 5-72 show similar activation times for the two systems in the first, second, and third steerings of the DLC maneuver, respectively, and differences between the two systems are minute, while System C-2 displayed a general performance outrigger contact improvement over System C. Figure 5-73 displays a seemingly large difference in the two systems in warning time, but the scale shown is quite small and there were no outrigger hits for System C-2. DLC results proved to be less than optimal again, as driver performance varied heavily from system to system. This is shown in Figure 5-74, which indicates the steering wheel input for eight different OERS+1.9% tests. System C tests shown were tested first, followed by the System C-2 tests, and finally by the baseline tests. The curves not only consist of different peak to peak times, but also different amplitudes. DLCs are highly inconsistent, and the results from their testing should not be considered too heavily.

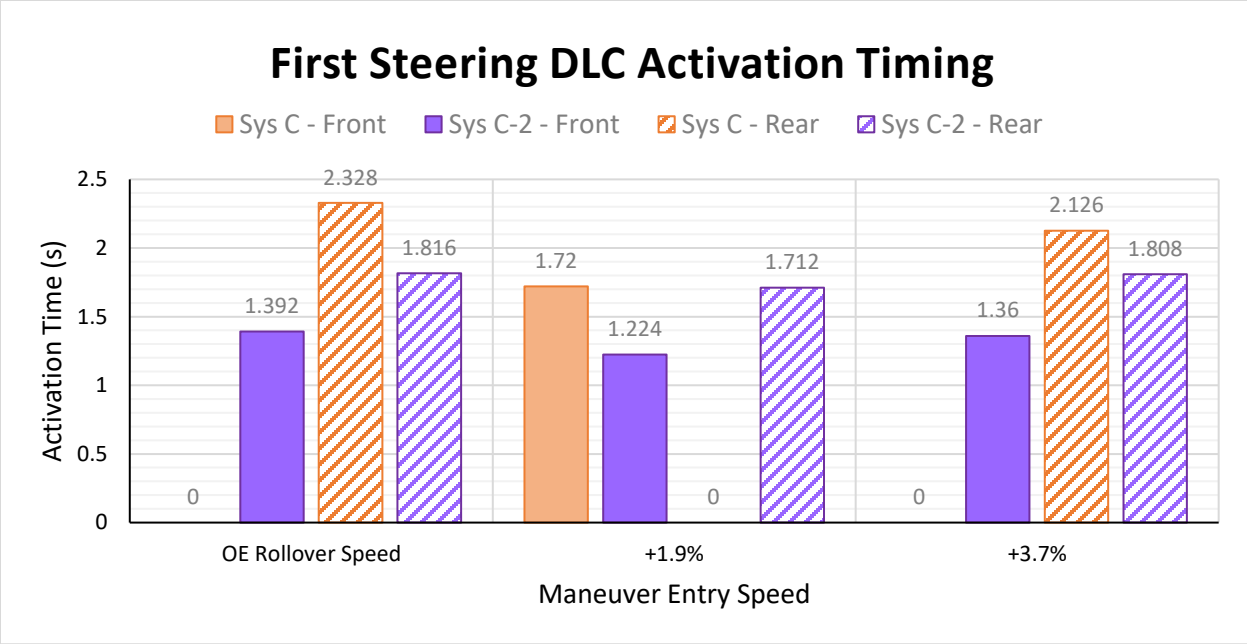

Figure 5-70. RSC activation times during first steering of double lane changes in 2S2M study, from OERS to +3.7% mph.

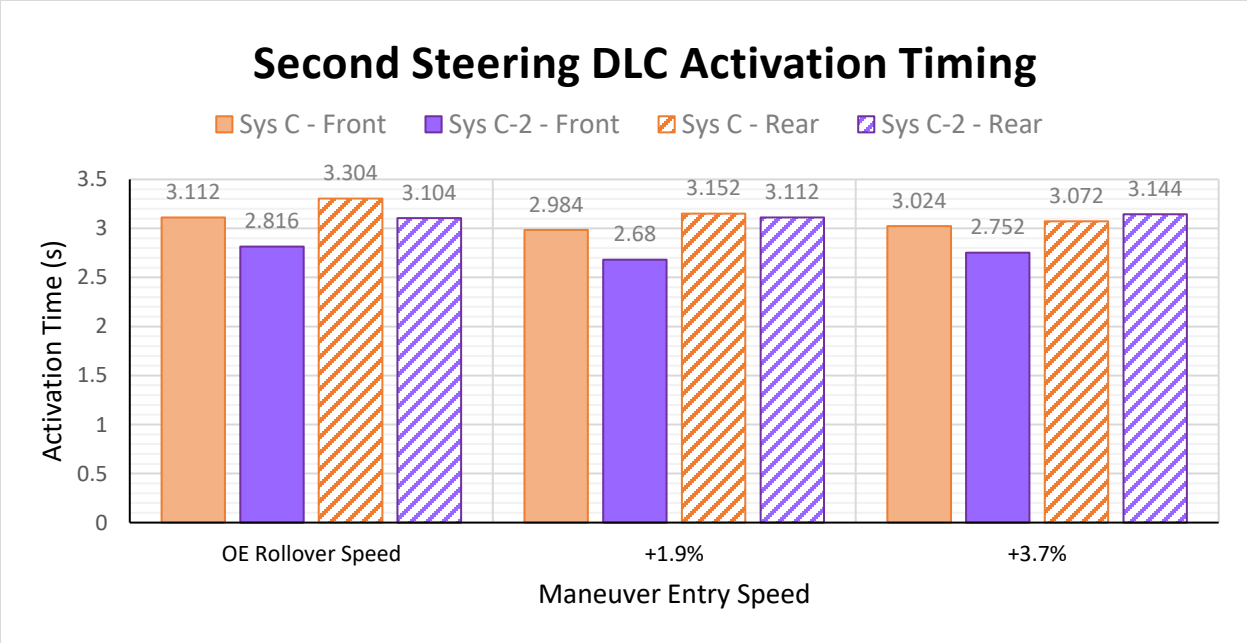

Figure 5-71. RSC activation times during second steering of double lane changes in 2S2M study, from OERS to +3.7% mph.

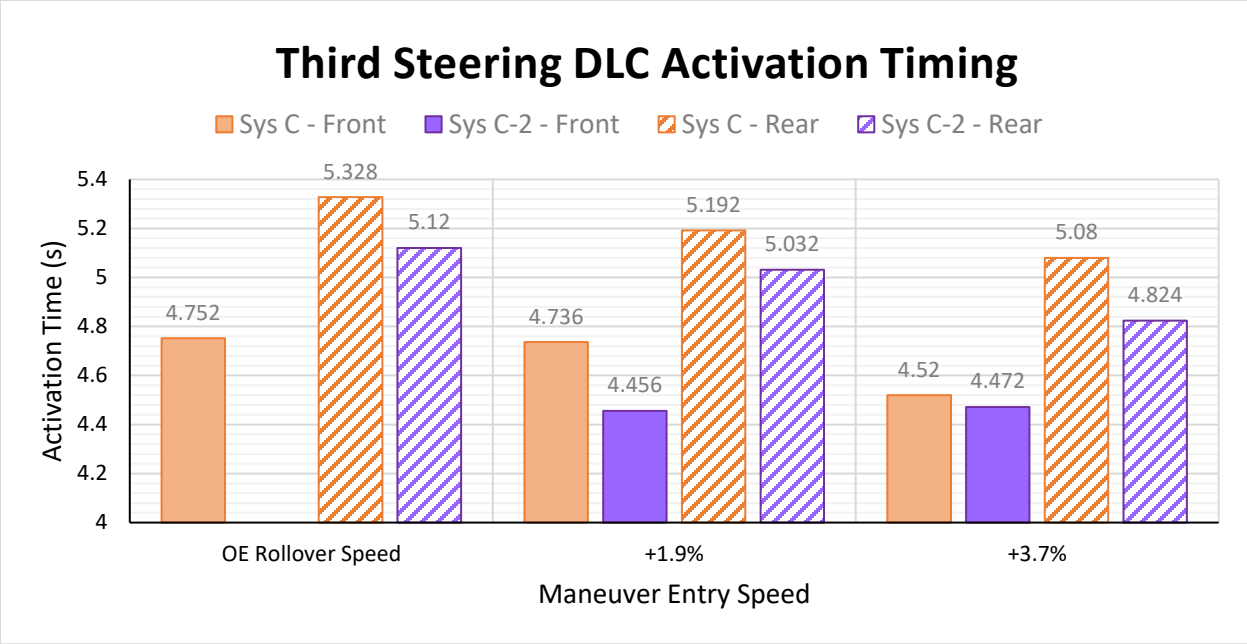

Figure 5-72. RSC activation times during third steering of double lane changes in 2S2M study, from OERS to +3.7% mph.

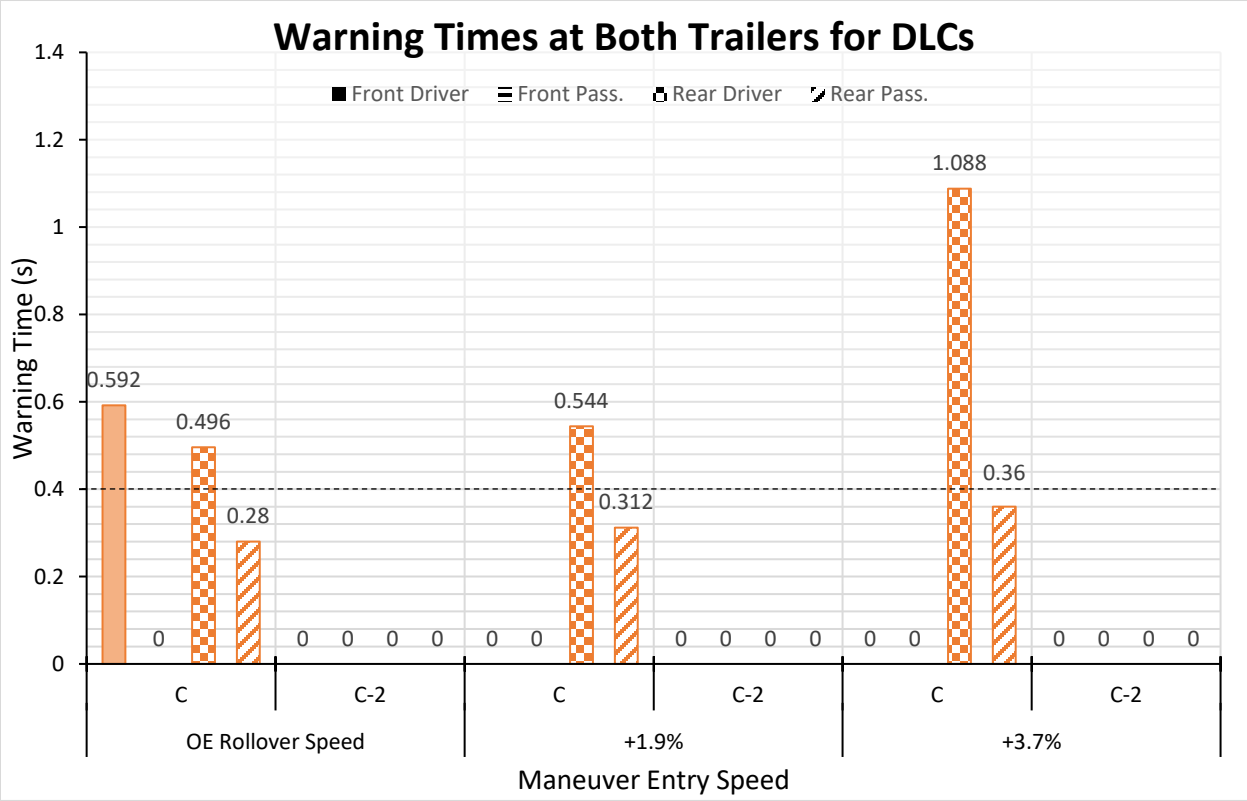

Figure 5-73. Warning times at both trailers during double lane changes in 2S2M study, from OERS to +3.7% mph.

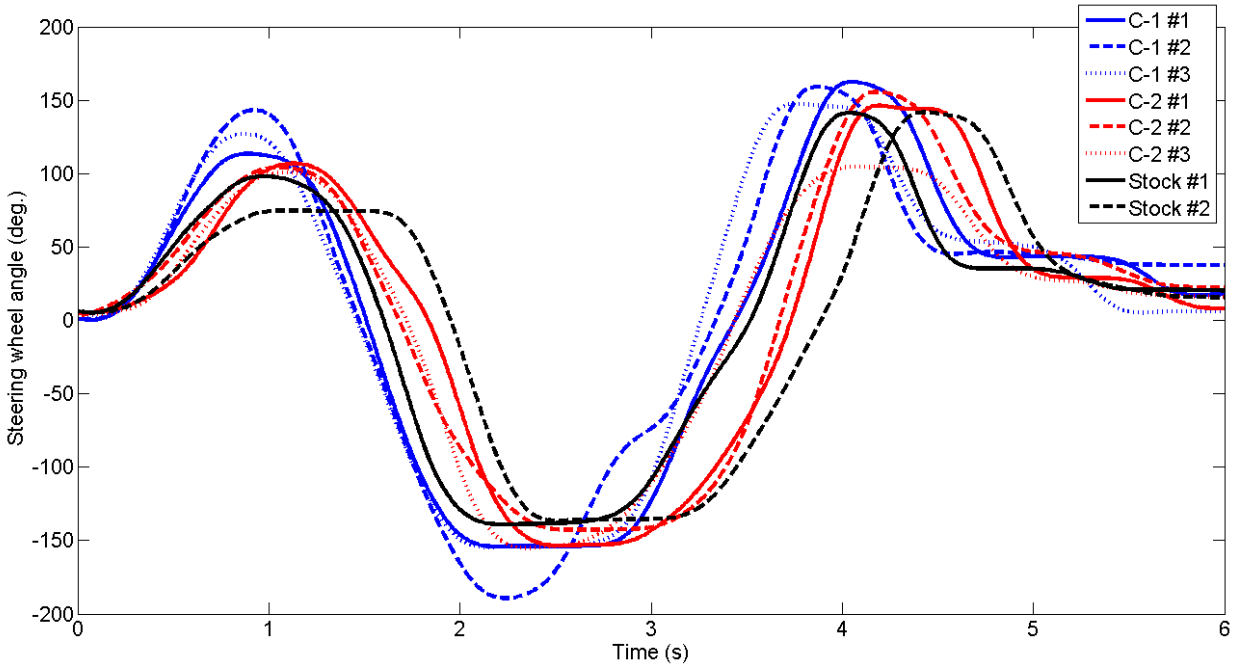

Figure 5-74. Steering wheel input for eight different OERS + 1.9% double lane change tests.

5.4.5 Summary (C vs. C-2)

Another secondary study was conducted with the objective of evaluating the differences between a single channel and a dual channel RSC system. It was found in all maneuvers that the dual channel system C-2 activated earlier and had longer warning times than did System C, yet the performance difference between the two systems points to System C being superior. Figures 5-75 and 5-76 display the outrigger contact improvements and the OERS threshold improvements for all maneuvers. The outrigger contact improvements are provided for a speed or steering one increment past the OERS only. Again, the outriggers under consideration are those of focus for each maneuver.

The Figure 5-75 results regarding a single and dual channel comparison are quite confusing. Although System C-2 repeatedly activated earlier and gave the driver a longer warning time, System C-2 actually yielded lower outrigger contact improvements over baseline at the next SWD increment over OERS, and the same improvement as System C in the next RSM increment over OERS. A small enhancement is found in J-turns, and the largest upgrade existed in DLCs. System C-2 showed no preference for types of maneuvers, as no pattern was found to differentiate better performances in either more static or more dynamic maneuvers. This study yielded quite inconclusive results regarding the selection of 2S2M systems over 2S1M and vice versa. Still, a decision can be made for installing System C-2 over System C for the specific maneuver of DLC, as a performance difference between System C-2 and the other Systems A, A-

D, and B is massive. Again, a decision regarding whether a 2S1M or 2S2M system is more cost-effective is not within the scope of this thesis.

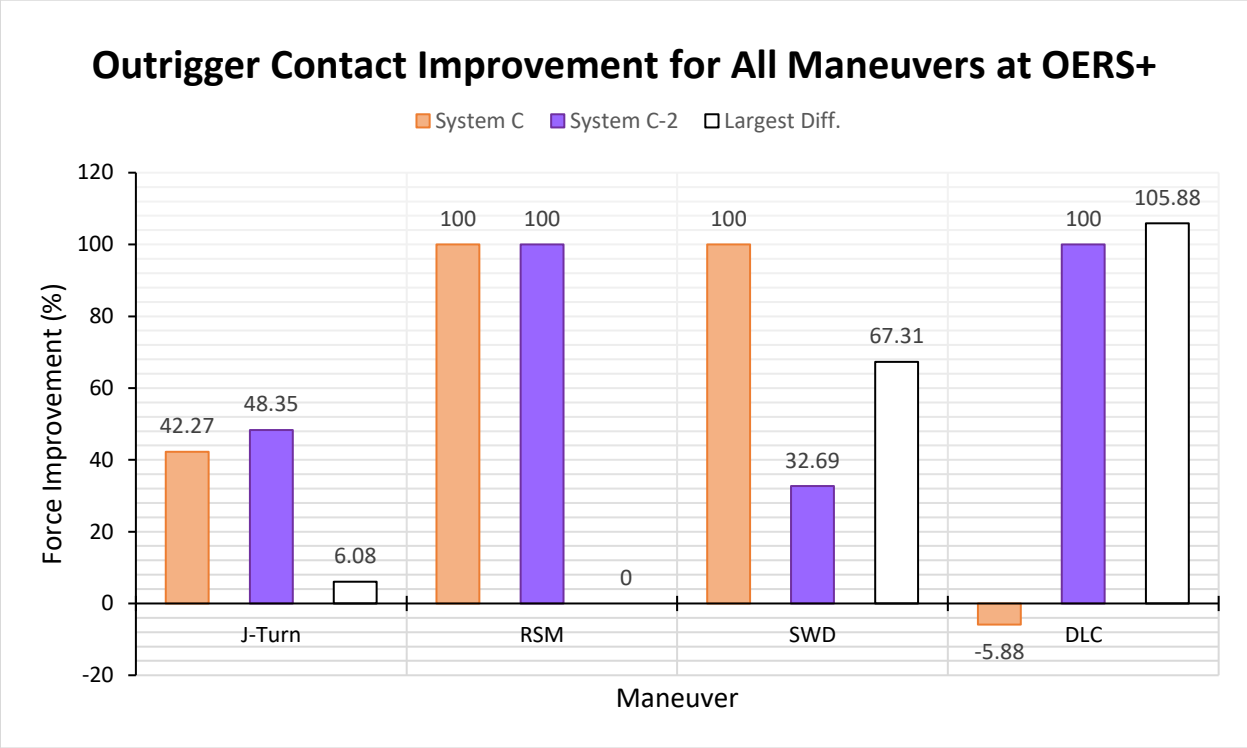

Figure 5-75. Outrigger contact improvements of Systems C and C-2 for all maneuvers at a speed or steering one increment past the OERS.

Figure 5-76 shows the OERS threshold improvements for all four maneuvers. Again, there is graphical evidence for a performance improvement gained from upgrading to a 2S2M system only in DLCs. It was at first theorized that System C-2 was more suited for static maneuvers, but it was later found that System C-2 has consistently lower activation times and longer waiting times. Because of its ability to detect impending rollovers correctly and to do so quickly, System C-2 presented stability improvements more for dynamic maneuvers than for static maneuvers. Although System C-2 does not necessarily show any speed or steering improvements over System C, this difference in activation time and warning time may yield significant differences in ride stability as the driver has more time to react. Figures 5-75 and 5-76 only appreciate RSC brake application, and the efficacy of the two systems can be portrayed in a vastly different manner if driver feedback were to be included in stabilizing the vehicle before roll.

Through the results from all three studies, it can be shown that System C-2 is the only system that yielded stability improvements to the test vehicle for all four maneuvers. Meanwhile, it can also be seen that the

differences between similar systems but from different manufacturers (i.e. Systems A, B, and C) are larger than those seen among different system models from the same manufacturer (i.e. Systems A-D and C-2).

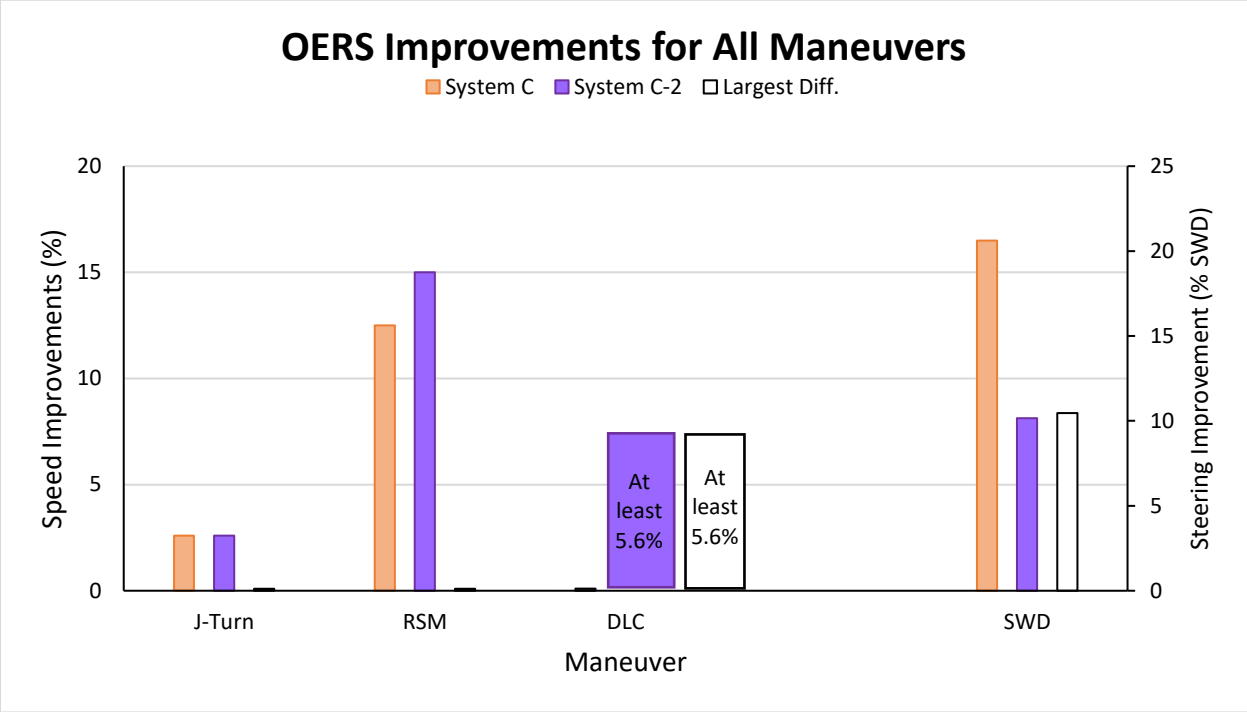

Figure 5-76. OERS threshold improvements of Systems C and C-2 for all four maneuvers.

Chapter 6 Conclusions and Recommendations

This chapter discusses the findings of this research and provides conclusions to the three studies and overall evaluation of RSC systems, as well as recommendations for future testing of RSC systems.

6.1 Conclusions

An evaluation of different RSC systems was conducted at Michelin Laurens Proving Grounds (MLPG) in Laurens, SC, using an instrumented A-Double in four steering maneuvers: J-turn, Ramp Steer Maneuver (RSM), Sine with Dwell (SWD), and Double Lane Change (DLC). Improvements in vehicle roll stability were demonstrated through roll severity reductions quantified by outrigger contact forces. A side-by-side comparison of trailers with and without RSC systems was performed in two quasi-static and two dynamic maneuvers. Both the J-turn and DLC tests were steered by a subjective, professional driver, while the RSM and SWD tests were steered by the steering robot created by the Center for Vehicle Systems and Safety (CVeSS). The J-turn and RSM were quasi-static maneuvers, and the DLC and SWD were more dynamic maneuvers, and by implementing different dynamic situations through the tested maneuvers, a more in-depth look at the performances of RSC systems was possible.

The test vehicle was instrumented with five separate RSC systems which were evaluated in a primary and two secondary studies in this document: a single channel (2S1M) RSC system comparison, a dolly RSC significance study, and a single channel and dual channel (2S2M) RSC system comparison. Direct and valid comparisons were made between the tested systems by evaluating the same variables in repeatable maneuvers in nearly the same test conditions at the test track. Outrigger contact forces, activation times, and warning times for the systems were recorded and analyzed for each maneuver. Outrigger contact forces directly indicated the roll severity of the vehicle, and an estimated contact force threshold of 300 lb was used to distinguish between a tip up and rollover. The activation time, defined as the time between maneuver initiation and RSC activation, was used as the metric for assessing each RSC system's ability to intervene with braking the trailer wheels in order to reduce the likelihood of rollover. The time between RSC activation and outrigger contact provides the warning time available to the driver for possibly executing a corrective steering maneuver to counter the roll dynamics. The warning time proved to be a good measure of RSC effectiveness when the difference in rollover speed or steering threshold between the systems is small or nonexistant.

Track testing of the 2S1M systems, or systems that applied one brake modulator and therefore applied brakes throughout each trailer axle, yielded results in a wide range, in terms of performance and

measurable RSC benefits. When comparing the three systems, the maximum outrigger contact force reductions varied by 6.08% for J-turn, 120.64% for RSM, 77.94% for SWD, and 5.58% for DLC . Somewhat lesser variations were noticed for maximum improvements in rollover speed threshold. The difference in rollover speed threshold among the three RSC systems were 2.6% for J-turn, 12.5% for RSM, and 0% for DLCs. A maximum of 20.63% increase in SWD steering amplitude before rollover was found in RSC usage over baseline, with the maximum difference between the two systems of 11.1 % SWD steering amplitude.

Results from the dolly RSC significance testing showed smaller differences between System A (a 2S1M system from Manufacturer A) and System A-D (System A with the inclusion of the dolly axle in controlled brake applications through RSC usage) than those found between Systems A, B (a 2S1M system from Manufacturer B), and C (a 2S1M system from Manufacturer C), despite hardware changes. The outrigger contact force data showed that dolly inclusion yielded a 16.98% improvement in RSM, and a 27.11% improvement in DLC. However, System A provided a 2.5% rollover speed threshold increase over baseline compared with System A-D at a 0% threshold increase, and posted faster activation times than did System A-D. These small improvements found in dolly-RSC usage failed to manifest rollover speed or maneuverability improvements.

The third and last study in which a 2S1M system (System C) was compared to an equivalent 2S2M system (System C-2) with all four maneuvers yielded mixed results. A comparison of the two systems saw System C and System C-2 each performing better at one quasi-static and one dynamic maneuver. The rollover speed and steering threshold improvements provided by the two systems are similar, with System C slightly outperforming System C-2. System C-2, however, repeatedly activated earlier and provided longer driver warning times than did System C, and provided more roll stability in maneuvers with high frequency steering inputs. An initial reasoning behind this result is the splitting of brake application from side to side with two modulators, reducing calculation effort and thus resulting in faster activation times and longer warning times.

There appears to be a direct correlation between activation time and warning time, but there is no relationship between either one and the outrigger contact force. The warning time in our tests does not include any driver steering feedback, since maintaining the same entry speed and driving path for each maneuver were the main two intentions of the driver. Any driver steering input, as it may occur in practice, could alter the performance of the systems. Hence, the RSC performances studied in this project represent stability improvements solely from controlled brake application.

Another important conclusion drawn from testing was that different commercially-available RSC systems perform differently from maneuver to maneuver, as Systems B and C yielded the largest outrigger contact improvements in at least one maneuver. The differences are estimated to be due to different algorithms, control schemes, and brake application specifics among the systems. Evaluating the specific control approach for each system, however, falls outside the scope of this study. Accordingly, measures such as the amount of braking, lateral accelerations, and brake timing were not evaluated in this study.

A minimum understeering was experienced with the RSC systems that were tested, and a small trade-off between maneuverability and earlier activation timing or increased brake contribution (such as from dolly brakes inclusion) was interpreted from the results. When the tractor was equipped with ESC, an increased propensity to jackknifing was observed in some of the maneuvers, in the presence of RSC on the trailers. Since the main goal of this project was to study RSC effectiveness on trailers with no ESC on the tractor, we did not evaluate any jackknifing effect that the absence of RSC may have for trucks that have an ESC-equipped tractor.

6.2 Recommendations for Future Testing

Further testing of the roll stability of A-Doubles with trailer-based RSC is needed to optimize the performance of trailer stability. Several aspects of the testing done in this study could have been enhanced in hindsight. These include, but are not limited to, the steering robot, GPS units, and the number of tests and retests.

The steering robot provided repeatable steering inputs, but was not capable of regulating vehicle speed as are most commercially-available steering robots. Several of the tests completed throughout this study resulted from maneuver entry speeds that were not as precise as desired. The GPS units were used along with the driver's witness of the speedometer, to log vehicle speeds, but due to the large resolution of the two GPS units installed on the truck, no speed data was considered to be accurate enough. Again, due to lead time and cost, a steering robot was created by CVeSS and used for this study. A steering robot that is fully in charge of vehicle speed as well as its steering input, and the added functionality of logging vehicle speed over time of operation, would be ideal.

To obtain a thorough evaluation of RSC systems for all driving situations, a robot-operated and a driver-operated version of each maneuver should be conducted. Using both a closed-loop and open-loop steering system would result in a comprehensive data set both showing repeatable maneuvers as well as driver feedback, as the latter was not used in evaluating the RSC systems in this study. Driver behavior

during warning time could then be analyzed, and the true value of the difference in warning times between RSC systems could then be determined. Allowing real LCV drivers to test-drive the RSC systems would also give user feedback regarding how intrusive or useful the RSC systems really are. These opinions could provide valuable information regarding the tuning of RSC systems.

Future testing of the RSC systems for particular maneuvers could be completed as well, with a more in-depth study made available by different tunings for the system. As mentioned in Chapter 2, RSC systems and their control schemes can be tuned for different sensitivities to lateral accelerations, marking rollover events earlier or later with the trade-off of intrusiveness. With driver/user feedback, an RSC system may be tuned accordingly for the maneuver a driver is more likely to do, such as for a driver who only drives on curved highways having RSC tuned for RSMs, for example. A future study into the benefit extremes of RSC tuning could open new doors for commercially available systems.

Finally, a study regarding the roll stabilities of triple trailer vehicle configurations with RSC, and the efficacy of commercially available RSC systems on triples can be evaluated in a future study using this study as a reference. It is recommended that a dolly significance study be completed similarly to the one conducted in this project, as the number of dollies doubles from doubles to triples, especially if the dollies used are A-Dollies. Since rearward amplification would play an even larger role in the dynamics of the last trailer in triples, and an additional trailer and trailer brake axle could distribute more vehicle braking effort to its trailers, RSC system usage with triples could prove to be more suitable than with doubles.

References

[1] Bureau of Transportation Statistics, *Number of U.S. Aircraft, Vehicles, Vessels, and Other Conveyances*, U.S. Department of Transportation, 2016.

[2] Statista, U.C.B., *Revenue of Specialized Long-Distance Freight Trucking in US from 2008 to 2020*, Statista, 2016.

[3] Federal Motor Carrier Safety Administration, *Large Truck and Bus Crash Facts 2015,* 2017.

[4] McKnight, J., Bahouth, G.T. *Analysis of Large Truck Rollover Crashes.* Association for the Advancement of Automotive Medicine, 2008. 52(5): p. 421-426.

[5] Green, S.D. *Prevent Heavy Truck Rollover.* Traffic Safety (Chicago), 2002. 2(4).

[6] National Highway Traffic Safety Administration, *Types of Rollovers.*

[7] Dilich, M., Goebelecker, J.M. *Truck Rollover.* Safety Bulletin, Triodyne Inc, 1997. 6(1).

[8] Winkler, C.B., Ervin, R.D. *Rollover of Heavy Commercial Vehicles*. 1999, Great Lakes Center for Truck and Transit Research: Ann Arbor, MI. p. 60.

[9] Winkler, C., Ervin R., Hagan, M. *On-board Estimation of the Rollover Threshold of Tractor Semitrailers*. The dynamics of Vehicles on Roads and On Tracks-Supplement to Vehicle System Dynamics*, Volume 33.* 2000.

[10] Svenson, A.L., et al. *Implementation of Stability Control for Tractor-Trailers Using the National Advanced Driving Simulator*. *21st International Techcnical Conference on the Enhanced Safety of Vehicles, Stuttgart, Germany*. 2009.

[11] Federal Motor Carrier Safety Administration. *Commercial Driver Handbook*. 2017.

[12] Segel, L., Ervin, R. *The Influence of Tire Factors on the Stability of Trucks and Tractor Trailers.* Vehicle System Dynamics, 1981. 10(1): p. 39-59.

[13] National Highway Traffic Safety Administration, *Title 49 Code of Federal Regulations (CFR) Part 571 Section 126 Electronic Stability Control Systems.* Washington, DC: Office of the Federal Register, National Archives and Records Administration, 2007.

[14] Federal Highway Administration. *Traffic Monitoring Guide*. 2014.

[15] Fancher, P.S. *A Vehicle Dynamics Handbook for Single-unit and Articulated Heavy Trucks.* 1987.

[16] Fancher, P. and C. Winkler, *Directional performance issues in evaluation and design of articulated heavy vehicles.* Vehicle System Dynamics, 2007. 45(7-8): p. 607-647.

[17] Independent Trailer & Equipment Co Inc. *Converter Dollies*. 2006, http://www.itec-inc.com/dolly/documnts.html.

[18] Jakubicek, P. *Get Your A B C's Straight*. 2014, http://www.bigtruckguide.com/get-your-a-b-cs-straight.

[19] Liu, P. *Analysis, Detection and Early Warning Control of Dynamic Rollover of Heavy Freight Vehicles,* 1999, Concordia University.

[20] Fancher, P., Winkler, C. *A Methodology for Measuring Rearward Amplification*. International Technical Conference on the Enhanced Safety of Vehicles. 1992. National Highway Traffic Safety Administration.

[21] Department of Motor Vehicles - Rhode Island, *Combination Vehicles*.

[22] Gillespie, T.D. *Vehicle Dynamics.* 1997.

[23] Winkler, C. *Improving the Dynamic Performance of Multitrailer Vehicles: A Study of Innovative Dollies. Volume I-Technical Report. Final Report.* 1986.

[24] Lu, J., Messih, D., Salib, A. *Roll Rate Based Stability Control-The Roll Stability Control System*. Proceedings of the 20th Enhanced Safety of Vehicles Conference. 2007.

[25] Li, Y., Meiry, J., Roeseler, W. *An Active Roll Mode Suspension System for Ground Vehicles.* JOURNAL OF BASIC ENGINEERING, 1968. 90(2): p. 167-174.

[26] Brown, T.A., Rhode, D.S. *Roll Over Stability Control for an Automotive Vehicle.* U.S. Patent No. 6,263,261. 17 Jul. 2001.

[27] Dang, J.N. *Statistical Analysis of the Effectiveness of Electronic Stability Control (ESC) Systems-Final Report*. 2007.

[28] Murray, D., Shackelford, S., Houser, A. *Analysis of Benefits and Costs of Roll Stability Control Systems for the Trucking Industry*. 2009.

[29] Toyota, *Toyota Brake Systems - Course 552*. 2002.

[30] Korn, A. *Safety Benefits of Stability Control Systems for Tractor-Semitrailers*. Meritor WABCCO Vehicle Control Systems.

[31] National Highway Traffic Safety Administration, *FMVSS No. 136, Electronic Stability Control Systems On Heavy Vehicles*. 2012, Office of Regulatory Analysis and Evaluation National Center for Statistics and Analysis.

[32] ATA Industry Technical Council, *RSC and ESC Systems for Trucks and Trailers*, A.T. Association, Editor. 2016.

[33] Sampson, D.J.M., Cebon, D. *Achievable Roll Stability of Heavy Road Vehicles.* Proceedings of the Institution of Mechanical Engineers, Part D: Journal of Automobile Engineering, 2000. p. 217.

[34] Maas, J. *Jackknife Stability of a Tractor Semi-Trailer Combination.* Mechanical Engineering Masterproject, Eindhoven, 2007. p. 11.

[35] Hou, Y., *Roll and Yaw Stability Evaluation of Class 8 Trucks with Single and Dual Trailers in Low- and High-Speed Driving Conditions*, in *Mechanical Engineering*. 2017, Virginia Tech: Center for Vehicle Systems and Safety.

[36] National Highway Traffic Safety Administration, *Tractor Semi-Trailer Stability Objective Performance Test Research - Roll Stability.* 2011.

[37] Day, A.J. *Braking of Road Vehicles*. 2014.

[38] Radlinski, R.W., *Braking Performance of Heavy US Vehicles*. SAE Technical Paper, 1987.

[39] Radlinski, R.W., Williams, S. *NHTSA Heavy Duty Vehicle Brake Research Program-Report No. 5: Pneumatic Timing*. 1985.

[40] Murphy, R.W., Lampert, R., Segel, L. *Bus, Truck, Tractor/Trailer Braking System Performance*. 1970.

[41] National Highway Traffic Safety Administration, *National Highway Traffic Safety Adminitration's Class 8 Tractor/Trailer Safety Outriggers.* 2010.

Appendix

A Vehicle Parameters

Figure A-1. Vehicle parameters for brake distribution calculations.

Variable	ST Parameters	AD Parameters
P	91665 (N)	91665 (N)
P_t	264311 (N)	
P_{t1}		70306 (N)
P_{t2}		70306 (N)
P_D		12192 (N)
z	0.6	0.6
L_1	3 (m)	3 (m)
L_2	2.600 (m)	2.600 (m)
L_3		3.622 (m)
L_4		3.200 (m)
L_5		3.622 (m)
L_6		3.200 (m)
L_D		.305 (m)
E_1	5.600 (m)	5.600 (m)
E_2	13.082 (m)	6.822 (m)
E_3		6.822 (m)
c_1	.178 (m)	.178 (m)
c_2		.648 (m)
c_3		1.994 (m)
c_4		-.102 (m)
h_1	1.350 (m)	1.350 (m)
h_2	1.143 (m)	1.143 (m)
h_3	2.460 (m)	2.410 (m)
h_4		.889 (m)
h_5		1.143 (m)
h_6		2.410 (m)
h_D		.699 (m)

B NI CompactRIO

The National Instrument (NI) CompactRIO platform, or simply cRIO, is a user-programmable FPGA that implements a standalone CPU and configurable IO modules. The cRIO-9024 has an 800 MHz CPU, 512 MB DRAM, and 4 GB storage controller that allows real-time monitoring applications, and is therefore perfect as a data acquisition system for this project. There are four module slots available in the cRIO-9024 chassis, but only two are used: two NI-9205 (analog output, or AO) modules.

The cRIO was used to log data from all of the AO sensors via DB-37 pin outs that are available for each junction box. Two separate DB-37 cables were used, one per NI-9205 module and therefore one for each trailer. Male-to-female DB-37 cables were used since the breakout boards in each junction box were female, and the NI-9205 modules were male. Each of the breakout boards in JBA and JBB use different pin outs, and are shown in Tables B-1 and B-2. As mentioned before, the junction boxes were designed for easy modifications, so the wires from the connector ports installed in the box all used the same wirings. In this way, any sensor could be used with any port, as long as the port's wires were pinned accordingly. These port wires are referred to in the last column of Tables B-1 and B-2.

Table B-1. Pin out table for JBA in Trailer A.

Pin # (Channel)	Sensor	Label	TDMS #	Paired with	Wire (Color)
1 (AI0)	Load cell #3 (Jerry Dri.)	LC-Jry-L	18	Pin #20	Output + (Blue)
2 (AI1)	Load cell #4 (Jerry Pass.)	LC-Jry-R	19	Pin #21	Output + (Blue)
3 (AI2)	Single-axis accel. on Jerry	A1-Jry	20	Pin #22	
4 (AI3)				Pin #23	
5 (AI4)				Pin #24	
6 (AI5)				Pin #25	
7 (AI6)	Pressure sensor #4	P-L	1	-	Output (Blue)
8 (AI7)				-	
9 (DO0)				-	
10 (COM)				-	Ground (Black)
11 (AI16)	LED flag		12	-	
12 (AI17)	Pressure sensor #5	P-R	2	-	Output (Blue)
13 (AI18)	String pot. #5	SP-L	3	-	Output (Blue)
14 (AI19)	String pot. 40	SP-40	4	-	
15 (AI20)	TOF Jerryy Dri.		16	-	

16 (AI21)	TOF Jerry Pas.		17	-	
17 (AI22)				-	
18 (AI23)	String pot. #6	SP-R	5	-	Output (Blue)
19 (AISENSE)				-	Ground (Black)
20 (AI8)	Load cell #3 (Jerry Dri.)			Pin #1	Output - (Green)
21 (AI9)	Load cell #4 (Jerry Pass.)			Pin #2	Output - (Green)
22 (AI10)	Single-axis accel. on Jerry	A1-Jry		Pin #3	
23 (AI11)				Pin #4	
24 (AI12)				Pin #5	
25 (AI13)				Pin #6	
26 (AI14)	3-g accel. #1 - Frame - X	A3-1	6	-	Output (Green)
27 (AI15)	3-g accel. #1 - Frame - Y	A3-1	7	-	Output (Blue)
28 (PFIO)					
29 (COM)				-	Ground (Black)
30 (AI24)	RSC Relay Dri.		8	-	Output (Purple)
31 (AI25)	Ground		13	-	
32 (AI26)	RSC Relay Pas.		14	-	
33 (AI27)	RSC Pres. Dri.		15	-	
34 (AI28)				-	
35 (AI29)	50-g accel. #2 - Jerry – X	A50-2	9	-	Output (Green)
36 (AI30)	50-g accel. #2 - Jerry – Y	A50-2	10	-	Output (Blue)
37 (AI31)	RSC Pres. Pas.	A50-2	11	-	Output (Purple)

Table B-2. Pin out table for JBB in Trailer B.

Pin # (Channel)	Sensor	Label	TDMS #	Paired with	Wire (Color)
1 (AI0)	Laser sensor #1 (Tom Dri.)	L-L	21	Pin #20	Output + (Blue)
2 (AI1)	Laser sensor #2 (Tom Pass.)	L-R	22	Pin #21	Output + (Blue)
3 (AI2)	Load cell #1	LC-L	23	Pin #22	Output + (Orange)
4 (AI3)	Load cell #2	LC-R	24	Pin #23	Output + (Orange)
5 (AI4)			25	Pin #24	
6 (AI5)			26	Pin #25	

7 (AI6)	Ground		27	-	
8 (AI7)	RSC Relay Dri.		28	-	
9 (DO0)					
10 (COM)				-	Ground (Black)
11 (AI16)			29	-	Output (Purple)
12 (AI17)	3-g accel. #2 - Tom - X	A3-2	30	-	Output (Orange)
13 (AI18)	3-g accel. #2 - Tom - Y	A3-2	31	-	Output (Blue)
14 (AI19)	3-g accel. #2 - Tom - Z	A3-2	32	-	Output (Purple)
15 (AI20)	Pressure sensor #1	P-L	33	-	Output (Blue)
16 (AI21)	Pressure sensor #2	P-R	34	-	Output (Blue)
17 (AI22)	Pressure sensor #3	P-T	35	-	Output (Blue)
18 (AI23)	String pot. #3	SP-L	36	-	Output (Purple)
19 (AISENSE)				-	Ground (Black)
20 (AI8)	Laser sensor #1 (Tom Dri.)	L-L		Pin #1	Output - (Green)
21 (AI9)	Laser sensor #2 (Tom Pass.)	L-R		Pin #2	Output - (Green)
22 (AI10)	Load cell #1	LC-L		Pin #3	Output - (Green)
23 (AI11)	Load cell #2	LC-R		Pin #4	Output - (Green)
24 (AI12)				Pin #5	Output - (Green)
25 (AI13)				Pin #6	Output - (Green)
26 (AI14)	String pot. #4	SP-R	37	-	Output (Purple)
27 (AI15)	TOF Tom Dri.		38	-	
28 (PFIO)					
29 (COM)				-	Ground (Black)
30 (AI24)	TOF Tom Pas.		39	-	
31 (AI25)	Ground		40	-	
32 (AI26)	RSC Relay Pas.		41	-	
33 (AI27)	RSC Pres. Dri.		42	-	
34 (AI28)	RSC Pres. Pas.		43	-	
35 (AI29)			44	-	
36 (AI30)			45	-	
37 (AI31)			46		

The CompactRIO is used with NI LabVIEW software; the data gathered by these NI 9205 modules are sent to the PC via an Ethernet cord in order to use the modules directly from LabVIEW Real-Time. LabVIEW is an engineering software for test, measurement, and control applications, and is specifically geared towards acquiring data with hardware. Its main feature is the ability to create custom GUIs quite easily.

Although the cRIO implements its own 4 GB hard drive that logs and stores collected data, using it with NI LabVIEW Real-Time allowed the team to monitor each sensor in real-time for an extended period of time. The LabVIEW Real-Time Module was a separate module purchased in order to extend LabVIEW's graphical environment to stand-alone embedded systems such as the cRIO. As an add-on to LabVIEW's development capabilities, the module acquired IO from the modules used and communicated with the PC to develop graphical applications to monitor both analog and digital data. This granted the team numerous benefits, most notably the ability to determine whether each test trial was successful, and to troubleshoot and check sensors before, during, and after testing. Live diagnostics turned out to be absolutely crucial when working with such a large vehicle and extensive system of sensors, especially when there was limited time for testing every week at the test track. LabVIEW also made the data transfer from the cRIO hard drive to the PC hard drive for post processing a quick and clean method.